**Title**

Leveraging the Bioeconomy for Carbon Drawdown



**Author**

Dees, John Paul

**Publication Date**

2022

Peer reviewed|Thesis/dissertation

# Leveraging the Bioeconomy for Carbon Drawdown

By

John Paul Dees

A dissertation submitted in partial satisfaction of the

requirements for the degree of

Doctor of Philosophy

in

Energy and Resources

in the

Graduate Division

of the

University of California, Berkeley

Committee in Charge:
Professor Daniel M. Kammen, Co-chair
Professor David Anthoff, Co-chair
Professor Matthew Potts
Professor Daniel L. Sanchez

Fall 2022

Abstract

Leveraging the Bioeconomy for Carbon Drawdown

By

John Paul Dees

Doctor of Philosophy in Energy and Resources

University of California, Berkeley

Professors Daniel M. Kammen and David Anthoff, Co-chairs

The role of the bioeconomy in climate change mitigation has been, at times, both contested or framed in a limited manner to include only bioenergy with carbon capture and sequestration (BECCS) technologies. This dissertation contributes to a more expansive framework wherein the bioeconomy services distinct and dynamic near, medium, and long-term decarbonization needs. Products of the bioeconomy can serve as both fossil fuel replacement in "hard-to-abate" sectors as well as providing a carbon storage medium for biomass carbon removal and storage (BiCRS), an emerging framework with a more expansive opportunity set for carbon removal than BECCS alone. This dissertation builds on existing literature, starting with a review of the BiCRS literature and a supplementary novel analysis of the climate impact potential of BiCRS technologies in the near-term. The subsequent chapters offer cost and climate impact assessments for biomass utilization in the transportation sector. The bioeconomy already services substantial decarbonization needs in light duty transportation in the form of biofuels derived from starch, sugars, and oil crops. Chapter 3 explores the potential to further decarbonize ethanol production by capturing fossil boiler emissions via the integration of an oxyfuel boiler. Chapter 4 explores the potential of drop-in biofuels in the "hard to abate" aviation sector through a comparative analysis of the cost, climate impact, and scalability of sustainable aviation fuel technologies and feedstocks. The overarching finding of this dissertation is that there are meaningful, cost-effective opportunities to deploy bio-based products for decarbonization and carbon removal, particularly in economic sectors where there are few if any other near-term options.

Stringent climate change mitigation scenarios rely on large-scale drawdown of carbon dioxide from the atmosphere. Amongst drawdown technologies, BECCS has received considerable attention in the climate mitigation literature. Recently, attention has shifted further from a relatively narrow focus on BECCS to a broader focus on BiCRS. The concept of BiCRS has the potential to enable a future where the climate mitigation value of biomass resources is more valuable than the energy value, due to the potential to remove and sequester large quantities of atmospheric $CO_2$. There are numerous opportunities to incorporate carbon removal and management within the bioeconomy, but the majority of immediate carbon removal potential

exists in four bioproducts: bioenergy, bioplastics, biochar, and wood products. Chapter 2 analyzes the life cycle greenhouse gas emissions and disposition of sequestered carbon over 10,000 years for four bioproducts representative of each broader category: an advanced BECCS pathway, biopolyethylene, oriented strand board, and biochar soil amendment. The analysis shows that the BECCS pathway has the greatest magnitude and durability of $CO_2$ storage over all time horizons. However, non-BECCS pathways achieve 34-64% of the drawdown magnitude relative to BECCS and retain 55-67% of their initial drawdown over 100 years (central estimate). This work identifies three engineering strategies for enhancing carbon drawdown: reducing biomass supply chain emissions, maximizing carbon stored in long-lived products, and extending the term of carbon storage. In the larger context of this work, the analysis demonstrates that the bioeconomy can service potentially higher-value economic needs than the energy sector alone, while removing and storing atmospheric carbon over climate-relevant timeframes.

Within the energy sector, the bioeconomy still has a near-term role to play in transport decarbonization. Decarbonization of transportation fuels represents one of the most vexing challenges for climate change mitigation. Biofuels derived from corn starch have offered modest life cycle greenhouse gas (GHG) emissions reductions over fossil fuels. This work shows that capture and storage of $CO_2$ emissions from corn ethanol fermentation achieves ~58% reduction in the GHG intensity (CI) of ethanol at a levelized cost of 52 \$/t$CO_2$e abated. The integration of an oxyfuel boiler enables further $CO_2$ capture at modest cost. This system yields a 75% reduction in CI to 15 g$CO_2$e/MJ at a minimum ethanol selling price (MESP) of \$2.24, a \$0.31/gallon increase relative to the baseline no intervention case. The levelized cost of carbon abatement is 84 \$/t$CO_2$e. Sensitivity analysis reveals that carbon neutral or even carbon negative ethanol can be achieved when oxyfuel carbon capture is stacked with low-CI alternatives to grid power and fossil natural gas. Conservatively, fermentation and oxyfuel CCS can reduce the CI of conventional ethanol by a net 44-50 g$CO_2$/MJ. Full implementation of interventions explored in the sensitivity analysis would reduce CI by net 79-85 g$CO_2$/MJ. Integrated oxyfuel and fermentation CCS is shown to be cost effective under existing U.S. policy, offering near-term abatement opportunities.

The role of biofuels is likely to diminish in ground transport as electrification provides more cost and climate effective alternatives. However, commercial aviation is not amenable to electrification at scale in the near future, thus there is an imminent role for the bioeconomy. Aviation is termed a “hard to abate” sector as there are few viable decarbonization options for air transport at present due to safety considerations, infrastructure, and technical hurdles. Drop-in sustainable aviation fuels (SAF) produced from biomass or $CO_2$ are widely-viewed as the most viable near-term alternatives to fossil jet fuel. There are many technical pathways to produce SAF, and their costs and impact on climate and food systems differ significantly. The work presented here sets sustainability and cost criteria to produce 10 billion gallons of SAF in the United States by 2030 and assesses the viability of SAF production technologies and feedstocks against those criteria. The analysis indicates the greatest opportunity in the production of Fischer-Tropsch and Alcohol-to-Jet fuels. These production pathways are amenable to waste and residue feedstocks, minimizing the impact on food systems and land use emissions. Moreover, they are compatible with relatively low-cost carbon capture and sequestration technologies which can yield carbon negative fuels. Given existing U.S. policies, the technoeconomic

assessment of these pathways indicates that in many contexts, subsidized costs may be competitive with commercial Jet-A.

The scope of the work in this dissertation highlights the significant and varied roles that the bioeconomy can play in climate mitigation while recognizing that sustainable biomass is a limited resource that should be targeted at its highest value uses.

## DEDICATION

I dedicate this work to all of the teachers, mentors, family, and friends who invested in me and believed in me. This is for my brothers in the recovery houses back home. This is for my support system in the writing center and the professors who took an interest in me at the University of North Georgia, Gainesville. Most importantly, this is for my mom, Jimmie Pearl Anderson Dees, who did not have the opportunities given to me, but whose tireless love and faith in me saved me time and again and delivered me here.

**TABLE OF CONTENTS**

Page

## LIST OF FIGURES

## LIST OF TABLES

## ACKNOWLEDGMENTS

I would like to thank my committee co-chairs, Dan Kammen and David Anthoff, and my committee members, Dan Sanchez and Matthew Potts for their guidance and support throughout the course of this research. Furthermore, I'd like to recognize Jalel Sager, who guided and supported my research in the early days of my graduate studies. Jalel helped me find the confidence and curiosity to chart my path through the PhD at a pivotal moment in my studies. I'd like to thank J.P. Carvallo, Seigi Karasaki, Sophie Major, Stephen Jarvis, and Ella Belfort for their friendship and for always being a sounding board for my ideas, whether they were fully-formed or not. I want to thank my colleagues A.J. Simon and Hannah Goldstein at Lawrence Livermore National Laboratory, Sean McCoy and Kafayat Oke at University of Calgary, and Joe Sagues and Ethan Woods at NC State for being excellent, supportive collaborators and intellectual partners. Moreover, I am indebted to Stephanie Karris, Erica Belmont, Pete Psarras, Julio Friedmann, and Charlie Parker for their support and collaboration on the sustainable aviation fuel chapter of this work. In addition, I would also like to thank my friends, colleagues, the department faculty, and staff for making my time at the Energy and Resources Group, UC Berkeley a wonderful experience.

# CHAPTER 1. BACKGROUND AND MOTIVATION

Anthropogenic climate change is a pressing existential challenge of our time. Human activities are responsible for an increase in average global temperature between 0.8$^{o}$C to 1.3$^{o}$C relative to 1850, resulting in rapid changes in the atmosphere, ocean, cryosphere, and biosphere [1]. The warming effect is the result of a change in earth's net energy balance catalyzed by the energy-trapping effects of well-mixed greenhouse gasses (GHGs) of anthropogenic origin, the most important of which are methane ($CH_4$), nitrous oxide ($N_2O$), and carbon dioxide ($CO_2$)[1]. Anthropogenic $CO_2$ has had the greatest impact on warming to date [1]. Unaddressed, global average temperatures in 2100 could exceed pre-industrial temperatures by 2 C or more, resulting in potentially catastrophic social and environmental harms [2].

The IPCC's use of 1750 as an inflection point for anthropogenic emissions is notable because it roughly marks a transition between humanity's reliance on a subsistence income of solar energy stored in the carbon-hydrogen bonds of recently living organisms (aka "biomass") and the rapid growth of industrialized societies fueled by vast deposits of solar energy stored in the carbon-hydrogen bonds of prehistoric organisms, aka "fossil fuels." To a great extent, the industrialized world transitioned from a "bioeconomy" to a fossil economy. The energy dense fossil trust fund enabled extraordinary expansion of human civilization. Surplus fossil energy served as a multiplier to human labor and subsequent technical advances paid compound interest in increased agricultural yields and cheaper, lighter, and more durable materials. Fossil fuel-enabled development came at a cost. The carbon excavated and released from those primordial bonds perturbed the delicate energy balance of the biosphere, shifting the climate away from conditions in which most of human history has transpired.

As the world grapples with the necessity of decarbonizing the global economy, biomass, civilization's original energy source, is again thrust to the fore as both a climate solution and a source of controversy. The bioeconomy has persisted alongside the fossil economy. Roughly 2.9 billion people and 14% of global heat consumption still rely on traditional biomass for heat and cooking [3]. Biomass is the intermediate source of every food calorie consumed. Working forests remain an indispensable source of construction materials and value-added products. Non-working lands and protected spaces house complex ecosystems that provide incalculable environmental services to the humans and the whole of the biosphere. These stores of biomass are increasingly under threat both from human exploitation as well as the impact of changing climate. It is because of the centrality of biomass to food systems, commerce, biodiversity, land use, water systems, and the carbon cycle that further human exploitation raises concerns.

The remainder of this introduction will situate my dissertation research in emerging narratives of sustainable biomass utilization for climate change mitigation. A summary of those narratives follows.

## 1.1 Biomass in decarbonization roadmaps

Climate mitigation scenarios implement two strategies to address rising atmospheric $CO_2$ concentrations. The first strategy is to reduce the flow of fossil $CO_2$ to the atmosphere through

low-carbon technology alternatives, efficiency, and other abatement methods. The second strategy involves increasing the flows of carbon from the atmosphere into natural or engineered sinks. Strategies of the second kind are termed carbon dioxide removal (CDR) or negative emissions technologies (NETs) when referring to the means of removal. Both immediate and deep emissions reductions as well as CDR will be necessary to meet climate targets. The IPCC's Sixth Assessment Report states unequivocally: "The deployment of CDR to counterbalance hard-to-abate residual emissions is unavoidable if net zero $CO_2$ or GHG emissions are to be achieved...(high confidence)" [4]. The same IPCC report also analyzed overshoot scenarios where CDR is needed to reverse a short-term exceedance of the 2$^{o}$C target.

Biomass can both reduce fossil emissions and function as a medium for CDR. Biomass leverages biotic productivity, storing both atmospheric carbon and energy in the process of photosynthesis. As such, biomass is an alternative to emissions intensive fuels and materials as well as a concentrated store of atmospheric carbon (biomass is typically 40-50% carbon by dry weight) [5]. The multifunctionality of biomass as well as constraints on biomass supply due to competing priorities for land, food, and natural ecosystems calls for an integrated approach to biomass utilization. David Keith's (2001) "Fourfold Way" offers a succinct conceptual model of climate mitigation options for biomass [6]. **Table 1-1** is an updated adaptation of this model that reflects more nascent opportunities such as biobased materials and innovative CDR solutions more representative of the contemporary option set. In the original depiction of this model, remote sequestration was a category unto itself, but there is growing recognition of the potential for engineered carbon removal in long-lived materials [7]–[9]. Specific opportunities for carbon removal via the bioeconomy will be addressed in Chapter 2.

**Table 1-1** An update to David Keith's "Fourfold Way." Adapted from [7]. BECCS = Bioenergy with Carbon Capture and Sequestration and many include any number of technologies that convert biomass to electricity, gaseous fuels (e.g. hydrogen), or liquid fuels (e.g. ethanol) and capture and store the resulting CO2 emissions, typically in the geologic subsurface.

| **[Terrestrial] Sinks** | **Bioenergy** |
|---|---|
| Carbon may be sequestered in situ in soil or standing biomass. Although the distinction between the protection of existing carbon pools and actions intended to increase carbon storage (e.g., forest protection versus reforestation) is vital for policy implementation, the tight biological coupling between the protection and enhancement of sinks leads me to treat them jointly. | Biomass may be harvested and used as fuel so that $CO_2$ emissions from the fuel's use are (roughly) balanced by $CO_2$ captured in growing the energy crops. |
| **[Non-BECCS Engineered] Sinks** | **BECCS** |
| [Original] *Remote sequestration*: Biomass may be harvested and separately sequestered; for example, by burying the trees.<br><br>[Updated] *Sequestration in long-lived products:* For example, storing biomass | Biomass may be harvested and used as fuel with capture and sequestration of the resulting $CO_2$; for example, we may use biomass to make hydrogen and sequester the resulting $CO_2$ in geologic formations. |

| | |
|---|---|
| carbon in recalcitrant materials such as polymers, harvested wood products, buildings. | |

Decarbonization strategies to date have deployed biomass inconsistently and no models, to my knowledge, address the full range of opportunities described above. Virtually all decarbonization roadmaps prioritize deep electrification and efficiency upgrades wherever possible across all sectors and significant deployment of low-carbon electricity [10]–[13]. Prominent decarbonization road maps deploy biomass broadly in the power sector, for liquid fuels, and for CDR utilizing BECCS to offset 'hard-to-abate' emissions [10]. Other strategies direct all biomass towards liquid fuels for transport and none for BECCS or power production [11]. Due to the extended turnover times of vehicle fleets, near-term roadmaps and indeed existing policies position liquid biofuels as complementary to electrification as a necessary bridge fuel for near-term decarbonization of light duty transport [14], [15]. Still other studies foreground BECCS for use in electricity production as a dispatchable source of power alongside intermittent renewable energy technologies while noting a higher relative value of the CDR component over the energy component of biomass [16], [17]. At least one seemingly aspirational study forgoes the biomass contribution to climate mitigation entirely [18], [19].

### 1.1.1 Feedstock potential and limits

Biomass deployment for climate mitigation is constrained by sustainable feedstock supply indicating a need to target biomass at highest value uses. Biomass availability and optimal use is spatially and temporally dependent [20]–[22]. Optimization models that consider interactions between biomass supply, food, land, and water tend to be complex and are targeted almost exclusively at the energy sector [23]–[25] although consideration of biomaterials is emerging [8], [26].

Estimates of sustainable biomass supply vary considerably. There are hard limits on sustainable biomass supply governed by land availability, nutrient cycling, and cost [27], [28]. The IPCC adopts a range 5-50 EJ/yr for wastes/residues and 50-250 EJ/yr for dedicated biomass production systems in 2050 when food security and environmental constraints are taken into account [29]. Dedicated biomass production systems include three potential subclasses of biomass: (1) First-generation (1G) edible crops like corn, sugarcane, or soy (2) Second-generation (2G) non-edible cellulosic crops such as miscanthus or poplar and (3) third generation (3G) algae. Wastes and residues (e.g., corn stover or forestry residues) are almost exclusively from the 2G category. The sustainability risks of 1G and dedicated production of 2G energy crops are well-documented [30], [31]. Unlike dedicated biomass production, wastes and residues do not compete for productive land, however, utilization of these materials removes key nutrients from ecological and agricultural systems, thus overutilization can initiate second-order effects on land and ecosystem productivity [32].

The biomass decarbonization strategies investigated in this dissertation are oriented toward near-term, low-risk opportunities to deploy biomass for climate mitigation. As such, it is assumed that 1G crops should be avoided beyond the low-hanging fruit of existing utilization. My research

emphasizes technologies that utilize wastes, residues, and limited 2G energy crops to address segments of the economy where there are few if any alternatives to fossil fuels.

**Figure 1-1** disaggregates global 2G biomass potential by category. The ranges represent a subset of those reported in Slade et al (2014), omitting scenarios that make heroic assumptions about behavioral and dietary change [33]. The result is a much narrower range and ultimately lower maximum potential than the ranges reported by the IPCC. Slade reports biomass EJ of total energy content. I converted this value to fuel energy equivalent using representative liquid fuel yields from Chapter 4. I further converted the ranges into carbon content assuming 50% C by mass and representative lower heating values (LHV) as well as $CO_2e$ stored in the biomass. To contextualize biomass decarbonization potential, high value sectoral demand is marked by the horizontal bars for comparison: (a) 2019 industrial heat demand to be compared with total energy content (b) 10 Gt/yr CDR to be compared with $CO_2e$ content (c) 2050 aviation fuel demand to be compared with fuel energy equivalent and (d) 2050 plastic production to be compared with C content of the biomass. While these conversions are an oversimplification of technical potential, they provide a reasonable intuition for the scalability of biomass to meet multiple decarbonization needs. Residues alone can address the needs of one or more categories, although some dedicated energy crop production would be indicated to decarbonize multiple sectors with biomass.

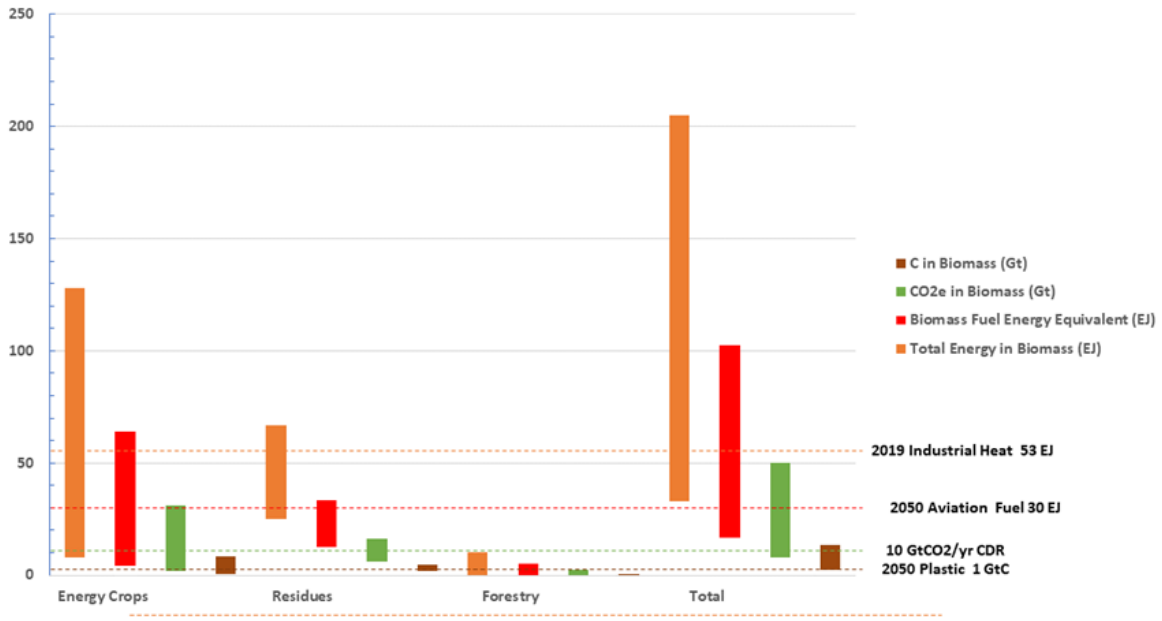


**Figure 1-1** Global 2G biomass potential by category. Original data adapted from Slade et al. (2014) [33]

There is a distinctly U.S. focus to the research presented in the subsequent chapters. The U.S. DOE has estimated biomass potential (primarily 2G) approaching one-billion BDT per year [34].

Chapter 4 offers a more granular analysis of near-term biomass potential in the context of sustainable aviation fuel.

### 1.2 Biomass for 'hard-to-abate' sectors

As discussed in Chapter 1.1, decarbonization roadmaps prioritize electrification and efficiency strategies to eliminate fossil emissions wherever possible. However, electrification is not a technically or economically viable option in many sectors. The IPCC and decarbonization literature more broadly have termed these sectors as 'hard to abate' and typically include: long distance transport (shipping and aviation), agriculture, and industrial processes (e.g. iron, steel, cement, and chemicals) [35]. As discussed previously, biomass energy and materials can be deployed to address these emissions either through direct substitution for fossil inputs or via CDR to offset emissions from sector that have yet to be decarbonized. The latter option will be discussed in the next section. In terms of substitution, there remains a near-term "bridge fuel" role for biomass in sectors that should eventually rely on low-cost renewable electricity from wind, solar, and other alternatives, for example as dispatchable power or liquid fuels for light duty transport [14], [20], [36]. In the medium to long-term, however, limited sustainable biomass supply will likely demand focused deployment to address residual emissions. **Figure 1-2** illustrates substitution possibilities for biomass feedstocks.

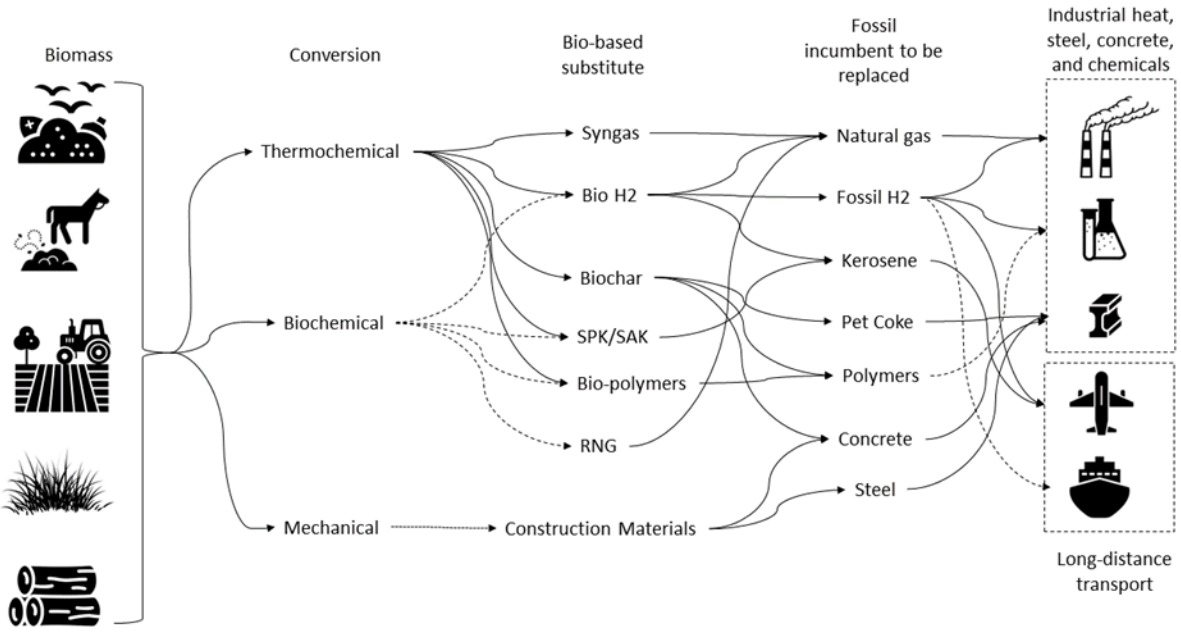


**Figure 1-2** Bio-based substitutes for high fossil emissions products. This list is not exhaustive.

Chapter 2 addresses the potential of biobased materials to replace fossil incumbents in polymers, steel, and construction materials while Chapter 4 addresses the cost and carbon intensity of bio-based substitutes for aviation fuels.

## 1.3 Negative emissions technologies

In addition to providing an alternative to fossil-derived energy and products, the bioeconomy is uniquely positioned to help remove $CO_2$ from the atmosphere. Biomass-based carbon dioxide removal (CDR) and negative emissions technologies (NETs) leverage the photosynthetic uptake of $CO_2$ by plants and algae either directly or indirectly (e.g. animal wastes) as a renewable source of carbon for long-term storage in living biomass, durable products, or durable sequestration in stable carbonaceous materials (biochar) and geologic stores.

The technical potentials of NETs vary widely and not all NETs technologies are biomass-based. Each approach (e.g. blue carbon [37], [38], enhanced weathering [39], [40], direct air capture [DAC] [41], and biomass-based pathways) has its own risks and challenges to reaching scale (these technologies are described in Chapter 1.3.2). However, engineered biomass approaches can achieve durable carbon removal and likely have the highest technological readiness at this time [42]. For instance, biomass-based carbon drawdown is lower in cost than DAC [42], and pathways are already more widely deployed than mineralization and other nascent engineered NETs.

CDR and NETs often raise questions of moral hazard [43]. Critics are concerned that an emphasis on CDR is a distraction and will stifle the urgency of decarbonization and the transition from fossil fuels. This criticism is typically leveled at CCS applied to fossil power generation or BECCS technologies that combust biomass for energy while capturing $CO_2$. This argument has merit, and as this dissertation should make clear, biomass-enabled CDR should be understood as a necessary but secondary tool alongside decarbonization of the economy. The remainder of Chapter 1.3 will describe why CDR is needed, the options available, describe the emerging framework of Biomass Carbon Removal and Storage (BiCRS) [44]as an alternative to the narrow category of BECCS CDR.

### 1.3.1 The Big Picture: The global carbon cycle

Fundamentally, increased atmospheric $CO_2$ concentrations are the result of human activities that altered the natural flux of carbon to and from other pools in the global carbon cycle. Some of those pools are transient with regard to the residence time of carbon, and carbon in these pools may shift between pools on human timescales. Transient pools include atmospheric carbon, soil carbon, terrestrial vegetation, and the organic carbon of the upper ocean (See **Figure 1-3**). Other pools cycle carbon on geologic timescales, such as the carbon stored in limestone (calcium carbonate), the deep ocean, and fossil carbon (coal, oil, natural gas). Emissions from terrestrial vegetation and soils as capture by the IPCC's Agriculture, Forestry and Other Land Use (AFOLU) category accounted for 36% of anthropogenic $CO_2$ emissions between 1850 and 2000 [45] and 14% between 2010 and 2019 [46]. The remaining anthropogenic $CO_2$ emissions over these time periods predominantly originated from geologic pools of carbon: fossil fuels and calcium carbonate (in the production of concrete) [47].

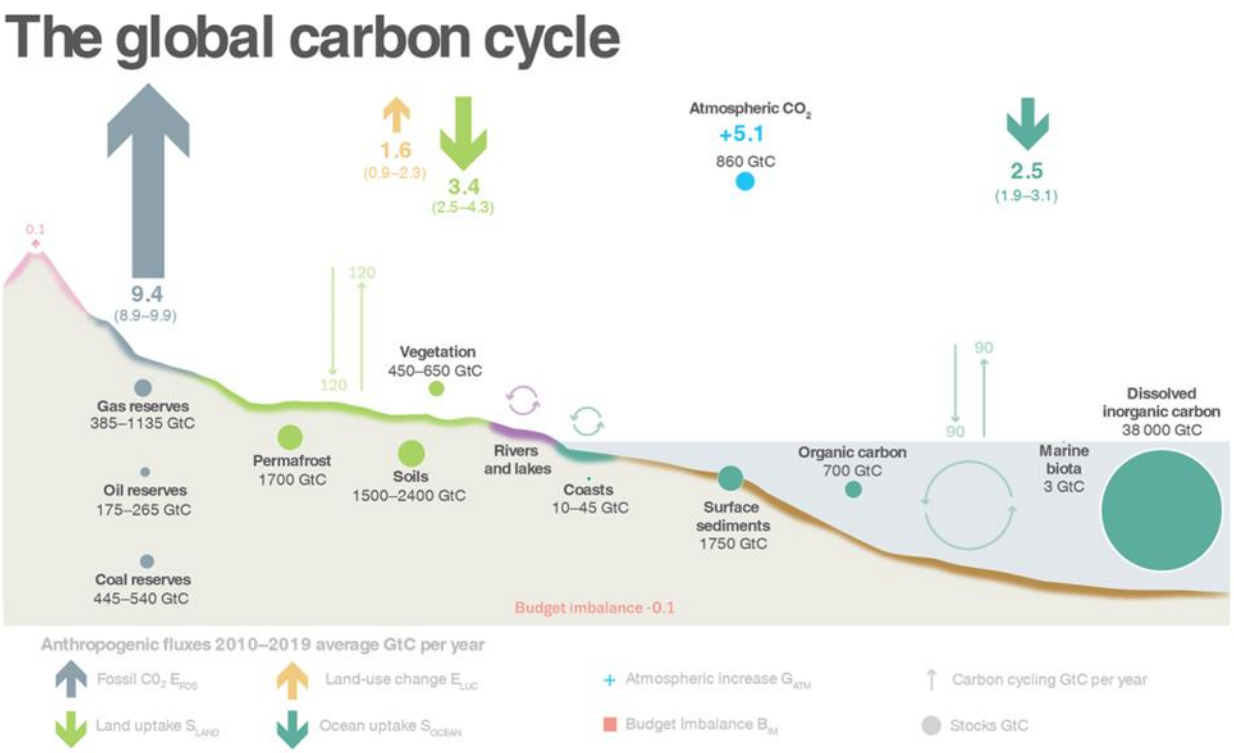


**Figure 1-3** The global carbon cycle. Image source: Friedlingstein et al (2019) [48]

The distinction between the transient and geologic pools of carbon are key to conceptualizing the challenge posed by climate change and potential mitigation options. While both terrestrial and geologic emissions have contributed to atmospheric $CO_2$ concentrations, geologic emissions represent a net increase to the transient carbon pool [45], [49]. Both the terrestrial pool and ocean pool draw down atmospheric $CO_2$ emissions, but only the ocean sink serves as a natural conduit to transfer carbon from the transient pools to the geologic pool at magnitudes and timescales relevant to humans. Between 2010 and 2019, 46% of anthropogenic $CO_2$ emissions accumulated in the atmosphere, 23% of anthropogenic $CO_2$ emissions were taken up by the ocean while 31% was stored in terrestrial vegetation [50]. In short, 77% of emissions remained in the transient pool and 86% of those emissions were additive emissions of geologic origin [46].

Ceasing fossil emissions is a necessary but not sufficient condition to restore climate equilibrium. If the terrestrial carbon pool returned to pre-industrial levels, the sum of atmospheric carbon and *potential* atmospheric carbon stored in transient pools remains irrevocably increased [45], [51] until either the ocean or human intervention return carbon to quasi-permanent storage in the deep ocean or the geologic subsurface. At present, anthropogenic additions to the atmosphere total approximately 279 GtC and growing while the net ocean flux is 2.5 GtC per annum [50]. As atmospheric concentrations of $CO_2$ decline, so does the uptake rate of the terrestrial and ocean sinks [52]. To compound the problem, the ocean is also storing heat which along with other climate feedback effects may continue to impact global temperatures and atmospheric $CO_2$ concentrations long after anthropogenic emissions cease [52]–[56], risking reversal of the terrestrial pool from sink to source [52] as well as the potential release of other

transient stores of GHG emissions such as the hundreds of gigatons of methane hydrate presently stored in permafrost [57].

### 1.3.2 Negative Emissions: Options, Costs, and Potential

Given the need for carbon drawdown via CDR and NETs, the bioeconomy will almost certainly play a central role. Engineered CDR solutions that do not involve biomass have been demonstrated or are in development. Direct air capture (DAC) and enhanced weathering (EW) represent two promising approaches. DAC involves capture of $CO_2$ directly from ambient air. Low concentrations of $CO_2$ in air creates a need for novel sorbents with maximal surface area. This challenge along with the very high energy intensity of these processes (electric power to move large quantities of air across the sorbent as well as high heat requirements to reconstitute sorbents in some designs) constrain this technology in terms of cost and access to low-carbon energy in the near-term. EW is also a promising and potentially low-cost approach that makes use of the natural formation of carbonates in silicate rocks (e.g. olivine) exposed to $CO_2$. This process is enhanced by increasing surface area via grinding of the rocks and spreading over a large area. While both of these approaches are feasible, they are still in early stages of development.

The bioeconomy, on the other hand, already exists. **Figure 1-4** show a conceptual diagram of the primary NETs approaches. While DAC and EW rely on chemistry, all approaches intersect the bioeconomy in some way. Afforestation and reforestation (AR) captures and stores carbon by improving and/or restoring forest carbon stocks. AR is a reversible process (e.g. wildfire), thus the durability of carbon storage is uncertain and is limited by available land. Still, AR is low-cost option with numerous co-benefits for biodiversity and ecosystems. Soil carbon sequestration (SCS) similarly seeks to restore carbon stocks depleted by changes in land use and agricultural practices. There are opportunities in the bioeconomy to restore soil carbon stocks through changes in agricultural practices, with potential to yield lower carbon intensity food and feedstocks for other sectors of the bioeconomy. Biochar (BC) is a product of pyrolysis of biomass yielding highly stable form of carbon that can be used to enhance agricultural soils and for a number of industrial applications (BC is discussed in detail in Chapter 2). Finally, bioenergy with carbon capture and storage (BECCS) makes use of the energy and carbon content of biomass to produce power or fuels while capturing $CO_2$ emitted from thermochemical and biochemical conversion processes for long-term storage. Storage of biomass carbon in long-lived products (construction, polymers) is notable absent from **Figure 1-4**, but this topic is discussed in detail in Chapter 2.

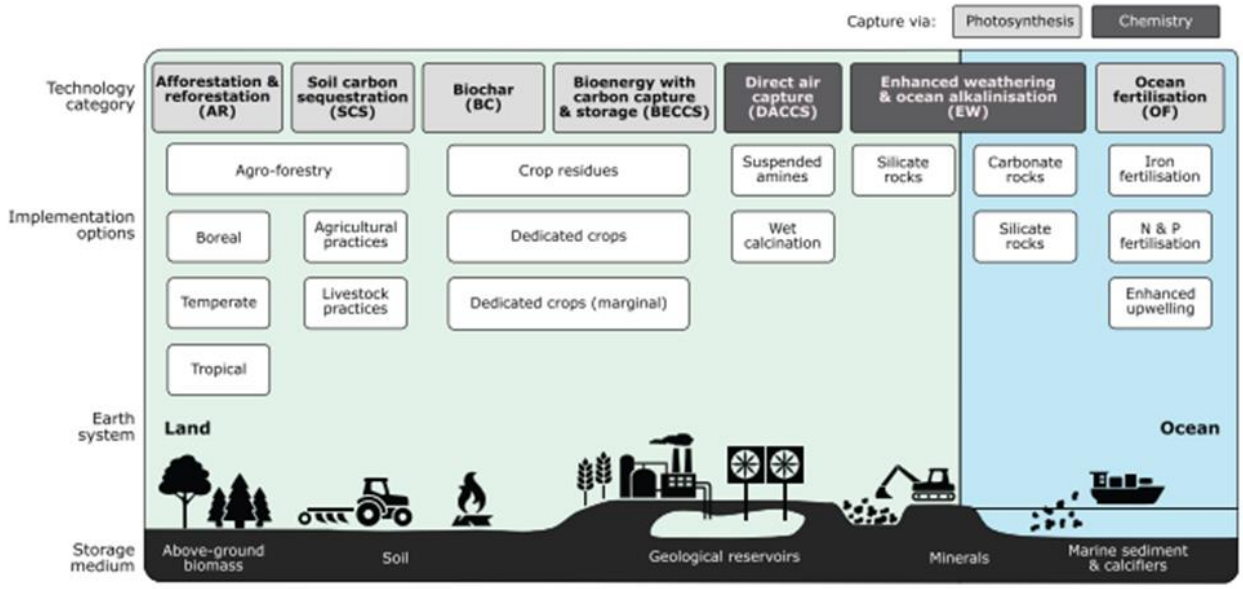


**Figure 1-4** A taxonomy of negative emissions technologies from Minx et al. 2018 [58]. Notably, durable carbon storage in long-lived products is excluded from much of current consideration.

The costs and ultimate potential of NETs technologies vary greatly. **Table 1-2** describes recent estimates along with an assessment of the durability of carbon storage and technology readiness level (TRL, See Appendix C1). In the near-term, the bioeconomy enabled approaches are the most promising in terms of cost, scale, and TRL. Moreover, engineered approaches (BC, BECCS) offer the most durable storage among the bioeconomy approaches.

**Table 1-2** NETs estimated costs, current tech potential, and durability. Potential, costs, and durability adapted from [42], except for biochar which is adapted from [59]. TRL = Technology Readiness Level. Typically, TRL is reported on a scale of 1-9. To cover the range of technologies within categories, the author categorized NETs as High = commercial or nearly commercial, Medium = Demonstrated, and Low = Concept to pilot scale.

| **Technology** | **TRL** | **Potential ($GtCO_2e/yr$)** | **Cost ($/tCO2)** | **Durability** |
|---|---|---|---|---|
| Afforestation/Reforestation | High | 2.5-9 (Eventual saturation) | 15-50 | Short-term (< 100 years) or reversable |
| Soil carbon | High | 3 (Eventual saturation) | 0-50 | Short-term (< 100 years) or reversable |
| Biochar | High | 0.5-2.6 | 30-120 | Medium-term (100-1000 years) |
| BECCS (Power) | High | 3.5-5.2 | 70 | Long-term (Geologic time scales) |

| | | | | |
|---|---|---|---|---|
| BECCS (Fuels) | Medium to High | 10-15 | 37-132 | Long-term (Geologic time scales) |
| DAC | Medium to High | 0 (Limited by cost and renewable energy supply) | 90-600 | Long-term (Geologic time scales) |
| Enhanced weathering and ocean alkalinization | Low to High | Unknown | <10 - 500 | Long-term (Geologic time scales) |
| Long-lived biobased or $CO_2$ derived materials | Low to High | Research need. See Chapter 2.3 | Research need. See Chapter 2.3 | Research need. See Chapter 2.3 |

### 1.3.3 BiCRS vs BECCS

To date, the focus of biomass-enabled CDR research has been on bioenergy with carbon capture and sequestration (BECCS). BECCS combines the production of energy with the capture and geologic sequestration of biogenic $CO_2$ emissions. However, the cost and complexity of BECCS pathways relative to their alternatives limit viability in respective markets for liquid fuels and energy in the near-term [60]. BECCS is also constrained geographically in that geologic storage of carbon is not possible everywhere. Recently, attention has shifted further from a relatively narrow focus on BECCS to a broader focus on Biomass Carbon Removal and Storage (BiCRS) [44]. BiCRS is relatively new nomenclature intended to supplant the energy product focus of BECCS, to include a much broader set of approaches that utilize biomass to capture and store atmospheric $CO_2$. BiCRS is defined by its progenitors to include all approaches that "(a) use[ ] biomass to remove $CO_2$ from the atmosphere, (b) store[ ] that $CO_2$ underground or in long-lived products, [and] (c) do[ ] no damage to—and ideally promote[ ]—food security, rural livelihoods, biodiversity conservation and other important values" [44].

In recent years, global climate mitigation policy and corporate agendas have embraced the goal of achieving "net zero" emissions by 2050 [35], [61]. While this is a laudable and necessary near-term target, it is not a panacea, and it does not address the climate risks described in the preceding sections. The net zero framework emerges from a global normative target of limiting warming to well under $2^0$C which implies a remaining carbon budget of 400-800 $GtCO_2$ [61], [62]. The framework implies a combination of emissions reductions and supplementary carbon removals to "offset" residual emissions that are either economically or technically challenging to address. In practice, net zero policy mechanisms and corporate offset purchases have overwhelmingly favored carbon removals in the form of nature-based solutions (NbS) that remove carbon via maintenance and restoration of the transient terrestrial pool [63]–[66].

## 1.4 Contributions

This dissertation contributes to a reframing of the critical near-term role of the bioeconomy in climate mitigation. Building upon the rapidly evolving BiCRS discourse,

increasing attention towards bio-based materials, and targeted opportunities in hard-to-abate sectors, my research focuses on immediate opportunities to utilize known sustainable feedstock supplies and existing technologies and policy frameworks to deploy bioeconomy climate solutions. **Figure 1-5** is conceptual diagram of the bioeconomy's role in carbon drawdown.

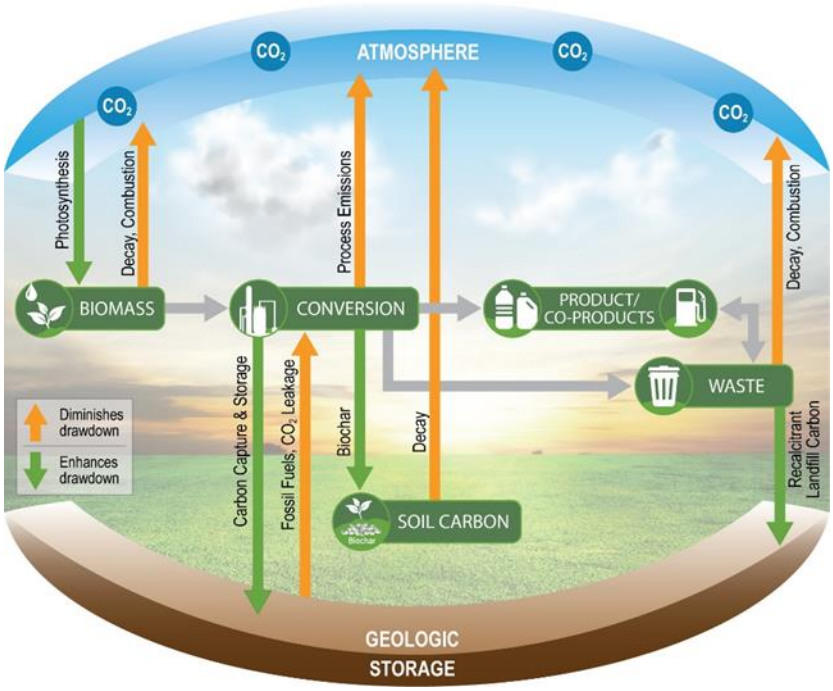


**Figure 1-5** Carbon flows associated with carbon drawdown from bioproducts. To enhance carbon drawdown, the flows represented by the green arrows need to increase in magnitude while minimizing the flows represented by the orange arrows. Credit:

My research is U.S.-focused, where I believe there is significant commercial opportunity for the bioeconomy and clear enabling policy leverage points to engage private market actors. This dissertation outlines three distinct goals as indicated by the subsequent chapter titles:

1. **Chapter 2. Beyond BECCS – The Bioeconomy for Climate Stabilization:** This chapter seeks to highlight a broader role for the bioeconomy by using biomass to store carbon in long-lived value-added products. I explore the opportunities for durable carbon storage in bio-based materials through literature review and analysis of carbon removal potential relative to BECCs. The chapter closes with an excerpt from a Viewpoint article that I authored on the unknown stability of fossil carbon in polymer materials and the role of that carbon in global carbon cycles.
2. **Chapter 3. Enhancing the climate benefits of the existing bioeconomy:** This chapter highlights opportunities to go after the "low-hanging fruit" in the existing ethanol industry by going to after process energy emissions via oxyfuel combustion, potentially enabling carbon-negative ethanol.

3. **Chapter 4. Targeting biomass at Hard-to-Abate sectors:** This chapter explores the essential role of the bioeconomy in addressing aviation emissions via the production of low-carbon and carbon negative sustainable aviation fuel (SAF). I analyze the technical readiness, cost, scalability, and emissions reduction potential of multiple sustainable aviation fuel technologies.

Each of these chapters addresses critical research needs in the rapidly evolving landscape of global decarbonization.

# CHAPTER 2. BEYOND BECCS: THE BIOECONOMY FOR CLIMATE STABILIZATION

## 2.1 Preface

This chapter seeks to highlight a broader role for the bioeconomy by using biomass to store carbon in long-lived value-added products. We explore the opportunities for durable carbon storage in bio-based materials through literature review and analysis of carbon removal potential relative to BECCs. The chapter closes with an excerpt from a Viewpoint article that I authored on the unknown stability of fossil carbon in polymer materials and the role of that carbon in global carbon cycles.

Stringent climate change mitigation scenarios rely on large-scale drawdown of carbon dioxide from the atmosphere. Amongst drawdown technologies, bioenergy with carbon capture and sequestration (BECCS) has received considerable attention in the climate mitigation literature. Recently, attention has shifted further from a relatively narrow focus on BECCS to a broader focus on Biomass Carbon Removal and Storage (BiCRS). The concept of BiCRS has the potential to enable a future where the climate mitigation value of biomass resources is more valuable than the energy value, due to the potential to remove and sequester large quantities atmospheric $CO_2$. This article provides a qualitative overview of prominent BiCRS technologies from which a set of the most promising technologies are assessed quantitively through life cycle assessment. There are numerous opportunities to incorporate carbon removal and management within the bioeconomy, but the majority of the near-term carbon removal potential exists in four bioproducts: bioenergy, bioplastics, biochar, and wood products. We analyze the life cycle greenhouse gas emissions and disposition of sequestered carbon over 10,000 years for four bioproducts representative of each broader category: an advanced BECCS pathway, biopolyethylene, oriented strand board, and biochar soil amendment. We find that the BECCS pathway has the greatest magnitude and durability of $CO_2$ storage over all time horizons. However, non-BECCS pathways achieve 34-64% of the drawdown magnitude relative to BECCS and retain 55-67% of their initial drawdown over 100 years (central estimate). We identify three engineering strategies for enhancing carbon drawdown: reducing biomass supply chain emissions, maximizing carbon stored in long-lived products, and extending the term of carbon storage. Finally, we highlight the need to characterize both the magnitude and permanence of carbon drawdown as a means for policymakers and technology developers to deploy limited biomass resources to maximize mitigation benefits.

## 2.2 Leveraging the Bioeconomy for Carbon Drawdown[1]

[1] Section 2.2 is under review at Green Chemistry, Manuscript ID: GC-CRV-07-2022-002483 under authorship Dees, J.P., Sagues, W.J., Woods, E., Goldstein, H.M., Simon, A.J., Sanchez, D.L. The main content of the paper in review has been placed in its entirety in the main body of the dissertation and
the supporting information has been placed in its entirety in the Appendix of the dissertation. This chapter may differ from the final published version.

### 2.2.1 Introduction

The bioeconomy is a complex set of economic activities that utilize renewable forms of biogenic carbon from agriculture, forestry, and aquaculture for their conversion into food, feed, fiber, polymers, bioenergy, and other bioproducts [67]. A central motive for the bioeconomy is the principle of circularity, which is applied at different steps of the value chain in order to retain the value of all resources in the economic cycle for as long as possible before these resources reach their end-of-life stage. One of the major benefits of adopting the principles of circularity is a reduction in greenhouse gas emissions, which mitigates the effects of climate change. Transitioning from the fossil resource-dependent linear economic model of "take-make-waste" to a circular bioeconomy will involve a coordinated effort from stakeholders across the value chain. As such, there is not just one singular bioeconomy, but many regional bioeconomies that vary technically, culturally, and politically.

Governments from many nations are formally embracing policies to enhance circularity, and their respective bioeconomies will play pivotal roles [68]. As primary stakeholders, governments play a key role both in agenda-setting and financial incentives and support for the bioeconomy. In the United States, the bioeconomy represents more than 22% of total economic activity, valued at more than $1 trillion, and employs ~28% of the workforce [69]. The US bioeconomy has evolved into a highly productive engine of economic activity providing essential products to societies around the globe; however, there are striking inefficiencies. Approximately 30 – 50% of mass in food and agricultural systems is lost between biomass cultivation and end product sale [69]. A significant portion of this waste is in the gaseous forms of carbon dioxide and methane, two of the leading greenhouse gases contributing to climate change, with the latter methane having a warming effect 27 to 83 times more powerful than carbon dioxide over 100 years and 20 years respectively [70]. Reducing inefficiencies through the principles of circularity and related practices, such as bioproduct cascading, will sequester carbon in useful products—thereby avoiding emissions and mitigating climate change. In addition to eliminating efficiencies, increasing the supply of affordable and sustainable biomass resources will increase the economic and environmental impacts of a particular bioeconomy.

In the US, the Department of Energy has estimated that ~1 billion dry tons of lignocellulosic biomass could be sustainably produced each year by 2040 [71]. Lignocellulosic biomass encompasses biomass material with lignin and cellulose within the cell wall, conferring woody characteristics, to include wood, grasses, agricultural residues, and similar materials. The intended application for a majority of the additional biomass resources has been toward avoiding fossil carbon emissions through the production and consumption of bioenergy products (e.g. biogas, biofuels, bio-hydrogen), which produce considerably less life cycle carbon emissions than fossil energy products. Notably, attention toward purely bioenergy products has shifted to bioenergy products with carbon capture and sequestration (BECCS) as the need for carbon-negative energy has become increasingly apparent [72]. BECCS technologies include biomass to power, heat, steam, hydrogen, or other gaseous or liquid fuels, combined with technologies that can capture carbon dioxide emitted by biochemical or thermochemical processes specific to the energy product conversion technology. Carbon capture and sequestration (CCS) technologies include capture via solvent adsorption, pressure swing adsorption, cryogenic, or membrane approaches, among others [73]. Process engineering, $CO_2$ concentration, energy requirements, and cost inform the selection

of CCS technologies, with dilute $CO_2$ streams, as are found in direct biomass combustion processes, requiring more technical intervention than high-purity streams such as are found in fermentation (e.g. fuel ethanol from corn). According to the IPCC, most emissions pathways that limit global warming to 1.5C – 2.0C require the removal and sequestration of 1 – 20 billion tonnes of atmospheric $CO_2$ per year by 2050 [72]. For reference, the global transportation sector emits ~10 billion tonnes of $CO_2$ per year.

Recently, attention has shifted further from a relatively narrow focus on BECCS to a broader focus on Biomass Carbon Removal and Storage (BiCRS) [44]. BiCRS is relatively new nomenclature intended to supplant the energy product focus of BECCS, to include a much broader set of approaches that utilize biomass to capture and store atmospheric $CO_2$. BiCRS is defined by its progenitors to include all approaches that "(a) use[ ] biomass to remove $CO_2$ from the atmosphere, (b) store[ ] that $CO_2$ underground or in long-lived products, [and] (c) do[ ] no damage to—and ideally promote[ ]—food security, rural livelihoods, biodiversity conservation and other important values"[44]. The concept of BiCRS has the potential to enable a future where the carbon content of biomass resources is more valuable than the energy content, due to the potential to remove and sequester large quantities atmospheric $CO_2$ [44]. In practice, BiCRS enables and expands the production of a variety of carbon-negative bioproducts including wood products (e.g. Oriented Strand Board / OSB), bioplastics (e.g. polyethylene), biocarbon (e.g. biochar), and purified biogenic $CO_2$ with geological sequestration, among others.

Such a future would require robust and reliable economic incentives for BiCRS, most likely through policy frameworks [44]. Stakeholders across the bioeconomy, including public and private sectors, must be engaged and involved in the process of crafting incentives that place a higher value on sequestered biocarbon [74], [75]. In the US, the bioeconomy is in the early stages of embracing the concept of BiCRS with the help of several policy tools, such as the low carbon fuel standard of California and the 45Q tax credit. However, a robust policy framework specific to BiCRS would significantly increase the bioeconomy's impact on mitigating climate change. The federal Renewable Fuel Standard is a good example of a policy framework that has a focused impact on the bioeconomy through rapid adoption and implementation of biofuels. A similar framework focused on BiCRS might catalyze rapid adoption and implementation of biomass-enabled carbon dioxide removal (CDR). Notably, to achieve the 1.5C target set forth by the IPCC, the implementation of carbon-negative technologies must not be limited to developed countries, likely requiring governments to be open to cross-cutting international agreements [76].

The number of carbon-negative technologies under development has expanded rapidly over the last 5 – 10 years to include a variety of disciplines such as genetic engineering, chemical engineering, and soil science, to name a few. Carbon-negative technologies have been refined into seven general classifications: bioenergy with carbon capture and storage (BECCS), afforestation and reforestation, direct air carbon capture and storage (DACCS), enhanced weathering, biochar, and soil carbon sequestration [58], [77]. Potential $CO_2$ removal capacities in the year 2050 were estimated to be 0.5–5$GtCO_2$ $yr^{-1}$ for BECCS, 0.5–3.6 $GtCO_2$ $yr^{-1}$ for afforestation and reforestation, 0.5–5 $GtCO_2$ $yr^{-1}$ for DACCS, 2–4 $GtCO_2$ $yr^{-1}$ for enhanced weathering, 0.5–2$GtCO_2$ $yr^{-1}$ for biochar, and up to 5$GtCO_2$ $yr^{-1}$ for soil carbon sequestration [58]. Cumulatively, these technologies combined could provide 9 – 24.6 $GtCO_2$ $yr^{-1}$, which would meet the aforementioned requirement set forth by the IPCC.

Estimated costs of leading carbon-negative technologies range from \$5 - \$300 per $tCO_2$, with BECCS costing \$100 - \$200 per $tCO_2$, afforestation and reforestation costing \$5 - \$50 $tCO_2$, DAC costing \$100 - \$300 per $tCO_2$ (for nth of a kind plant), enhanced weathering costing \$50 - \$200 per $tCO_2$, biochar costing \$90 - \$120 per $tCO_2$, and soil carbon sequestration costing \$0 - \$100 per $CO_2$ [77]. Notably, the aforementioned costs do not incorporate degree of carbon permanence or risk of reversal. Afforestation, reforestation, and soil carbon sequestration have the lowest cost, but also have the lowest permanence and highest risk of reversing carbon storage through re-emission to the atmosphere. The life cycle carbon intensity of emerging carbon negative technologies must be thoroughly and responsibility assessed on cradle-to-grave bases to avoid the promotion of unrealistic carbon removal benefits [78].

Overall, costs of strictly capturing and sequestering atmospheric $CO_2$ are not justified with existing policy frameworks [73]. Opportunities for $CO_2$ capture, utilization, and sequestration appear to be more economically feasible in the near-term [79]. However, the carbon permanence of technologies aimed at strictly removing $CO_2$ from the atmosphere, particularly geologic storage of $CO_2$, are overall greater than for technologies that incorporate $CO_2$ utilization [80]. Soil carbon sequestration is one particular approach that has uncertain carbon permanence based on many factors, thereby requiring significant advancements in carbon monitoring and LCA methodologies to reduce risk and improve carbon permanence reliability [81]. BECCS relying on dedicated energy crops with geologic storage of $CO_2$ has high permanence, but has significant implications regarding land use change, thereby warranting caution to avoid food displacement and biodiversity loss [82].

Although widespread commercial deployment of BiCRS technologies has not yet been achieved in the US or abroad, there has been significant advancement in the research, development, and demonstration of BiCRS technologies. This article provides a qualitative overview of the leading BiCRS technologies from which a set of the most promising technologies are assessed quantitively through life cycle assessment.

### 2.2.2 Carbon negative bioproducts

The bioeconomy is essentially a facilitator and promoter of organized biological $CO_2$ fixation into a wide range of different end products with varying degrees of permanence. There are numerous opportunities to incorporate carbon removal and management within the bioeconomy, but the majority of the near-term carbon removal potential exists in four bioproducts: bioenergy, bioplastics, biochar, and wood products. Herein, we explain the various mechanisms by which carbon removal can be incorporated into each of these four bioproducts (see conceptual diagram in **Figure 2-1**). We also provide a qualitative assessment of two emerging bioproducts for carbon removal, namely steel and concrete, that have significant potential for carbon removal of the long-term.

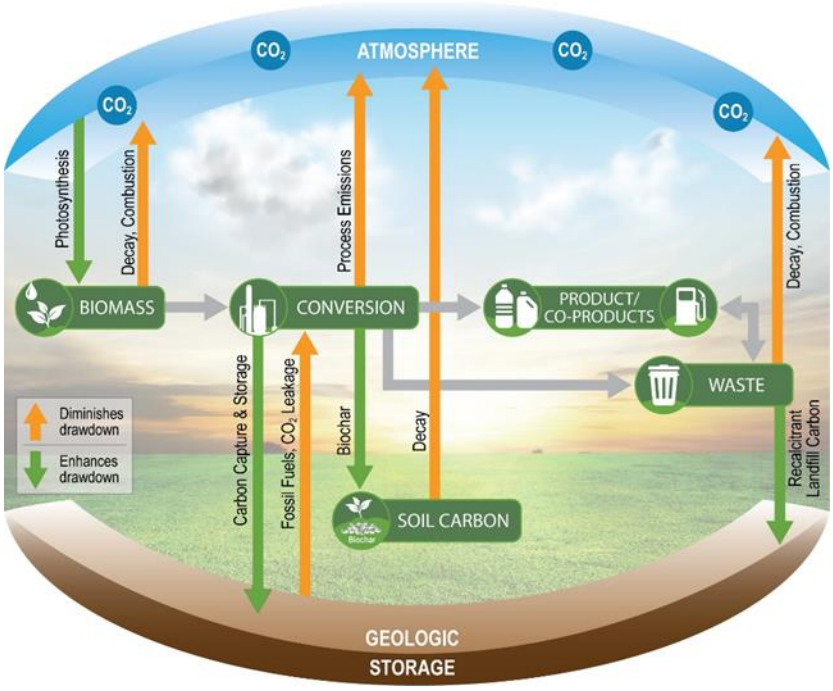


**Figure 2-1** Carbon flows associated with carbon drawdown from bioproducts. To enhance carbon drawdown, the flows represented by the green arrows need to increase in magnitude while minimizing the flows represented by the orange arrows. Credit:

#### 2.2.2.1 Bioenergy

Many different bioenergy technologies exist and span a wide range of technology readiness levels (TRLs), but they can generally be classified as either thermochemical or biochemical. Biochemical technologies use microorganisms and/or enzymes to convert the biomass resource into a bioenergy product, whereas thermochemical technologies rely on heat and catalysts. There are four primary, high TRL thermochemical pathways for bioenergy products with carbon removal, as shown in **Figure 2-2**.

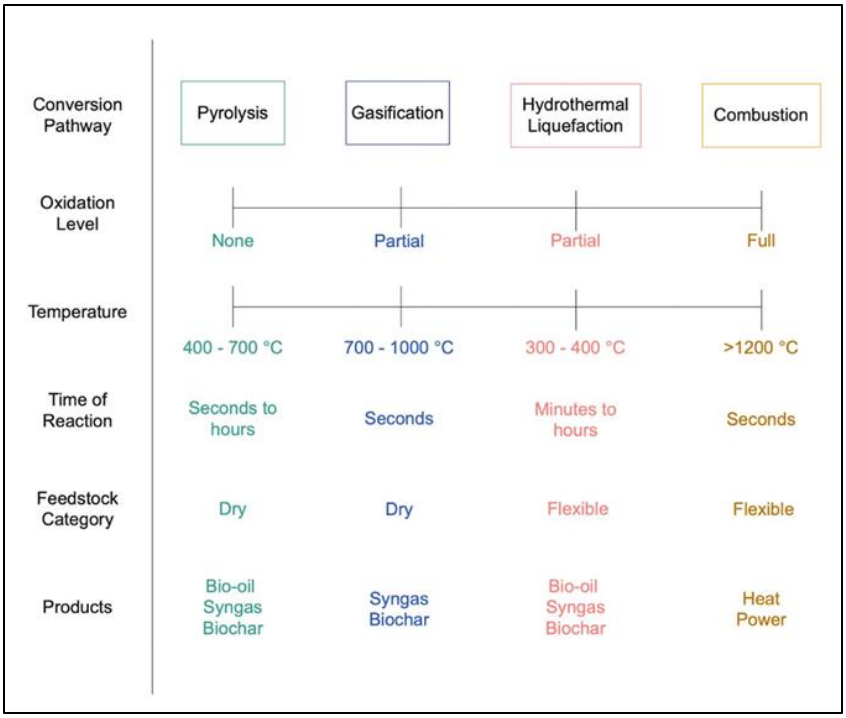


**Figure 2-2** Thermochemical bioenergy pathways

Pyrolysis entails the thermal treatment of biomass in an oxygen-free environment, wherein biocarbon is transformed into bio-oil, pyrogas, and biochar. Gasification entails the thermal treatment of biomass in an oxygen-lean environment, wherein biocarbon is partially oxidized into syngas (CO, $CO_2$, and $H_2$). Combustion entails the thermal treatment of biomass in an oxygen-rich environment, wherein biocarbon is fully oxidized into $CO_2$. Hydrothermal liquefaction is a thermochemical biomass conversion process in which feedstocks with high moisture content are converted to bio-oil, syngas, and biochar. The process entails the degradation of biomolecular compounds in the feedstock by high pressure water in a medium temperature setting to form bio-oil which can then be upgraded into hydrocarbons vis hydrotreating [83], [84]. Complex thermochemical biomass conversion processes for carbon removal including gasification [85]–[87] and combustion [20] typically require large scales of operation to be economically viable, thereby limiting opportunities to areas with high densities of low-cost biomass feedstocks. Hydrothermal liquefaction (HTL) [84] and pyrolysis [85], [88] have the potential to be economically viable at smaller scales due to the relatively mild process requirements. However, should they be necessary, operations for upgrading of biocrude and bio-oil from HTL and pyrolysis typically require economies of scale [89]. Fortunately, thermochemical biomass conversion technologies are amenable to processing multiple different biomass feedstocks, whereas biochemical approaches typically require one feedstock.

Pyrolysis and gasification both have potential for relatively low-cost carbon removal due to the generation of biochar in the former case and high purity $H_2$, fuels, and $CO_2$, in latter case. Specifically, the biochar generated via pyrolysis can be land applied for soil carbon sequestration and the concentrated $CO_2$ generated via gasification and gas clean up can be sequestered

geologically with $H_2$ and catalytically-produced fuels providing additional revenues. It is important to note that only gasification to $H_2$ and power can achieve 100% carbon removal. When gasification yields liquid fuels (GtL), a significant portion of the carbon is carried by the liquid fuel which may be impractical to capture at the point of combustion (e.g. tailpipe). The bio-oil generated via pyrolysis has traditionally been viewed as a potential fuel precursor, but more recent work has illuminated its potential to store carbon via geological sequestration.[90] The efficacy of bio-oil geological sequestration is still uncertain and requires continued research [90]. Incorporating carbon removal in the combustion of biomass for electrical power, traditionally referred to as bioenergy with carbon capture and sequestration (BECCS), requires costly $CO_2$ capture technologies, such monoethanolamine (MEA) scrubbing and stripping or oxycombustion. In general, BECCS for biopower is not viewed as an ideal pathway for biomass carbon removal and storage (BiCRS) due to the significant land requirement and high costs relative to alternative, low-carbon power generation technologies (solar, wind, geothermal, nuclear, etc) [44], [91]. Nonetheless, there exists the potential to sequester 737 million metric tons of $CO_2$ per year at costs of $42 - $92 per metric ton by 2040 with widespread implementation of BECCS for biopower across the United States [92]. Relative to combustion, gasification-enabled BECCS for biopower has advantages, although most experts believe hydrogen, not electrical power, will be the most economically competitive bioenergy product from gasification [93], [94]. The decreasing costs of carbon-free electricity (e.g. solar and wind power) coupled with the need to remove carbon from the atmosphere and decarbonize hydrogen production have made biomass gasification highly advantageous [95]–[97].

Regional biomass availability, climate, water availability, and land type, process conditions, and scale of operation all play critical factors in determining the techno-economic feasibility a particular BECCS technology [98], [99]. Coupling thermochemical BECCS with other carbon removal technologies, including DACCS and soil carbon sequestration, has the potential to offer benefits such as locational flexibility and enhanced carbon removal per unit area [100]. Leveraging existing thermochemical bioenergy facilities for carbon removal also has the potential to enhance carbon removal and reduce costs. For example, US pulp mills emit ~115 million tonnes of biogenic $CO_2$ per year that are available for carbon removal without the new capital and extensive land use that is required of greenfield BECCS plants [101]. Thus, near-term efforts for carbon removal via thermochemical energy processes could focus on the existing pulp and paper industry.

Relative to thermochemical pathways, biochemical pathways for bioenergy offer several advantages, including the ability to operate under mild conditions, generate relatively pure products, and produce gaseous waste streams of high $CO_2$ concentration. However, the volumetric productivity (g/L/h) of biochemical pathways may be one to two orders of magnitude lower than those of thermochemical pathways and thus require large reactors to achieve the same level of production [102], [103]. Thus carbon removal will generally be an auxiliary benefit to biochemical conversion for energy and materials. There are two primary, high TRL biochemical pathways for bioenergy products with carbon removal, as shown in **Figure 2-3**.

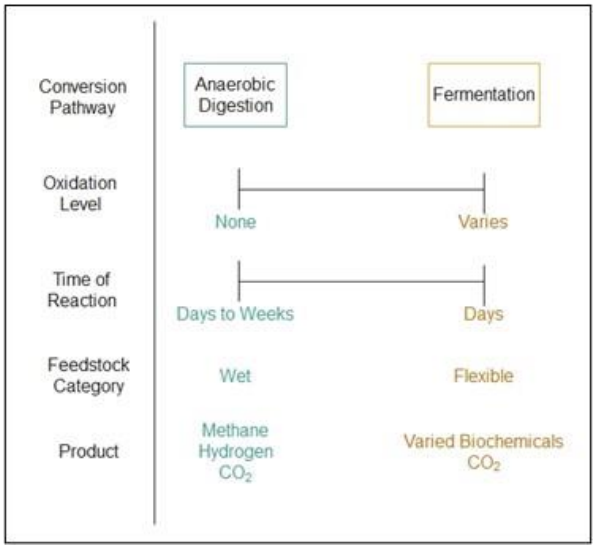


**Figure 2-3** Two primary biochemical energy pathways

Fermentation, in the context of this review article, entails the conversion of biomass to biofuels via pure culture fermentation under aerobic or anaerobic environments. Anaerobic digestion, in the context of this review article, entails the conversion of biomass to biofuels via mixed culture fermentation under anaerobic environments. In the US, existing industrial operations for the fermentation of corn starch to ethanol and anaerobic digestion of biowaste to biogas have the potential to remove ~45Mt-$CO_2$ and ~110Mt-$CO_2$, respectively [104]–[107]. For comparison, in Brazil, existing industrial operations for the fermentation of sugarcane to ethanol have the potential to remove ~28Mt-$CO_2$ per year [108]. Thus, near-term efforts for carbon removal via biochemical energy processes could focus on the existing ethanol and biogas industries. The $CO_2$ concentrations in waste streams associated with ethanol fermentation and anaerobic digestion are relatively high, thereby justifying their consideration for carbon removal since the costs of $CO_2$ capture and sequestration are highly dependent on incoming $CO_2$ concentration [109]. In the US, 60% of $CO_2$ from ethanol refineries could be captured and compressed for less than $25 per tonne, which is considerably less than costs for traditional BECCS [104]. Ethanol fuel prices would increase by ~3.5% with incorporation of $CO_2$ capture and sequestration, which is not significant. Notably, the $CO_2$ off gassed during ethanol fermentation requires minimal separation, allowing for such low costs of removal. Historically, $CO_2$ from ethanol fermentation has been used for carbonating beverages and other food applications, but there is significant potential for geological sequestration [110]. Archer Daniels Midland (ADM) successfully captured, compressed, and injected over 1 million metric tons of fermentation-derived $CO_2$ into the Mt. Simon Sandstone geological formation in Decatur, Illinois, thereby demonstrating the ethanol industry's ability to rapidly and successfully scale carbon capture & sequestration [111]. In addition, techno-economic assessments have shown the potential for microalgae growth and cultivation using $CO_2$-derived from ethanol fermentation [112]. The $CO_2$ concentration and availability from biogas operations is a bit less clear given the diversity of sources (landfills, agricultural digesters, and wastewater treatment plants) and biogas end-uses (venting, flaring, and combustion).

Although there is significant potential to utilize and sequester existing biogenic $CO_2$ from industrial operations in the US, the need for new biorefining pathways for enhanced carbon removal are required. Several recent studies have shown the immense potential for carbon removal via soil carbon sequestration coupled with fermentation of lignocellulosic biomass into ethanol [113], [114]. Specifically, the cultivation of switchgrass for biofuel production coupled with $CO_2$ capture and sequestration has climate mitigation potential 4 and 15 times larger than forest and grassland restoration, respectively [113]. Second generation bioenergy crops have significant potential to address climate change when the $CO_2$ emitted during the biorefining process is captured and sequestered, ultimately achieving carbon-negative biofuels (< -22 $gCO_2$ per MJ) [113], [114]. Decentralized biorefineries have been proposed as a means of utilizing disperse, low-density biomass feedstocks, but the relatively small scales of operation pose a challenge due to the lack of economies of scale. Conversely, large, centralized biorefineries are challenged by high feedstock costs. Techno-economic modeling indicates that carbon-negative biorefineries should aim for biomass supply rates of ~2000 metric tons per day [114]. Unlike ethanol fermentation, the $CO_2$ from anaerobic digestion of biogas requires purification prior to compression and sequestration. Traditionally, biogas is utilized in one of two ways: direct combustion or upgrading followed by combustion. Anaerobic digestion produces both hydrogen and methane. Both are valuable energy products, but the methane portion is preferred for electricity generation. Biogas destined to be pipeline-ready biomethane, or renewable natural gas (RNG), must undergo an upgrading process wherein $CO_2$ and $H_2S$ are removed via a separation process [115]. Pressure swing adsorption, chemical absorption, water scrubbing, and membrane separation are the leading technologies used for biogas upgrading, with water scrubbing being most common method due to its low cost and high efficiency [116], [117]. However, water scrubbing is not the best choice for high purity $CO_2$ production. New swing adsorption technologies provide flexible load operations, high energy efficiency, and low capital costs, relative to baseline systems [118]. However, sulfur containing species reduce efficacy and increase cost. Biological treatments are emerging as a low-cost method for removing H2S before the aforementioned non-biological upgrading methods. In particular, chemo- and photo-trophic methods of biofiltering, biotrickling, and bioscrubbing show promise for sulfur contaminate removal [119]. Moving forward, continued advancements are needed in the modularization of biogas upgrading systems to enable low-cost $CO_2$ capture from small AD systems [118]. Small scale biogas upgrading systems could enable the purification and sequestration of regionally diffuse biogas sources from readily available organic wastes [120]. Methane leakage from anaerobic digestion systems is a great concern due to the high global warming impact of methane, relative to $CO_2$, and therefore must be tightly regulated as biomethane production increases in a growing bioeconomy. Dark fermentation is an emerging method of anaerobic digestion wherein $CO_2$ and $H_2$ are the primary products, thereby eliminating the risk of methane leaks [121]. For both biochemical and thermochemical pathways, initial deployment efforts should focus on sustainable feedstocks from marginal agricultural lands or existing waste materials to minimize transport costs and avoid indirect land use change [122]. In addition, near-term siting of biorefineries should prioritize regions with suitable geology for permanent $CO_2$ sequestration, such as the Illinois basin, Gulf region, and western North Dakota in the United States [123].

#### 2.2.2.2 Bioplastics

Polymers and plastic materials are ubiquitous in modern life and store significant quantities of carbon for extended periods of time, albeit the majority of such carbon is derived from fossil resources. Specifically, over 380 million metric tonnes of plastic are currently produced globally each year, storing over 285 million tonnes of carbon with an emissions potential of over 1 billion tonnes of CO2 (assuming plastics are 75 wt% carbon on average) [124], [125]. The production of plastics is expected to reach over 1 billion metric tonnes by 2050 each year, storing over 750 million tonnes of carbon with an emissions potential of over 2.75 billion tonnes of $CO_2$ [124]. Traditionally, there have been four end-of-life applications for plastics: landfilling, incineration, recycling, and littering. Less than 10% of plastics are recycled, leaving the majority of the plastic-carbon either being landfilled, incinerated, and littered [126]–[128]. Over the past several decades, a variety of bioplastics have risen to industrial relevance to help reduce the use of fossil carbon resources and associated emissions during refining and at end-of-life. As shown in **Table 2-1**, a significant fraction of the leading bioplastics are biodegradable, meaning the carbon is biologically released/decomposed as $CO_2$ or CH4 in natural or controlled environments, with the remainder being relatively inert [129], [130].

**Table 2-1** Relative market share of bioplastics. Adapted from European Bioplastics[123] PE = polyethylene, PA = polyamide, PTT = polytrimethylene terephthalate, PET = polyethylene terephthalate, PP = polypropylene, PEF = polyethylene furanoate, PBAT = polybutylene adipate terephthalate, PLA = polylactic acid, PBS = polybutylene succinate, PHA = polyhydroxyalkanoates

| Bio-based/Non-biodegradable | % of Total | Biodegradable | % of Total |
|---|---|---|---|
| PE | 9.5 | PBAT | 19.2 |
| PA | 9.1 | PLA | 18.9 |
| PTT | 8.1 | Starch Blends | 16.4 |
| PET | 6.2 | PBS | 3.5 |
| PP | 1.9 | Cellulose Films | 3.2 |
| Other | 1.0 | PHA | 1.8 |
| PEF | 0.0 | Other | 1.2 |

Currently, bioplastics make up less than 1% of the global plastics market, however that is expected to increase significantly if the plastics industry is to achieve net-zero emissions by 2050 [129]. Bioplastics face similar limits to scale as other bioproducts in that feedstocks often compete with land for food production and will also compete directly with other uses of biomass

[131]. Moreover, fossil polymer production systems are highly optimized and generally low-cost making many biopolymer options uncompetitive with current technology and infrastructure. Still, industrial systems models have been utilized to highlight the potential of removing over 1 billion tonnes of $CO_2$ per year via bioplastic production in the year 2050, thereby justifying increased research and development into the development of carbon-negative bioplastics [124]. Based on recent trends, the global bioplastics industry is expected to grow by 216% between 2021 and 2026, thereby providing strong evidence that bioplastics will likely be at a significant scale by mid-century [130].

There are two main pathways for bioplastic-enabled carbon removal: 1) capture and sequestration of gaseous carbon at end-of-life decomposition or 2) long term carbon storage in the product itself. Option 1 is the only viable pathway for carbon removal with biodegradable and compostable bioplastics, whereas both options are viable for carbon removal with inert bioplastics. In 2021, the five most popular bioplastics represent 73% of production and include PBAT, PLA, starch blends, PE, and PA, of which PE and PA are the only non-biodegradable, inert bioplastics (**Table 2-1**) [130]. Traditionally, biodegradable bioplastics have been preferred over inert due to concerns over pollution and accumulation in the environment and associated effects on marine and terrestrial ecosystems. However, inert bioplastics are more amenable to carbon removal and thus climate change mitigation. Currently, bioplastic production does not prioritize carbon removal, with the majority of biocarbon entering the atmosphere as methane or $CO_2$ at end-of-life via degradation in landfills, compost, and energy recovery. Composting of bioplastic has gained significant attention due to its production of value-added soil amendment, but the majority of carbon in the bioplastic is lost as $CO_2$ via respiration [132]. Notably, cradle-to-grave LCAs have shown that the carbon intensities of certain bioplastics with end-of-life composting are higher than their petroleum-derived counterparts, particularly for bioplastics made from land-intensive feedstocks such as corn starch [133]. The carbon intensities associated with bioplastics can be decreased with high solids compositing techniques that limit microbial respiration, and should be investigated further [134]. Negative carbon intensities were shown to be possible with the production of PLA from waste biomass feedstocks and landfilling at end-of-life, although the permanence of the sequestered carbon was unclear [135].

PE has an increased potential for carbon removal relative to other bioplastics for a variety of reasons, including its composition that is resistant to microbial degradation, the opportunity for $CO_2$ capture during its manufacturing process, and the existing fossil-PE market of which it can serve as a drop-in replacement. Specifically, the lack of oxygen in PE makes it highly inert and an ideal material for carbon sequestration. The manufacturing of bio-based PE requires upstream ethanol fermentation, thereby offering an opportunity for low-cost $CO_2$ capture from the fermentation vessels. Finally, PE is the most popular plastic in the world, representing 31% of global demand, thereby offering an opportunity for carbon removal at significant scale. Specifically, over 100 million tonnes of primary PE are produced each year, equivalent to 86 million tonnes of carbon. Thus, the current PE market demand has the theoretical potential to remove 315 million tonnes of $CO_2$ if all carbon is derived from biomass [136]. Moreover, the intermediate chemical ethylene, which is also made from ethanol and used in a variety of different polymers, has a global demand of 200 million tonnes per year, equivalent to 630 million tonnes of $CO_2$ if all carbon is derived from biomass [137], [138].

The majority of bioplastics currently on the market are indirectly derived from $CO_2$ in the form of biomass feedstocks rich in carbohydrates or lipids, such as sugarcane, corn starch, and soybean oil, or cellulose, such as pine and poplar. Recently, there has been significant interest in producing plastics directly from $CO_2$ using novel biological or chemical routes, which reduces the use of land-intensive biomass feedstocks. A particularly promising route for producing PE in a sustainable fashion with minimal impact on land use and food crops is via fermentation of $CO_2$ and $H_2$ into ethanol with subsequent conversion to PE. Advancements in genome engineering of acetogens with tools such as CRISPR-Cas9 have enabled cost competitive fermentation of $CO_2$ into ethanol, thereby warranting serious attention from decision makers interested in decarbonization [139]. Unlike PE, which can be synthesized using a variety of biological substrates other than $CO_2$, several bioplastics require $CO_2$ for synthesis. **Figure 2-4** illustrates representative direct and indirect polymer production from $CO_2$.

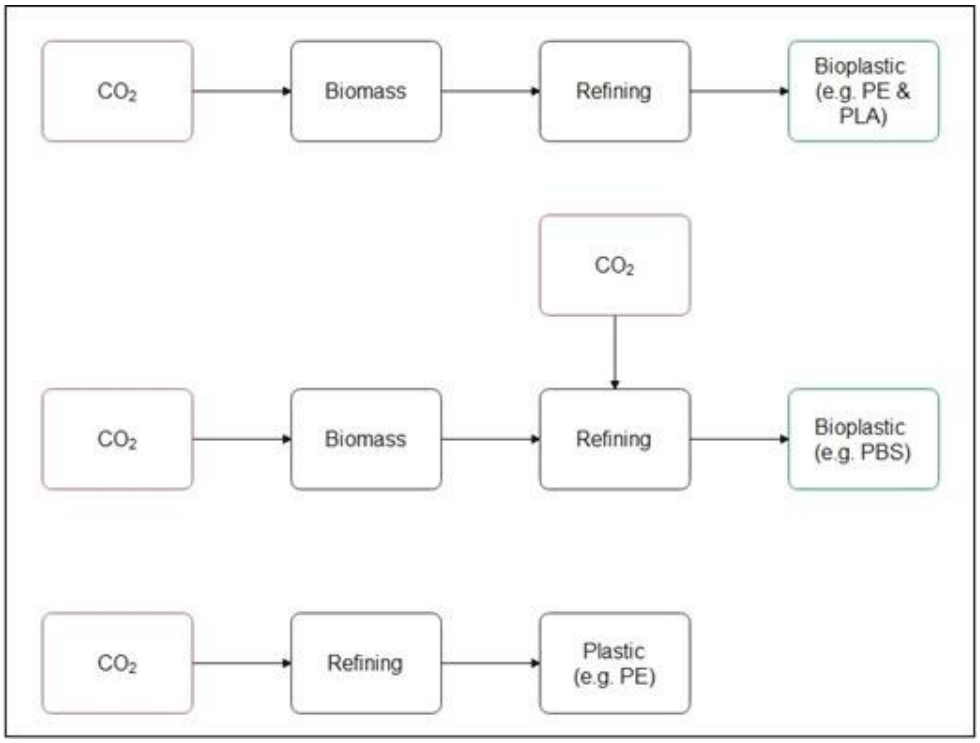


**Figure 2-4** Indirect and direct utilization of CO2 for polymer production. PE = polyethylene, PLA = polylactic acid, PBS = polybutylene succinate.

For example, the primary metabolic pathways used by industrial microbes for producing succinic acid, the intermediate biochemical to polybutylene succinate (PBS), require $CO_2$. PBS is on track to the best the 2$^{nd}$ highest demand bioplastic by 2026, meaning that significant quantities of $CO_2$ will be required for synthesis [130]. Notably, PBS synthesis typically involves co-fermentation of carbohydrates with $CO_2$, thereby still requiring biomass feedstocks. A recent cradle-to-grave LCA study demonstrated the potential carbon-negative PBS production when using wheat straw and miscanthus as biomass feedstocks for fermentation and land management practices that promote soil carbon sequestration [140]. Another LCA study assessed a multitude of the most common bioplastics and determined that PBS and PE had the lowest carbon intensities [141].

Similar to PBS, biomass-derived polycarbonates require $CO_2$ as a reagent in synthesis. Polylimonene carbonate is particularly intriguing since it requires the catalytic reaction of biomass-derived limonene with $CO_2$ gas and can serve as a direct replacement to fossil-derived poly(propylene carbonate) [142]. Carbon-negative polylimonene carbonate production has been demonstrated to be possible with direct mineralization of $CO_2$ gas and use of waste biomass for energy generation in the process [143]. Notably, the chemistry of poly(limonene carbonate) can be modified quite easily, thereby presenting an opportunity to use this $CO_2$-derived material as a platform polymer in the production of many functional materials. Currently, the TRL of bio-based poly(limone carbonate) is still relatively low, and thus there is a need for continued innovation and large-scale demonstration. As the technology matures, LCA modeling will be needed to quantify and compare its carbon intensity with other, higher TRL, bioplastics such as polyethylene and polylactic acid [144]–[146]. Finally, polyhydroxyalkonates (PHAs) are an emerging class of bioplastic with tunable properties that might make them more amenable to carbon sequestration. Microbes directly synthesize the PHAs from various carbon substrates, including biomass-derived compounds and air-derived $CO_2$, and genome engineering holds the potential to enable tailored bioplastics [147], [148].

Moving forward, research on carbon-negative bioplastics must involve thorough and reliable LCA methodologies to ensure reported carbon intensities are realistic. Inconsistencies in LCA methodologies have been identified in the accounting of biogenic carbon in the bioplastic materials. End-of-life distinction between biogenic and fossil carbon in the bioplastic must be made to enable accurate cradle-to-grave CI values, particularly when recycling is involved [141]. In addition, dynamic accounting of biogenic carbon indicates that rapid biomass growth and harvest cycles are required to ensure beneficial climate impacts; thus, the traditional assumption of carbon neutrality without time consideration may no longer be defensible. However, dynamic accounting is less important if biomass waste materials or sustainable, highly productive crops with short rotations are used. Overall, LCA modelers must be transparent and consistent in the methods used to account for biogenic carbon when quantifying the carbon intensity of a particular bioplastic [141].

#### 2.2.2.3 Biochar

Biochar is a carbon-rich, highly porous, and solid material produced from pyrolysis where biomass is thermally treated at 400 – 700C in the absence of oxygen. Biochar products have been developed for a multitude of different applications, including adsorbents, catalyst supports, soil amendments, electrodes, carbon fibers, and many more (see **Figure 2-5**). Importantly, biochar is highly inert and thus offers an opportunity for carbon sequestration [149]. Activated biochar products, often referred to as activated carbon, undergo physical or chemical activation after pyrolysis to enhance physiochemical properties, such as specific surface area and functionality [150]. Activated biochar products primarily include adsorbents, catalyst supports, and electrodes and are used for many applications, including environmental remediation, heterogenous catalysis, $CO_2$ capture, and energy storage, to name a few [150].

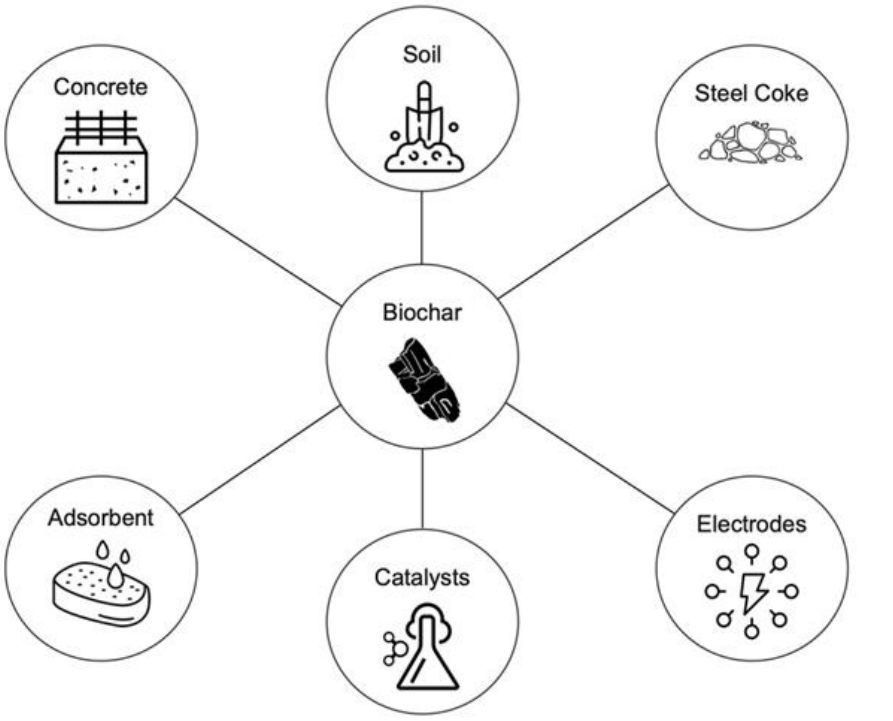


**Figure 2-5** Biochar product applications

Regarding $CO_2$ capture, biochar is a unique material that has the potential to capture and store atmospheric carbon in two different ways: 1) in the structural make-up of the char via carbonized biomass and 2) on the surface of the char via $CO_2$ gas adsorption. Biochar composition and textural properties can vary widely and are critical predictors of performance as an adsorbent [151]. Activation of biochar via chemical treatment, including amine functionalization, can provide high-performing $CO_2$ adsorption/desorption materials (~5 mmol per gram at 1 bar and 25C). However, there is a significant lack of data demonstrating durability and recyclability of activated biochar for CO2 adsorption at large scale and with representative flue gas streams [152], [153]. Activated biochar is also highly effective as adsorbing other compounds of interest, particularly inorganic nitrogen and phosphorous from wastewater and agricultural runoff. Notably, the mechanisms involved in N and P adsorption to biochar differ, with N involving ion exchange and electrostatic adsorption and P involving surface deposition and precipitation with metallic compounds. In addition, fluctuations in pH have the potential to significantly affect N & P adsorption. Thus, activated biochars for nutrient removal from wastewater often require custom design for optimal performance, which increases cost [154]. Biochar has been shown to be a beneficial additive to anaerobic digestion processes through increased biogas productivity. Specifically, biochar provides micropore habitats for robust growth, buffer capacity for stable operation, and electrical conductivity for enhanced electron transfer [155]. Electrodes for energy storage are an emerging class of biochar products that have the potential for large scale carbon sequestration. Electric vehicles and modular stationary energy storage systems have created a fierce demand for lithium-ion batteries, which is in turn causing a dramatic increase in demand for graphite anode materials [156], [157]. Recently, several new methods of catalytic pyrolysis

have been developed to convert biomass into battery-grade biographite [158]–[164]. Other ion batteries, such as sodium and potassium, typically also require carbon anodes, thereby providing another market for biochar electrodes. In addition, energy storage devices based on capacitance, such as supercapacitors, are typically comprised of activated carbon. The energy storage industry is growing rapidly, and more attention is warranted towards using biomass precursors to develop carbon-negative energy storage devices. Carbon fibers are used in high performance, high strength, lightweight materials for structural supports in applications including transportation, athletics, and buildings. The incumbent carbon precursor used in carbon fibers is polyacrylonitrile, which is expensive and derived from fossil carbon precursors. There is growing interest in using biocarbon precursors such as lignin and bio-based PAN for carbon fiber synthesis [165], [166]. The multi-stage process of carbon fiber synthesis involves pyrolysis around 1000C, thereby classifying biocarbon fibers as a form of biochar product. Lignin carbon fibers have been under development for several decades, but have yet to reach commercial adoption due primarily to high costs and poor performance [167]. Moving forward, lignin carbon fiber products should be tailored for applications that require relatively low strength and performance properties. A recent innovation has enabled the production of PAN from biocarbon precursors, thereby offering an opportunity to produce a drop-in PAN carbon fiber material derived from sustainable biomass [168]. The process of producing bio-based PAN carbon fibers is energy-intensive, and thus thorough life cycle assessment is still required to understand the potential for carbon sequestration [167], [169].

All of the aforementioned biochar products and applications have the potential to create value and sequester atmospheric carbon, but not at any appreciable scale ($< 0.5\ GtCO_2\ yr{-}1$) [150]. However, there is significant potential in carbon sequestration via application of biochar to soils ($0.5–2GtCO_2\ yr{-}1$) [58]. In addition to carbon sequestration, biochar offers of a multitude of benefits to soil health including increased biological activity and organic carbon accumulation, reduced runoff, increased crop productivity, and reduced nutrient leaching [170]. Also, recent evidence shows the ability of biochar to reduce $N_2O$ emissions from soils, which is important given the strong global warming impact of $N_2O$.

**Table 2-2** Advantages and drawbacks to biochar in soil applications

| Pros | Cons |
|---|---|
| Reduction in runoff | Potential leaching of heavy metals and polycyclic aromatics |
| Decrease in soil organic carbon priming | Efficacy dependent on many variables |
| Potential for high carbon permanence | Relatively expensive |
| Reduction in $N_2O$ emisions | Lack of robust LCA data |
| Increase in crop yields when applied at appropriate dosages | Decrease in crop yields when applied at excessive dosages |

Specifically, a meta-analysis showed that biochar application leads to an average reduction of ~50% in soil $N_2O$ emissions across laboratory and field trials, particularly in sandy soils. Notably, reductions in $N_2O$ emissions have been found to diminish with time, and thus further research is needed to better understand this dynamic [171]. Although $N_2O$ emissions reductions are highly beneficial, the majority of long-term benefits from biochar application to soils are in the form of carbon sequestration. The extent of carbon storage durability for particular combinations of biochars and soil types is a major research gap that requires continued investigation. Nonetheless, there has been significant progress in understanding biochar durability in soils over the last 5-10 years. Through meta-analysis, the rate of biochar decomposition was found to vary significantly with experimental duration, feedstock, pyrolysis temperature, and clay content [172]. On average, over 95% of biochar mass results in long-term carbon sequestration of greater than 500 years. Biochar application has a substantial effect on soil microbial activity, particularly for sandy soils where the mineralization of soil organic matter has been shown to increase by 20% with application of biochar. Also, crop-derived biochar, fast pyrolysis, low pyrolysis temperature, and small application amounts all had negative soil priming effects, meaning the SOM degradation rates of the soils are reduced upon application [172]. Upon initial application of biochar there is a relatively rapid increase in $CO_2$ emissions from the labile carbon followed by a reduction in priming [173]. Overall, the stability of carbon in biochar is proportional to the temperature used during pyrolysis. Regardless of feedstock, temperatures in the range of 500 – 700C were found to be optimal for carbon stability [174]. Highly stable biochars are achievable at lower temperatures with other process modifications, including extended reaction times, pressurized reactors, and feedstocks with high initial lignin contents.

Typically, highly stable biochars are produced in relatively low yields [174]. The optimal composition of biochar for soil carbon sequestration was found to have an $O/C_{org}$ ratio < 0.2 and

$H/C_{org}$ ratio < 0.4 [173]. Notably, particular biomass feedstocks and pyrolysis conditions, excessive application of biochar, as well as other variables can decrease soil health, thereby warranting more research into elucidating these complexities [172]. Specifically, potential negative impacts of biochar application to soils include suppression of soil nutrient availability and crop productivity, reduction in carbon mineralization, and accumulation of polycyclic aromatic hydrocarbons (PAHs), polychlorinated dibenzodioxins, and dibenzofurans (PCDD/DF) [175]. Excessive application of biochar, exceeding 72 tonnes per hectare, has been found to decrease maize and wheat grain yields by 46 and 70%, respectively. The reduced crop productivity was due to immobilization of nutrients, most notably nitrogen [175]. Fast pyrolysis biochar was found to immobilize substantially more nitrogen than biochar made via slow pyrolysis. Pyrolysis reactors that do not sufficiently separate tars and vapors produce biochar products saturated in polycyclic aromatic hydrocarbons, which have the potential to negatively affect soil and human health. Thus, standards for allowable PAH concentrations in biochar products must be established to ensure producers are using the appropriate pyrolysis technologies and avoiding the risk of PAH contamination [175]. A thorough risk assessment of biochar application to soils for carbon sequestration determined the majority of risk is not present in the feedstock variability, supply chain logistics, or pyrolysis process scale-up, but rather in the ability to predict and monitor the carbon sequestered in soils.

In summary, permanence of biochar carbon in soils is highly variable and new tools must be developed to cost-effectively monitor and verify soil carbon sequestration. Precision agriculture tools that rely on robotics and remote sensing have the potential to address the issue of permanence in soil carbon sequestration [176]. In addition, LCAs of biochar for soil carbon sequestration must prioritize multiple impact categories. Global warming potential is often the impact category of sole interest. A recent review indicates a small but growing body of research that includes other impact categories of import such as abiotic depletion, eco-toxicity, and human toxicity, among others [177]. Given the diversity of biochar feedstocks and processes, it is essential that these important categories be included alongside climate impacts when assessing the impacts of soil amendments. Positive benefits of biochar application to soils, including moisture retention and reduced irrigation, are captured in abiotic depletion. Conversely, the negative impacts of incorporating polyaromatic hydrocarbons (PAHs) into soils will be captured in eco-toxicity and human toxicity [178].

#### 2.2.2.4 Wood products

The wood products industry removes significant quantities of atmospheric carbon in the form of long-lived products each year. A summary of products is shown in **Figure 2-6**. In the US, over 100 million tonnes of $CO_2$ are removed and incorporated into wood products each year [179]. Thorough assessments have demonstrated that wood products emit considerably less greenhouse gases over their lifetime relative to their non-wood (e.g. metal or plastic) counterparts [180]. For example, a standard new house has the potential to sequester 17.5 tonnes of $CO_2$ if lumber, oriented strand board (OSB), and plywood are utilized [180]. The use of wood in place of non-wood materials reduces lifecycle emissions by an average of 3.9 tonnes of $CO_2$ for each tonne of dry wood used [181]. Many wood product systems models have been developed to track forest carbon accumulation, harvesting, processing, and distribution, but few models accurately account for end-of-life carbon emissions, thereby warranting more research into wood product

degradation in different environments [182]. The degradation of a variety of wood products, including hardwood, softwood, oriented strand board (OSB), plywood (PW), particleboard (PB), and medium-density fiberboard (MDF), was carried out under landfill conditions over a 2.5 year period, from which exposed holocellulose content was determined to be readily degradable, relative to lignin, thereby highlighting the importance of lignin content for carbon permanence in wood products [183].

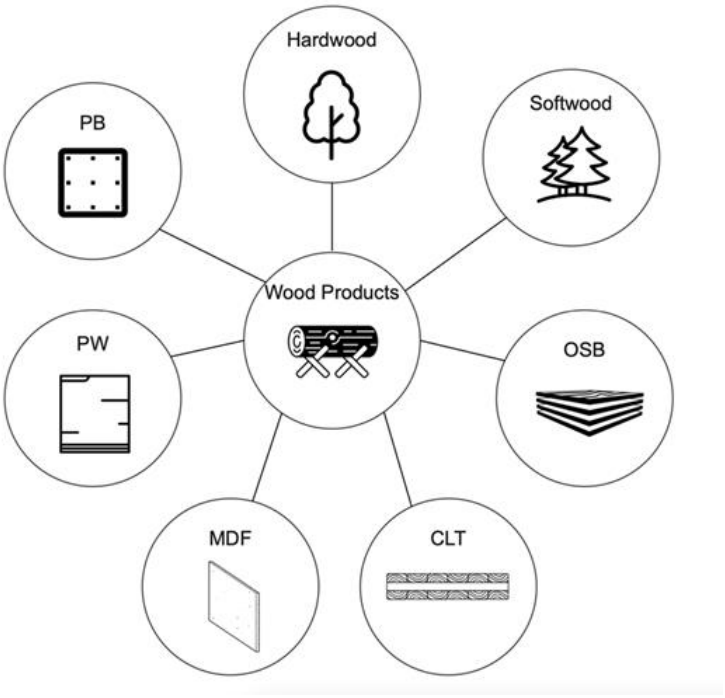


**Figure 2-6** Harvested wood products for carbon storage. OSB = oriented strand board, CLT = cross-laminated timber, MDF = medium-density fiber board, PW = plywood, PB = particle board.

Multiple studies have demonstrated the recalcitrance of lignin in landfills, while the rate and extent of holocellulose decomposition are dependent on the type of wood product and its physical form (e.g. particle size and surface area) [184]. A detailed assessment of the forest products industry in Portugal using two different carbon accounting methods determined that net negative emissions are possible with long product lifetimes and sufficient landfill management practices [185]. However, further research is required to create reliable permanence data for a variety of wood products under various end-of-life conditions, particularly for life cycle modeling where there is significant uncertainty in permanence of carbon in wood products at end-of-life [9]. Notably, optimizing forests for long-term carbon storage typically involves harvesting of biomass for wood products. Thus, overall, significant reductions in forest biomass harvesting generally do not maximize carbon storage [186]–[188]. Accumulation of forest residues with minimal removal can lead to negative environmental and social impacts including intensified wildfire severity and probability [189], [190]. Thus, more effort into the sustainable removal of forest residues for valorization and carbon storage is encouraged [191].

Dimensional lumber and OSB have been shown to be significant sinks of carbon over their life cycle when made from forest residues, as opposed to virgin timber [192]. Most lumber products have been shown to reliably store 50% of their carbon for at least 100 years, thereby providing significant potential for carbon removal [193]. Notably, a ~10% improvement in wood mill efficiency has been shown to decrease waste and increase the quantity of carbon sequestered in lumber products by ~7% [194]. However, there is considerable variation in the composition and permanence of lumber products, therefore requiring detailed assessments for each product and avoiding generalization. For example, alkaline copper quaternary (ACQ) treated lumber and wood plastic composite (WPC) are two common lumber materials used in decking, but the emissions associated with former over its life cycle are roughly 30% of the emissions of the latter [195]. In addition, borate-treated lumber was found to generate 1.8 times lower GHG emissions and use 83 times less water than galvanized steel framing members (the closest non-wood competitor) [196]. Other emerging engineered wood products with significant carbon storage potential include cross-laminated timber, glulam, laminated veneer lumber, parallel strand lumber, and mass plywood panels [197].

Globally, the life cycle of pulp and paper products represent 1.3% of greenhouse gas emissions, and there is considerable potential to reduce emissions with end-of-life carbon management and storage [198]. Notably, recent research indicates that increasing the rate of pulp and paper product recycling will not necessarily reduce emissions due to the high quantity of fossil fuel consumption in the recycling pulping process, compared to the chemical pulping of virgin biomass wherein the vast majority of fuels consumed for energy are bio-based [199]. Thus, implementing the concept of circularity with heavy reliance on recycling may not reduce emissions in the pulp and paper sector, warranting further research. Landfill practices have been found to be especially important in reducing emissions from the pulp and paper sector, given that approximately 100 tonnes of waste are landfilled per 550 tonnes of pulp produced. There is significant potential for capture and sequestration of the biogenic carbon emitted from paper waste at landfills [200]. In addition, there is considerable potential to capture and sequester biogenic $CO_2$ emitted at chemical pulp mills. In the US, the pulp and paper industry is the largest consumer of biomass for stationary heat and power production, emitting ~115 million metric tons of biogenic $CO_2$ each year. There are intriguing opportunities to integrate $CO_2$ capture into the lime kiln operation and to utilize $CO_2$ for pH adjustment and lignin precipitation. Also, the alkaline chemistry of the kraft pulping process lends itself well for $CO_2$ capture, thereby offering the opportunity for *in-situ* $CO_2$ capture in the recovery boiler [101], [201].

#### 2.2.2.5 Emerging biocarbon products

The aforementioned biocarbon products and associated industries are relatively mature and of high technology-readiness-level (TRL > 7). There are several new biocarbon products emerging that have significant potential to sequester carbon, with bio-steel and bio-cement holding particularly impactful potential. The manufacturing of iron and steel represents ~7% and cement and concrete ~6% of global $CO_2$ emissions, and traditional low-carbon energy technologies, such solar and wind, are not suitable for decarbonizing these industries. Traditional manufacturing of virgin steel relies on carbon-rich petroleum- or coal-derived coke for iron ore reduction in the blast furnace. Recently, process modeling has shown the techno-economic feasibility of using pyrolysis-derived biocoke, which is similar to biochar, or gasification-derived biohydrogen as

substitutes to fossil coke in the blast furnace [202], [203]. Preliminary assessments indicate carbon-negative steel production is feasible with capture of the $CO_2$ from the blast furnace. Notably, a small percentage (0.2 – 2.0 wt%) of the final steel product is carbon from the blast furnace, thereby offering another avenue for carbon sequestration. Carbon is intentionally incorporated into the steel to provide specific strength properties. Although the weight percentage of biocarbon in the final steel product is small, the large quantities of steel produced each year (~2 billion tonnes of steel) justify its consideration for carbon removal; note that steel produced from virgin iron ore and recycled scrap both require the incorporation of carbon.

Similar to steel, the incorporation of carbon into cement mixes has been shown to provide desirable strength properties. When 1% weight of the concrete mix is replaced with biochar, the compressive strength of the concrete improves, the flowability, static elastic modulus, drying shrinkage, and flexural strength are not significantly impacted, and permeability decreases [204], [205]. Notably, inclusion of < 1% biochar to global concrete production has the potential to sequester 0.5 Gt of $CO_2$ per year [205]. Recent studies show that no more than 3% biochar can be added to concrete without negatively impacting strength properties [206], [207]. In addition, the use of biogenic or atmospheric $CO_2$ in the concrete curing has the potential to significantly reduce emissions and achieve negative carbon intensities [208], [209].

### 2.2.3 Assessment of Drawdown Potential

In the second part of this paper we demonstrate the potential of four representative BiCRS products to facilitate carbon drawdown. Estimating the carbon drawdown potential of BiCRS products necessitates reliable estimates of the magnitude and durability of sequestered carbon. We analyze an advanced BECCS pathway, bio-polyethylene, oriented strand board (OSB), and biochar soil amendment. We first present estimates for the durability of carbon in geologic reservoirs, durable products, and biochar soil amendments over a 10,000-year time horizon, while acknowledging the shortcomings of assessments over such long horizons. We then estimate the life cycle GHG emissions of the four products, including a discussion of the long-term drawdown potential of each pathway. Finally, we discuss the relevance of this analysis to long-term climate mitigation goals, future research directions, and supportive climate policy.

#### 2.2.3.1 Results Part 1: Durability of sequestered carbon over time

Biogenic carbon can be sequestered in engineered sinks for climate-relevant timescales. The durability of sequestration can vary from days to millennia. We estimate optimistic, moderate, and pessimistic bounds for sequestration in onshore and offshore geologic reservoirs, polyethylene products, oriented strand board (OSB), and biochar soil amendment. The estimates should not be understood as a statistical likelihood of a given outcome but rather a plausible range of outcomes. The estimates reported here are the result of the synthesis of the best available data. Representative cases are selected for the main text, while the full range of analyzed scenarios is presented in greater detail in the Supplementary Information (see Appendix A1 for methods specific to each pathway).

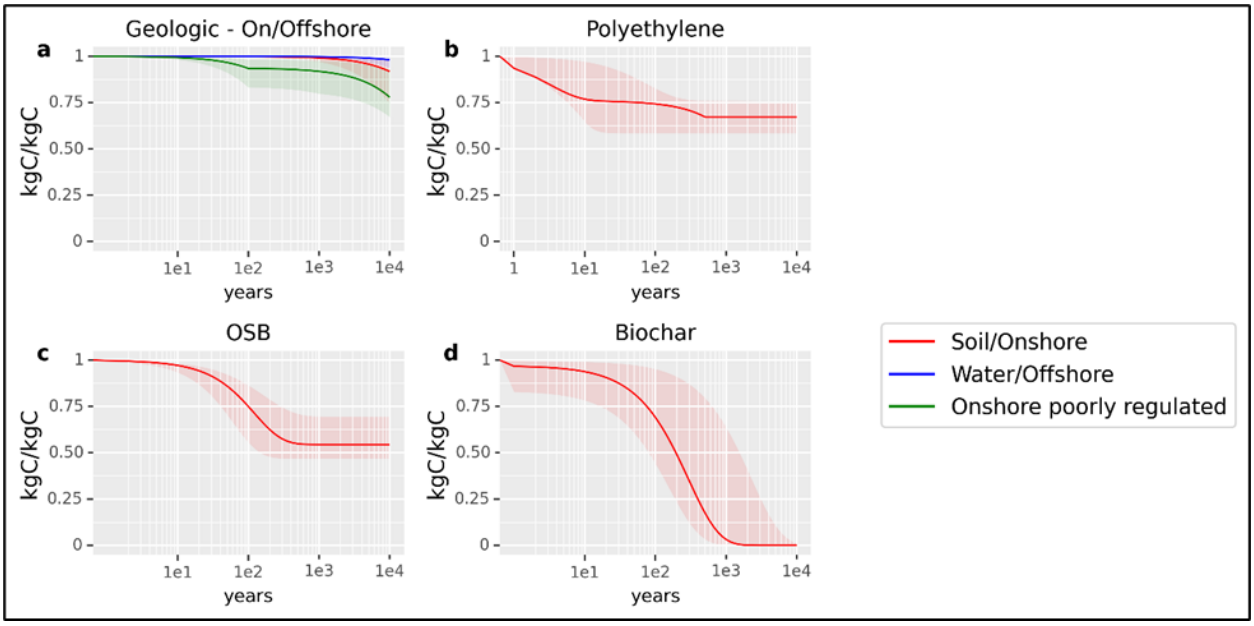


**Figure 2-7** Estimated carbon sequestration over 10,000 years. This figure illustrates a range of optimistic, pessimistic, and moderate cases for carbon sequestration over time. The dark red line in each panel is the moderate estimate for each analyzed scenario. The dark blue and dark green lines in panel (a) represent the P50 estimate (Appendix A1.1) for offshore and onshore poorly-regulated geologic sequestration. The dark red line in panel (a) is the P50 scenario for onshore, well-regulated wells. This is the baseline for geological sequestration in this analysis. The functional form in each case considers a pulse of carbon entering the carbon cycle in the form of a product or sequestration co-product. From the production gate, the function may consider (where appropriate) operational use-life, recycling, secondary use, and sequestration of carbon in the product or biosphere. Panels: a. Geologic sequestration of industrially captured CO2 in either onshore well-regulated or poorly-regulated or offshore well-regulated reservoirs b. carbon sequestered in a polyethylene product. Note that the discontinuity and shape of the function results from the interaction of both linear (landfill decay) and exponential (use-life decay) decay assumptions in the function. c. carbon sequestered in oriented strand board (OSB) construction material d. carbon sequestered in biochar soil amendment applied to agricultural soil.

#### *2.2.3.1.1 Geologic Sequestration*

Geologic sequestration of $CO_2$ is the most secure form of sequestration analyzed here, serving as a baseline for comparison to other modes of sequestration. Here, $CO_2$ is compressed into a supercritical fluid and injected into deep geologic formations. Injected $CO_2$ is trapped in porous rock beneath an impermeable cap-rock formation through buoyancy, adhesion, solubility, or mineralization [210]. Leakage can occur through structural failure of the caprock or well or from unidentified and improperly abandoned wells proximate to the storage project [210]. **Figure 2-7a** illustrates the $5^{th}$ to $95^{th}$ percentile range for the fraction of carbon remaining in (globally aggregated) on-shore and off-shore reservoirs (adapted from Alcalde et al. (2018)[210]). In the least optimistic estimate, > 67% of the sequestered $CO_2$ remains in storage after 10,000 years. The remaining fraction of sequestered carbon at 100; 1,000; and 10,000 years

in onshore and offshore reservoirs is estimated to be within the ranges 0.83-0.99 (0.99), 0.79-0.99 (0.99), and 0.67-0.99 (0.92) respectively. The values in parenthesis reflect the representative case of onshore, well-regulated geological sequestration.

#### *2.2.3.1.2 Carbon storage in polyethylene products*

Long-term sequestration of biogenic carbon can also be achieved in thermoplastics such as polyethylene (PE). PE's stable structure and resistance to degradation give it desirable qualities for many commercial uses as well as long-term carbon storage. At the end of its useful life, PE may be recycled, re-used, combusted, landfilled, or discarded. In the U.S. context, most PE is landfilled [211] (also see A1.2), where only a fraction of the degradable carbon will return to the atmosphere. The lifetime of plastics in the environment is not well-understood and estimates vary widely [212]. Once in the environment, PE is subject to physical (photodegradation from UV light, thermooxidation, and hydrolysis) as well as biological degradation [213], [214]. Degradation rates are subject to physical properties such as volume, surface area, and chemical composition as well as environmental factors such as temperature, humidity, pH, and the presence of oxygen [215]. **Figure 2-7b** shows the optimistic, moderate, and pessimistic estimates for carbon remaining in PE over time based on estimated use-life, recycling and secondary use rates, and a physical decay model for HDPE pipe, HDPE bottles, and LDPE bags in soil. We estimate the fraction of sequestered carbon at 100; 1,000; and 10,000 years stored in PE to fall within the ranges 0.58-0.83 (0.74), 0.59-0.76 (0.67), and 0.59-0.75 (0.67) respectively. The values in parentheses reflect the representative case of carbon stored in HDPE bottles.

#### *2.2.3.1.3 Carbon storage in oriented strand board (OSB)*

There is an extensive literature on the mitigation benefits of storing carbon in long-lived wood products, particularly in buildings [179], [181], [216]. Oriented strand board (OSB) is widely-used as a load-bearing construction material. After its useful life expires, OSB's end-of-life phase may involve recycling, secondary use, and a significant portion may arrive in landfills or open dumps. **Figure 2-7c** shows optimistic, moderate, and pessimistic estimates for carbon sequestered in OSB over time based on estimated use-life, energy reclamation rates, and physical degradation rates for OSB panels in a landfill environment. In all cases, > 46% of the OSB carbon is permanently sequestered in landfills. We estimate the fraction of carbon sequestered at 100; 1,000; and 10,000 years stored in OSB to be within the ranges 0.56-0.87 (0.75), 0.47-0.70 (0.54), and 0.47-0.70 (0.54) respectively. The values in parenthesis reflect the representative moderate decay rates (use-life and landfill) and degradable organic carbon fraction for OSB.

#### *2.2.3.1.4 Carbon storage in biochar soil amendment*

Finally, biogenic carbon can be sequestered in biochar as a soil amendment. We rely on published estimates of labile and recalcitrant carbon fractions [172] and mineralization rates [217] for biochar in soils. Physical characteristics of the biochar and feedstock as well as environmental factors such as precipitation and soil conditions influence biochar stability; as such, there is a large degree of uncertainty in the durability of sequestration [218]–[220]. **Figure 2-7d** illustrates optimistic, moderate, and pessimistic estimates for biochar carbon remaining sequestered in soils over time. We estimate the fraction of sequestered carbon at 100; 1,000; and

10,000 years stored in biochar in soils to be within the ranges 0.44-0.95 (0.69), 0-0.64 (0.03), and 0-0.01 (0) respectively. The values in parenthesis reflect the representative case.

#### 2.2.3.2 Results Part 2: Drawdown in products

The carbon physically stored in bio-based products is only half of the story. Net carbon removal must also account for the full life cycle of production prior to final end-of-life. The four BiCRS pathways explored here are representative but not exhaustive in terms possible production methods. They were selected for near-term viability and to represent a variety of second generation (cellulosic) feedstocks (see A2.2 for details), conversion methods, and end-uses. After estimating cradle-to-gate life cycle emissions, the moderate case 100-year sequestration durability estimates (from Results Part 1, fully derived in Appendix A1 for each technology) are applied to calculate cradle-to-grave net carbon removals or emissions, as the case may be. We estimate the 1,000 and 10,000-year emissions profile for each pathway in Appendix A (A2.3.2, A2.4.2, A2.5.2, A2.6.2). We apply 100-year global warming potentials (GPW) to non-$CO_2$ emissions, expressed as $CO_2$ equivalents or $CO_2$e [221]. This decision amplifies the relative climate impact of emissions that occur late in a project's lifetime (e.g. landfill emissions) when considering the 100-year time horizon, causing the estimates of net carbon removal presented here to be conservative within the GWP framework (See Appendix A2.1.1) [222]. Dynamic life cycle assessment methods [222] can be used to account for these temporal discrepancies, but for the illustrative purposes here, we focus on the physical carbon drawdown rather than assessing the benefits of delayed impacts over a fixed time horizon. The temporal impact considerations are out-of-scope and would only serve to enhance the apparent climate benefits of pathways that delay release of stored carbon ($CO_2$ emissions occurring near year 100 would approach zero impact). This is a distraction from the nominal carbon removal estimate we are after. The life cycle model assumptions for each of the four pathways are described in greater detail in Appendix A2.3-A2.6.

##### *2.2.3.2.1 Goal, Scope, Functional Unit, and System Boundaries*

The goal of this analysis is to quantify the carbon removal potential of various products in the bioeconomy. The scope of the analysis is cradle-to-grave net carbon removal 100, 1,000, and 10,000 years. Carbon durability over millenia is uncertain and speculative, thus here we focus on the 100-year time horizon. We report our estimates for 1,000 and 10,000 years in Appendix A. The functional unit for this analysis is "per metric tonne of carbon in biomass feedstock." This approach allows us to compare the carbon removal efficiency and resulting product outputs of different product categories on a consistent basis.

The system boundary for our analyses includes feedstock production/collection, feedstock transport, production of biomass product, and product end-of-life. Two BiCRS pathways considered here generate co-products alongside the primary product. The corn stover to polyethylene pathway generates excess electricity which is assumed via system expansion to displace average regional electric grid emissions. The oriented strand board pathway also generates a small quantity of wood residues. The quantity is small and thus we made a simplifying assumption that these materials are combusted to support process heat needs. The potential displacement effects of primary product outputs are not considered in the life cycle GHG

assessment. Consistent comparison between the variety of products analyzed here would be challenging and perhaps misleading. We instead offer GHG estimates for incumbent products which might be replaced in the sections below without factoring those avoided emissions into the quantitative analysis.

#### *2.2.3.2.2 Feedstock selection*

The BiCRS pathways analyzed in the sections that follow utilize cellulosic wastes, residues, and purpose-grown energy crops as feedstocks. These feedstocks avoid or at least minimize sustainability challenges associated with food-crop feedstocks (e.g. corn) that compete for land, water, and nutrients with the food sector. In the case of wastes and residues, the upstream life cycle emissions associated with these feedstocks are minimal, limited to the activities of collection and transport because typically environmental impacts associated the production of the primary product are allocated to the primary product rather than wastes and residuals. Purpose-grown energy crops such as switchgrass, poplar, and miscanthus have received attention because they can potentially generate high yields on marginal lands not suitable for agricultural production. **Table 2-3** below describes the feedstocks considered in this analysis.

**Table 2-3** Cellulosic feedstocks considered in this analysis

| **Feedstock** | **Assumed Carbon % (Dry basis)** | **Description** |
|---|---|---|
| Switchgrass | 46.6% | Switchgrass is a fast-growing perennial crop that can generate high yields in diverse environments, including marginal lands unsuitable for conventional agriculture [223]. This is especially beneficial since limited land resources and competition for food production are key challenges for scaling up biomass production for carbon drawdown. |
| Corn Stover | 46.6% | Corn stover is agricultural residue consisting of leaves, stalks, and cobs left over after harvest. As much as half of corn crop yield consists of stover residues. Agricultural wastes/residues have the advantage of not requiring additional land for cultivation. Most of the resources have already been expended to produce the primary agricultural good. The wastes would otherwise degrade in situ, releasing a significant portion of their carbon back into the atmosphere. |
| Forest Residues | 50.3% | Residues consist of the unmerchantable wood left over from logging activities in managed forests. Transport of residues presents logistical challenges [224]. When it is not cost-effective to transport or utilize residues, they may be burned onsite or left to decompose. |

#### *2.2.3.2.2 Bioelectricity from Switchgrass with CCS*

The selected BECCS pathway considers an integrated gasification combined cycle (IGCC) power plant with carbon capture and sequestration (CCS) and that sequesters carbon in geologic storage. Switchgrass cultivation, the IGCC facility, and geologic carbon storage are all assumed to take place in California, USA. There are suitable conditions for switchgrass cultivation throughout the state [225]. The feedstock is assumed to travel an average of 100 km by heavy diesel truck to the IGCC facility. At the IGCC facility, gasification of switchgrass generates syngas—a mix of hydrogen, carbon monoxide, and $CO_2$. Carbon monoxide is converted to additional $CO_2$ via the water-gas shift reaction [226]. $CO_2$ is separated from the syngas mix before the remaining gas is combusted for electricity production. We model pre-combustion capture of $CO_2$ after physical scrubbing with a methanol-based system as described in an analysis of a coal slurry IGCC system [227]. There are suitable formations for geologic carbon sequestration throughout California, and it is assumed that the IGCC facility is located proximate such that additional compression outside of the plant boundary is unnecessary to deliver supercritical $CO_2$ to subsurface storage. CSS system operation causes a 22% relative drop in plant efficiency in order to achieve an 85% capture rate. The separation of the high-purity $CO_2$ stream prior to combustion offers a more cost-effective option than conventional biomass combustion with post-combustion capture [228]. Further details on our IGCC LCA assumptions can be found in Appendix A2.3.

The carbon drawdown potential of the IGCC facility with CCS is substantial. The process sequesters 3,113 $kgCO_2/tC$ in geologic storage while generating 3,124 kWh (11,249 MJ) of electricity for the grid. Once captured and stored, 92% of the carbon remains sequestered over 10,000 years. The life cycle net drawdown of the process is -2,811 $kgCO_2e/tC$ or -0.90 $kgCO_2e/kWh$ (-0.25 $kgCO_2e/MJ$). For comparison, a Natural Gas Combined Cycle facility without CCS emits roughly 0.40 kg $CO_2e/kWh$ [229].

Taking the moderate case for onshore geological sequestration, at 100; 1,000; and 10,000 years, 99.9%, 99% and 91% of the original drawdown benefit remains, respectively (Appendix A, **Figure A3**). Net drawdown at 100 years is -2,811 kgCO2e/tC (**Figure 2-8**).

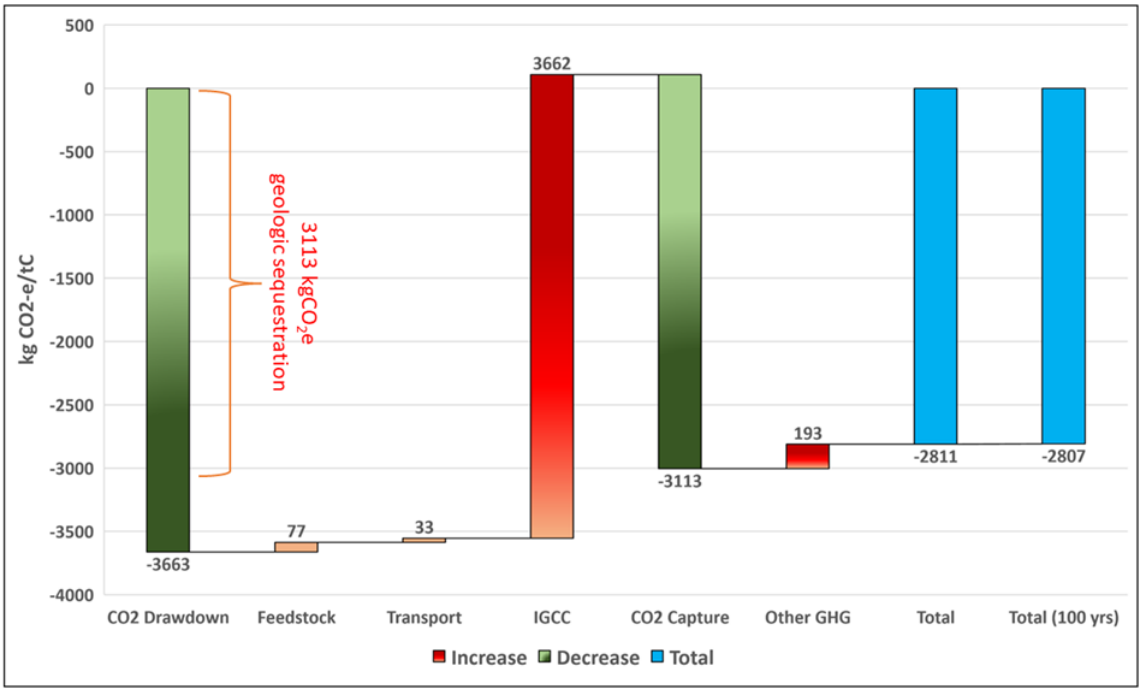


**Figure 2-8** IGCC-CCS electricity production from switchgrass drawdown over 100 years (moderate case). Note that in the waterfall diagrams, green and red bars represent magnitudes of drawdown and emissions subsequent to the initial drawdown in biomass. The blue bars represent totals. The sum of all red and green bars is equal to the first blue bar.

#### *2.2.3.2.3 Polyethylene production from corn stover with CCS*

Next, we consider conversion of corn stover to polyethylene (PE) with CCS. The process modeled here assumes corn stover is enzymatically treated to make cellulosic sugars available for fermentation. The resulting ethanol is then dehydrated to ethylene intermediate and finally polymerized to PE. Process heat and power for ethanol production is generated via combustion of a fraction of the stover (40%), thus fossil $CO_2$ emissions are avoided at the facility. Subsequent processing into to PE is assumed to use regional grid electricity as well as utility natural gas. Collection of corn stover is assumed to take place in Iowa, USA, and the stover travels 2,896 km (1,800 miles) by diesel rail car to a refinery in California, USA. The fermentation stage generates a high-purity stream of $CO_2$ which can be captured and sequestered geologically at lower cost than combustion streams of $CO_2$ [104]. As in the IGCC case, the facility is assumed proximate to suitable geologic formations such that additional compression outside of the plant boundary is unnecessary to deliver supercritical $CO_2$ to subsurface storage. Additional biogenic carbon is sequestered in the PE product. Further details on our polyethylene LCA assumptions can be found in Appendix A2.4.

The drawdown potential of stover-based PE with CCS is substantial. This pathway sequesters 2,159 $kgCO_2/tC$ in engineered sinks while producing 351 kg of polyethylene. 1,064 $kgCO_2/tC$ is sequestered in geologic reservoirs while 1,102 $kgCO_2/tC$ is sequestered in the PE product as stable carbon. Approximately 92% of the geologic carbon and 67% of the carbon in PE remains

sequestered over 10,000 years. The PE carbon losses are emitted by combustion in energy recovery projects or by landfill emissions. The methane in the unflared fraction of landfill emissions is a significant contributor to the reduction of drawdown benefits over time. We estimate the life cycle net drawdown of the process at the gate of the PE resin facility to be -1,595 $kgCO_2e/tC$ or -4,544 $kgCO_2e/t$ of PE. Additional emissions arise in our representative case from injection molding to produce HDPE bottles. The net drawdown of the completed product is -1,197 $kgCO_2e/tC$ or -3,410 $kgCO_2e/t$ of PE. This compares to an approximate life cycle emission for fossil-based HDPE injection molded products of 2,080 $kgCO_2e/t$ of PE produced [229].

Taking the moderate case which assumes well-managed, flared landfills, at 100; 1,000; and 10,000 years, 67%, 53% and 46% of the original drawdown benefit remain, respectively. Assuming no landfill flaring, the benefits fall to 41%, 3.6%, and net emissions at 10,000 years (Appendix A, **Figure A5** and **Figure A6**). The representative pathway, which assumes methane management at the landfill, retains a net drawdown of -807 $kgCO_2e/tC$ at 100 years (**Figure 2-9**).

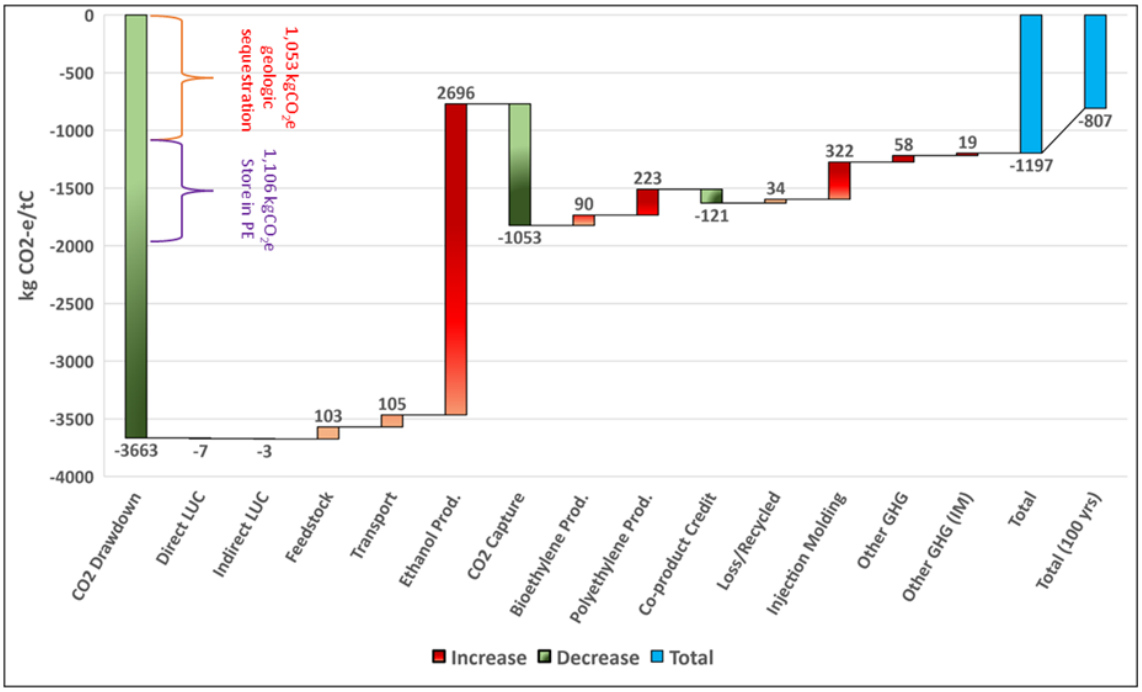


**Figure 2-9** Polyethylene with CCS drawdown over 100 years (moderate case/flared landfills)

#### *2.2.3.2.4 Biochar from Forest Residue*

We next consider carbon sequestration in biochar as an agricultural soil amendment. Biochar can be a co-product of syngas production (gasification) or bio-oil production (fast pyrolysis), or it can be the primary product (slow pyrolysis). We analyze a simple biochar process using a modified air curtain burner (ACB) to pyrolyze forest management residues. The ACB is a refractory-lined box with a blower that is used for low-emissions incineration but can also be

operated to produce biochar (Appendix A2.5 for additional details.) External energy requirements include start-up accelerant and fuel for heavy equipment in collection and handling of residues. The portable unit can be set up at remote locations for the management of forest residues which otherwise face logistical challenges to utilization [224]. Forest residues and biochar production are assumed to be co-located in Northern California, USA. Biochar is substantially less costly to transport as it is lighter than wood waste and has a higher energy density. It is also preferable to open pile burning from a climate mitigation and emissions perspective [230]. Produced biochar is assumed to be transported roughly 129 km (80 miles) by truck from forest site to agricultural soils in the California Central Valley region. Further details on our biochar LCA assumptions can be found in Appendix A2.5.

We estimate moderate drawdown potential for biochar on centennial timescales with large uncertainties on millennial timescales. This biochar initially sequesters 1,296 kg $CO_2$e/tC in 397 kg of biochar applied to agricultural soils. Over 10,000 years, no carbon remains sequestered in the biochar (See **Figure 2-7d**). We assume all biochar carbon degradation in soils results in $CO_2$ emissions. We do not consider potential biochar sequestration benefits from increased agricultural yields, nor do we consider soil priming impacts. We estimate a net drawdown of -963 kg $CO_2$e/tC or -2,426 kg $CO_2$e/t of biochar. Alternatively, the fate of forest residues could be natural decay, open pile burning, or forest fire. Assuming sustainable forest management practices, the alternative fate of onsite combustion would conservatively yield emissions near 0 kg$CO_2$e/tC due to the biogenic nature of the carbon. We do not consider alternative productive uses of forest residues, although there are other possible counterfactuals.

At 100 years, 59% of the original drawdown benefit from biochar application as a soil amendment remains. At 1,000 and 10,000 years the process yields net positive emissions (see Appendix A, **Figure A8**). The pathway retains significant drawdown benefit with life cycle emissions of -564 kg $CO_2$e/tC at 100 years **Figure 2-10**. See A2.4 for a detailed discussion the life cycle emissions of the biochar pathway.

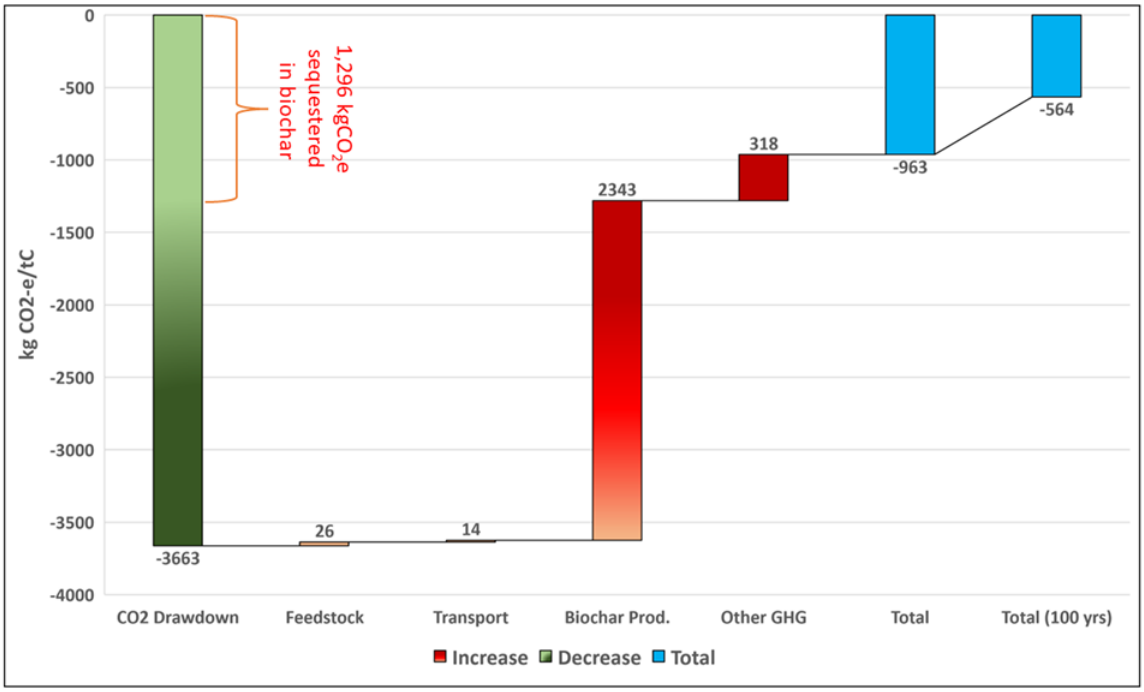


**Figure 2-10** Biochar soil amendment drawdown over 100 years (moderate case). Note that in the waterfall diagrams, green and red bars represent magnitudes of drawdown and emissions subsequent to the initial drawdown in biomass. The blue bars represent totals. The sum of all red and green bars is equal to the first blue bar.

#### *2.2.3.2.5 Oriented Strand Board (OSB) from forest residues*

Finally, we assess the conversion of forest residues into oriented strand board (OSB). OSB is a ubiquitous construction material with an estimated North American production volume of 19,885 million $ft^2$ per year as of 2015 [231]. A standard production unit of OSB is measured at 1,000 $ft^2$ at 3/8" thickness. One metric tonne of forest residue feedstock will produce roughly 1.3 units (2.58 units/tC) with an estimated mass of 769 kg (1,529 kg/tC). We assume forest residue collection in Northern California, USA and transport by heavy diesel truck approximately 145 km (90 miles) to a hypothetical OSB production facility also located in Northern California. Wood strands approximately 2.5 cm x 15 cm are layered at opposing angles and compressed under high temperatures with resin and wax (about 5% by mass) [232] to produce a strong construction material. The life cycle of OSB production involves fossil fuels in the collection, handling, and transport of forest residue feedstock. Onsite processes include energy and emissions from flaking, drying/screening, blending, pressing, finishing, and emissions controls. Roughly 90% of the onsite heat requirement comes from wood fuel (about 23% of the feedstock requirement) [233], with the remainder supplied by natural gas, liquified petroleum gas, and fuel oil [233]. In addition to wood feedstock, the process uses 25 kg of PF resin, 5 kg of MDI resin, and 11 kg of slack wax per metric tonne of feedstock processed. Further details on our OSB LCA assumptions can be found in the Appendix A2.6.

The carbon drawdown potential of OSB is substantial. This pathway sequesters 2,541 kg$CO_2$e/tC in the OSB product. Approximately 54% of the carbon is eventually permanently sequestered in landfills. The balance of carbon is released when the OSB reaches the end of its functional life, either from combustion in an energy recovery system or as landfill emissions. Methane from the unflared fraction of landfill emissions is a significant contributor to the loss of drawdown benefits over time. We estimate the net drawdown potential to be -1,806 kg $CO_2$e/tC or -700 kg$CO_2$e per production unit (-1.18 kg $CO_2$e/kg). A recent meta-analysis estimates an average of 4 tons of $CO_2$e avoided for each ton of dry wood that displaces non-wood materials (assuming similar operation phase emissions), with a middle range of 1.5 to 22.0 tons of $CO_2$ emissions avoided by displacement of non-wood materials per ton of wood carbon employed in building construction (See A2.6.3 for explanation of the reported displacement factors) [181].

Assuming well-managed landfills that flare emissions, 55% of the original drawdown benefit remains at 100 years (24% if all landfills were unflared), and 11% at 1,000 and 10,000 years (net emissions if all landfills are unflared; see Appendix A, **Figure A10** and **Figure A11**). The 100-year net $CO_2$ drawdown of this pathway assuming all landfills are flared is -987 kg$CO_2$e/tC (**Figure 2-11**). See A2.5 for a detailed discussion the life cycle emissions of the OSB pathway.

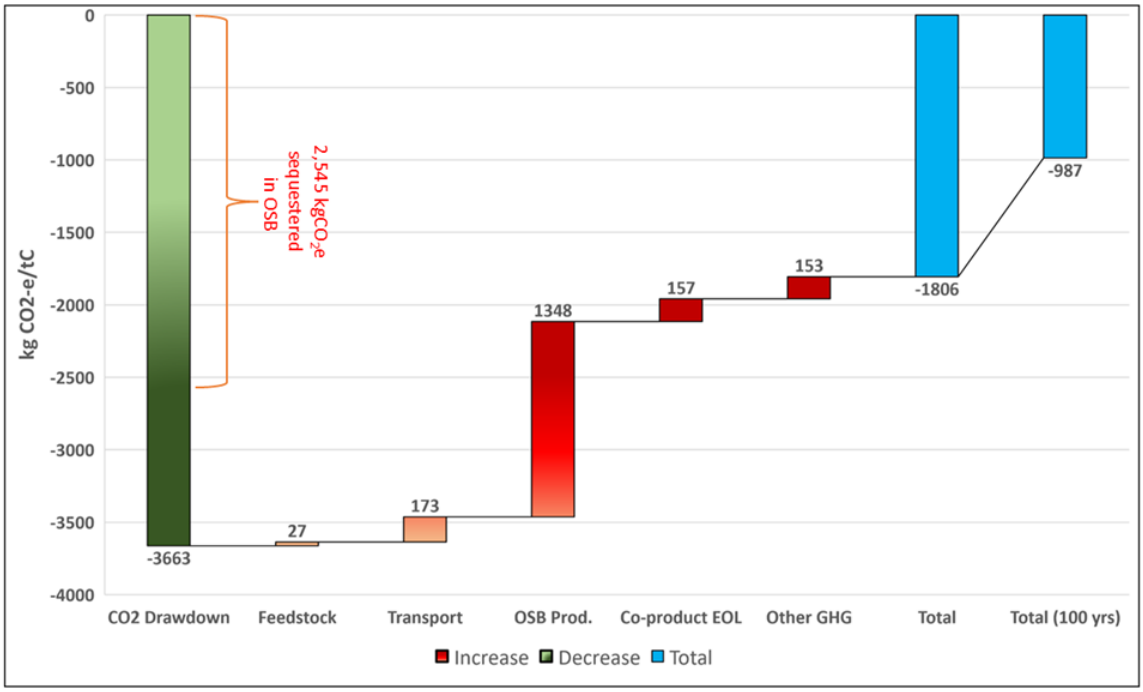


**Figure 2-11** Oriented strand board drawdown over 100 years (moderate case/flared landfills). Note that in the waterfall diagrams, green and red bars represent magnitudes of drawdown and emissions subsequent to the initial drawdown in biomass. The blue bars represent totals. The sum of all red and green bars is equal to the first blue bar.

#### *2.2.3.2.6 Pathway comparison*

**Table 2-4** provides an overview of pathway analysis results. We include the cradle-to-gate emissions for each pathway, the quantity of atmospheric carbon sequestered (reported in $CO_2e$), and both the initial and 100-year disposition of sequestered $CO_2$, as well as the net $CO_2$ drawdown benefits (negative emissions). Life cycle sequestration durability and net $CO_2$ are reported on both a per tC in feedstock and per-unit-product basis. Non-BECCS pathways achieve 34-64% of the initial drawdown magnitude relative to BECCS and retain 55-67% of the initial drawdown over 100 years (central estimate).

The IGCC plant with CCS attains the most drawdown potential per ton of feedstock, with 91% of the initial drawdown benefit expected to persist over millennia. However, the performance of the other pathways is notable. The role of biopower may be limited by the increasing role of other low-carbon energy options. But there are many other sectors of the economy where the carbon removal potential of biomass feedstock can play a significant role. By combining geological sequestration with carbon storage in long-lived products, the PE pathway achieves 29% of the drawdown benefit of the IGCC plant at 100 years and maintains about 46% of the initial drawdown benefit at 10,000 years. The biochar pathway achieves 20% of the IGCC drawdown benefit at 100 years but yields net positive emissions over 10,000 years. The OSB pathway achieves 35% of the drawdown benefit of the IGCC plant at 100 years, with 11% of the initial drawdown benefit persisting over 10,000 years.

**Table 2-4** Comparison of bioproduct $CO_2$ drawdown potential

| | **Product type** | **Sequestration** | **Initial sequestration ($kgCO_2e$/t C)[a]** | **100-yr sequestration ($kgCO_2e$/tC)[a]** | **Initial drawdown ($kgCO_2e$/t C)** | **100-yr drawdown ($kgCO_2e$/t C)** | **Initial drawdown ($kgCO_2e$ per unit product)** | **100-yr drawdowon ($kgCO_2e$ per unit product)** | **Product Unit** |
|---|---|---|---|---|---|---|---|---|---|
| **IGCC w/ CCS** | Electricity | Geologic reservoir | 3113 | 3109 | -2811 | -2807 | -900 | -899 | MWh |
| **Polyethylene w/ CCS** | Durable polymer | Geologic reservoir | 1053 | ~1053 | -1197 | -807[b] | -3410 | -2299[b] | t |
| | | Polyethylene/landfill | 1106 | 822[b] | | | | | |
| **Biochar** | Soil amendment | Agricultural soils | 1296 | 899 | -963 | -564 | -2426 | -1421 | t |
| **OSB** | Durable wood product | OSB/landfill | 2541 | 1819[b] | -1806 | -987[b] | -700 | -383[b] | 1,000 $ft^2$ of 3/8" panel |

a. These quantities reflect the atmospheric carbon sequestered converted into equivalent quantities of atmospheric $CO_2$

b. The 100-year sequestration values reflect the amount of atmospheric carbon remaining sequestered in $CO_2e$ while the 100-year drawdown quantities take into account carbon that has been released as methane. Therefore, the change in drawdown benefit may be larger than the change in carbon sequestered.

### 2.2.4 Discussion

Our analysis demonstrates a range of opportunities for the bioeconomy to contribute to carbon drawdown. BECCS likely remains a key component of drawdown strategies and serves as a useful baseline for comparing alternatives. Advanced biomass gasification pathways can facilitate access to higher-purity streams of $CO_2$, minimizing the plant efficiency impacts of $CO_2$ separation and capture. Geologic sequestration remains the benchmark given the greater security

of long-term sequestration. However, other biomass utilization alternatives may present unique advantages. For instance, alternative markets may present fewer obstacles to scale or offer synergies with existing operations, production externalities (jobs, environmental impacts) may be more regionally beneficial, or processes may be able to utilize a broader range of feedstocks. We discuss our key findings, research needs, and the implications for existing climate mitigation policy.

All of the non-BECCS drawdown pathways analyzed store carbon at climate-relevant timescales. Fermentation pathways are promising because of the potential to produce carbon-negative polymers in addition to low-carbon fuels all while capturing high-purity streams of $CO_2$ for geologic storage. Wood construction materials are a potentially carbon negative alternative to emissions intensive concrete and steel. Markets for polymers and wood products are already mature and do not face the same challenges to scale as more speculative pathways. Biochar can contribute to drawdown efforts while addressing challenges in forest management and improving agricultural yields and soil health.

Furthermore, our analysis highlights the importance of waste management in a comprehensive carbon mitigation system. The drawdown potential of durable goods is blunted by the impact of landfill emissions, namely $CH_4$. Policymakers should take seriously the role of landfills in engineered carbon sequestration. Increased utilization or oxidation of methane across the full life of waste management projects would greatly enhance the potential of bio-based durable goods as negative emissions pathways [42].

Our analysis suggests linked mitigation priorities of emissions reduction and carbon drawdown. The performance of drawdown pathways can be enhanced by reducing the energy and emissions intensity of supply chains and conversion, maximizing carbon stored in long-lived goods, and increasing the time which carbon is stored. Policymakers should be mindful that increasing the inflow of atmospheric carbon to engineered sinks relative to the outflow is a sufficient condition to increase the net stock of sequestered carbon. Moreover, magnitude and permanence of drawdown pathways are key policy considerations. Climate change is an intergenerational challenge and analyses should consider the fate of carbon beyond the conventional 100-year horizon.

Our analysis highlights the utility of flow-based accounting in life cycle models. Policymakers need consistent metrics to compare the magnitude, permanence, and temporal evolution of carbon drawdown pathways. Life cycle assessments and models (e.g. GREET) often adopt a “net zero” approach when dealing with biogenic carbon [234]. This practice assumes biogenic emissions are accounted for at the point of harvest and is consistent with the stock change approach used in national GHG accounting.[235] However, this approach is not suited to track biogenic carbon stored in durable goods, landfills, and soil amendments at the product system level [236]. To consistently value carbon stored by biomass products, the magnitude of sequestration must be temporally resolved. Flow-based accounting facilitates that quantification, and the field of dynamic life cycle assessment has developed methods which allow comparison of time-dependent impacts for temporary sequestration [236].

Given estimates of magnitude and permanence of carbon drawdown, metrics could be developed to compare the relative value of sequestration in biobased goods. Existing policies such as California's Low Carbon Fuel Standard (LCFS), Section 45Q of the US Tax Code and the proposed Section 45T incentivize geologic sequestration (LCFS and 45Q) and utilization (45Q) of industrial emissions and land management-based sequestration (45T). The policies could offer a framework for policy support of drawdown in biomass-based goods. Moreover, consistent biogenic carbon accounting could support performance-based mechanisms similar to the LCFS to reduce the carbon intensity of other high-volume markets (e.g. polymers, construction materials). For example, biorefineries, which often produce multiple products, could play a larger role in mitigation efforts by producing carbon negative durable goods in addition to the fuels they supply to existing low-carbon fuels markets.

### 2.2.5 Conclusion

This article provides a qualitative overview of prominent BiCRS technologies from which a set of the most promising technologies are assessed quantitively through life cycle assessment. There are numerous opportunities to incorporate carbon removal and management within the bioeconomy, but the majority of the near-term carbon removal potential exists in four bioproducts: bioenergy, bioplastics, biochar, and wood products.

We analyze the life cycle greenhouse gas emissions and disposition of sequestered carbon over 10,000 years for four bioproducts representative of each broader category: an advanced BECCS pathway, biopolyethylene, oriented strand board, and biochar soil amendment. We find that the BECCS pathway has the greatest magnitude and durability of $CO_2$ storage over all time horizons. However, non-BECCS pathways achieve 34-64% of the initial drawdown magnitude relative to BECCS and retain 55-67% of the initial drawdown over 100 years (central estimate).

We identify three engineering strategies for enhancing carbon drawdown: reducing biomass supply chain emissions, maximizing carbon stored in long-lived products, and extending the term of carbon storage.

Finally, we highlight the need to characterize both the magnitude and permanence of carbon drawdown as a means for policymakers and technology developers to deploy limited biomass resources to maximize mitigation benefits

A research agenda should begin to think beyond BECCS and take a holistic view of the potential role of biomass in carbon drawdown. Within the broader bioeconomy, carbon drawdown is an opportunity to create economic value, support working lands, and achieve climate benefits with an innovative systems approach to carbon management through biomass.

## 2.3 Excerpt from: Microplastics and their Degradation Products in Surface Waters : A Missing Piece of the Global Carbon Cycle Puzzle[2]

Since the mid-1950s, plastics have become an increasingly ubiquitous component in industrial and domestic products with an estimated 6,300 million metric ton (MMT) of plastic waste generated by 2015 [136]. At current rates of plastic production of 350–400 MMT per year, the volume of plastic waste could triple over current levels by 2050 [213]. The magnitude of plastic waste generation presents a formidable challenge for waste management systems and a threat to ecosystems [237]. The impact of anthropogenic carbon from plastics and degradation byproducts on marine and terrestrial environments is particularly concerning. For a polymer carbon content of 80–90%, the current annual flow of plastic carbon into the global carbon cycle is roughly 280–360 MMT. These carbon amounts are enormous. For reference, this carbon flow from plastics is about 10% the magnitude of the 2.7 Gt of carbon added by the global combustion of coal for electricity [238]. Herein, we highlight this emerging biogeochemical cycle and the need for research to understand to what degree anthropogenic carbon from plastic is impacting surface water ecosystems and, more broadly, the global carbon cycle.

Researchers now recognize plastics pollution beyond the effect of their bulk characteristics on aquatic and terrestrial environments. Due to the nature of terrestrial and aquatic interactions, it is not feasible to discuss either system in isolation. As shown in **Figure 2-12,** the flow of plastics and their degradation products through the environment is complex. The contribution of these flows to carbon stocks in aquatic and terrestrial systems is poorly understood. Roughly 99% of this carbon originates in fossil hydrocarbons, with a much smaller (but growing) 1% originating in the atmosphere in the form of biomass-based polymers [239]. This anthropogenic carbon enters the global carbon cycle as plastic products which can remain in use from days to decades. After a product's useful life, over the last ~70 years, roughly 9% was recycled, 12% incinerated, and about 79% was either managed in landfills or entered the natural environment [136]. Once in the environment, plastics degrade to smaller particles, nano and microplastics (NMPs) under different conditions. Plastics also contain additives which may leech into the surrounding environment more readily that the parent polymer.

[2] Section 2.3 was originally published as:
Dees, J.P., Ateia, M., Sanchez, D.L. 2020. Microplastics and their Degradation Products in Surface Waters : A Missing Piece of the Global Carbon Cycle Puzzle. EST Water. Reprinted with permission from ACS EST Water 2021, 1, 2, 214–216, Publication Date: November 13, 2020, https://doi.org/10.1021/acsestwater.0c00205, Copyright © Published 2020 by American Chemical Society

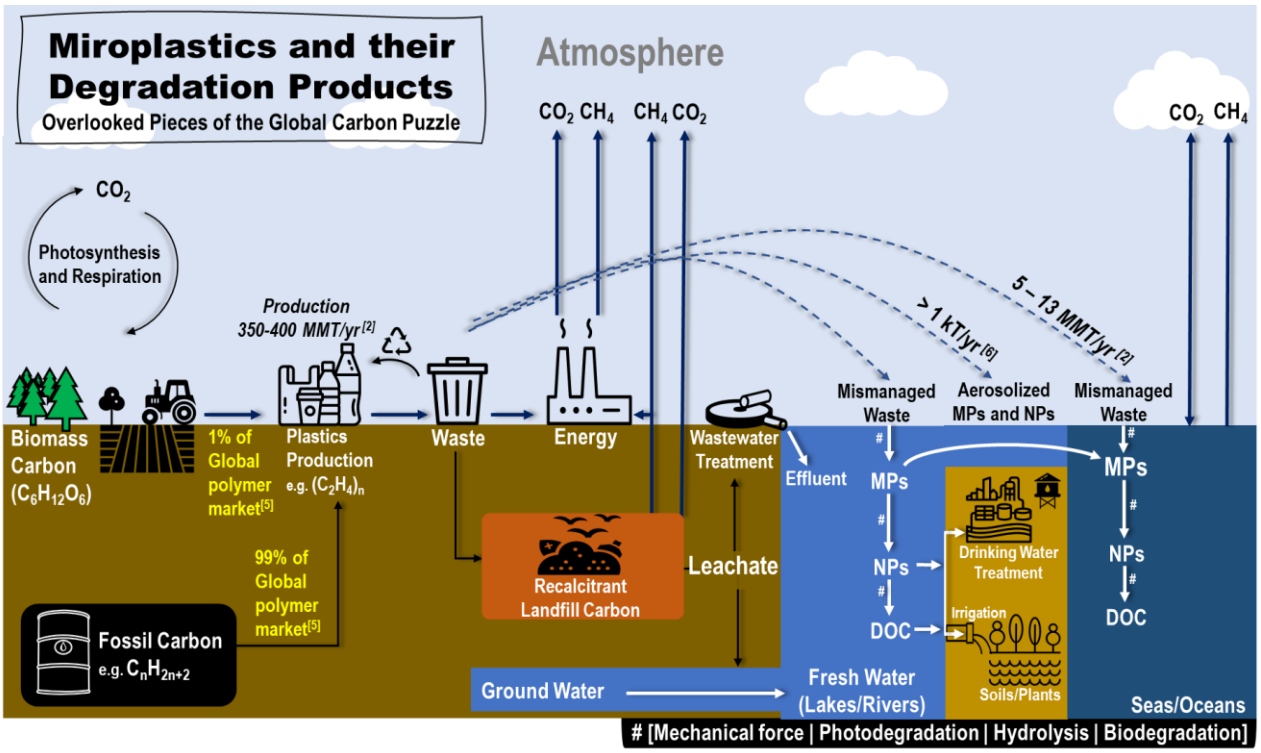


**Figure 2-12** Plastics in the carbon cycle

Although current literature strongly supports the mobility of NMPs and the leached additives, the development of a framework to describe and quantify this complex and dynamic system is unrealized and is an urgent research need. Unmanaged plastic waste may degrade through physical or biological processes on land, in soils, or find its way into groundwater or freshwater rivers and streams, and eventually the ocean. Thus, NMPs have been detected in air, soils, freshwater, oceans, and biota. Aerosolized particles may also be deposited on land and water via storms and air currents [240]. The plastic that reaches landfills may release some fraction of carbon to the atmosphere in the form of landfill emissions ($CO_2$, methane). Carbonaceous degradation products also have high potential to escape the landfill and infiltrate groundwater or directly pass into freshwater as leachate [241]. This pathway is particularly understudied. Once in water, it is hard to distinguish the carbon coming from plastics and those of natural organic matter (NOM). Recent studies have shown similar reactivity of both carbon sources in forming of disinfection byproducts (DBPs). Finally, water-born plastic may cycle back to land, e.g. NMPs can be transported in waste water treatment sludge applied as fertilizer [242].

The lifetime of plastic in the environment and the stability of its carbon matrix is not well-understood. Much conventional wisdom assumes that plastics persist indefinitely, and there is very little data backing the degradation estimates that are available [243]. Laboratory experiments have shown complete photochemical oxidation of polystyrene to $CO_2$ on centennial timescales and partial photochemical oxidation to dissolved organic carbon on decadal timescales [244]. Other common consumer plastics such as polyethylene and polypropylene have shown similar photo-reactivity in laboratory conditions [245], [246].

An estimated 13 MMT per year of NMPs is released to aquatic ecosystems,[213] where they undergo different degradation pathways: 1) biodegradation, 2) photodegradation by UV light, 3) thermooxidative degradation under low temperature, 4) thermal degradation at high temperature, and 5) hydrolysis in water. The resulting organic carbon will interact with biotic systems, and mineralized carbon will impact the magnitude of stocks and exchange between aqueous, terrestrial, and atmospheric carbon pools as well as having an effect water chemistry (e.g. pH). To date, however, the impact of NMP and degradation product carbon on existing stocks is not well-quantified, but it is likely that carbon of plastic origin is showing up in measurements of total and dissolved organic carbons [247], [248]. Moreover, recent research has asserted that plastics represent an important flux missing from the global carbon budget accounting [249]. Understanding the role of plastic degradation products in aquatic environments may have important implications for estimates of future biogeochemical feedbacks between the geosphere and the atmosphere—underscoring an urgent research need in the face of accelerating climate change.

Overall, the role of plastics in the global carbon cycle puzzle is not quantified or well-understood. Anthropogenic carbon from plastics may have important implications for scientists studying biogeochemical dynamics, climate science, life cycle assessment, soil and agricultural sciences, and for materials scientists and engineers. The emerging realization of the ubiquity of microplastics in all facets of the environment has led some researchers to describe a “microplastic cycle” [250]. But it is perhaps also correct to conceptualize plastics as an emerging anthropogenic component of the global carbon cycle. Research is needed to better characterize the fate of microplastics in surface waters and terrestrial systems and to characterize the dynamics between these flows of anthropogenic carbon and biogeochemical and ecological systems.

# CHAPTER 3. ENHANCING THE CLIMATE BENEFITS OF THE EXISTING BIOECONOMY

## 3.1 Preface

This chapter highlights a near-term opportunity for carbon drawdown by addressing the "low-hanging fruit" in the existing bioeconomy. We explore the potential for carbon negative ethanol by addressing process energy emissions via oxyfuel combustion paired with carbon capture and sequestration. We are the first, to our knowledge, to propose carbon-negative ethanol in the academic literature.

Decarbonization of transportation fuels represents one of the most vexing challenges for climate change mitigation. Biofuels derived from corn starch have offered modest life cycle greenhouse gas (GHG) emissions reductions over fossil fuels. Here we show that capture and storage of $CO_2$ emissions from corn ethanol fermentation achieves ~58% reduction in the GHG intensity (CI) of ethanol at a levelized cost of 52 $/tCO2e abated. The integration of an oxyfuel boiler enables further $CO_2$ capture at modest cost. This system yields a 75% reduction in CI to 15 $gCO_2e/MJ$ at a minimum ethanol selling price (MESP) of $2.24, a $0.31/gallon increase relative to the baseline no intervention case. The levelized cost of carbon abatement is 84 $/$tCO_2e$. Sensitivity analysis reveals that carbon neutral or even carbon negative ethanol can be achieved when oxyfuel carbon capture is stacked with low-CI alternatives to grid power and fossil natural gas. Conservatively, fermentation and oxyfuel CCS can reduce the CI of conventional ethanol by a net 44-50 $gCO_2/MJ$. Full implementation of interventions explored in the sensitivity analysis would reduce CI by net 79-85 $gCO_2/MJ$. Integrated oxyfuel and fermentation CCS is shown to be cost effective under existing U.S. policy, offering near-term abatement opportunities.

## 3.2 Cost and life cycle emissions of ethanol produced with an oxyfuel boiler and carbon capture and storage[3]

### 3.2.1 Introduction

Carbon dioxide emissions from the power, transport, and industrial sectors are key drivers of anthropogenic climate change [251]. Efforts to limit global anthropogenic warming to 2 °C by 2100 have spurred efforts to decarbonize these sectors and eliminate emissions from fossil fuels. One solution in the mitigation portfolio is use of biomass as an alternative fuel or feedstock that displaces use of fossil fuels and fossil-based products and, if biomass is sustainably produced, result in an overall emissions reduction. Sustainable biomass supplies are limited, thus energy transition models tend to rely on electrification and efficiency where possible with a targeted role for biomass, primarily in the transportation sector [252]–[254]. Biofuels can be a low-carbon

[3] This chapter is under review at Environmental Science and Technology, Manuscript ID: es-2022-07847b under authorship Dees, J.P., Oke, K., Goldstein, H.M., McCoy, S.T., Sanchez, D.L., Simon, A.J., Li, W. The main content of the paper in review has been placed in its entirety in the main body of the dissertation and the supporting information has been placed in its entirety in the Appendix of the dissertation. This chapter may differ from the final published version.

alternative in challenging sectors such as heavy transport, steel, cement and aviation and can assist in decarbonizing light-duty transportation alongside vehicle electrification in the near-term [36]. When combined with capture and storage (CCS) of high purity $CO_2$ streams made available during the conversion of biomass to liquid fuels, the carbon intensity of biofuels can be driven lower or in some cases, achieve net removal of carbon from the atmosphere [255].

Biobased ethanol represents a significant component of the transportation fuel mix in the United States and Brazil (4% [256] and 20% [257] by energy content, respectively). Recent research has highlighted near-term opportunities to develop CCS capabilities for existing ethanol capacity [104], [258]. In the U.S., approximately 15.8 billion gallons of ethanol, primarily from corn, are produced annually for blending with gasoline [259]. An estimated 45 Mt/yr of high-purity $CO_2$ generated from fermentation is available for capture at these facilities.[104] Fermentation $CO_2$ is considered "low-hanging fruit" due to the relative purity of the $CO_2$ stream. Similarly, Brazil consumes 7.4 billion gallons of fuel ethanol, primarily derived from sugarcane [260] but with a growing contribution from corn [261]. The fermentation $CO_2$ capture potential at Brazilian ethanol facilities is as high as 28 Mt $CO_2$/y [108]. There is also considerable interest in upgrading ethanol and other alcohol-based fuels into sustainable aviation fuels, at high energy and carbon conversion efficiency [262].

Carbon dioxide from fermentation can be captured at relatively low-cost, requiring only dehydration, and compression [263]. Unlike other $CO_2$ point-sources, ethanol production generates a high purity (99%) stream of fermentation $CO_2$ containing only $CO_2$, $H_2O$ and small amounts of sulfur and organic compounds [264], [265]. The technical feasibility of fermentation CCS and permanent geologic storage in saline aquifers has been demonstrated at one U.S. site owned by ADM where captured $CO_2$ was sequestered in the Mt. Simon Sandstone formation [266] : additional projects are proposed, some interconnected by common-carrier $CO_2$ pipelines [267]–[271]. There is a growing literature around CCS in the Brazilian ethanol context, as well [108], [258].

Policy support is key to the development of low-carbon biobased fuels. In the United States, production volumes are largely supported by the Renewable Standard (RFS) which established annual biofuel blending requirements that result in approximately 10% blend of ethanol in most gasoline used in light duty transport [272]. Continued improvement in the CI of ethanol has largely been driven by performance-based policies implemented at the state level such as California's Low Carbon Fuel Standard (LCFS) [273] and both federal and state policies supporting the deployment of CCS [273], [274]. Brazil's ethanol industry has been supported by blending requirements as well. These requirements have varied since the implementation of the Brazilian National Alcohol Program (Proálcool) in 1975. In addition to tax incentives driving large scale adoption of flex fuel vehicles since the early 2000s, more recently, Law No. 12,490 (2011) set ethanol blending requirements at 18%, and the executive branch has adjusted volumes as high as 27% in recent years [275], [276]. Brazil's adoption of the RenovaBio policy (2017) is of particular import as there is now a performance-based market mechanism at the national level for low-CI biofuels analogous to the LCFS program [277]. In these policy contexts, interventions such as CCS can substantially reduce the carbon intensity of ethanol while providing the necessary revenue support to compete with conventional fuels, learn-by-doing, and ultimately bring down costs. There is potential to not only reduce the climate impact of current light duty transport but

can also provide low-carbon feedstocks to chemicals manufacturing or sustainable aviation fuel, a rapidly growing market, with some market research firms estimating a compound annual growth rate (CAGR) of 60% or more through 2030 [278].

The above context motivates exploration of interventions to reduce the CI of ethanol beyond capture and storage of $CO_2$ from fermentation. Researchers and operators have already explored many options. Switching from first-generation starch and sugar feedstocks to second-generation cellulosic feedstocks has clear CI benefits, as these feedstocks typically have much lower production emissions and less concern regarding emissions from land use change. However, there remain substantial technological barriers to make cellulosic ethanol cost-effective [279]–[282]. Other interventions target process engineering and facility operations to achieve higher efficiencies and protect equipment functionality. Improved boiler and condenser integration, high gravity fermentation, pervaporation membranes, substitution of dewatering processes, multi-effect distillation, and mechanical vapor recompression in the distillation column are examples of potential interventions [283]–[285].

The heat and power requirements of a corn ethanol facility typically represent a substantial fraction of emissions and a concurrent opportunity to decarbonize the industry. Sugarcane and cellulosic ethanol facilities substantially improve ethanol CI by utilizing cellulosic wastes/residues as a biogenic source of fuel for heat and power needs [279], [286], [287]. However, conventional corn and sugar beet ethanol facilities often rely on fossil-fuel boilers and grid power to supply process heat and electricity. Only one study, to our knowledge, has explored the potential for capture and storage of carbon from fossil co-generation at conventional ethanol refineries from conventional boilers [288]. This earlier study considered use of a first-generation (monoethanolamine or MEA) solvent for post-combustion capture from on-site heat and electricity power generation for production of ethanol from sugar beets. This reflects a significantly different route to ethanol production than is dominant in North America. Moreover, in this case, the capture process absorbs $CO_2$ in aqueous solution, requiring substantial heat inputs for regeneration of the capture solvent. The combustion of additional natural gas to meet this demand results in an increase of non-renewable energy consumption and a penalty on emissions reductions [288]. As such, alternatives to solvent capture of diffuse post-combustion $CO_2$ streams have been proposed [227], [289], [290].

Oxyfuel combustion is one potential alternative to solvent-based post-combustion capture. In an oxyfuel process, high-purity oxygen takes the place of ambient air in the combustion vessel, greatly reducing the volume of nitrogen and other species in combustion resulting in a high purity CO2 stream in the combustion products. Oxyfuel process designs have been studied and demonstrated in the fossil fuel power [291]–[294], petrochemical [295], cement [296], and steel [297] industries. While it is not considered commercial (e.g., TRL 9) at the scale of a large power plant [298], demonstrations of the technology have been undertaken at the scale of the boiler used in an ethanol mill (e.g., 30-50 $MW_{th}$). In this context, one benefit of oxyfuel combustion is that the energy requirements for capture are largely electrical, which means that the system can benefit from decreasing electricity grid CI over time (or be directly served by renewable generation). Moreover, an oxyfuel boiler does not have conventional “stack” emissions. However, the resulting reduction in air emissions may come at the cost of increased amounts of solid or liquid waste [299]. Operational data on criteria pollutants from natural gas oxyfuel boilers is limited but boilers can likely meet regulatory limits in the United States [300].

This analysis explores oxyfuel combustion combined with CCS to address boiler emissions in a corn-based ethanol plant. We propose the integration of an oxyfuel natural gas boiler to supply refinery heat demand. In this process design, natural gas is combusted in high-purity oxygen (95-99%) with a fraction of the flue gas recycled to the boiler to control combustion temperature. An air separation unit (ASU) is required to supply oxygen for oxycombustion. The flue gas is composed primarily of water and $CO_2$ making the flue gas stream compatible with the fermentation $CO_2$ stream, allowing greater process integration and dehydration in the same $CO_2$ purification unit (CPU). To our knowledge, this is the first analysis of potential integration of oxyfuel combustion in the production of ethanol combined with CCS.

Here we estimate the emissions mitigation benefits and costs of integrating fermentation and oxyfuel boiler CCS to produce low-carbon corn ethanol. We consider a conventional dry mill corn ethanol facility located in the Midwestern United States. We calculate the well-to-wheel life cycle carbon intensity (CI) and production costs of two intervention scenarios: (1) fermentation $CO_2$ capture only and (2) fermentation and oxyfuel $CO_2$ capture. Cost estimates are presented without policy incentives to estimate minimum ethanol selling price (MESP) and unit cost of carbon abatement. Key life cycle input and cost sensitivities as well as MESP sensitivity to existing policy support such as California's LCFS program and the U.S. 45Q tax credit are presented in the final section. Our analysis tests the hypothesis that oxyfuel combustion is a cost-effective option to decarbonize corn ethanol production under existing policy regimes.

### 3.2.2 Materials and Methods

**Baseline Facility:**

The baseline facility (BASE) for this study is assumed to be a modern dry mill ethanol refinery in the midwestern United States with a capacity of 40 M-gal of ethanol per year. The Midwest is home to a high density of existing corn production and ethanol refineries, and parts of the region are proximate to suitable formations for geologic sequestration of CO2 such as the Forest City and Illinois Basins [266], [301]. The facility produces dried distiller's grains and solids (DDGS) and corn oil co-products. BASE utilizes a conventional natural gas boiler for thermal energy requirements and utilizes a direct natural gas-fired drying system for the DDGS co-product. This drying configuration is a conservative choice, as the selection of an indirect steam dry system will make more $CO_2$ available for capture from the boiler. We explore the steam dry option in the sensitivity analysis and SI. Electricity is supplied by the Midwestern Reliability Organization (MRO) for which we assume 2019 grid average emissions and costs. BASE life cycle inventory data is consistent with Argonne National Lab's GREET.net 2019 model [302], except for power and heat demand and the relative ethanol and co-product yields, which are adjusted to match our own Aspen Plus model results. BASE energy demand is based on Mueller's 2008 report which reports an average natural gas thermal energy requirement for dry grind refineries of 29,009 btu/gal (HHV) and 0.73 kWh/gal electricity requirement [303]. Approximately 62% of the thermal energy requirement is steam, equivalent to a thermal duty of 24,427 kWth. Corn is assumed to travel an average of 50 miles by heavy diesel truck to the ethanol refinery. Ethanol travels an additional 50 miles by heavy truck for denaturing and blending into transport fuel. The facility is assumed to operate 7,882 hours per year.

**Fermentation CO2 capture:**

For the fermentation-only CCS (FERMCCS) scenario, we performed a full material balance to determine the quantity of CO2 capturable from a 40 M-gal per year ethanol plant. The composition of corn is reviewed from several literature sources [285], [304], [305] and given in Appendix B (See **Table B1**). Fermentation is assumed to have 93.2% conversion efficiency, while liquefaction and saccharification conversion efficiency and ethanol recovery is 99%. Corn is assumed to be composed of 40.5% carbon. The density of ethanol is 0.79 kg/L. The reaction equations are given in S1.1. Overall yield from 1 kg corn is 0.33 kg ethanol, 0.28 kg DDGS, 0.01 kg corn oil, and 0.32 kg $CO_2$. Fermentation $CO_2$ is captured at a rate of 13,089 kg/hr and assumed to be at 100% purity. Fermentation $CO_2$ is dehydrated, compressed, liquefied, and pumped at 150 bar, which is assumed to be sufficient to transport the gas by pipeline 100 miles to geologic storage without need for further compression. This is carried out by the $CO_2$ processing unit (CPU) and modeled using Aspen Plus® V11. The additional electricity demand for the CPU is estimated to be 110 kWh/t $CO_2$ using this model.

**Integration of the Oxyfuel Boiler with CO2 Capture:**

For the integrated oxyfuel CCS scenario (FERMOXYCCS), we modeled the steam requirement of the BASE plant to be supplied by the oxyfuel boiler, with integrated capture of the $CO_2$ streams produced during the combustion and fermentation steps. We modeled additional power requirements for oxygen provision by the ASU and for handling additional $CO_2$ throughput in the CPU. The overall additional power requirement is 2730 Btu/gal of ethanol. An additional 5,056 kg $CO_2$/hr are captured from the oxyfuel boiler, assuming a 98% capture rate. Energy and carbon balance results from the Aspen model can be found in Appendix B1.

**Figure 3-1** shows a block-flow representation of the FERMCCS and FERMOXYCCS processes with the BASE plant. In the FERMOXYCCS case, steam requirements are supplied by an oxyfuel utility boiler. Oxygen is separated from air by cryogenic distillation in the ASU and is used for combustion of fuel in the oxy-combustion unit for steam generation. The combustion stream joins the fermentation stream. In both CCS cases, the $CO_2$ is sent to the CPU for final cleanup and compression prior to pipeline transportation.

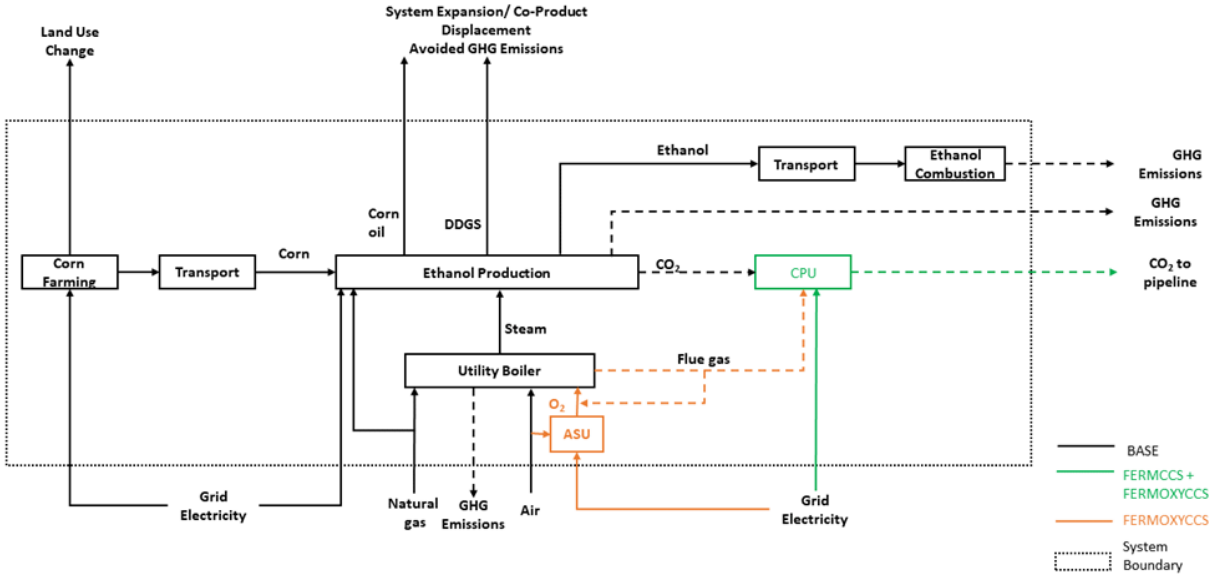


**Figure 3-1** Process configuration for integration of fermentation CCS (FERMCCS) and the oxyfuel boiler (FERMOXYCCS) with the BASE facility. The dashed box represents the system boundary for the LCA. Land use change and co-product displacement are handled via system expansion. DDGS = Dry Distillers Grains and Solids, CPU = $CO_2$ Processing Unit, ASU = Air Separation Unit.

**Techno-economic Assessment**

We perform a techno-economic assessment (TEA) to determine the minimum ethanol selling price (MESP) for each of the scenarios and cost sensitivity cases. The TEA is informed by a (1) conceptual-level process design based on research data, rigorous material and energy balance calculations via commercial simulation tools such as Aspen Plus®, (2) capital and project cost estimations using an in-house model, (3) and a discounted cash flow economic model used to determine MESP.

We adapted an in-house version of the United States Department of Agriculture (USDA) Dry Mill Ethanol Production to serve as the basis for our TEA. This model is utilized and regularly updated by the National Renewable Energy Laboratory (NREL) [306], [307]. This is a capacity factored model that uses flow rates and equipment duties to estimate the purchased cost of equipment based on reference costs and applies an installation factor to arrive the installed or inside battery limit (ISBL) capital cost. The reference costs are primarily based on detailed equipment costs reported in previous NREL cost assessments [306]–[310]. The operating expense (OPEX) calculations are also based on material and energy balance calculations using process simulations and are consistent with previously developed TEA models [307]–[310]. Raw materials include feedstocks, chemicals, catalysts, and utilities. All costs are adjusted to 2020

U.S. dollars using the U.S. Bureau of Labor Statistics's Labor Cost Index [311] and Chemical Cost Index [312] as well as the Chemical Engineering Plant Cost Index [313].

We perform a discounted cash flow analysis using the financial assumptions shown in **Table 3-1**. The MESP is the minimum fuel selling price necessary to generate a net present value of zero assuming a 10% after tax return on equity

**Table 3-1** Main assumptions of ethanol economic analysis

| **Economic parameters** | **Assumed basis** |
|---|---|
| **Basis year for analysis** | 2020 |
| **Debt/equity for plant financing** | 60%/40% |
| **Interest rate and term for debt financing** | 8%/10 years |
| **Internal rate of return for equity financing** | 10% |
| **Total income tax rate** | 21% |
| **Plant life** | 20 years |
| **Construction period** | 3 years |
| **Fixed capital expenditure schedule (years 1–3)** | 32% in year 1, 60% in year 2, 8% in year 3 |
| **Start-up time** | 0.5 year |
| **Revenues during startup** | 50% |
| **Variable costs during startup** | 75% |
| **Fixed costs during startup** | 100% |
| **Outside battery limit (OSBL) costs** | 10.5% of ISBL |
| **Total installed cost (TIC)** | Total of ISBL and OSBL costs |
| **Indirect costs** | % TIC |
| *Prorated expenses* | 10% |
| *Home office and construction fees* | 25% |
| *Field expenses* | 10% |
| *Project contingency* | 10% |

| | |
|---|---|
| **Total plant cost (TPC)** | TIC + Indirect Costs |
| **Other costs (start-up and permitting)** | 10 % TPC |
| **Total capital investment (TCI)** | TPC + Other costs |
| **Working capital** | 5% TPI |

**Table 3-2** shows estimated capital costs, operating costs, and product prices used in the cash flow analysis to calculate the MESP. Feedstock, electricity, fuel costs, and co-product selling prices are scaled to 2020 dollars from costs representative of a 2016 base year. The $CO_2$ capture costs were scaled from reported costs from the Archer Daniel Midland Demonstration in Decatur, IL [314] based on the Aspen Plus energy and mass balance. Similarly, the ASU costs and assumptions are scaled from Air Liquide Engineering and Construction Technology Handbook [315]. No additional plant employee was assumed to run the plant under intervention scenarios. In the FERMOXYCCS scenario, the boiler installation factor was increased from a factor of 3 to 4. Detail on the $CO_2$ capture cost model is reported in SI, Section S3.

**Table 3-2** Capital and OPEX assumptions and costs (2020 USD Basis)

| **Capital Costs** | |
|---|---|
| **BASE** | |
| Total installed equipment cost (ISBL) | $74.5M |
| Total installed cost (TIC) | $82.3M |
| Total plant cost (TPC) | $127.6M |
| **Total capital investment (TCI)** | $140.3M |
| **CCS and Oxyfuel Assumptions** | |
| CCS Installed Cost (ISBL, Direct Dry Cases) | $9M |
| CCS Installed Cost (ISBL, Direct Dry with Oxy Cases) | $11.2M |
| ASU Installed Cost (ISBL, Direct Dry Cases) | $10.6M |
| CCS Utilities and Labor (Scaled from ADM Decatur, IL) | +33% & +35% of ISBL |
| **OPEX Assumptions** | |
| Fixed operation costs | $7M/yr |

| | |
|---|---|
| Corn | $3.30/bushel |
| Electricity (Midwest) | $0.072/kWh |
| Electricity use for $CO_2$ Compression (Direct Dry) | 110 kWh/tonne-$CO_2$ |
| Natural Gas | $4.20/mmBtu |
| **Co-product** | **Selling price** |
| DDGS | $0.074/lb |
| Corn Oil | $0.28/lb |

**Life Cycle Assessment**

The goal of the life cycle assessment is to quantify the incremental change in the well-to-wheel carbon intensity (CI) of corn fuel ethanol from a dry mill ethanol refinery resulting from the integration of CCS and an oxyfuel combustion boiler. We consider the impact of these interventions relative to a BASE refinery where a conventional natural gas-fired industrial boiler is used and CCS is not employed. The results are not intended to represent a particular ethanol mill, but are generally representative of a modern dry mill ethanol facility in the midwestern United States. The life cycle inventory for BASE is drawn from Argonne National Lab's GREET.net 2019 model (see Appendix B2 for further details) [302]. Ethanol and co-product yield as well as baseline and intervention scenario thermal energy and power requirements have been calculated using Aspen model results and calibrated where necessary to ensure consistency between the techno-economic model and the LCA model, The functional unit for a life cycle assessment quantifies the function of a product system, and is a reference unit for reporting of results (ISO 14040). For this study, life cycle results and comparisons are made on the basis of 1 MJ of ethanol measured as the lower heating value (LHV), as this allows for reasonable comparisons between liquid transportation fuels and conforms to relevant policy contexts such as California's Low Carbon Fuel Standard.

The system boundary in a life cycle assessment specifies which unit processes are modeled explicitly in the product system (ISO 14044). Clear definition of the boundary is important to assure consistency in product system comparison. For this analysis, the system includes production of corn at the farm, transportation of corn from farm to refinery, production of ethanol from the corn starch, and transport of finished ethanol product to blending/denaturing facility (see **Figure 3-1** above). While we do not consider the impact of blending and denaturing in this analysis, we consider the final combustion of the ethanol and assume that all embodied biogenic carbon returns to the atmosphere at $CO_2$.

Treatment of multifunctionality: Dry mill corn ethanol refineries produce DDGS and often corn oil co-products alongside ethanol. The question arises as to how to allocate emissions and other life cycle impacts between products and co-products. Typical options include system expansion

to account for market displacement of co-product alternatives or allocation of life cycle burdens proportionally by energy content, mass, or market value. We opt for system expansion. Ethanol carries all environmental benefits and burdens of production while co-products are assumed to displace similar products in the market. This choice conforms to the practice under the California LCFS program methodology whereby DDGS is assumed to displace alternative agricultural feed. The type and mass of feed displaced relative to the total mass of DDGS is corn (78%), soybean meal (31%), and urea (2.3%). Note that due to displacement ratios greater than 1, the above weight percentages exceed 100%. Corn oil displaces soy oil on a 1:1 basis. Similarly, we adopt system expansion to include direct and indirect land use change (LUC) impacts of corn production, as quantified in the most recent CA-GREET 3.0 model under the LCFS program.

Biogenic $CO_2$ emissions are assumed to be "net zero"—that is, we assume that annual crops such as corn will uptake equivalent quantities of $CO_2$ in the next growth cycle, thus carbon originating in corn feedstock adds no net $CO_2$ to the atmosphere.

### 3.2.3 Results and Discussion

We first present the results of the life cycle assessment (LCA) of BASE, FERMCCS, and FERMOXYCCS scenarios followed by the results of our economic analysis. For benchmarking, we first compare our BASE LCA results to industry data. The approved fuel pathways database for California's LCFS program reports GHG emissions intensities (CI scores) for corn-only dry mill ethanol facilities ranging between 53 and 86 $gCO_2e/MJ$. The mean certified CI is 70.2 $gCO_2e/MJ$ [316]. Our BASE scenario yields a CI of 57 $gCO_2e/MJ$, comparable to facilities participating in the LCFS program. Corn production is responsible for the largest share of life cycle emissions, followed by onsite natural gas combustion to fire the boiler and dry the DDGS co-product. LUC emissions are the next largest contributor to the CI score followed by electricity generation. Avoided emissions credits awarded for co-product displacement reduce the overall CI in all three scenarios by 11.8 $gCO_2e/MJ$. Tailpipe $CO_2$ emissions from combustion of the ethanol are assumed to be net zero, due to the biogenic origin of the carbon.

FERMCCS yields a CI of 24 $gCO_2e/MJ$, approximately half that of BASE. Emissions from electricity generation increase by 44% due to the extra power required for dehydration and compression of captured CO2. Approximately 36 $gCO_2/MJ$ are captured from the fermentation stage by the CCS system. Onsite combustion of natural gas remains the largest share of onsite facility emissions, accounting for 21 $gCO_2e/MJ$.

FERMOXYCCS targets $CO_2$ emissions both from the fermentation column and the oxyfuel boiler. This scenario yields a CI of 15 $gCO_2e/MJ$, a 75% reduction from BASE. Additional grid power is required for the ASU and to dehydrate and increased duty on the CPU from the combined fermentation and oxyfuel combustion streams. This results in a 108% increase in emissions from electricity generation. However, the boiler combustion emissions are reduced by 62% through integration of the oxyfuel boiler and the CCS system. The remaining 38% of natural gas combustion emissions are associated with the direct dry DDGS system and are uncaptured in this configuration. An alternative case of indirect steam drying of DDGS allows for capture of most of the emissions from natural gas combustion. We present results for this steam dry scenario in the Appendix B2.2. However, we preview the CI result in the sensitivity

analysis section below. The captured fermentation $CO_2$ remains unchanged in all CCS scenarios at 36 $gCO_2/MJ$.

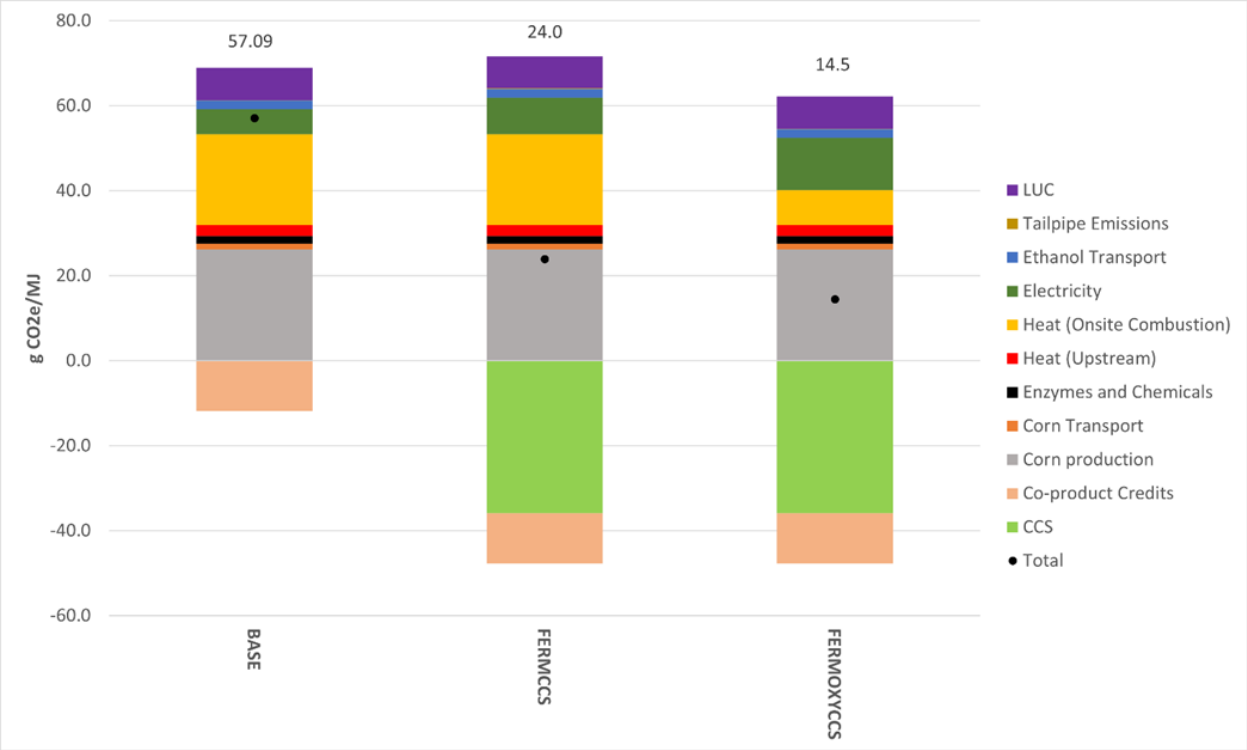


**Figure 3-2** Life cycle carbon intensity (CI) of three ethanol process configurations BASE = Baseline facility with direct drying of DDGS, FERMCCS = CCS on fermentation gas only, FERMOXYCCS = Oxyfuel boiler added with CCS on both fermentation and boiler flue gas streams, CCS = Carbon Capture and Sequestration, LUC = Land Use Change (Direct + Indirect).

We next assessed the relative costs of CCS in both intervention cases. We benchmarked the MESP for the BASE scenario to the Ethanol Profitability Model developed by Iowa State University Extension Office [317]. Between January 2020 and December 2021, the model reports monthly average spot prices between \$0.77-\$3.12/gallon, with an average market price of \$1.70/gallon. Production costs over the same period range between \$1.81-\$2.03/gallon. The MESP resulting from our TEA of the BASE scenario is \$1.93/gallon, comparable to the benchmark estimates.

FERMCCS includes added capital costs from the CPU and additional OPEX costs associated with increased grid power demand and $CO_2$ transport and storage. These additional costs result in a MESP of \$2.08/gallon. The 58% reduction in CI score in this scenario comes at a cost of \$52/$tCO_2e$ avoided. We compare our estimated costs to IEA estimates for bioethanol CCS, which estimates the breakeven cost between \$25-\$35/$tCO_2$ captured [318]. Note, that the cost of $CO_2$ captured (and stored) and the cost of $CO_2$ abatement are different measures. Our costs reflect the latter metric, which is the cost of the net reduction in emissions resulting from integration of the CCS system across the life cycle. Additional emissions from grid electricity negate a fraction of the $CO_2$ captured, thus the cost of $CO_2$ abated will be greater than the cost of

$CO_2$ stored. Moreover, the IEA estimate does not include transport and storage cost, which we model at $10/tCO2. When these differences are accounted for, our modeled cost is reasonably consistent with the upper range of the IEA estimate.

FERMOXYCCS incurs additional CAPEX for a larger CPU, the ASU, as well as higher costs for the oxyfuel boiler. OPEX increases due to additional power demand as well as additional $CO_2$ handling costs. This scenario yields an MESP of $2.24/gallon. The 65% reduction in CI relative to BASE comes at a cost of $85/t$CO_2$e avoided. The oxyfuel boiler component of the avoided emissions comes at a cost of $154/t$CO_2$e. While this is significantly higher than published estimates of post-combustion capture using conventional methods such as amine solvents estimated to be under $100/t$CO_2$ [289], [319], most capture system cost-estimates are for much larger systems (e.g., on the order of 1 Mt$CO_2$/y) rather than the 139 kt$CO_2$/y captured here. In addition, because carbon removal in an oxyfuel boiler comes at the expense of greater electricity use, a lower carbon-intensity grid could improve the cost competitiveness of this approach. We explore this possibility in section 3.1.2. A comparison of MESP and cost of GHG abatement is shown in **Figure 3-3**.

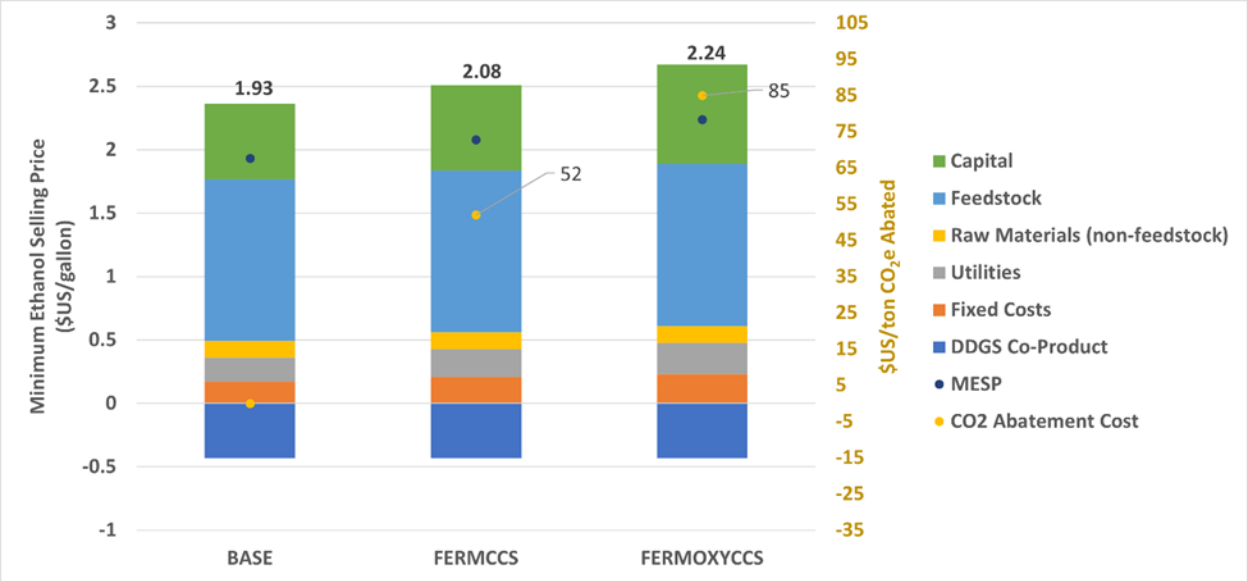


**Figure 3-3** MESP and cost of GHG abatement in the BASE, FERMCCS, and FERMOXYCCS scenarios. There is no abatement or related cost in the BASE case. BASE = Baseline facility with direct drying of DDGS, FERMCCS = CCS on fermentation gas only, FERMOXYCCS = Oxyfuel boiler added with CCS on both fermentation and boiler flue gas streams, CCS = Carbon Capture and Sequestration.

#### 3.2.3.1 Sensitivity Analysis

##### *3.2.3.1.1 Carbon intensity*

Ethanol facilities will differ in geography, process design, and intersection with power and fuel markets. We identified grid carbon intensity, oxyfuel $CO_2$ capture efficiency, thermal energy

demand, and natural gas CI as key sensitivities to test. We test these sensitivities on FERMOXYCCS only. Results are shown in **Figure 3-4**. We omit sensitivities not directly relevant to the oxyfuel and CCS system. The aim is to highlight the incremental benefits and costs of the modeled interventions rather than to precisely model all potential well-to-wheel life cycle scenarios for ethanol.

For electricity, we test a hypothetical zero marginal emissions electricity source (e.g. hydro) and the average distributed U.S. Central / Southern Plains Mix at 730 $gCO_2e/kWh$. The latter case is the only average grid CI greater than MROW in GREET and is greater by a factor of 1.2x. In the low-CI test, the CI of ethanol is reduced to 2 $gCO_2e/MJ$. The high-end test yields a CI of ethanol of 17 $gCO_2e/MJ$.

We also test capture efficiency of the oxyfuel $CO_2$ stream. Capture efficiency performance will be affected by transient operations (e.g., start-up and shut down), during which operations the boiler may be operated on air and the flue gas vented. Boiler capture efficiency is already assumed to be 98%, thus we do not consider a high-end case. A low-end case where 90% of the $CO_2$ from the oxyfuel boiler is captured yields an ethanol CI of 17 $gCO_2e/MJ$.

Thermal energy requirements in ethanol facilities have trended downwards as reflected in a recent GREET retrospective published by Lee et al [320]. The low-end thermal energy requirement tested here reflects the 2017 update to GREET model at 26,487 Btu/gal, approximately 9% lower than BASE. The high-end case tests a thermal requirement of 32,043 Btu/gal which is the assumption in the 2016 iteration of the NREL ethanol cost model that served as the basis of the TEA [307]. This requirement is just over 10% higher than BASE. The thermal energy requirement has a dynamic effect on FERMOXYCCS CI. Upstream natural gas emissions as well as ASU and CPU power demand are positively correlated with increased or decreased thermal requirements. Although BASE boiler emissions are correlated with the thermal requirement, CCS abatement is largely correlated, as well. With respect to the boiler, only the change in leakage (~2%) as a result of throughput materially impacts the CI sensitivity. The low-end thermal requirement yields a CI of 12 $gCO_2e/MJ$. The high-end case yields a CI of 17 $gCO_2e/MJ$.

Of the parameters tested, the CI of ethanol is most sensitive to the CI of the boiler fuel. The modeled scenarios assumed natural gas from both North American shale (51.5%) and conventional recovery (48.5%). Methane leakage from the shale portion is assumed to be 0.6% while leakage from the conventional portion is assumed to be just over 2% [302]. The upstream CI of this natural gas is 7.3 $kgCO_2e/mmBtu$. For the low-end estimate, we assume procurement of renewable natural gas (RNG) from landfill gas with an upstream CI of -49.3 $kgCO_2e/mmBtu$. The negative value arises from avoided landfill emissions in the GREET model. Recent remote sensing analysis of natural gas recovery in the Permian Basin found methane leakage rates as high as 8% [321]. For the high-end case, we assume an 8% leakage rate with natural gas procured from conventional recovery only, increasing upstream CI to 61.3 $kgCO_2e/mmBtu$. The low-end test case yields an ethanol CI of -6 $gCO_2e/MJ$. The high-end case yields and ethanol CI of 4 $gCO_2e/MJ$.

In our scenario design, we modeled an alternative process configuration whereby DDGS is dried indirectly by the steam cycle. We present the scenario results here alongside the sensitivity analysis. A full set of results for the steam dry scenario to include a steam dry BASE, FERMCCS, and FERMOXYCCS can be found in Appendix B, **Figure B2**. Alternative mass and energy balances can be found throughout the tables in S1.2 under Scenario 2. The essential difference in this scenario is that all natural gas combustion occurs in the oxyfuel boiler for steam generation rather than diverting a portion to a direct dry system. This configuration allows for increased capture of $CO_2$ from natural gas combustion. In **Figure 3-4** below, we show that this configuration is improved relative to the direct dry system with a CI of 9 $gCO_2e/MJ$ or 39% lower than direct dry FERMOXYCCS and 85% lower than direct dry BASE.

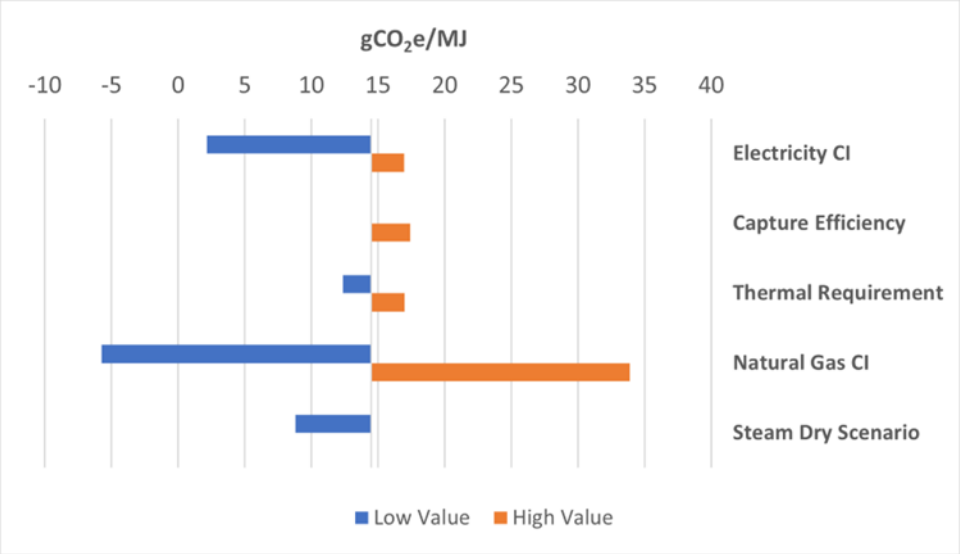


**Figure 3-4** Results of the carbon intensity sensitivity analysis. The Steam Dry case is not a sensitivity but rather an alternative configuration burns all natural gas in the oxyfuel boiler and DDGS is dried indirectly using steam heat. This case is presented alongside the sensitivities for comparison purposes. See Appendix B2 for more details.

Finally, we assess the impact of all these interventions combined on corn ethanol production. The left side of **Figure 3-5** illustrates a progression of emissions reductions from the BASE facility to include FERMCCS, FERMOXYCCS, steam drying, renewable electricity, and renewable natural gas. This system has a carbon intensity of -26 $gCO_2e/MJ$. Without RNG, CI is -6 $gCO_2e/MJ$, while without renewable electricity CI is 9 $gCO_2e/MJ$. However, we note that some existing corn and sugar ethanol facilities already have a CI lower than the BASE scenario modeled here and, with the addition of CCS on fermentation and stack emissions, could achieve negative CI scores with fewer interventions. The right-hand side of **Figure 3-5** illustrates this potential using the benchmark LCFS ranges discussed previously. Some of these facilities already utilize interventions such as renewable heat and power. For instance, the low range CI score depicted by the gray bar (53 $gCO_2e/MJ$) is utilizing landfill gas. Moreover, given lower CI electricity, the incremental improvement of an oxyfuel CCS system will be greater than the shift depicted below. Other CCS configurations (e.g., post-combustion capture) might achieve similar results. While carbon negative sugarcane ethanol has been proposed [108], to our knowledge, we

are the first demonstrate in the academic literature that corn ethanol production systems could result in net-negative emissions, removing $CO_2$ from the atmosphere over the entire fuel life cycle.

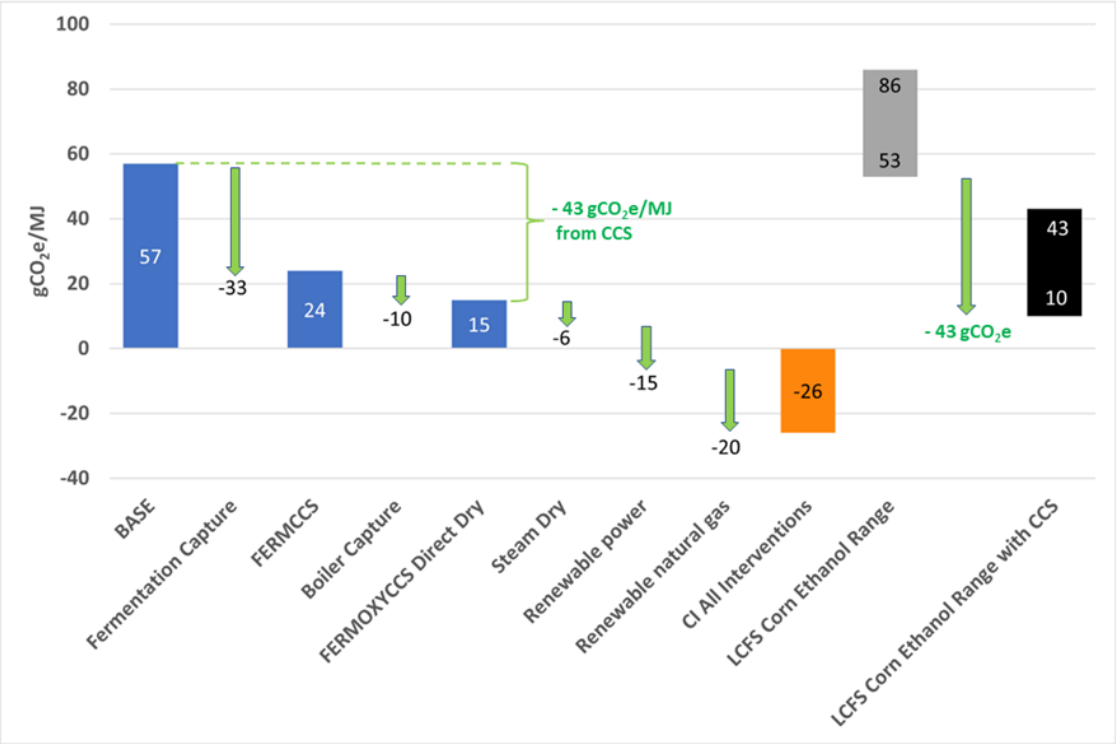


**Figure 3-5** Carbon-negative ethanol can be achieved assuming all interventions. We adjust the range conservatively using the "net" CI reduction of the direct dry case which accounts for the additional power required for oxycombustion rather than the "gross" CO2 captured.

#### *3.2.3.1.2 Cost of emissions abatement*

Any change in CI of the ethanol facility also results in a change in cost of carbon abatement for most cases, as both the BASE and FERMOXYCCS CI scores are affected. CAPEX and OPEX may be altered, as well as the distribution of costs over shifting relative CI reductions between BASE and FERMOXYCCS. The tested sensitivities primarily impact costs related to boiler capacity, ASU and CPU energy demand, and $CO_2$ transport and storage. A summary of unit cost of emissions abatement sensitivities is shown in **Figure 3-6**.

The electricity CI sensitivity impacts the relative CI difference between BASE and FERMOXYCCS primarily by impacting carbon emissions associated with additional power requirements for the ASU and CPU. The low emissions case lowers abatement cost to $73/ton CO2e, while the high emissions case increased abatement cost to $87/ton $CO_2$e. Notably, the low CI electricity case reduces the $CO_2$ avoidance cost of the oxyfuel boiler component to $116/t$CO_2$e. Electric grid decarbonization or purchase of renewable power (at a similar cost) can contribute to greater cost competitiveness of oxycombustion relative to post-combustion capture.

Low $CO_2$ capture efficiency trades off lower $CO_2$ clean-up and handling costs with lower overall abatement. Because costs in this case are spread over a smaller magnitude of $CO_2$ reduction, the cost of emissions abatement increases to \$88/t $CO_2$e.

The change in thermal energy requirement has a dynamic effect on both costs and the emissions differential between the BASE and FERMOXYCCS scenario. OPEX is positively correlated with the thermal requirment, in both BASE and FERMOXYCCS. In BASE, this is entirely fuel cost. In FERMOXYCCS, ASU and CPU capacity CAPEX and OPEX power demand are also affected, as well as $CO_2$ handling costs. Boiler emissions increase or decrease in the BASE scenario in the high and low cases. Captured boiler emissions increase or decrease in the FERMOXYCCS scenario. Boiler capture leakage (2%) alters the relative abatement between the two cases. Upstream natural gas emissions are altered in both cases, but the impact is equivalent and does not affect the unit cost. In the low thermal energy requirement case, the cost of $CO_2$ abatement decreases to \$82/t $CO_2$e while in the high thermal energy case, the cost increases to \$87/t $CO_2$e.

The upstream CI of natural is a fixed component and equivalent in both BASE and FERMOXYCCS cases in both the high and low sensitivity tests. As such, the unit cost of abatement is unaltered. Real-world costs for low-CI RNG are likely to be greater than conventional natural gas. While this would impact MESP, it would have no effect on the unit cost of abatement in the sensitivities as tested here because these costs would be equivalent in both BASE and FERMOXYCCS.

In the alternative steam dry scenario, the cost structure of $CO_2$ abatement for FERMOXYCCS has significant differences to the direct dry BASE case. In this scenario, the boiler is sized larger to accommodate combustion of all natural gas for steam production. There are increased CAPEX costs for the larger boiler and increased demand on the ASU and CPU in FERMOXYCCS to handle both more fuel throughput in the boiler and greater volumes of $CO_2$ in the capture stream. $CO_2$ transport and storage cost OPEX increases, as well. Although this configuration results in a much lower overall CI, the cost of carbon abatement is increases by approximately 6% relative to the direct dry FERMOXYCCS. The cost of carbon abatement is estimated to be \$90/t$CO_2$e. (More on the steam dry case can be found in the SI, S1.2 & S2.2).

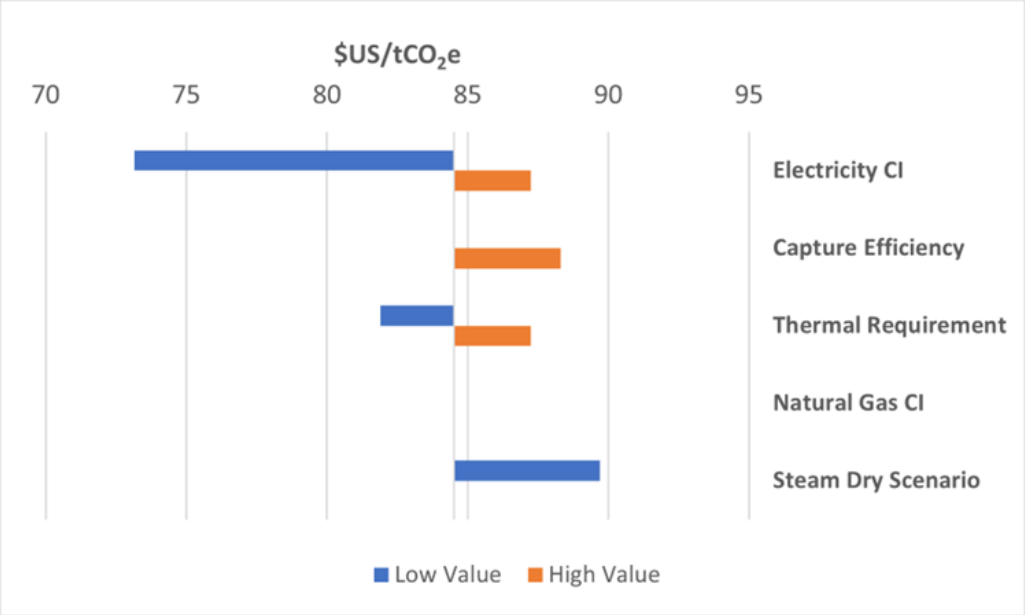


**Figure 3-6** Sensitivity of carbon abatement costs to CI sensitivity scenarios. The alternative steam dry configuration is presented here as a sensitivity.

#### *3.2.3.1.3 CAPEX and OPEX Sensitivities*

Here we test the sensitivity of the MESP of the FERMOXYCCS system to variation in key CAPEX and OPEX assumptions (see **Figure 3-7**). We tested CAPEX sensitivities only on the major components unique to FERMOXYCCS system relative to the BASE system. We apply a +/- 20% variation to the oxyfuel boiler, CPU, and ASU quoted costs before scaling factors for installation, equipment size and cost index adjustments are applied. Similarly, feedstock, utilities, labor, and co-product revenues are the largest contributors to OPEX, with each category representing >10% of total operating costs. We apply a +/- 20% variation to base year costs to test the impact on the MESP relative to capital costs.

The sensitivity of the MESP ($2.24/gallon) to capital costs is modest. Individual CAPEX components move the MESP by less than 1%. The combined sensitivity on the oxyfuel boiler, CPU, and ASU results in MESP ranging between $2.21-$2.28/gallon. Electricity and natural gas both individually impact MESP by -0.9% to 1.3% yielding ranges between $2.22-$2.27/gallon. Labor has a similar impact yielding MESP between $2.21-$2.28/gallon. The most significant impacts result from feedstock price sensitivity and the selling price of the DDGS co-product, yielding MESP in the ranges of $1.98-$2.51/gallon (+/- 12%) and $2.16-$2.33/gallon (+/- 4%) respectively.

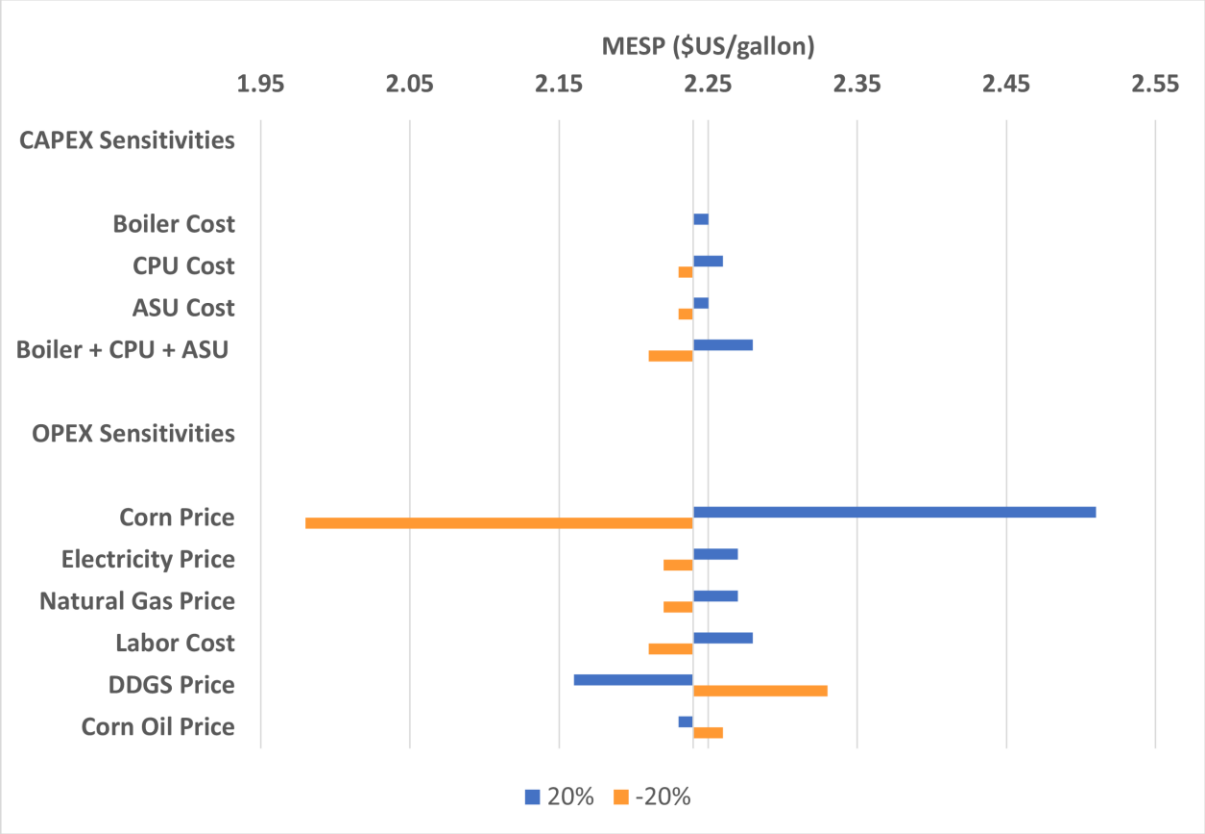


**Figure 3-7** Sensitivity of MESP to a +/- 20% adjustement of CAPEX and OPEX assumptions.

#### *3.2.3.1.4 Impact of policy support on MESP*

Several state-level low-carbon fuel policies currently enacted in the U.S. have played a substantial role in the development of new low-carbon fuels projects. The California LCFS, in particular, has incentivized improvements in fuel CI in existing and proposed conventional ethanol facilities, as evidenced by the influx of program applicants and a steady trend in declining CI scores of approved production pathways [322]. Thus, we elected to test the sensitivity of FERMOXYCCS MESP scenario to a low and high policy support market environment. We model policy incentives on the two most prominent policies in the U.S. context, California's Low Carbon Fuel Standard (LCFS) and U.S. 45Q tax credit.

The LCFS is a performance-based standard that created a market for alternative fuel producers to sell avoided emissions credits. These credits are calculated based on the difference in CI between the alternative fuel and a state-mandated threshold for the average CI of fuels sold in the state. These credits can be sold to obligated fuel producers participating in the market such that fuels exceeding the CI threshold are brought into compliance. The $gCO_2e/MJ$ differential is converted to credits functionally equivalent to "tonnes of $CO_2e$ avoided" based on the energy content of volumes of fuel sold into the market. As of 2022, the CI threshold for gasoline (for which ethanol is a substitute) is $89.5gCO_2e/MJ$. The modeled FERMOXYCCS facility would produce 244,530 credits per year based on production of 38.9 MMgal/yr (~3.2 billion MJ). See Appendix

B4 for the LCFS credit calculation equations. Between July 2021 and May 2022, LCFS credit prices fell from $187 to $115 per tonne. Informed by this, we model a low policy support scenario at a credit price $100/tonne and a high policy support scenario credit price of $200/tonne.

Fuel projects that incorporate CCS can also participate in the federal U.S. 45Q tax program. This policy stacks with LCFS revenues. U.S. 45Q is intended to incentivize carbon capture projects which result in permanent sequestration or utilization. As of May 2022, the highest incentive was for geologic sequestration, which awards a $50/ton credit for the first 12 years of operation. We model this value stacked with the LCFS in our low policy support scenario. we model an increase in the tax credit consistent with recent legislative adjustments to U.S. 45Q, increasing the credit to $85/ton. The modeled FERMOXYCCS facility would capture and sequester 139,432 $tCO_2e$ /year. The resulting MESP for the stacked low policy support case is $1.45/gal. While the high policy support case reduces the MESP to $0.70/gal. Holding the U.S. 45Q credit fixed at $50/$tCO_2$, we also varied the LCFS credit to find the breakeven value with the BASE case (MESP = $1.93/gal). Breakeven occurs at an LCFS credit price of $26 per tonne.

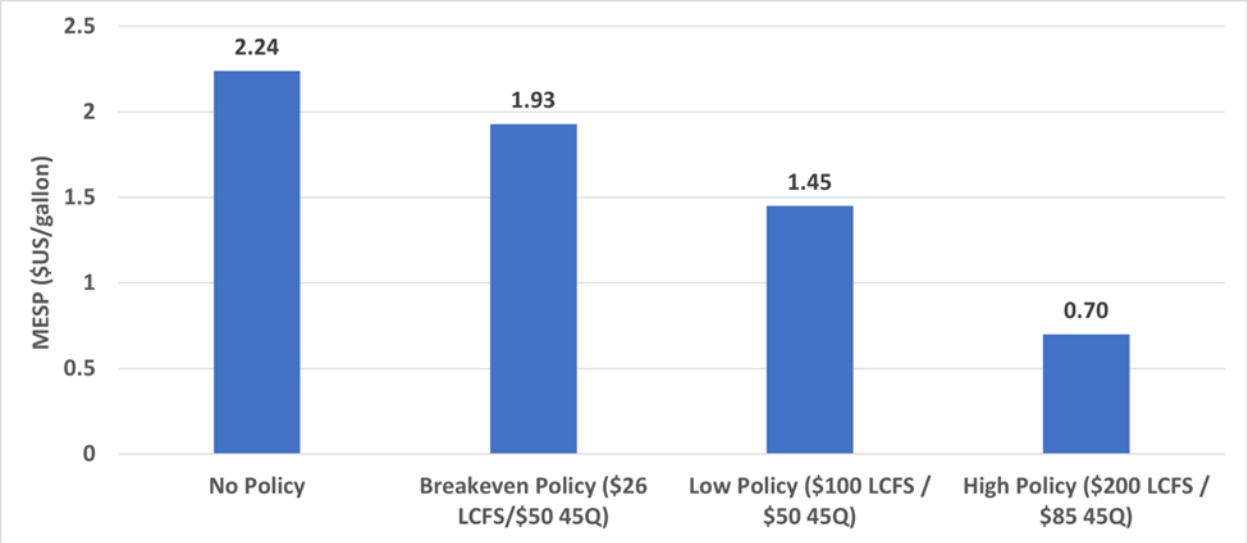


**Figure 3-8** Sensitivity of MESP to policy support. LCFS = California Low-carbon Fuel Standard, 45Q = U.S. 45Q Tax Credit.

#### *3.2.3.1.5 Discussion*

Ethanol continues to play an important role as the most ubiquitous biofuel alternative to gasoline. The industry has the potential to play an even greater role in decarbonizing the transport sector through continued improvements in life cycle emissions. Decarbonization of light transport and performance-based low-carbon fuels policy incentives may soon favor electrification over liquid fuels. Nonetheless, low-carbon ethanol can serve as an important low-carbon platform in other market segments where policy support for CI performance exists such as sustainable aviation fuels or where it may soon exist, such as the chemicals and polymers industries [323]. There is ample runway to further improve the CI of existing capacity and reduce the costs of doing so

while maintaining the cost and CI competitiveness of ethanol as a sustainable transportation fuel. We are mindful of potential limits to the sustainable utilization of first-generation (food-based) crops for fuel production which will depend on the extent to which agricultural yields can meet increasing demand without deleterious effects on land and food systems. However, the findings herein are generally applicable to ethanol production from many potential feedstocks with lower sustainability risk and greater CI reduction potential than conventional corn. Applied to existing sugarcane and emerging cellulosic supplies of feedstock, the carbon removal potential of the ethanol industry is substantial.

The "low-hanging fruit" for corn ethanol refineries remains integration of CCS to capture and store biogenic $CO_2$ from the fermentation process. This analysis along with other studies and commercial projects have demonstrated the technical and economic potential of this option. The low cost of $CO_2$ capture from fermentation relative to other $CO_2$ sources can help to facilitate learnings on carbon management and play a role in the development of a rapidly growing carbon removal and storage industry. Even so, conventional ethanol with fermentation CCS is still far from carbon neutral. If ethanol is to continue to play a role in deep decarbonization and achieving climate stability targets, the CI of ethanol must continue to be driven down.

Process and fuel interventions that address fossil emissions associated with heat and power represent another promising opportunity to realize very low carbon or even carbon negative ethanol. Several options to address those emissions have been analyzed here. CCS on oxyfuel boiler and fermentation emissions can reduce ethanol carbon intensity by as much as 71% at prices under \$100/ton $CO_2$e. Moreover, sensitivity analysis has demonstrated that in combination with other interventions such as renewable energy and fuel switching to bio-derived fuels, conventional ethanol refineries can produce carbon neutral or even negative fuel, potentially at profit under existing policy support.

Integration of oxyfuel combustion and CCS at ethanol facilities will present unique challenges and opportunities for learnings. Further research, process engineering design, and demonstration will be necessary to understand the full potential and compare with the technical and economic feasibility of alternative interventions. Further research could investigate alternatives to oxyfuel combustion such as increased electrification of refinery heat demand, improved efficiency, pre-combustion and post-combustion CCS configurations, and alternative bio-heat production (e.g. anaerobic digestion) such that additional synergies and opportunities may be realized. Each could present new opportunities to further reduce the CI of conventional biofuels.

# CHAPTER 4. TARGETING BIOMASS RESOURCES AT HARD-TO-ABATE SECTORS

## 4.1 Preface

This chapter explores the essential role of the bioeconomy in addressing aviation emissions via the production of low-carbon and carbon negative sustainable aviation fuel (SAF). Aviation is widely recognized as a "hard-to-abate" sector of the economy, with few near-term substitutes for fossil fuels and a significant growth trajectory between now and 2050.

Internationally, the aviation sector has committed to reducing net air transport emissions to 50% of 2005 levels by 2050 and to carbon neutral growth from 2020 onward [340]–[342]. Until recently, aviation has relied on carbon offset programs to realize emissions reductions. The Carbon Offsetting and Reduction Scheme for International Aviation (CORSIA) standard laid the groundwork for aviation offsets, but the standard also laid the groundwork for a direct solution through the development of renewable drop-in fuels (SAF) to replace fossil jet fuel. National policy in the European Union and United States, among other nations, have embraced regulations and supportive policies to incentivize SAF production and adoption in alignment with CORSIA.

SAF alternatives are not created equal. Multiple biochemical and thermochemical processes and feedstocks can yield SAF with differing implications for sustainability, climate, logistics, and cost. Most SAF today is a product of waste vegetable and animal oil refinement using the HEFA process. However, given the intersection of vegetable oils with food systems and limited supply of waste oils, HEFA SAF is unlikely to remain sustainable at scale. Other conversion processes and feedstocks may offer greater sustainability and cost advantages. In this chapter, I analyze the technical readiness, cost, scalability, and emissions reduction potential of multiple SAF technologies with particular focus on climate impact, potential for carbon removal, and intersection with existing supportive policy frameworks. To our knowledge, this is the first cross- comparison of its kind.

## 4.2 A comparison of sustainable aviation fuel pathways across emissions, cost, and feedstock sustainability criteria[4]

### 4.2.1 Introduction

Aviation is widely recognized as of the most challenging sectors of the economy to decarbonize [324]. Domestic and international aviation made up approximately 1.9% of global emissions and 9% of transportation emissions in 2020 [325], [326]. The aviation sector is responsible for as much as 4% of global warming that has occurred to date [327], [328] with non-$CO_2$ effects, primarily comprised of NOx induced $CH_4$ formation, contrails, and contrail cirrus formation responsible for more than 50% of that warming [329].

[4] Full authorship for this chapter is as follows: Dees, J.P, Karris, S., Sanchez, D.L, Belmont, E.B., Psarras, P., Friedman, J., McCormick, C.

Decarbonization options available to land-based transport are not viable for aviation in the near-term. Battery electric aircraft contend with low energy density [330], with equivalent battery energy weighing 30 times more than jet fuel [331]. Electrification of aircraft via hydrogen fuel cell shares similar energy density challenges, limiting the technology to short-range segments. Hydrogen combustion as an aviation propellant overcomes the range issues of batteries and fuel cells; however, hydrogen fuel necessitates a full redesign of aircraft and airport infrastructure that is likely many decades away [332]. Due to the constraints on decarbonization in the aviation sector, low-carbon drop-in fuels, termed broadly "sustainable aviation fuel" or SAF, are the most viable near-term option for deep decarbonization of the sector. For the purposes of this analysis, SAF refers to a variety of biomass-derived kerosene-like fuels. We also include synthetic fuels produced from $CO_2$ under the SAF umbrella.

Despite the need for SAF fuels, very little supply exists today. In 2019, less than 200,000 tonnes (6 million gallons) of SAF were produced globally, which corresponds to less than 0.1% of the ~300 million tonnes (90 billion gallons) of aviation fuel used globally [333]. Virtually all of this SAF fuel was produced from waste vegetable oils and fats utilizing the HEFA process, which has very limited scale-up potential due to feedstock economics and sustainability [334], [335]. Alternatives to HEFA SAF such as Fischer-Tropsch (FT) fuels and alcohol-to-jet (ATJ) are nearing commercialization while more nascent technologies remain in the pilot phase [334].

A range of biochemical and thermochemical conversion processes can produce SAF from agricultural residues, waste and non-edible oils, forest residues, municipal solid waste, and point source or atmospheric $CO_2$. The American Society for Testing and Materials (ASTM) has certified seven SAF pathways as drop-in fuels that can be blended with conventional Jet-A up to a specified blending limit, summarized in **Table 4-1** [335], [336].

**Table 4-1** ASTM certified SAF pathways and fuel blending limits

| Acronym | Full Name | Blending Limit |
|---|---|---|
| FT-SPK | Fischer-Tropsch Synthetic Paraffinic Kerosene | 50% |
| FT-SPK/A | FT-SPK with Aromatic Component | 50% |
| HEFA | Hydroprocessed Esters and Fatty Acids | 50% |
| HFS-SIP | Hydroprocessing of Fermented Sugars (Farnasene) – Synthetic Iso-Paraffinic Kerosene | 10% |
| ATJ-SPK | Alcohol-to-Jet Synthetic Paraffinic Kerosene | 50% |
| ARA CHJ | Applied Research Associates Catalytic Hydrothermolysis Jet | 50% |

**Figure 4-1** shows a sampling of SAF feedstocks and conversion pathways to produce ASTM certified SAF as well as potential fuel pathways under consideration. The properties of Jet-A and SAF drop-in fuels have been covered in depth in other literature [337]. ASTM certified SAF at present is primarily paraffinic, low in aromatic content, and must be blended with conventional Jet-A.

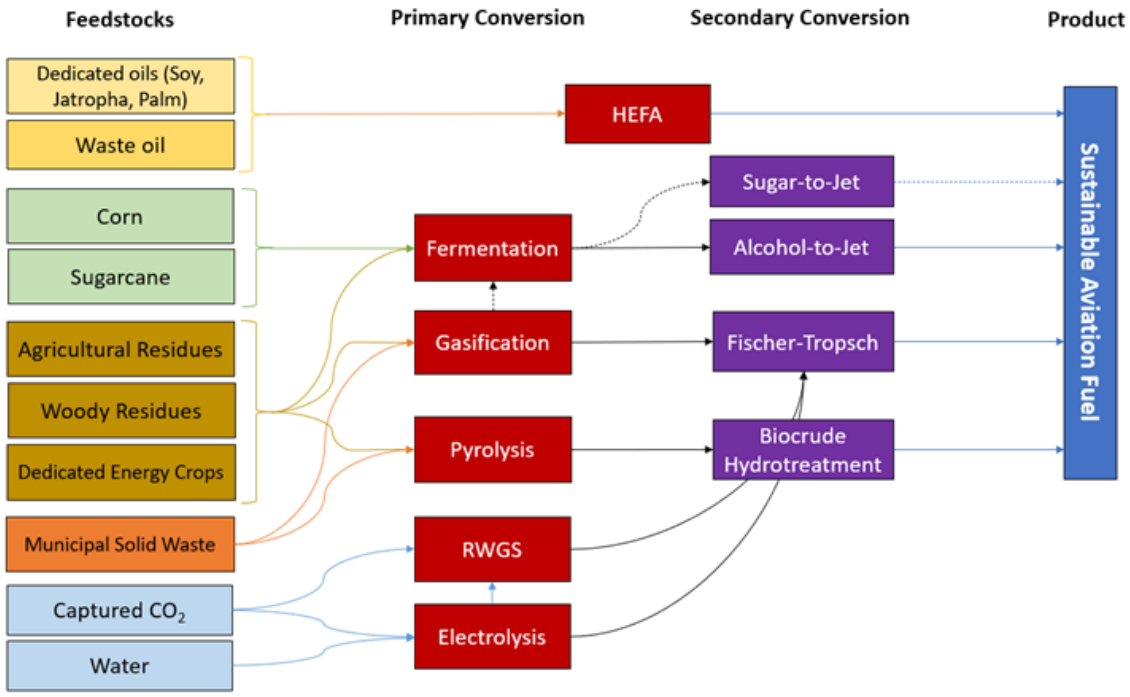


**Figure 4-1** Feedstocks and biochemical and thermochemical conversion processes or the production of sustainable aviation fuel.

Notably, carbon capture and sequestration (CCS) can be integrated with some SAF technologies with relatively minor modification to enable carbon dioxide removal (CDR). FT and ATJ conversion pathways produce high-purity streams of $CO_2$ during the product life cycle. These $CO_2$ streams represent "low hanging fruit" for CCS. In the FT process, $CO_2$ is separated after gasification in a process called acid gas removal (AGR) [338]. In the ATJ process, fermentation to produce the ethanol intermediate yields a high-purity stream of $CO_2$ requiring only dehydration and compression of the gas prior to storage [263]. CCS of fermentation $CO_2$ is a particularly low-cost opportunity that has already been demonstrated and deployed in existing ethanol refineries [339]. CDR integrated with fuel production can offset presently un-addressable climate impacts resulting from SAF blending limits and the atmospheric warming stemming from contrail emissions, making these fuels particularly attractive for near-term decarbonization of aviation.

Synthetic SAF catalytically derived from captured $CO_2$ and hydrogen, termed Air-to-Fuels (ATF) herein, is also a promising pathway for aviation. While costs of $CO_2$ capture and low-carbon hydrogen remain prohibitively high, constrained supply of sustainable biomass feedstock could make this attractive alternative in the medium to long-term.

**Policy Support for SAF**

Global institutions and industry have recognized the need to address the climate impacts of aviation. The International Civil Aviation Organization (ICAO), a specialized agency of the

United Nations, and the Air Transport Action Group (ATAG), an industry proxy, committed in 2014 to reducing net air transport emissions to 50% of 2005 levels by 2050 and to carbon neutral growth from 2020 onward [340]–[342]. These commitments include sectoral targets focused on four pillars: 1) technological improvements; 2) operational improvements; 3) market-based measures; and 4) alternative fuels [343]. Despite measurable improvements [342], technical and operational mitigation efforts have been unable to keep pace with increased activity levels in the aviation sector [344], [345]. This is due in part to the long fleet turnover cycles and the limited incremental improvements possible relative to already high fuel-efficiencies in aircraft engines [334], [342], [346]. Market-based measures and alternative fuels fall under the Carbon Offsetting and Reduction Scheme for International Aviation (CORSIA) standard. CORSIA requires airlines to offset $CO_2e$ emissions that exceed 2019 levels. These offsets can take the form of conventional carbon offsets or the purchase of CORSIA eligible fuels (CEFs) [347].

CEFs must meet several sustainability criteria to qualify. In terms of climate impacts, CEFs must achieve a life cycle carbon intensity at least 10% lower than conventional Jet A (< 80.1 $gCO_2e/MJ$ relative to 89 $gCO_2e/MJ$) based on CORSIA's life cycle accounting methodology [347]. In addition, feedstocks must be classified as renewable or wastes and must not originate from lands classified as having high carbon stocks. Sustainability criteria also include a number of stipulations to protect air, water, and soil quality as well as human rights, labor rights, land and water rights, and local food security [348]. CORSIA maintains a framework for independent sustainability certification schemes that are allowed to qualify CEFs, which as of this writing include only two organizations: 1) Roundtable for Sustainable Biomaterials and 2) International Sustainability and Carbon Certification.

CORSIA promises to offer a robust standard for SAF. The European Union moved to incorporate standards and norms of the CEF framework into the Renewable Energy Directive and Emissions Trading System. The U.S. is also a CORSIA signatory. Until recently, the U.S. had enacted little in the way of SAF policy to align with CORSIA, but the passage in 2022 of The Inflation Reduction Act (IRA) created SAF production incentives ranging from $1.25 to $1.75 per gallon for fuels meeting CORSIA life cycle criteria and achieving 50% or greater reduction in greenhouse gas emissions intensity relative to Jet-A [349]. Near-term policy support is needed across the value chain to support SAF scale-up [334], [342], [349]. Prior to the IRA, opt-in programs such as the U.S. Renewable Fuel Standard (RFS) and California's Low Carbon Fuel Standard (LCFS) were the primary incentives for SAF deployment in the U.S. [349]. These latter two policies are central to the analysis in this research and a detailed description of their impact on the economics of SAF will be discussed in later sections of this chapter. Because this research was carried out prior to the introduction of the IRA, the incentives in that legislation are absent from the analysis in subsequent sections of this chapter.

**Table 4-2** Supportive SAF policies in the U.S.

| Policy Name | Description | Financial Impact | Enactment |
|---|---|---|---|

| | | | |
|---|---|---|---|
| **Federal Renewable Fuel Standard** | A program that requires transportation fuel sold in the US to contain a minimum volume of renewable fuels. | Renewable fuels are subsidized via a tradable permit system of Renewable Identification Numbers (RINs). Average RIN values in 2020 ($/GGE) ranged between $0.25-$1.31, depending on the fuel. | Originated with the Energy Policy Act of 2005 and was expanded and extended by the Energy Independence and Security Act of 2007. |
| **Federal 45Q tax credits** | Provides a tax credit on a per-tonne basis for $CO_2$ that is sequestered. Tax credits are also available for non-EOR $CO_2$ utilization and direct air capture projects. | The Section 45Q tax credit will increase to $35 per tonne for EOR and $50 per tonne for geologic storage by 2026, available for 12 years.<br><br>Proposed CATCH act would increase to $85 per tonne for saline sequestration, and increase value to $60 per tonne for EOR. | |
| **Biomass-based diesel (also known as renewable diesel) tax credit (BTC)** | A type of federal fuel production tax credits. In its current form, qualified taxpayers may claim the tax credit, at $1.00 per gallon, when the required amount of biodiesel or renewable diesel is blended with petroleum diesel for sale or use in a trade or business. | $1.00/gallon biodiesel mixture credit [97] | BTC was created under the American Jobs Creation Act of 2004. The Further Consolidated Appropriations Act, 2020 (HR 1865) reinstated the BTC tax credit through 2022.[98] |
| **Volumetric ethanol excise tax credit (VEETC)** | A type of federal fuel production tax credits. Expired at the end of 2011. | "VEETC allows an ethanol blender that is registered with the Internal Revenue Service (IRS) to be eligible for a tax incentive in the amount of $0.45 per gallon of pure ethanol (minimum 190 proof) blended with gasoline."[99] | |
| **Alternative fuel blender's tax credit** | A type of federal fuel production tax credits | | |
| **Low Carbon Fuel Standard (LCFS) Programs** | Aim to reduce the carbon intensity (CI) of transportation fuels as compared to conventional petroleum fuels such as gasoline and diesel. | Prices in 2020 have been $125-150 / $tCO_2$-eq in Oregon and British Columbia, and in excess of $150/$tCO_2$-eq in California. | LCFS programs are operating in California, Oregon, and the province of British Columbia. Washington, the remainder of Canada, Colorado, New York, Iowa, Minnesota, and South Dakota are also considering or implementing a LCFS. |
| **Federal 40B** | A production credit to incentivize production of SAF fuels with a 50% GHG reduction relative to Jet-A | $1.25/gallon credit for fuels with >50% reduction in GHG intensity relative to Jet-A. An additional $0.01 paid out for each % reduction below 50% | Originated in the Inflation Reduction Act of 2022 |

| | | | |
|---|---|---|---|
| | | to a maximum total credit of $1.75. Sunsets in 2024 | |
| **Federal 45Z** | A production tax credit to incentivize production of SAF fuels with a 50% GHG reduction relative to Jet-A | $1.75/gallon credit for fuels with >50% reduction in GHG intensity relative to Jet-A. Replaces 40B in 2024. Sunsets in 2027 | Originated in the Inflation Reduction Act of 2022 |

## Overview

The goal of this analysis is to characterize near-term opportunities to produce SAF at scale within the context of the U.S. We ask which SAF pathways meet criteria for technology readiness level (TRL), feedstock scalability, carbon intensity (CI), and subsidized cost to meet roughly 10% of SAF demand by 2030 given existing policy support. We explore six SAF production pathways and eleven unique feedstocks. We assessed TRL by searching for evidence of existing or announced commercial or demonstration projects, by assessing the technical and commercial readiness of process components, by surveying existing literature produced by academia and U.S. National Lab reports, and expert input. We assess economically recoverable and sustainable feedstock supply using data from a national-level assessment for cellulosic feedstocks, residues, and wastes. We estimate first-generation (food-crop) feedstock availability based on market data describing capacity growth and exports. CI scores ($gCO_2e/MJ$) for SAF pathway and feedstock combinations are calculated using life cycle assessment methodologies consistent with the approach used for fuel pathways under California's LCFS. We assess costs with a technoeconomic model, drawing upon and harmonizing previous estimates in the literature to quantify the minimum fuel selling price (MFSP) as well as the unit cost of CI reductions. Both unsubsidized and subsidized MFSP are modeled, taking advantage of relevant enabling policies in the U.S. to include California's LCFS, the U.S. RFS program, and the U.S. 45Q tax incentive (for pathways involving carbon capture and sequestration).

To our knowledge, this is the first SAF assessment of its kind. Staples et al. estimated the aggregate feedstock availability, life cycle emissions impact, and the scale of investment needed for SAF through 2050 [350]. Prior studies analyzed GHG emissions alongside costs for ATJ [350] and FT SAF [338]. Moreover, the ICAO Committee on Aviation Environmental Protection (CAEP) produced a set of default CI values under the CORSIA standard for many of the SAF pathways analyzed herein, the findings of which were published after completion of this work [351]. The life cycle assessment methodology under the CORSIA standard differs from the approach taken by California's LCFS program. This independent analysis does not attempt to compare approaches. Rather, we explore SAF opportunities over the next five to ten years to highlight SAF technologies that can simultaneously achieve sustainability targets and price parity under existing policies in the U.S. In addition, carbon capture and sequestration opportunities are a key feature of many the SAF pathways investigated here. The implementation of CCS and the interaction with U.S. low-carbon fuel and CDR policies is a novel contribution of this work. We ultimately identify alcohol-to-jet (ATJ) and Fischer-Tropsch (FT) fuels using cellulosic biomass and waste feedstocks as the most promising medium to long-term opportunities to supplant HEFA, which is unlikely to remain sustainable at scale. Long-term,

Air-to-Fuels pathways may supplant biomass pathways in the face of constrained supplies of sustainable biomass. We lay out the following criteria to guide our conclusions:

- SAF pathways should be at a technology readiness level (TRL) of 6 or higher.
- SAF feedstock supply should be sufficient to sustainably scale to meet 10% of existing SAF demand by 2030.
- SAF pathways should have a 70% reduction in life cycle GHG emissions relative to fossil Jet-A.
- Subsidized SAF selling price should be $5/gallon or less. Ideally, SAF minimum fuel selling price (MFSP) should be at parity (< $2.50) with conventional Jet-A

Displacing Jet-A with SAF will likely require a portfolio approach, with no single SAF technology capable of providing sustainable supply. Thermochemical and biochemical conversion processes that yield SAF require different feedstocks, economies of scale, and logistics, thus SAF production that makes optimal use of available feedstocks is likely to vary by region and context. This analysis is not intended to describe a "best" technology, but rather to highlight the technologies with the most potential in the current U.S. context.

### 4.2.2 Materials and methods

#### 4.2.2.1 SAF Pathway Descriptions and Technology Readiness Level (TRL)

We first assessed Technology readiness level (TRL) when determining which SAF pathways to analyze in-depth. TRL definitions (See Appendix C1, **Table C1**) are adapted from the National Academies of Science, Engineering, and Medicine report *Negative Emissions and Reliable Sequestration: A Research Agenda (2019)* [42]. We initially screened for SAF pathways with a TRL of 7 or greater. The TRL 7 definition indicates a "system prototype demonstrated in a plant environment" [42]. It is important to recognize, however, that TRL includes all components of a system, from feedstock, to conversion, and where applicable, carbon capture and sequestration. Individual components of a SAF pathway could be at TRL 7 or greater, but if those components have never been demonstrated together, then a TRL 6 designation is appropriate: "Engineering/pilot-scale prototypical system demonstrated in a relevant environment" [42]. We judged that TRL 7 unnecessarily excluded pathways that could advance in technical and commercial viability rapidly. We thus adjusted our TRL criteria to 6 to allow for inclusion of commercial or nearly commercial pathways combined with CCS, even if the pathway has not been combined with CCS at demonstration or commercial scale.

SAF pathways analyzed in this research are summarized in **Table 4-3**, including summaries of the technologies, their technology maturity (TRL), feedstocks, and the status of their ASTM approval in terms of their maximum approved blending limits. NASEM 2019 [42], Mawhood 2016 [334], as well as expert judgement and observation of the SAF industry were used to determine TRL levels of SAF pathways (See **Table C2** in Appendix C1 for TRL assessments). TRL 6 criteria necessarily excluded aromatic SAF fuels that could theoretically be blended above the current ASTM 50% limits. ASTM approved HFS-SIP fuels were also excluded. While the companies Amyris and LS9 have demonstrated HFS-SIP, those projects were abandoned, and the companies are now pursuing biochemicals, cosmetics, and materials [334]. Given ASTM

blending limits of 10%, we do not consider HFS-SIP to be a major contributor to SAF at scale. All of the considered pathways yield not only SAF but also a range of other products such as synthetic diesel, naphtha, biochar, or chemicals – products commercially relevant in automotive, petrochemical, and other sectors.

**Table 4-3** SAF pathways considered in this analysis

| | HEFA | Alcohol-to-Jet (ATJ) | Fischer-Tropsch (FT) | HDCJ | Air-to-Fuels (ATF) |
|---|---|---|---|---|---|
| **Technology maturity (TRL)** | Mature (7-9) | Commercial pilot (7-8) | Commercial pilot (6-7) | In development (5-6) | In development (5-6) |
| **Technology Summary** | • A series of hydrogenation, cracking, isomerization, deoxygenation, and distillation processes to convert triglyceride feedstocks such as vegetable oils and other oil-based feedstocks, such as algae, to SAF. | • Alcohols, such as ethanol, undergo dehydration, oligomerization, hydrogenation, and fractionation. to produce SAF. The upstream production of ethanol can proceed via commercially available sugar fermentation technology, and syngas fermentation as an alternative ethanol production technology is under development. | • A catalytic chemical process that yields liquid hydrocarbon fuels, including SAF, from a mixture of carbon monoxide (CO) and hydrogen ($H_2$) called synthesis gas or syngas | • A pyrolysis-based process whereby feedstocks, such as lignocellulose, are heated in the absence of oxygen to produce biochar, biogas and bioliquids. The bio-liquids, also called pyrolysis oils or biocrude, are upgraded to liquid fuels via hydroprocessing to remove the significant oxygen content of biocrude and hydrogenate the hydrocarbons. | • Syngas is produced through a combination of: electrolysis of air-captured $CO_2$ to CO, electrolysis of water to $H_2$, and/or a reverse water gas shift reaction between $CO_2$ and $H_2$. Renewable electricity is used to generate $H_2$, making the $H_2$ green, and minimize electrolysis emissions. Syngas is then converted into hydrocarbons such as jet fuel via Fischer-Tropsch synthesis. |
| **Feedstocks** | • Oil crops (soy, jatropha, palm), Used cooking oils | • Corn, Sugarcane, Cellulosic biomass* | • Cellulosic biomass, Municipal solid waste | • Cellulosic biomass, Municipal solid waste | • Carbon dioxide, Hydrogen |
| **Maximum ASTM-approved blending limit (vol%)** | 50 | 50 | 50 | 0 | 50 |

*Note: *Ethanol production for ATJ is limited to fermentation of sugar and cellulosic feedstocks. Ethanol production via gasification, such as of MSW, and fermentation of syngas is excluded from the scope of this report because of the low maturity of the technology. Further information on the Technology Readiness Level (TRL) in* ***Appendix C1****,* **Table C1** *and* **Table C2***. HDCJ stands for hydrotreated depolymerized cellulosic jet.*

#### 4.2.2.2 Feedstock sustainability

Sustainable feedstock supply is a key criterion for scalable SAF. Feedstock cost is a major component of fuel cost for many SAF pathways. Moreover, SAF is not truly sustainable if the feedstock supply is at high risk of inducing land use change, increasing food prices, or causing other social or ecological harms (The CORSIA standard contains an extensive treatment of key

sustainability criteria) [351]. In this analysis, we limit U.S. "economically and sustainably recoverable" feedstock supply to cellulosic feedstocks, wastes, and residues recoverable at a $50/bdt roadside price as indicated by the U.S. DOE's 2016 Billion Ton Report [71]. We consider first-generation starch, sugar, and oilseed crops. However, we limit supply to existing excess capacity, exports (for geographically constrained corn and sugar ethanol) and extrapolate future supply by applying secular production growth rates. In essence, only current underutilized food crop supplies as well as new volumes resulting from secular growth in the sector (as opposed to new fuel policies or demand) are available for SAF production. We assume that any increased SAF demand on food crops will induce sustainability risks. In the sections below, we detail feedstock availability and the calculations used to estimate supply.

#### *4.2.2.2.1 First-Generation Feedstocks*

First-generation (1G) feedstocks encompass edible sugars, starches, and oil crops such as sugarcane, corn, and soybean. 1G feedstocks are associated with high land use, nutrient and water demand [352]–[354]. These crops are utilized to produce fuel products such as ethanol (sugarcane and corn) and biodiesel/SAF (soybean, palm oil), but they are also food crops, thus they compete with food production for arable land, water, and resources. The food versus fuel debate has been studied extensively, with particular concern for the impact of 1G biofuel on food prices and food insecurity [31], [355], [356]. While there is debate about the extent to which 1G feedstocks and fuels can be sustainable, supply is clearly not limitless.

In this analysis, we consider pathways utilizing corn, sugarcane, soy oil, and palm oil. We assume existing 1G feedstock supply cannot support SAF at scale nor would these feedstocks be available for SAF alone. Thus, for each 1G feedstock, we assessed the size of the current market, current utilization and exports, as well as projected growth to establish the excess supply that may be available today and in 2030 for SAF production without substantial sustainability and cost risk. A key concern from a climate perspective is that demand shocks for feedstocks in already tight commodity markets can only partly be met by increased yields. Higher prices are likely to induce land use change (LUC) impacts and associated emissions that are not factored into the already substantial LUC penalties associated with 1G feedstocks under current policy regimes.

*Corn ethanol* - U.S. ethanol capacity grew 3% in 2019 to 17.3 billion gallons/year with production of fuel ethanol reaching 15.8 billion gallons [357]. Of the total supply, 1.5 billion gallons were exported, primarily to Canada, Brazil, and India [358]. Domestic demand for corn ethanol is primarily tied to its use as a fuel additive. The U.S. RFS program requires U.S. fuel refiners to purchase and blend volumes up to 10% into nearly all gasoline. However, current production capacity has already exceeded the "blend wall," and the ethanol industry is seeking revisions to Federal policy to allow for greater blending limits [359]. We restrict corn ethanol supply for SAF to current excess capacity over and above U.S. consumption and include additional potential assuming 9% growth between now and 2030. The strong incentives to produce and sell low-CI ethanol into California's LCFS program likely preclude the diversion of most existing low-CI ethanol to SAF production and much of existing supply is already spoken for by Federal blending requirements.

*Sugarcane ethanol* - Brazil is the primary producer of sugar-crop ethanol, producing 8.57 billion gallons in 2019 [360]. Brazil and the U.S. combined make up 84% of global ethanol production. 47% of the sugar produced in Brazil is used for ethanol production to meet the national blending requirements of 27% in automotive gasoline [361], [362]. Most of Brazil's ethanol production is used to meet domestic needs with exports of roughly 500 million gallons in 2019 [276] We assume sugarcane ethanol supply for use in U.S. SAF production to be limited to current Brazilian exports.

*Soybean for Soy Oil* – Soybean is the dominant commodity oil crop with 361 million metric tonnes produced and sold in 2020. Soy oil production reached 60 million metric tonnes in 2020, centered primarily in China and the United States [363]. Vegetable oil markets are tight, and the price of exported oils doubled between 2019 and 2020 [364]. Refined oils for SAF compete with biodiesel and heating oil, which currently fetch higher prices than jet fuel, in addition to competition from a host of other end-uses [342], [365]. Increased demand for refined oilseed products raises unambiguous sustainability challenges. We limit soy oil supply for SAF to 3% of current supply and consider new supply from secular growth in the soy oil market of 9% by 2030.

*Palm Fresh Fruit Bunch (FBB) for Palm Oil* - Palm oil is derived primarily from the outer fruit, but oils are also derived from the palm kernel. Palm oil production is forecast to reach 75 million metric tonnes in 2022, primarily centered in Malaysia and Indonesia [364]. Expansion of oil palm in tropical climates is linked to deforestation and biodiversity loss in primary and secondary forests [342]. Palm oil by-products (POME) are responsible for large-scale water pollution, and palm plantations have been linked to the draining of peatlands, which are valuable carbon sinks, turning them into landscapes which produce net GHG emissions [342]. Due to the sustainability and price risks associated with palm oil, we assume no sustainable supply for SAF. The 1G feedstock supply criteria for near-term SAF production are detailed in **Table 4-4.**

**Table 4-4** Sustainable and economically recoverable supply criteria for 1G feedstocks

| Feedstock | Supply |
|---|---|
| Corn ethanol | Current - excess production capacity over-and-above U.S. blending requirements (1.5 billion gallons)<br>2030 – Additional capacity assuming 9% growth between now and 2030 (3.1 billion gallons) |
| Sugar ethanol | Current and 2030 – Equivalent to current Brazilian exports (500 MM gallons) |
| Soybean | Current – 3% of soybean supply (10.8 MM tonnes)<br>2030 - Additional capacity assuming 9% growth between now and 2030 (33.5 MM |

| | |
|---|---|
| | tonnes) |
| Palm FBB | Given sustainability risks associated with Palm oil, we assume no sustainable supply for SAF |

#### *4.2.2.2.2 Second-Generation Feedstocks*

Second-generation (2G) feedstocks include non-edible cellulosic feedstocks such as energy crops and wastes. Energy crops include perennial grasses (switchgrass, miscanthus) and short-rotation woody crops (poplar, willow). Wastes can be further subdivided into agricultural residues (corn stover, bagasse) and wastes (soybean hulls, sugarcane field trash), woody wastes (forest residues, sawmill wastes), and food and municipal wastes [71], [342]. 2G feedstocks avoid many of the challenges facing food crops. National analyses in the U.S. context have confirmed the relative abundance of these feedstocks [71]. The lack of present demand for these feedstocks make them an attractive alternative to 1G feedstocks on a cost and sustainability basis [342]. The drawbacks of 2G feedstocks are technical and associated with accessing the sugars within a recalcitrant lignocellulosic cell matrix at costs that can scale commercially [342], [366]. For this analysis, we rely on available feedstock supply estimates in the U.S. Department of Energy's 2016 Billion Ton Report (BTS) [71]. We incorporate supply estimates for 2G feedstocks at a $50/BDT (bone dry tonne) cost at the farm-gate or roadside in 2022 and 2030. These supply estimates are "in addition to" current utilization of biomass feedstocks. Based on this data, we estimate the supply of 2G feedstocks suitable for SAF production to be 238 million BDT growing to 354 million BDT by 2030.

*Agricultural Residues and Secondary Wastes* - Agricultural residues make up the largest portion of current supply at 103 million tonnes in 2022 and 132 million dry tonnes in 2030 [367]. More than 80% of this supply is corn stover. The remainder in this category is primarily wheat straw. Agricultural residues carry the sustainability advantage of requiring no additional land to meet demand. Residue collection is subject to sustainability limitations because removing too much residue can lead to increased nutrient demand in subsequent planting cycles and leave soils vulnerable to water and wind erosion [368]. Secondary agricultural wastes have an estimated availability in 2022 of 17 million dry tonnes, with orchard and vineyard pruning representing approximately one-third, rice straw another third, and the remainder composed of "field trash" and crop hulls. The 2030 estimate for these feedstocks increases by less than one-million tonnes in the BTS model.

*Dedicated Energy Crops* - This category is composed of perennial grasses and short rotation trees. Both feedstocks typically have low nutrient requirements and can grow on marginal lands not suitable for 1G crops. The BTS projected 18.5 million dry tonnes in 2022 and 100 million tonnes in 2030 [71]. Note, however, that little of this projected supply exists today. A little over half of the projected supply would come from switchgrass in 2022. The remaining supply is comprised of miscanthus and a small contribution from coppiced trees. Switchgrass would remain the dominant energy crop in 2030 with increasing contributions from coppiced and non-coppiced trees over time and at higher prices.

*Woody Biomass* - Here we focus on industrial logging residues and residues from non-commercial thinning operations. Logging residues could supply roughly 30 million tonnes in 2022 and 35 million dry tonnes in 2030 [71]. An additional 13 million dry tonnes are available each year from secondary thinning operations (unused wood from forest land conversion and pre-commercial thinning). Other wood wastes (mill wastes) are heavily utilized and thus require high prices to divert to fuel production. They are not considered here.

*Non-edible oilseed* - 2G oil crops are toxic to humans and thus do not face direct competition with food production. Two candidates for SAF production are jatropha and castor bean (castor oil). Jatropha garnered widespread attention from researchers in the early 2000s [369], [370]. Jatropha has strong scalability characteristics due to the crop's high oil content (30-40%), low nutrient requirements, and resistance to drought, which allows it to grow in environments inhospitable to many other crops [342], [371], [372]. SAF production from jatropha has been tested at demonstration scale and jatropha blended fuels have been used in commercial flights [373]. However, early cultivation experiments failed to achieve expected yields, and interest in jatropha waned. Recently, however, there is renewed interest in jatropha cultivation for SAF. While there is no significant commercial market for jatropha oil, there are multiple commercial parties engaged in research and development of jatropha in recent years, including Lufthansa and NesteOil [374], [375]. Castor oil has also shown promise as a potential feedstock for SAF [342], [376]. However, like jatropha, supply of castor oil is small, with a production volume of 2 million tonnes of castor seed in 2020 [377].

*Municipal Solid Waste* - Municipal solid waste (MSW) accounts for 55 million tonnes of waste feedstocks in the United States [71]. The recoverable supply of MSW is expected to remain stable in the near-term. Separated MSW feedstocks (refuse-derived fuels or RDF) are primarily composed of paper/paperboard, plastics, and textiles. These feedstocks are suitable for thermochemical conversion via gasification or pyrolysis into precursors for SAF. MSW utilization comes with a unique set of benefits and challenges. Utilization of these wastes can promote circular economies and reduce landfill requirements and concomitant GHG emissions, but face social opposition for some utilization pathways, particularly in the United States [378], [379]. MSW offtake is often associated with tipping fees paid to the receiving party rather than costs. We assume zero cost or revenue associated with MSW feedstocks for SAF.

*Waste Oils* - Secondary agricultural wastes also include animal fats and yellow grease. Because animal fat supply is limited and contains high levels of saturated fatty acids which can cause problems in fuels at colder temperatures, only vegetable-based (yellow grease, i.e. used cooking oil) oils are considered here. Supplies of yellow grease (UCO) have been relatively constant at about 1 million tonnes/year [71].

#### *4.2.2.2.3 $CO_2$ and Hydrogen for Air to Fuels*

Air-to-Fuels (AIR) pathways begin with the chemical feedstocks $H_2O$ and $CO_2$, the former providing the source of $H_2$ and the latter providing CO to the syngas blend. Both the procurement of $CO_2$ via direct air capture (DAC) and the electrolytic splitting of $CO_2$ and $H_2O$ are energy intensive processes; thus, the availability of low-carbon renewable energy is essential to AIR viability [380], [381]. Further, the reverse water gas shift (RWGS) catalytic conversion of $CO_2$ to CO occurs at high temperature (in excess of 1,000 ˚C) which typically requires natural

gas-fired heaters; hence, the development of low-carbon heating technologies like resistive, solar thermal or solid biomass is crucial to reducing fossil dependency and related emissions [382]. Three different AIR pathways are explored in this study and are presented in **Figure 4-2** below. The pathway outlined in blue proceeds through a co-electrolysis route. Here, $CO_2$ is captured from the atmosphere via DAC and co-fed with $H_2O$ to a high temperature solid oxide electrolysis cell (SOEC) where they are converted into a 2:1 syngas mixture in one step. The second pathway outlined in green involves independent electrolytic steps: $CO_2$ captured from the atmosphere via DAC is fed to a SOEC where it is reduced to CO, and separately $H_2O$ is fed to a PEM electrolytic cell for conversion to $H_2$. These separate streams are then combined in a 2:1 H:C ratio to produce the desired syngas FT precursor. In the third pathway outlined in orange, $CO_2$ captured from the atmosphere via DAC is co-fed with $H_2$ produced electrolytically through PEM water electrolysis into a reverse water gas shift (RWGS) reactor, which takes as a feed $H_2$ and $CO_2$ at a higher ratio (>3:1) to produce the 2:1 syngas blend required for FT processing.

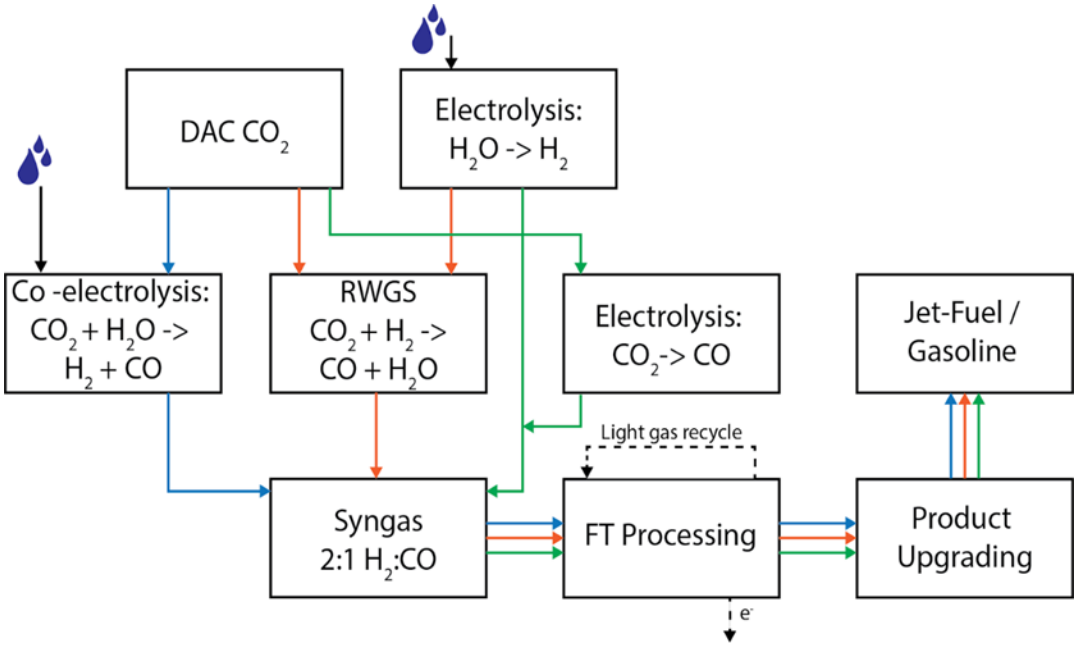


**Figure 4-2** Schematic of Air-to-Fuels routes to jet fuel production using DAC-sourced CO2. The blue pathway indicates co-electrolysis, the orange indicates the RWGS route, and the green route indicates independent electrolysis steps to yield $H_2$ from $H_2O$ and CO from $CO_2$.

ATF feedstocks are less constrained than those discussed for 1G and 2G pathways: $CO_2$ from air and process water are essentially limitless in the sense that they are always expandable to meet supply. However, geographic and techno-economic constraints could limit supply in the near-term. Unlike in the above sections where local and global availability dictated fuel production, it is more instructive to project how ATF pathways impact various feedstock supply chains given the resource requirements outlined above. Results are presented in **Table 4-5** given a SAF production target of 1 billion gallons per year.

While each ATF pathway has slightly different feedstock requirements, they all align in the need to source low-carbon hydrogen. The key difference is that the RWGS pathway requires much

more $H_2$ per unit of syngas produced (and thus, likewise, per finished fuel product) since $H_2$ is used to drive the RWGS forward at high temperature. Increased $H_2$ requirements will thus increase both water consumption and renewable energy needs in the RWGS relative to the two electrolytic pathways. Likewise, all pathways require $CO_2$, however, the co-electrolysis route – where $CO_2$ and $H_2$ are co-fed to the same electrolytic cell – has a slightly lower conversion efficiency, meaning more $CO_2$ is required per finished fuel product. The impact of this incremental $CO_2$ will depend on how the $CO_2$ is sourced. Currently, the only large-scale[5] DAC facility in planning uses the solvent-based architecture. Under the current design, these plants are heavy consumers of natural gas and water. This leads to increased use of those resources for the co-electrolysis case. The natural gas supplies heat and on-site power to the DAC facility through an oxy-fired kiln and integrated power block. Carbon capture is applied to capture 90% of the $CO_2$ emissions associated with natural gas combustion, with the remaining 10% fed back through the contactor for additional capture. Upstream natural gas supply chain leakage can result in non-trivial $CO_2e$ emissions and are assigned to the $CO_2$ feedstock. The implications of these DAC-related emissions will be discussed later in the context of pathway carbon intensities.

**Table 4-5** Resources required to produce 1 billion gallons/yr of SAF using three unique ATF pathways. Note: The $CO_2$ is assumed to be derived from a solvent-based DAC technology, using natural gas to supply both onsite heat and power. Carbon capture is applied to approximately 97.5% of the emissions from oxy-fired natural gas combustion. The majority of natural gas is used for DAC, with more in the co-electrolytic route due to a higher amount of $CO_2$ required. Likewise, despite less $CO_2$ required in the RWGS route, additional natural gas is needed for RWGS process heating. Process water is needed for electrolytic routes, with PEM sensitive to impurities. Additional process water is required for steam generation in the RWGS route.

| Pathway | Natural Gas (PJ/yr) | $CO_2$ (Mt/yr) | Renewable Energy (TWh/yr) | Water (Ggal/yr) |
|---|---|---|---|---|
| Electrolysis | 90 | 16 | 135 | 7.4 |
| Co-electrolysis | 121 | 21 | 91 | 4.2 |
| RWGS | 100 | 14 | 108 | 9.0 |

As shown in **Table 4-5** above, these three different ATF pathways have slightly different feedstock requirements. However, more so than sustainability, the feedstock requirements impact the economic viability for these processes. Ambiently sourced $CO_2$ via DAC is far more expensive than that sourced from high purity industrial streams, with active commercial costs ranging from \$600 - \$1,100/t$CO_2$ and projected best-case costs of \$200-\$300/t$CO_2$ near-term and under \$200/t$CO_2$ long term. Less expensive point sources of carbon dioxide could be used as a feedstock for SAF, but at best, this represents delayed emissions. Direct Air Capture (DAC) provides greater emissions reductions and the opportunity for a carbon neutral fuel cycle. Operational expenditures naturally increase when sourcing $CO_2$ from DAC, which in turn leads

[5] As of 2021, Carbon Engineering, in partnership with Oxy Low Carbon Ventures, is in development of a million-tonne per year scale, solvent-based DAC facility in the US Permian Basin region.

to higher jet fuel production costs. Generally, an increase in \$100/t$CO_2$ to the feedstock $CO_2$ price leads to an increase of between \$1.25 to \$1.50/gallon in the jet fuel selling price.

While the impact of $CO_2$ source is noted, overall SAF production costs are far more sensitive to the secondary reactant $H_2$. For example, where doubling the cost of $CO_2$ generally translates to a 30% increase in jet fuel selling price, doubling the cost of $H_2$ will lead to a 50% increase. The cost of green $H_2$ is largely contingent on the cost of electricity and electrolysis technology.

In the co-electrolysis route, $CO_2$ and $H_2O$ are co-fed to a solid oxide electrolytic cell (SOEC) to produce a syngas mixture. SOEC technology is generally less developed and more expensive than other electrolytic pathways like alkaline electrolysis (AEC) or proton-exchange membrane electrolysis (PEM), with capital costs projected in the near-term at over \$3,000/kW and projected costs of ~\$2,000/kW by 2030 [383]. Further, the projected stack lifetime of SOEC cells are less than AEC and PEM, leading to potential risk of cost increase due to a greater frequency of replacement schedule and lower utilization of capital. In the other routes, water electrolysis is used to provide the $H_2$ feedstock. More mature technologies like AEC and PEM are used to produce $H_2$, with optimistic projections in capital reduction of <\$1,000/kW by 2030, and as low as \$500/kW [383].

In the techno-economic analysis that follows, we use feedstock costs of \$3.50/kg $H_2$ and \$250/t$CO_2$. The impacts of these feedstock costs are further explored in *Chapter 4.2.4.*

#### 4.2.2.3 SAF Scenarios

We selected twenty-two feedstock and conversion pathway combinations for detailed life cycle assessment (LCA) and technoeconomic assessment (TEA) analysis. We consider 1G, 2G, and ATF feedstocks where appropriate. We elected to analyze three high TRL biomass SPK pathways with 50% ASTM approved blending limits: (1) HEFA, (2) FT, and (3) ATJ. We selected one moderate TRL pathway (4) HDCJ that is not yet ASTM certified. Given that biomass is not a limitless resource, future SAF may rely on circular economy pathways, thus we consider three potential (5) ATF pathways alongside the biomass routes. ATF technologies are at moderate TRL levels, but requisite costs remain prohibitive. We analyze ATJ and FT scenarios both with and without CCS. The FT and HDCJ thermochemical pathways are amenable to a wide range of feedstocks. We include MSW as potential feedstock for these pathways. We employ TEA methodology and discounted cashflow analysis (DCF) to determine minimum fuel selling price (MFSP) both with and without applicable policy support, i.e. a "subsidized" and "unsubsidized" case. An overview of the scenarios is shown in **Table 4-6**. Each feedstock option within a technology category represents a separate modeled pathway.

**Table 4-6** SAF LCA and TEA scenario overview

| SAF Pathway | Feedstock Options | Applicable Policy |
|---|---|---|
| Fischer-Tropsch (FT) | Forest residues (FR), Switchgrass (SG), Municipal Solid Waste (MSW) | LCFS, RFS D7 RINs (FR&SG), RFS D5 RINs (MSW) |

| | | |
|---|---|---|
| Fischer-Tropsch (FT) with CCS | Forest residues (FR), Switchgrass (SG), Municipal Solid Waste (MSW) | LCFS, RFS D7 RINs (FR&SG), RFS D5 RINs (MSW) |
| Alcohol to Jet (ATJ) | Sugarcane (S), Corn (C), Corn Stover (CS) | LCFS, RFS D5 RINs (S), D7 RINS (CS), No RINs (C) – Fails 20% reduction criteria |
| Alcohol to Jet (ATJ) with CCS | Sugarcane (S), Corn (C), Corn Stover (CS) | LCFS, RFS D5 RINs (S), D7 RINS (CS), D6 RINS (C), U.S. 45Q |
| HDCJ | Forest Residues (FR), Municipal Solid Waste (MSW) | LCFS, RFS D7 RINs |
| HEFA | Soy Oil (SY), Palm Oil (PAL), Jatropha Oil (JAT), Used Cooking Oil (UCO) | LCFS, RFS D4 RINs (JAT & UCO). No RINs (SY & PAL) - Fails 20% reduction criteria |
| Air-to-Fuels (ATF) | Reverse Water Gas Shift (RWGS), Co-electrolysis (COEL), Electrolysis (ELEC) | LCFS |

#### 4.2.2.4 Life cycle GHG assessment

The goal of the life cycle assessment is to quantify the well-to-wake CI of SAF production pathways across a variety of potential feedstocks and conversion processes in order to identify pathways with substantial emissions reduction potential relative to conventional Jet A. ISO 14040 and 14044 define the functional unit for life cycle assessment as the "quantified performance of a product system for use as a reference unit." For this study, all life cycle results and comparisons are made on a lower heating value (LHV) basis of 1 MJ of fuel, as this allows for reasonable comparisons between liquid transportation fuels and conforms to relevant policy contexts such as California's Low Carbon Fuel Standard.

The system boundary in a life cycle assessment specifies which unit processes are modeled explicitly in the product system (ISO 14044). Clear definition of the boundary is important to assure consistency in product system comparison. For this analysis, the system includes production of feedstock, transportation of feedstock from source to conversion facility, production of SAF and intermediate pre-cursors, transport of intermediates to final SAF upgrading, where appropriate, and transport of finished SAF product to end-use, and final combustion of SAF, assuming that all embodied biogenic carbon returns to the atmosphere as $CO_2$. For pathways that involve CCS, energy or parasitic energy load required for separation, capture, and compression are also included in the system boundaries. See Appendix C2 for system diagrams illustrating carbon flow and for selected LCA results.

Because early SAF deployment will likely be supported by existing policy frameworks, LCA system boundaries and allocation are carried out in a manner that is as consistent as possible with the approach used in the California LCFS program, thus we rely on data and modeling choices

consistent with California GREET 3.0 and the Argonne National Lab (ANL) GREET 2019 models [302], [384]. Because the latter ANL model is updated more frequently and contains SAF pathways not available in the California version of the model, it is the primary source of inventory data. Before selecting processes from the GREET.net model, we screened background literature to ensure sufficient documentation to support GREET model assumptions. Of the biomass-based conversion technologies, only the FT and the ATF (which are also FT pathways) pathways did not meet completeness criteria in our judgment. A summary of original data sources for each pathway can be found in **Table 4-7.** We manually extracted life cycle inventories for most feedstocks and fuel production processes from the GREET model. We cleaned and normalized data to the functional unit using a set of custom applications written in R Studio. We retained only the inventory data relevant to life cycle GHG emissions. GREET does not track biogenic $CO_2$ emissions unless the emissions arise as a consequence of combustion (e.g. no fermentation or gasification emissions). We performed an independent carbon balance in order to explicitly quantify biogenic $CO_2$ emissions at each stage of the fuel production life cycle. Finally, we scaled $CO_2$, $CH_4$, and $N_2O$ emissions with the 100-year global warming potential (GWP) multipliers of 1, 30, and 265, respectively [385]. Feedstock, intermediate product, and final fuel product inventories were rescaled to 1 MJ of output for each stage of the life cycle. We constructed our own Excel-based LCA model from the inventory data. We discarded transportation and land use change (LUC) emissions from GREET in the initial cleaning stage and added these emissions back during our LCA modeling, relying on the most recent values for LUC under the LCFS program [384]. We remain consistent with GREET, but due to our use of IPCC AR5 GWP factors as well as rounding losses inherent in GREET data extraction, our results do not match GREET precisely.

#### *4.2.2.4.1 LCI data and analysis outside of ANL GREET 2019*

Fischer-Tropsch - The background documentation on the GREET.net 2019 FT SPK Jet pathway is sparse, and the assumed products and co-products were not congruent with other analyses we have seen in the academic literature. We opted to rely on a detailed process analysis for FT fuels and electricity by Larson et al. (2010) [386]. This analysis models conversion of cellulosic feedstocks to diesel and gasoline products with co-production of electricity both with and without CCS. The feedstock energy density and dry basis carbon content assumptions in the source material differed from similar feedstocks in the GREET model. For consistency across pathways, we assume GREET feedstocks and reanalyzed the system to derive a new mass-energy balance from the modified feedstock inputs. We also update energy requirements for carbon capture to maintain consistency with other modeled pathways.

Municipal Solid Waste (MSW) – We adopted MSW handling and sorting energy and emissions from California GREET 3.0 [384], borrowing from the anaerobic digestion and renewable natural gas production pathways. We assume a 2:1 MSW to refuse derived fuel (RDF) mass ratio. RDF is assumed an LHV of 15 MJ/kg. The emissions factor for RDF separation and preparation is approximately 1.04g/MJ. The utilization of MSW implies a counterfactual scenario where MSW is, instead, landfilled or incinerated. We credit the use of MSW feedstock for avoided methane emissions. We assume feedstock derived from MSW is 82% biogenic and 18% fossil in origin. Our counterfactual case assumes that 50% of MSW is landfilled and 50% incinerated. We assume a 10% degradable organic carbon (DOC) fraction in the fossil material

and 26% in the biogenic material. Finally, we assume the landfill collects and flares 75% of methane emissions. A full accounting of the counterfactual would also account for forgone biogenic sequestration of non-DOC due to diversion of the MSW from the landfill. Given the assumptions above, we estimate an 80% reduction in the MSW credit relative to the credit reported.

Used Cooking Oil (UCO) – We use LCI data from California GREET 3.0 to inform collection and refining requirements for UCO. The emissions factor for combined collection of waste oil and rendering to finished oil is approximately 86 $gCO_2e$/lb.

Direct Air Capture - Life cycle inventory data for a solvent-based DAC system are taken from the analysis *Natural Gas vs. Electricity for Solvent-Based Direct Air Capture* by McQueen et al. [387]. The configuration is assumed to use natural gas with carbon capture to provide thermal energy and renewable energy (solar with battery storage) to provide electricity. The configuration is assumed to achieve 81% removal (0.19 $tCO_2e$ emitted for every 1 $tCO_2$ captured), with most emissions occurring through leakage of natural gas at the rate of 2.3%. Material embodied emissions for the DAC system are included and amount to less than 1% of the total footprint.

Hydrogen and $CO_2$ Electrolysis - Life cycle inventory data for electrolytic routes were built from two sources. The first from Pellow et al. [388] describes the embodied emissions in the electrolytic cells, and the second from NREL (2012) [389] describes the embodied emissions in solar energy with Li-ion battery storage, which amount to 25 $gCO_2e$/kWh.

Air-to-Fuels – Upgrading of $H_2$ and CO to final fuels in all ATF pathways assumes FT conversion with LCI assumptions consistent with the other FT pathways minus the gasification of biomass stage.

RWGS – The LCI for RWGS is taken from Rezaei and Dzuryk (2019) [390]. System components were compiled from the study, and emissions were assigned based on the methods for natural gas, $H_2$ electrolysis, and renewable energy described in the preceding sections.

**Table 4-7** Data sources for SAF life cycle inventory

| Pathways | LCI Data Source | Auxiliary Data Sources |
|---|---|---|
| Ethanol to Jet | GREET.net 2019[302] | Han, Tao, and Wang (2017)[391] |
| HEFA | GREET.net 2019[302] | Pearlson (2011)[392], Stratton (2010 & 2011)[393] |
| Biocrude (Pyrolysis) to Jet (HDCJ) | GREET.net 2019[302] | Wright et al. (2010)[394], Jones et al. (2009)[395] |

| | | |
|---|---|---|
| Fischer-Tropsch to Jet | Larson et al. (2010)[396] | GREET.net 2019[302] |
| Air to Fuels | Larson et al. (2010)[396] | GREET.net 2019[302], Rezaei and Dzuryk (2019)[390], Schmidt et al. (2017)[397], McQueen at al. (2021)[387], [398] |
| **Feedstocks** | | |
| Biomass Feedstocks | GREET.net 2019[302] | |
| Used Cooking Oil | California GREET 3.0[384] | |
| Municipal Solid Waste (MSW) | California GREET 3.0[384] | Adapted material handling emissions, assumed 2:1 MSW to RDF conversion |

#### *4.2.2.4.2 System expansion / Allocation to multiple products*

Feedstock conversion to intermediate products and final SAF fuel generate multiple co-products that differ between technologies. The question arises as to how to allocate emissions and other life cycle impacts between products and co-products. ISO guidelines offer several options for dealing allocation with the ultimate decision is left to the analyst given the context of the analysis. Options include system expansion to account for market displacement of co-product alternatives or allocation of life cycle burdens proportionally by energy content, mass, or market value. Consistent with the goal of the LCA, we selected allocation methods for each SAF scenario that we determined to be consistent with the approach for similar fuels under California's LCFS program. **Table 4-8** gives an overview of allocation or system expansion approach applied to co-products at each stage of the fuel production life cycle. No feedstock harvest or collection phase produces co-products. However, some feedstocks could be considered co-products or wastes of other processes, thus we explicitly assume MSW, corn stover, and forest residues are "true wastes," carrying no upstream allocation of burdens. The production of intermediates (e.g. ethanol, refined vegetable oils, and pyrolysis biocrude) in many cases indicates electricity co-generation and/or material co-products such as DDGS animal feed, corn oil, soy meal, and palm kernel expeller. Electricity, DDGS, and corn oil do not receive allocation but rather generate avoided emissions credits via system expansion and displacement of other market goods. Soy meal and palm kernel expeller, on the other hand, share in the emissions burdens of production proportional to the share of energy content among all products and co-products. Final production of SAF typically yields of mixed array of hydrocarbon chain lengths consistent with SAF, diesel, naphtha, and other hydrocarbon fuels. In all cases, environmental burdens are allocated to SAF on an energy basis.

**Table 4-8** Allocation method used for attribution of SAF life cycle GHG emissions

| Pathway | Feedstock | Intermediate | Final fuel |
|---|---|---|---|
| **Alcohol to Jet** | | | |
| Corn ethanol | None | Displacement (DGS/Corn Oil) | Energy |
| Stover ethanol | Treated as waste. Feedstock does not carry any upstream burdens from corn production | Displacement (U.S. Grid) | Energy |
| Sugarcane ethanol | None | Displacement (U.S. Grid) | Energy |
| **HEFA** | | | |
| Palm oil | None | Energy (Palm Kernel Expeller) | Energy |
| Jatropha oil | None | Displacement (U.S. Grid) | Energy |
| Soy oil | None | Energy (Soy meal) | Energy |
| Used Cooking Oil | None | None | Energy |
| **HDCJ or Pyrolysis Oil to Jet (SKA)** | | | |
| Stover biocrude | Treated as waste. Feedstock does not carry any upstream burdens from corn production | None. Biochar co-product is utilized onsite for energy. | None |
| Forest residue biocrude | None | None. Biochar co-product is utilized onsite for energy. | None |
| MSW biocrude | Waste – no upstream emissions burden. Credits assigned for avoided methane emissions in counterfactual | None. Biochar co-product is utilized onsite for energy. | None |

| FT Jet | | | |
|---|---|---|---|
| Forest residue | None | | Energy |
| Switchgrass | None | | Energy |
| MSW | Methane credit (no biogenic landfill sequestration) | | Energy |

#### *4.2.2.4.3 Biogenic carbon*

Biogenic $CO_2$ is assumed to be "net zero." It is assumed that short rotation crops such will uptake equivalent quantities of $CO_2$ in the next growth cycle and that residual wood waste emissions are accounted for in national level accounting as stock changes in the agriculture, forestry, and other land use (AFOLU) sectors. While this latter assumption is imperfect, the range of counterfactuals for forest residues include pile burning and energy recovery as well as sequestration scenarios such as slow degradation in forests, incorporation into wood products. It is a simplifying assumption that these feedstocks add no net $CO_2$ to the atmosphere in terms of GWP. Sustainable forestry practices and a hierarchy of waste utilization are a necessary pre-condition for this assumption to hold.

#### *4.2.2.4.4 Transportation*

Transportation ultimately represents a small fraction of emissions impacts for a given fuel pathway. However, long transport distances and method of transport do have an impact on final CI. The LCA models analyzed assume a general case rather than a specific facility. Feedstocks, intermediates, and final fuels are transported either by heavy duty truck (with backhaul), diesel rail, or ship with GHG intensities of 0.23, 0.03, and 0.01 $gCO_2e$/kg-mile respectively. Transport scenarios are tailored to be reasonable approximations for each SAF pathway.

**Table 4-9** Transportation assumptions for SAF life cycle analysis

| Transport Scenarios | Feedstock | | Intermediate | | Final fuel | |
|---|---|---|---|---|---|---|
| **Pathway** | **Method** | **Distance** | **Method** | **Distance** | **Method** | **Distance** |
| **Ethanol to Jet** | | | | | | |
| Corn ethanol | Truck | 200 | Truck | 100 | Rail | 1000 |
| Stover ethanol | Truck | 200 | Truck | 100 | Rail | 1000 |
| Sugarcane ethanol | Truck | 200 | Truck | 100 | Ship | 7000 |

| | | | | | | |
|---|---|---|---|---|---|---|
| **HEFA** | | | | | | |
| Palm oil | Truck | 200 | Truck | 100 | Ship | 7000 |
| Jatropha oil | Truck | 200 | Truck | 100 | Ship | 7000 |
| Soy oil | Truck | 200 | Truck | 100 | Rail | 1000 |
| Used Cooking Oil | | | Truck | 200 | Rail | 1000 |
| **HDCJ or Pyrolysis Oil to Jet (SKA)** | | | | | | |
| Stover biocrude | Truck | 100 | | | Rail | 1000 |
| Forest residue biocrude | Truck | 100 | | | Rail | 1000 |
| MSW biocrude | Truck | 100 | | | Rail | 1000 |
| **FT Jet** | | | | | | |
| Forest residue | Truck | 200 | | | Rail | 1000 |
| Switchgrass | Truck | 200 | | | Rail | 1000 |
| MSW | Truck | 200 | | | Rail | 1000 |

#### *4.2.2.4.5 Carbon Capture and Sequestration (CCS)*

We only employ CCS on processes which emit a high-purity stream of $CO_2$. Energy requirements for capture are assumed to be 200 kWh/tonne for capture, dehydration, and compression sufficient to transport captured $CO_2$ as a supercritical fluid up to 100 km for storage. This energy requirement is higher than published estimates for ethanol CCS (100-150 kWh/t) and more representative of the lower $CO_2$ concentrations in the FT process [399]. As a simplifying assumption, we selected this value for all CCS pathways. For pathways that co-generate electricity, CCS power requirements are deducted from net electricity export and matching reduction in co-product emissions credits. For processes that do not produce onsite electricity, it is assumed electricity is sourced from the U.S. average grid with an GWP of 479 $gCO_2e/kWh$.

### 4.2.2.5 Technoeconomic assessment

The minimum fuel selling price (MFSP) under both unsubsidized and subsidized conditions are calculated with a discounted cash flow (DCF) model assuming a 20-year plant life, 1 year construction period, and 15% IRR. All results are presented in 2020 USD. Where possible, TEA assumptions draw from the source literature that also informed GREET.net LCA assumptions. Final determination of TEA assumptions relied on expert judgement to ensure consistency across pathways. Data sources for each pathway are shown in **Table 4-10**.

Co-product revenues have secondary impacts on the cost of SAF production; while we include the revenues from co-product sales in our model, to be conservative, we do not attempt to include additional policy revenues that may be associated with those co-products, e.g. we do not apply LCFS credits to revenues for co-products. See Appendix C3 for a snapshot of the discounted cashflow model.

**Table 4-10** Data sources for SAF techno-economic assessment

| **Pathways** | **TEA Data Sources** |
|---|---|
| Ethanol to Jet | Han, Tao, and Wang (2017) [391]<br>Restrepo-Valencia and Walter (2019) [400] |
| HEFA | Pearlson (2011)[392]<br>Stratton (2010 & 2011)[393] |
| Biocrude (Pyrolysis) to Jet (HDCJ) | Wright et al. (2010)[394]<br>Jones et al. (2009)[395]<br>Kreutz et al. (2020)[338] |
| Fischer-Tropsch to Jet | Larson et al. (2010)[396]<br>Kreutz et al. (2020)[338] |
| Air to Fuels (ATF) | Larson et al. (2010)[396]<br>Rezaei and Dzuryk (2019) [390]<br>Pellow et al. (2015)[388]<br>NREL (2012)[389]<br>McQueen et al. (2021)[387] |

**Table 4-11** describes the price of feedstocks, assumed utility electricity prices for CCS and for electricity exported to the grid, co-product sales prices, and the value of policy credits used in the subsidized scenarios. Note that due to the number of pathways modeled, we do not independently model cost of utilities for each of the pathways. We adopt aggregate fixed and variable OPEX from the referenced studies. This is a limitation of this work. We only model feedstock variable cost and selling price of co-products independently. The CAPEX cost of CCS infrastructure and the OPEX cost for transportation and storage of captured $CO_2$ are added components to our model.

**Table 4-11** SAF TEA model inputs

| **Biomass Inputs** | **Price** |
|---|---|
| Corn | $144/BDT |
| Sugarcane | $16/BDT |
| Soy oil | $2.27/gal |
| Palm oil | $2.10/gal |
| Jatropha oil | $1.39/gal |
| UCO | $2.13/gal |
| All cellulosic biomass (stover, forest residues) | $50/BDT |
| RDF from MSW | $0/BDT |
| **Air to Fuels Inputs** | |
| $CO_2$ feedstock | $250/tonne |
| $H_2$ feedstock | $3.50/kg |
| **Co-Product Prices** | |
| DDGS selling price | $116/tonne |
| Corn oil selling price | N/A |
| Naphtha selling price | $500/tonne (1.40/gal) |
| Gasoline | $3.50/gal ($2.42 in ATJ)(1.31 HEFA) |
| Diesel | $1.29/gal |
| Electricity price | $0.04/kWh |
| **CCS** | |
| CCS CAPEX | $12M |
| $CO_2$ T&S cost | $10/ton |
| **Cost of Capital and Policy Incentives** | |
| WACC % | 10 % |
| LCFS Credit Price | $150/tonne $CO_2e$ |
| 45Q | $50/ton for first 12 years of operation |
| D4 RINs (Renewable Diesel) | $0.51 |
| D5 RINs (Advanced Biofuel) | $0.55 |

| | |
|---|---|
| D6 RINs (Renewable Fuel) | $0.36 |
| D7 RINs (Cellulosic Diesel) | $1.30 |

**Table 4-12** shows annual production volumes, feedstock requirements, CAPEX and annual non-feedstock OPEX (fixed and variable with feedstock component removed) for each of the SAF technologies. Different SAF technologies and feedstock types will operate at different optimal scales. We make no attempt to determine an optimal facility size or to normalize facility scale. This would lead to misleading results. Instead, we rely on the facility capacities in the reference literature and fix feedstock input within technology type to capture differences in SAF yield. This is particularly relevant in the ATF pathways and the ATJ pathways, as well as HDCJ.

**Table 4-12** SAF Pathways – Production volumes, feed rate, CAPEX, and non-feed OPEX

| **Pathway** | **Annual SAF (MMgal/yr)** | **Feed (per day)** | **CAPEX MM USD** | **Non-Feedstock OPEX MM USD/yr** |
|---|---|---|---|---|
| Corn ATJ | 39.6 | 2000 BDT | 448 | 74 |
| Stover ATJ | 27.6 | 2000 BDT | 731 | 63 |
| Sugar ATJ | 23.3 | 3365 BDT | 149 | 8 |
| HEFA Palm | 33.2 | 4,000 BBL | 103 | 25 |
| HEFA Soy | 33.2 | 4,000 BBL | 103 | 24 |
| HEFA Jatropha | 33.2 | 4,000 BBL | 103 | 31 |
| HEFA UCO | 33.2 | 4,000 BBL | 103 | 25 |
| HDCJ | 35 | 2000 BDT | 455 | 25 |
| FT | 44.6 | 3044 BDT | 1639 | 18 |
| AIR RWGS | 69.9 | 2740 BDT $CO_2$ | 561 | 511 |
| AIR COELEC | 48.1 | 2740 BDT $CO_2$ | 1168 | 294 |
| AIR ELEC | 63.8 | 2740 BDT $CO_2$ | 2274 | 532 |

### 4.2.3 Results

#### 4.2.3.1 Scalable Feedstock Supply

In general, 1G feedstocks will not be suitable for SAF production at scale. Food-based feedstocks compete with alternative uses in existing commodity markets. As shown in **Figure 4-3**, oil crops, sugar cane, and corn are already heavily utilized for energy and fuels as well as food and alternative uses. As discussed previously, corn ethanol capacity in the U.S. already exceeds domestic demand and is continuing to grow despite limited markets for industry output and little expansion in land use. For this reason, we suggest that in the near-term, some corn

ethanol based SAF production may be viable as a stepping-stone to ethanol intermediate fuels produced from other feedstocks (cellulosic). We do not see evidence that sugarcane ethanol shares these characteristics. Brazil, the largest producer of sugarcane ethanol, exports relatively little supply, and demand for sugarcane is leading to expansion of sugarcane agriculture. 2G feedstocks, on the other hand, currently demonstrate little to no utilization or competition and do not require agricultural expansion to meet current demand. Air-to-Fuels feedstocks, water ($H_2$) and air ($CO_2$), are essentially limitless and require much less land use to source, so production costs wind up being a more appropriate metric for determining their availability / potential growth compared to biomass-based pathways. DAC and green hydrogen production technologies are still relatively nascent, and significant cost reductions are expected with continued scale up.

Based on this data, we estimate the supply of 2G feedstocks suitable for SAF production to be 238 million BDT growing to 354 million BDT by 2030. While these estimates are optimistic, we find that there is ample supply of 2G feedstocks to meet demand for SAF production in the near-term. For instance, we estimate that 1 billion gallons of SAF would require < 10% of available 2-G feedstocks agricultural and woody residues at the $50/bdt price-point in 2022 (utilization of all 2-G feedstocks available at $50/bdt could supply 10 billion gallons of SAF in 2030.

Given the effectively limitless supply of ATF feedstocks, we present alongside the percentage (%) of existing renewable electricity capacity that would need to be dedicated to SAF to achieve 1 billion and 10 billion gallons of SAF.

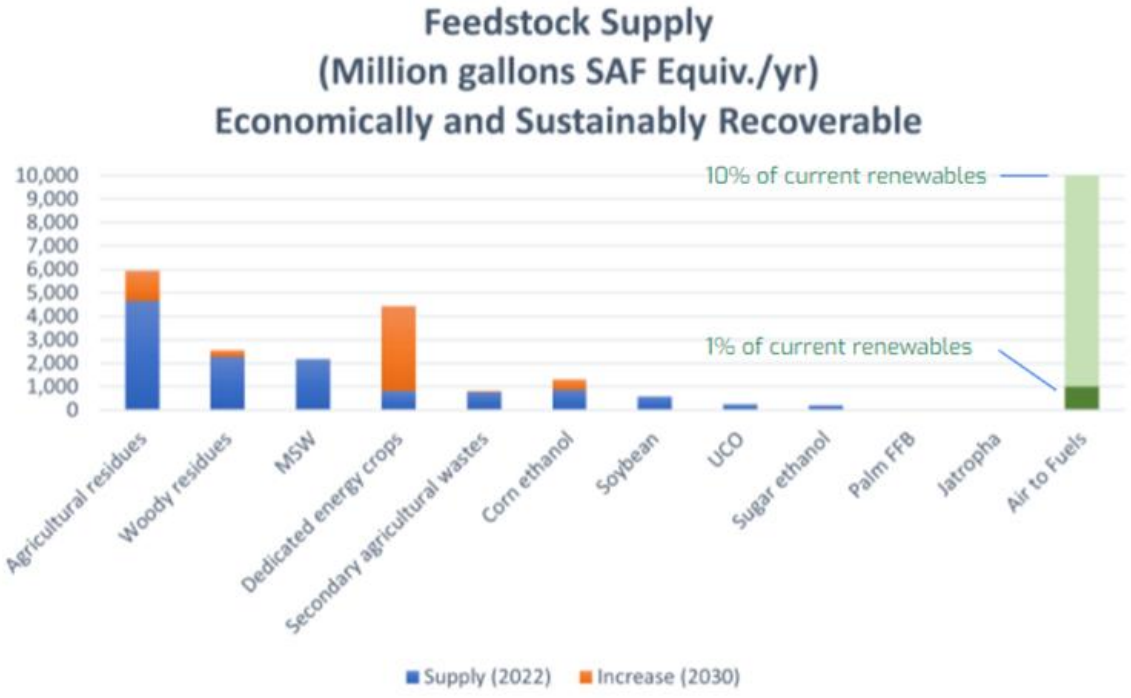


**Figure 4-3** Economically and sustainably recoverable feedstock supply for SAF

#### 4.2.3.2 Life cycle carbon intensity

A target of >70% life cycle CI reduction from Jet-A (CI = 89.37 gCO2e/MJ) translates to a maximum SAF life cycle CI of 26.8 $gCO_2e/MJ$; see **Figure 4-4** below. Food-based feedstocks are generally unable to achieve the target, with the notable exception of sugar ATJ with CCS. Corn ATJ with CCS nears 70% with a CI of 31 $gCO_2e/MJ$. This raises the possibility that further improvements in the life cycle CI could allow corn ethanol-based ATJ as a bridge to cellulosic ATJ (for example, dramatic reductions in fertilizer use or life cycle). Use of MSW and the pairing of cellulosic feedstocks with CCS can result in negative CI values for SAF, indicating net carbon removal. The greatest potential for carbon negativity is found in Fischer-Tropsch pathways combined with CCS or FT pathways that utilize MSW as feedstock, with the most carbon-negative SAF fuel arising from the combination of FT with CCS and MSW as feedstock. A credit for avoided methane emissions comprises a significant portion of the “negative emissions" for MSW pathways. While all the FT with CCS pathways remain carbon-negative and superior to the other pathways without the credit, the methane component is not true carbon removal. The ATJ pathway with CCS also achieves carbon removal when corn stover or, to a lesser degree, sugarcane is used as feedstock. The implications of negative CI fuels for broader SAF carbon reduction targets are significant.

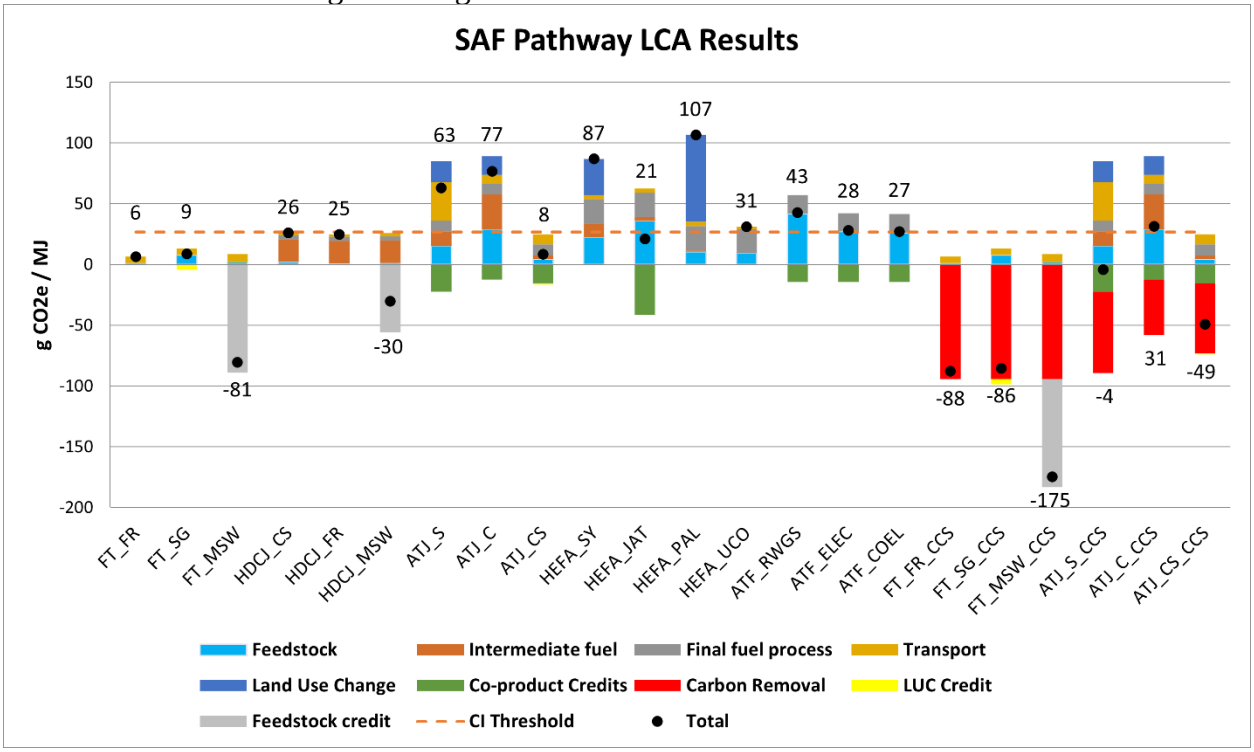


**Figure 4-4** Process contributions to life cycle emissions for SAF pathways.

Pathway key: FR = forest residue, SG = switchgrass, MSW = municipal solid waste, S = sugar, C = corn, CS = corn stover, SY= soy oil, JAT = jatropha oil, PAL = palm oil, UCO = used cooking oil, FT = Fischer-Tropsch, HDCJ = Hydrotreated Depolymerized Cellulosic Jet (pyrolysis biocrude), ATJ = alcohol to jet, HEFA = hydroprocessed esters and fatty acids, ATF = Air to Fuels, CCS = carbon capture and sequestration, RWGS = reverse water gas shift, ELEC = electrolysis, COEL = co-electrolysis

The primary drivers of carbon intensity vary by SAF pathway. **Figure 4-5** illustrates the relative contribution of the primary stages of the fuel life cycle to total fossil emissions (including fossil $CO_2$, $CH_4$, $N_2O$, and LUC emissions). The CI of FT pathways that rely on residues or wastes as feedstocks are dominated by biomass and fuel transportation, with feedstock collection playing a lesser role.

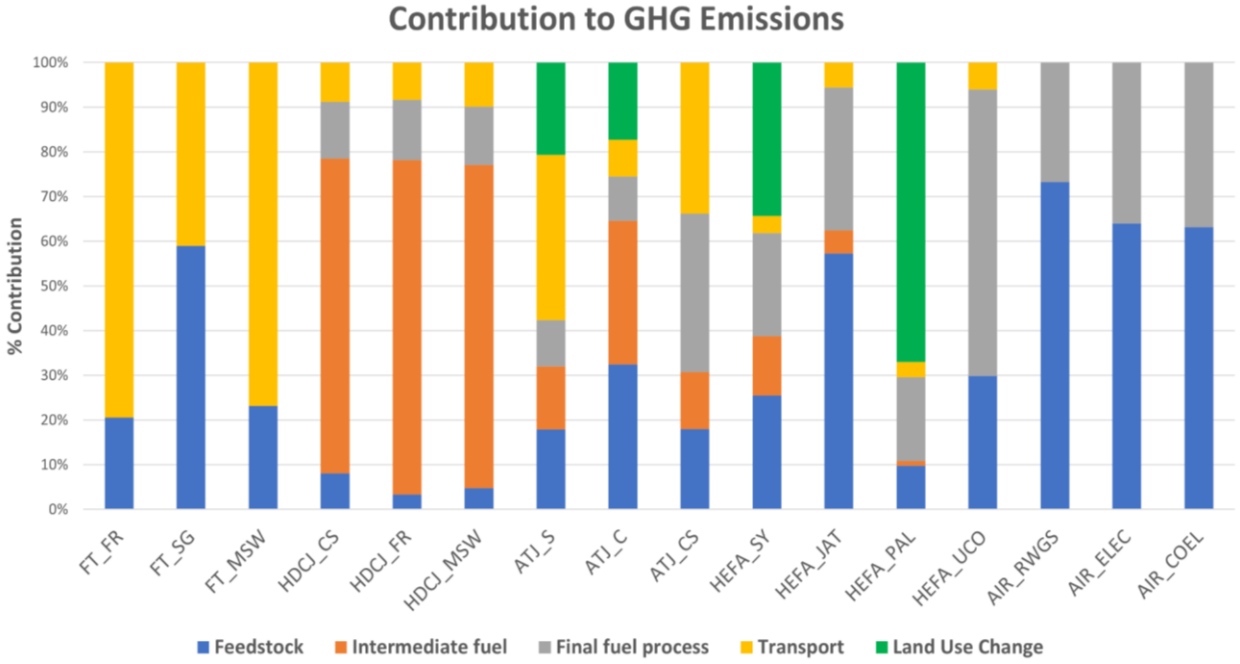


**Figure 4-5** Drivers of non-biogenic (fossil and LUC) GHG emissions in SAF production life cycle. CCS pathways are omitted because the emissions contribution from energy required to capture CO2 are imperceptible relative to the non-CCS version of the same pathway. Pathway key: FR = forest residue, SG = switchgrass, MSW = municipal solid waste, S = sugar, C = corn, CS = corn stover, SY= soy oil, JAT = jatropha oil, PAL = palm oil, UCO = used cooking oil, FT = Fischer-Tropsch, HDCJ = Hydrotreated Depolymerized Cellulosic Jet (pyrolysis biocrude), ATJ = alcohol to jet, HEFA = hydroprocessed esters and fatty acids, AIR = Air to Fuels, RWGS = reverse water gas shift, ELEC = electrolysis, COEL = co-electrolysis

FT pathways primarily utilize their own internal energy, which is supplied by biogenic sources - this diminishes the contribution from fossil emissions. Dedicated feedstocks like switchgrass indicate a small increase in emissions for feedstock production relative to residues, but the impact is small and largely offset by LUC benefits (dedicated energy crops are assumed to increase carbon storage in terrestrial pools, see Land Use Change for more details). The HDCJ

(biocrude) pathway CI is dominated by the production of the intermediate pyrolysis oil, which requires some fossil fuels to initiate pyrolysis and to run auxiliary processes.

First generation feedstocks potentially compete with food crops for arable land and thus threaten terrestrial carbon sinks if agricultural lands expand to meet demand. Sugar and starch ATJ pathways have significant GHG emission contributions from all process stages, and notably LUC is a significant source. Corn ethanol uses more fossil energy for distillation than sugar ethanol, leading to a larger CI contribution in the production of the intermediate for ATJ. Corn stover ATJ, on the other hand, produces most of the internal heat and energy required for ethanol production from biomass. The CI of HEFA pathways is dominated by LUC and feedstock production emissions.

The ATF routes are comparatively poor in terms of carbon reductions, with no pathway achieving the requisite 70% CI reduction, although the two electrolysis routes are borderline at 69% under current assumptions. Higher emissions in the RWGS case are on account of additional natural gas used in process heating. Much of the limitation in carbon reductions has to do with a key difference between ATF and biomass pathways: ATF can, at best, achieve a 1:1 tradeoff between $CO_2$ incorporated into the fuel and the $CO_2$ released upon combustion. In other words, you can never do better than stoichiometry. In the biomass pathways, not all of the carbon fixated into the biomass ends up in the fuel. A fraction of this carbon is captured and sent to storage which results in an emission credit. ATF pathways are not designed to achieve these types of removals.

Other factors lend to the modest emission reductions in ATF pathways. For one, there are potential significant emissions resulting from feedstock production ($CO_2$ capture and water electrolysis). Natural gas provides thermal energy and on-site electricity for the DAC facility. Even when CCS is applied, leakage in the supply chain can result in significant $CO_2e$ emissions; these, combined with other process and embodied emissions result in a DAC $CO_2$ CI of 0.2 $kgCO_2e$ per $kgCO_2$ delivered. Additionally, electrolytic systems have tremendous electricity requirements of near 20 MW per million gallons of jet fuel capacity, just for green $H_2$ alone. Hence, even very low-carbon energy sources, like wind (~11 $gCO_2e$/kWh) or solar (~25 $gCO_2e$/kWh) can result in noticeable contributions to the overall CI of ATF pathways. This could be improved with incorporation of hydrogen generated from biomass with carbon removal and storage (BiCRS), all-electric DAC-sourced $CO_2$, or progressive reductions in renewable energy CI. For example, as the CI of solar converges to 0.0 $gCO_2e$/kWh, the CI of ATF pathways drops to between 14 and 30 $gCO_2e$/MJ fuel.

#### 4.2.3.3 Cost structure and Minimum Fuel Selling Price

We first look at cost drivers for each SAF pathway by analyzing the net present value and relative contribution of CAPEX, feedstock, OPEX, and CCS transport on total project costs (**Figure 4-6**). Sugar ATJ and HDCJ have the lowest total costs. For all MSW-fed pathways, CAPEX comprises more than 60% of total cost. All FT, HDCJ, and cellulosic ATJ pathway costs are primarily CAPEX driven (>40%). All 1G pathways (starch and sugar ATJ, HEFA) have less than 20% contribution from CAPEX. 1G pathway costs are primarily driven by feedstock cost. In general, ATF pathway costs are OPEX driven with a significant contribution from feedstock

(DAC $CO_2$, hydrogen) production. Notably, the presence or absence of CCS makes little relative difference in CAPEX costs and associated $CO_2$ transport costs are relatively negligible.

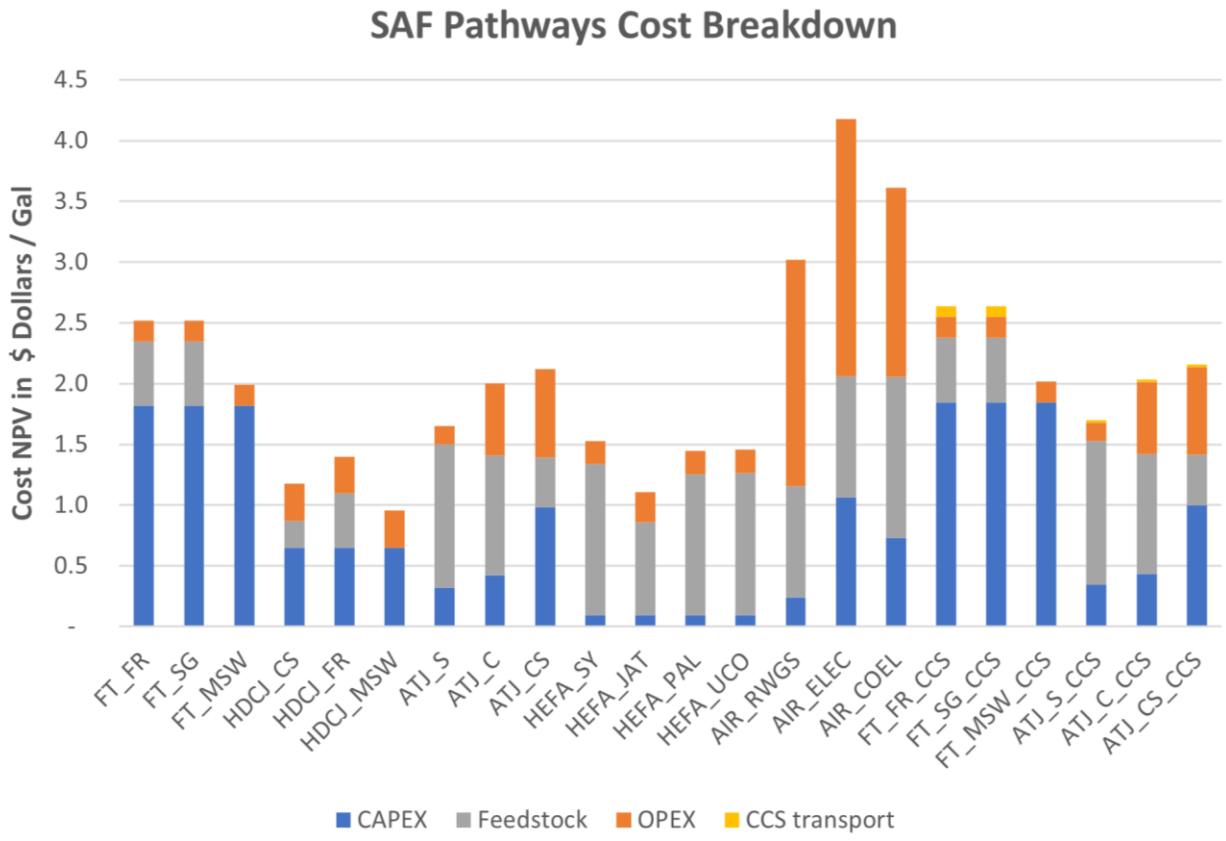


**Figure 4-6** SAF pathways cost contribution breakdown. Note that this figure shows the net present value of costs over the life of the project averaged over the total fuel produced. Discounted future costs result in smaller values than the undiscounted variable costs in the current year. See the unsubsidized minimum selling price estimates in **Figure 4-11** to get a sense of discrete cost estimates for each SAF pathway. Note that minimum selling price incorporates a 15% IRR assumption. Pathway key: FR = forest residue, SG = switchgrass, MSW = municipal solid waste, S = sugar, C = corn, CS = corn stover, SY= soy oil, JAT = jatropha oil, PAL = palm oil, UCO = used cooking oil, FT = Fischer-Tropsch, HDCJ = Hydrotreated Depolymerized Cellulosic Jet (pyrolysis biocrude), ATJ = alcohol to jet, HEFA = hydroprocessed esters and fatty acids, AIR = Air to Fuels, CCS = carbon capture and sequestration, RWGS = reverse water gas shift, ELEC = electrolysis, COEL = co-electrolysis

Next, we analyze the sources of positive cashflow (**Figure 4-7**). We select a static selling price of $3/gal to illustrate a representative proportion of cash flow coming from policy relative to sales for each pathway, and this represents a modest green premium above the typical price of Jet-A. Available subsidies, including 45Q (tax credit), LCFS, and RFS, are included in selling price estimates where applicable. Low selling price and low carbon intensity are somewhat correlated, as the revenue stream for very low CI pathways is dominated by the sale of LCFS and RFS credits. At $3/gal, all FT and HDCJ pathways generate more cash flow from policy than

from sales. 1G pathways without CCS rely much more heavily on fuel sales. This is especially true for 1G HEFA pathways.

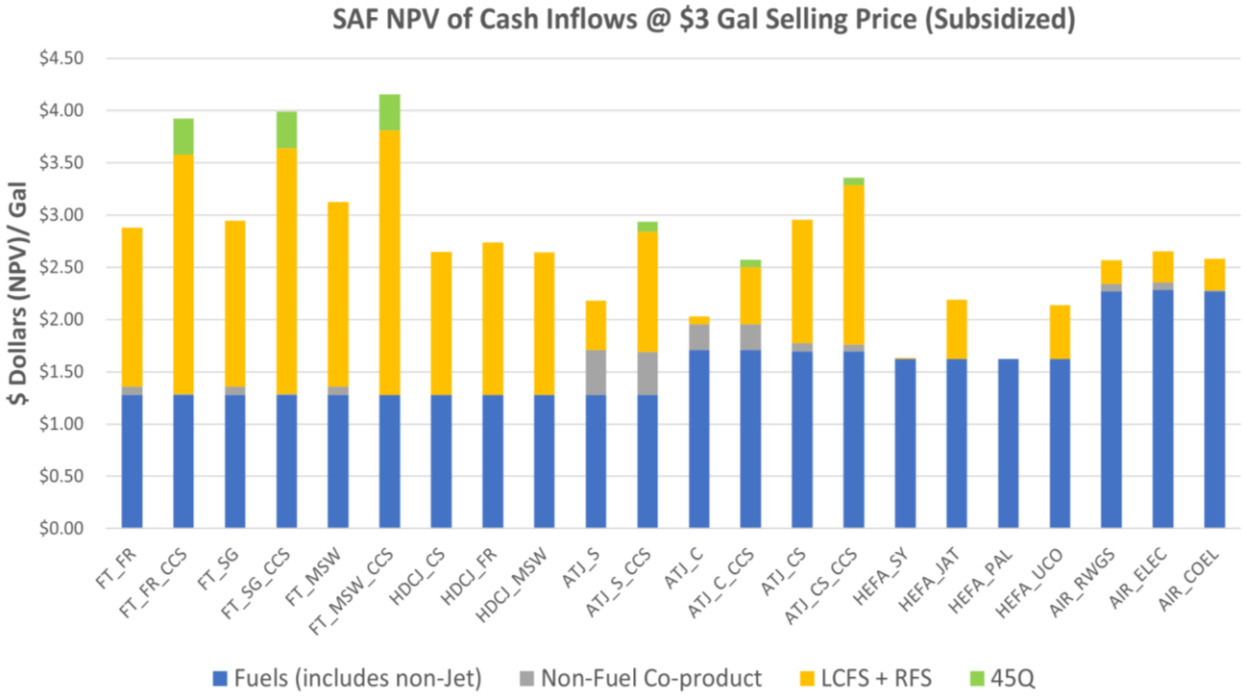


**Figure 4-7** SAF pathway NPV of subsidized cash inflows at $3/gal jet fuel price. Note that this figure shows the net present value of cash inflows over the life of the project averaged over the total fuel produced. Discounted future cash flows result in smaller values than the undiscounted cash flows (e.g. fuel price) in the current year. Pathway key: FR = forest residue, SG = switchgrass, MSW = municipal solid waste, S = sugar, C = corn, CS = corn stover, SY= soy oil, JAT = jatropha oil, PAL = palm oil, UCO = used cooking oil, FT = Fischer-Tropsch, HDCJ = Hydrotreated Depolymerized Cellulosic Jet (pyrolysis biocrude), ATJ = alcohol to jet, HEFA = hydroprocessed esters and fatty acids, AIR = Air to Fuels, CCS = carbon capture and sequestration, RWGS = reverse water gas shift, ELEC = electrolysis, COEL = co-electrolysis

Our SAF price criteria is a subsidized SAF selling price <$5 per gallon assuming a 15% IRR. Currently ASTM-approved HEFA price estimates (as well as our own estimates for soy and palm oil HEFA) hover near this value and our analysis reveals a significant divergence in prices above and below this threshold for other SAF pathways. In comparison, recent prices for Jet-A have been less than $2 per gallon. **Figure 4-8** shows the subsidized and unsubsidized MFSP for pathways analyzed in our TEA and discounted cashflow analysis. Differences between cellulosic feedstocks (e.g. forest residues, corn stover) were small, and thus they have been aggregated here under the “cellulosic” category, taking the higher of the prices as representative.

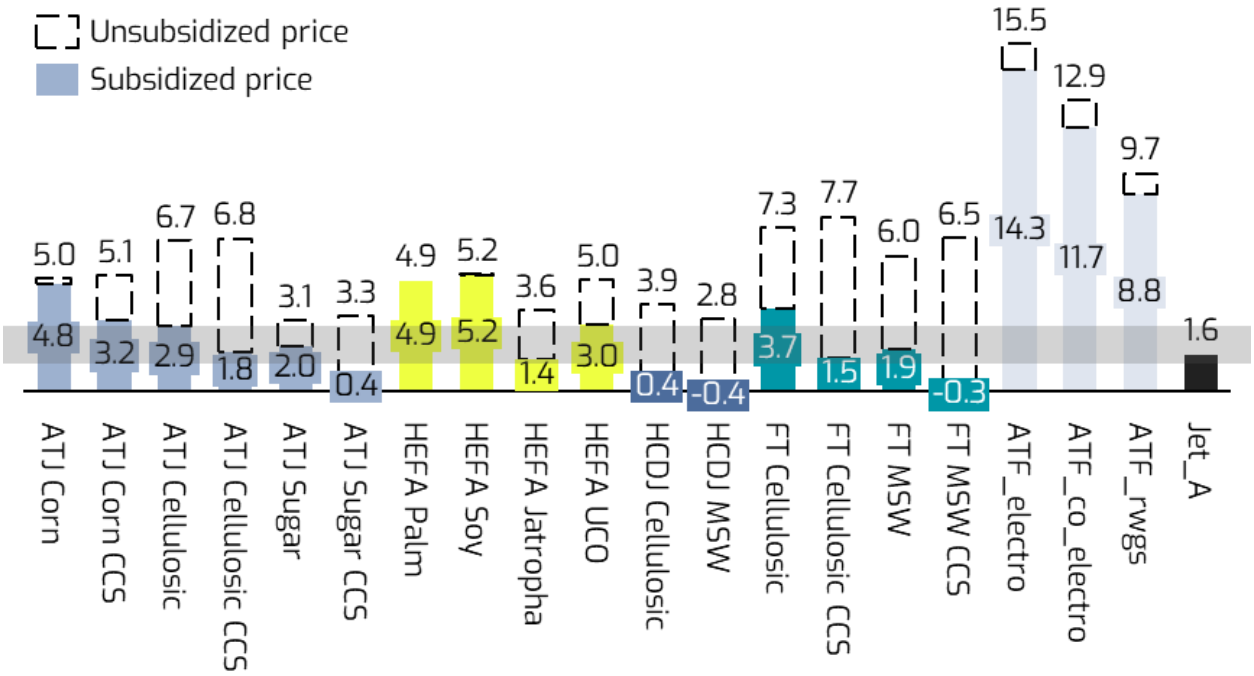


**Figure 4-8** Subsidized and unsubsidized MFSP. Typical Jet-A range is represented by the grey bar. Jet-A spot price is indicative of 2020 prices. Subsidies include LCFS credit price and U.S. 45Q tax credit for CCS where applicable. Pathway key: FR = forest residue, SG = switchgrass, MSW = municipal solid waste, S = sugar, C = corn, CS = corn stover, SY= soy oil, JAT = jatropha oil, PAL = palm oil, UCO = used cooking oil, FT = Fischer-Tropsch, HDCJ = Hydrotreated Depolymerized Cellulosic Jet (pyrolysis biocrude), ATJ = alcohol to jet, HEFA = hydroprocessed esters and fatty acids, AIR = Air to Fuels, CCS = carbon capture and sequestration, RWGS = reverse water gas shift, ELEC = electrolysis, COEL = co-electrolysis

**Figure 4-9** shows which pathways meet or exceed a 15% IRR at price points between $1.50 and $5.00. With the exception of soy-based HEFA and Air-to-Fuels pathways, all SAF pathways meet the selling price criteria. More importantly, FT paired with CCS and/or MSW, HDCJ, Sugar ATJ with CCS, Cellulosic ATJ with CCS, and Jatropha-based HEFA meet or exceed price parity with Jet-A when provided with relevant subsidies.

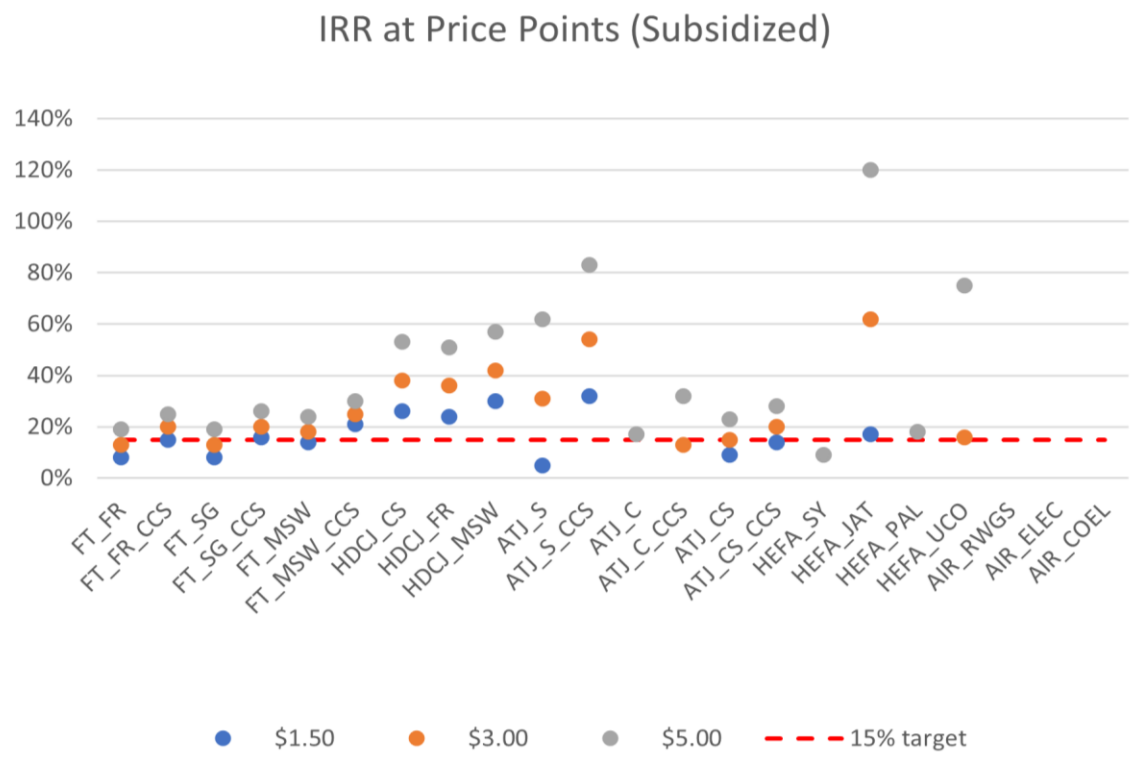


**Figure 4-9** Expected IRR with subsidies at various jet fuel selling prices. Return rates less than zero are excluded. No ATF pathways make a return at $5 or under. The RWGS ATF pathway has the lowest return threshold of the three ATF pathways at about $7.90 per gallon. Pathway key: FR = forest residue, SG = switchgrass, MSW = municipal solid waste, S = sugar, C = corn, CS = corn stover, SY= soy oil, JAT = jatropha oil, PAL = palm oil, UCO = used cooking oil, FT = Fischer-Tropsch, HDCJ = Hydrotreated Depolymerized Cellulosic Jet (pyrolysis biocrude), ATJ = alcohol to jet, HEFA = hydroprocessed esters and fatty acids, AIR = Air to Fuels, CCS = carbon capture and sequestration, RWGS = reverse water gas shift, ELEC = electrolysis, COEL = co-electrolysis

#### 4.2.3.2 Summary findings

To synthesize, we compare the price, carbon intensity, and estimated supply of SAF pathways. This allows us to evaluate many of our criteria simultaneously. Results are summarized in **Figure 4-10** and **Figure 4-11**, and **Table 4-13**.

Looking at subsidized costs (**Figure 4-10**), scalable technologies in the lower left quadrant are best-qualified to meet our stated criteria. Current subsidies make a number of pathways attractive options. The most important additional option is MSW-based FT with CCS, which is not only price competitive but has an excellent footprint (substantial $CO_2$ removal) amongst currently accepted accounting protocols. This suggests that as a fuel it has additional value in decarbonizing aviation on a miles-traveled basis. However, the heterogeneous nature of MSW feedstocks likely positions this option more long-term than FT utilizing more conventional feedstocks.

Aside from MSW, we believe biomass wastes and residues could produce SAF at prices approaching our stated criteria and, in some cases, price parity with existing policy support. Both ATJ and FT processes appear promising, especially when coupled with CCS. We anticipate both of these pathways could play a role by 2030. Several other pathways meet the cost and CI criteria but are either at lower TRL or we have assessed scaling risks to the feedstock supply.

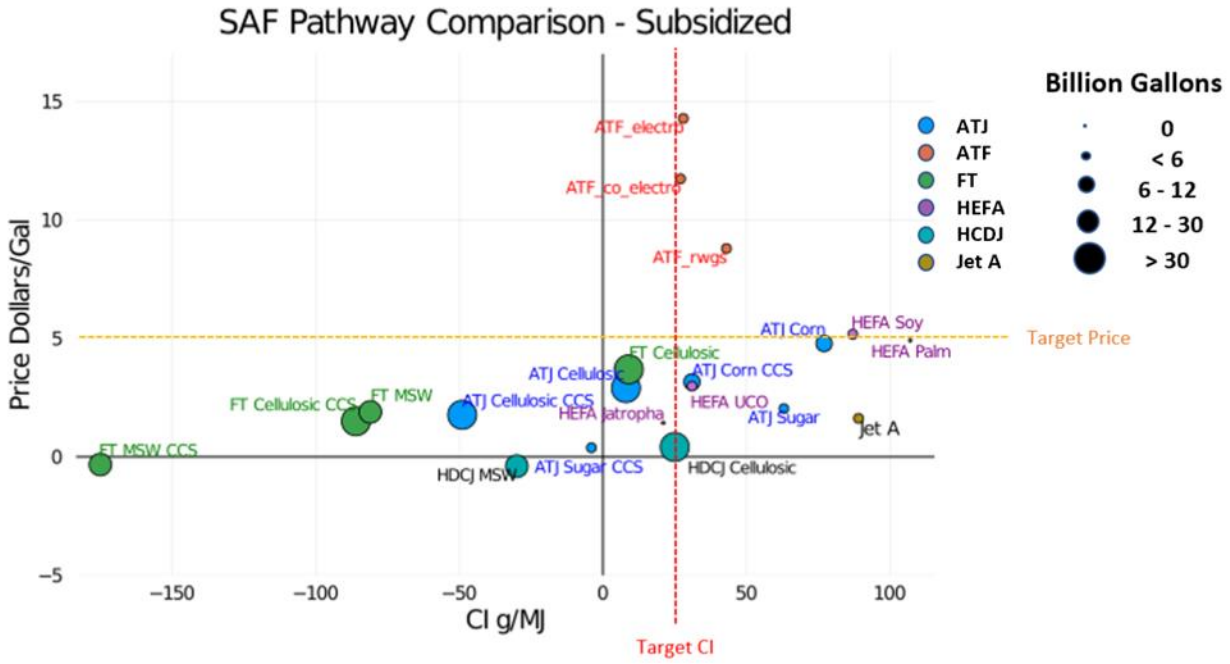


**Figure 4-10** Subsidized selling price at 15% IRR, CI, and feedstock availability (marker size) for pathways. Fossil-derived Jet-A is provided for comparison. Feedstock/scale potential for ATF pathways is theoretically unlimited. However, near-term potential is limited by costs and lack of commercial deployment. We anticipate < 1 billion gallons (low end of the < 6 Billion category) over the next 10 years. Scale potential is not depicted for Jet-A.

For comparison, the unsubsidized costs are provided in **Figure 4-11** to illustrate the significant impact of policy and related subsidies on SAF prices. In the absence of subsidies, SAF prices range from approximately $3-15/gal, and none are at or below the price of Jet-A. All of the pathways that meet cost and emissions criteria without subsidy face technology readiness challenges (HDCJ) or feedstock sourcing/supply challenges (Sugarcane ATJ, Jatropha HEFA). The implication is that policy support will be essential to meet SAF cost criteria.

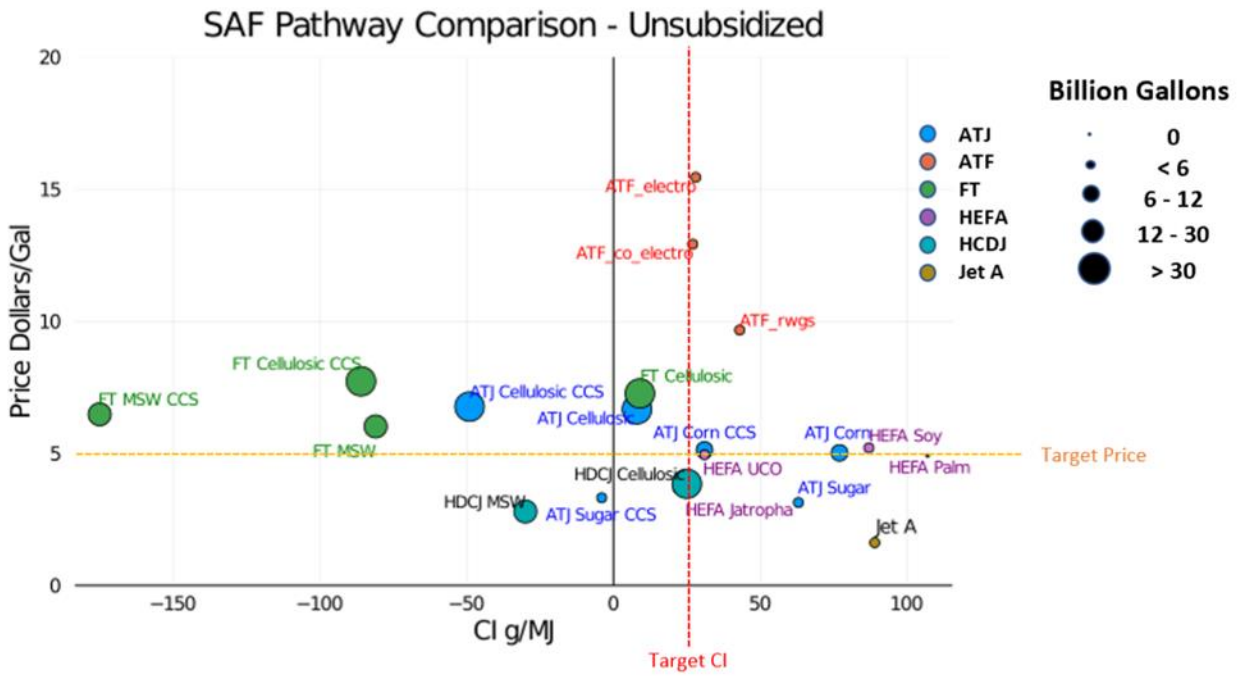


**Figure 4-11** Unsubsidized costs, CI, and feedstock availability (marker size) for pathways. Fossil-derived Jet-A is provided for comparison. Feedstock/scale potential for ATF pathways is theoretically unlimited. However, near-term potential is limited by costs and lack of commercial deployment. We anticipate < 1 billion gallons (low end of the < 6 Billion category) over the next 10 years. Scale potential is not depicted for Jet-A.

The replacement of Jet-A with SAF could impact ticket prices because fuel costs represent a substantial component of the overall cost of a flight. **Table 4-13** shows the range of impacts on ticket price for the SAF pathways analyzed in this report assuming 1:1 replacement of Jet-A (and assuming that $2/gal Jet-A constitutes 25% of existing ticket price). In practice, SAF is currently blended at volumes up to 50%. The realized impacts of SAF on ticket price will ultimately be a function of SAF price, blending volumes, and the carbon intensity of fuel, as it will require smaller blending volumes of very low carbon or carbon negative fuels to achieve aggregate emissions targets

**Table 4-13** Summary MFSP, CI, and CI reduction relative to Conventional Jet-A

| | | HEFA | Alcohol-to-Jet | Fischer- Tropsch | HDCJ | Air-to-Fuels |
|---|---|---|---|---|---|---|
| **% Carbon Reduction vs. Jet-A** | *With CCS* | N/A | 65-155% | 197-297% | N/A | N/A |
| | *Without CCS* | 2-76%<br>Palm (+20%) | 13-91% | 90-191% | 72-134% | 52-69% |
| **Price** | *Sub.* | $1.43-$5.17 | $0.38-$4.78 | $0.00-$3.69 | $0.0 -$0.41 | $8.79-$14.28 |

| | | | | | | |
|---|---|---|---|---|---|---|
| **Range $/gal** | *Unsub.* | $3.60-$5.21 | $3.14-$6.77 | $6.02-$7.73 | $2.80-$3.85 | $9.67-$15.45 |
| **Change in ticket price** | *Sub.* | -7% to +40% | -20% to +35% | -25% to +21% | -25% to -20% | +85%-154% |
| | *Unsub.* | +20-40% | +14-60% | +50-72% | +10-23% | +96-168% |

### 4.2.4 Discussion

No SAF is price competitive without subsidies. Historically (2018 & 2019), Jet-A prices were roughly $2/gallon. Unsurprisingly, this makes fierce competition against unsubsidized SAFs. It appears that HDCJ from MSW and cellulosic feedstock pyrolysis are relatively promising, although limited today by low technical readiness (TRL 5).

Given the reliance of SAF on policy support, understanding the value and stability of key subsidies is important for assessing the markets for SAF in 2025, 2030, and beyond. For example, uncertainty in future markets for the LCFS affect financing of early projects. Conversely, enhancements to 45Q or the renewable fuel standard can improve the competitiveness of these systems for those systems where CCS and DAC contribute (see below on air-to-fuels). Alternatively, if biochar production and use is supported, that would alter the financial profile for pyrolysis-based HDCJ technology.

The carbon intensity of these SAF pathways is sensitive to LUC and LCA input of the feedstocks. For waste streams, qualification and certification of waste footprints is emerging rapidly as an important standard setting exercise. If these pathways shift feedstocks from wastes to dedicated energy crops, that could dramatically affect both the climate/carbon value of the product and the magnitude of subsidies.

It is evident that feedstocks can greatly impact the economic viability of these SAF pathways. In particular, Air-to-Fuels pathways suffer from high costs to capture $CO_2$ directly from the atmosphere and electrolytically split water to produce $H_2$, with the latter having a larger impact. While only green hydrogen is considered in this analysis, several alternative low-carbon hydrogen routes are emerging. Blue hydrogen involves fitting steam methane reformation with CCS, typically on the post-shift and/or PSA tail gas, which can add $0.50 - 1.00/kg $H_2$ to the cost of production while reducing the CI by ca. 70% [401]. However, regional variance is expected - similar to that seen in green routes where economics are largely tied to the cost of local electricity - blue hydrogen routes are largely dependent on the availability of low-cost natural gas and an offtake partner for the captured $CO_2$. Overall, replacing green hydrogen at $3.50/kg $H_2$ with blue hydrogen at $2.00/kg $H_2$ could reduce the jet fuel selling price from $11/gal to ~ $8.40/gal, albeit at a slightly higher CI of 56 $gCO_2e$/MJ fuel.

A host of less mature options for $H_2$ production have also entered the conversation. Hydrogen from biomass has been posited (under the umbrella of BiCRS - Biomass Carbon Removal and Storage138), where fast pyrolysis or gasification of biomass and subsequent storage of $CO_2$ can lead to $H_2$ with a carbon negative footprint. Turquoise hydrogen involves the pyrolytic splitting

of $CH_4$ into $H_2$ and solid carbon. It remains unclear whether these new options can be considered economic alternatives for an ATF feedstock at this time.

To help explore future scenarios, $H_2$ sourced at \$1.00/kg and at a CI of 0.5 kg CO2e/kg $H_2$ would yield a low ATF-derived jet fuel selling price of \$6.12/gal. If DAC-sourced $CO_2$ can simultaneously fall to \$150/t$CO_2$, the jet fuel selling price drops to under \$5/gal. Thus, significantly reducing these renewable feedstock costs as the associated technologies scale up could eventually bring these ATF pathways closer to commercial viability.

For comparison, we estimate what the abatement cost would be to mitigate conventional jet fuel emissions with direct air capture and geologic sequestration instead. Considering two cases of DAC (90% capture) at \$250/t$CO_2$ and \$600/t$CO_2$ with \$20/t$CO_2$ for transport and storage, the incremental cost would be roughly \$1.67/gal and \$6.06/gal, respectively. In addition to the price for conventional Jet Fuel (\$1.62/gal), this yields an all-in cost of \$3.29/gal and \$7.68/gal used (see Table A-7). Thus, investing in DAC for sequestration rather than SAF production might prove to be a more cost-effective means of getting to net-zero emissions. Importantly, a full analysis of the economic, social and environmental impacts of this pathway ought to be considered when evaluating this option against the SAF routes presented herein.

#### 4.2.4.1 Why Air to Fuels?

It is clear from the above analysis that ATF pathway fuels are economically unattractive given current feedstock prices and could only potentially enter the conversation with aggressive cost reductions in both DAC-$CO_2$ and low carbon $H_2$, but these are not likely to become cost competitive with incumbent pathways nor best case 1G and 2G biomass options. A similar though less drastic gulf exists in the comparative LCA footprints. The question then begs, why ever consider ATF pathways? We believe that despite non-competitive economics in the near-term, ATF pathways will continue to gather interest for the following reasons: 1) biomass availability for the specific purpose of SAF production is subject to geographical and competitive limitations. There are several emerging uses for biomass, including in energy production, hydrogen production and chemical production, so it remains uncertain how much biomass can be earmarked for SAF production, 2) there are logistical advantages to ATF pathways including siting and co-location of feedstocks, and a much more straightforward calculation of the full life cycle emissions, 3) there exist indirect benefits to ATF pathways in the form of technology learnings gained from DAC deployment. Here, ATF pathways play a role in subsidizing DAC deployment which can help drive down costs for future DAC deployment.

# CHAPTER 5. CONCLUSION

This dissertation makes several advances in the rapidly emerging Biomass Carbon Removal and Storage (BiCRS) literature as well as indicating the indispensable role of the bioeconomy in global decarbonization strategies. While methodologically rooted in life cycle assessment (LCA) and techno-economic assessment (TEA) and the intersection of these analyses with existing policy regimes, the research, in sum, also highlights that the role of the bioeconomy is necessarily limited by ecological and social boundary conditions. This work points towards the highest value uses of these limited resources and indicates that the highest value uses of these resources are likely to change over the near, medium, and long-term.

The findings of this work indicate substantial near-term opportunities to deploy commercially viable decarbonization strategies within the bioeconomy at its intersection with the agriculture, chemical, construction, and energy industries. Supportive policies and capital investment are available today to scale these technologies as well as to innovate and improve. The chapters leading up to this point serve as important technical contributions for government, industry, and private market actors to guide the transition to a decarbonized economy and to sustainably position the bioeconomy within that transition. My research is motivated by the question "How should biomass be used in decarbonization efforts?" The answer to this question is not straightforward. But my research indicates priorities by asking about impact, cost, scalability, sustainability, and commercial viability. Several themes emerge from this work.

## 5.1 Decarbonization with biomass is bigger than BECCS

Bioenergy with carbon capture and sequestration— or BECCS –has dominated the conversation around biomass and decarbonization until recently. However, the bioeconomy is bigger than bioenergy. Low-cost, low-carbon sources of electricity like wind and solar, along with battery storage and perhaps even nuclear power seem poised to dominate the power sector and light-duty transport in the medium to long-term. While the energy content in biomass resources may remain valuable in the near to medium term, the value of the carbon and other chemical/physical properties of biomass feedstocks may increasingly represent a larger share of the value in bioproducts. The emerging BiCRS framework embraces this distinction and recognizes a broad spectrum of opportunity to remove atmospheric carbon for storage in value-added products and long-lived goods.

## 5.2 Highest value use of biomass

While this dissertation did not seek to assess the highest value uses of biomass directly, the results of my work and the frameworks that I have drawn upon perhaps sketch a trajectory. Just as BECCS dominated the biomass conversation before it became clear that utility scale wind and solar could be made reliable and cheap, other potential biomass interventions may be obviated as the global economy decarbonizes. What is clear, for now, is that a limited role likely remains for bioenergy (fuels, hydrogen, and power) as a light-duty vehicle fleets phase over to electric vehicles. There would seem in the near-term an indispensable role for biomass feedstocks in the production of drop-in aviation fuels. Even as fossil fuels phase out of use for energy, there will

remain demand for hydrocarbons for plastics, polymers, and building materials, and biomass may well play a pivotal role in "greening" those hard-to-decarbonize sectors, as well. We currently do not have enough biomass resources to service all of the sectors of the economy where there is potential. We will increasingly be forced to direct biomass resources to sectors where the bioeconomy is the most impactful or only option. Increasingly, recycled $CO_2$ and hydrogen may serve as the basis feedstock for many of the end-uses that biomass can provide today. However costs remain high for $CO_2$ utilization. In the meantime, photosynthesis draws upon the nearly inexhaustible resource of the sun to provide the carbon, hydrogen, and energy that serve as the only cost-effective and ready analog for fossil resources. Eventually, it may prove that carbon storage potential of biomass is one of its most valuable attributes.

### 5.3 Life Cycle and Technoeconomic Assessment are indispensable decision support tools for assessing decarbonization opportunities.

Given the scale of transition implied by global decarbonization, new technologies, business models, market actors, policies, and public private partnerships will continue to emerge. Policymakers, investors, and stakeholders need frameworks to separate real opportunities from dead-ends. Climate solutions emerging from the bioeconomy must both have real impact and commercial viability. LCA and TEA are two decision support methodologies that can identify scalable, impactful new sectors in the economy more broadly, but this is particularly true and needed in the bioeconomy. These tools can be deployed at every stage of development, from early-stage planning to commissioning. While no tool is perfect, best practices and consistent, transparent comparisons of cost and impact within these frameworks provide invaluable benchmarks for supportive policy, project development, and decision-making among all decarbonization stakeholders. Chapters 3 and 4 offer the clearest examples of the utility of these approaches in tandem.

# CHAPTER 6. REFERENCES


[1] IPCC, "Summary for Policymakers," in *Climate Change 2021: The Physical Science Basis. Contribution of Working Group I to the Sixth Assessment Report of the Intergovernmental Panel on Climate Change*, V. Masson-Delmotte, P. Zhai, A. Pirani, S. L. Connors, C. Péan, S. Berger, N. Caud, Y. Chen, L. Goldfarb, M. I. Gomis, M. Huang, K. Leitzell, E. Lonnoy, J. B. R. Matthews, T. K. Maycock, T. Waterfield, O. Yelekçi, R. Yu, and B. Zhou, Eds. Cambridge, United Kingdom and New York, NY, USA: Cambridge University Press, 2021, p. 3−32.

[2] IPCC, *Climate Change 2021: The Physical Science Basis. Contribution of Working Group I to the Sixth Assessment Report of the Intergovernmental Panel on Climate Change*, vol. In Press. Cambridge, United Kingdom and New York, NY, USA: Cambridge University Press, 2021.

[3] United Nations Department of Economic and Social Affairs, "SDG Indicators - 7 Affordable and Clean Energy," *unstats.un.org*, 2022. https://unstats.un.org/sdgs/report/2021/goal-07/ (accessed Oct. 16, 2022).

[4] IPCC, "Summary for Policymakers," in *Climate Change 2022: Mitigation of Climate Change. Contribution of Working Group III to the Sixth Assessment Report of the Intergovernmental Panel on Climate Change*, P. R. Shukla, J. Skea, R. Slade, A. Al Khourdajie, R. van Diemen, D. McCollum, M. Pathak, S. Some, P. Vyas, R. Fradera, M. Belkacemi, A. Hasija, G. Lisboa, S. Luz, and J. Malley, Eds. Cambridge, UK and New York, NY: Cambridge University Press, 2022.

[5] R. C. (Robert C. Brown, *Biorenewable resources : engineering new products from agriculture* , 1st ed. Ames, Iowa: Iowa State Press, 2003.

[6] D. W. Keith, "Sinks, energy crops and land use: Coherent climate policy demands an integrated analysis of biomass. An editorial comment," *Climatic Change*, vol. 49, no. 1–2. Springer, pp. 1–10, 2001, doi: 10.1023/A:1010617015484.

[7] S. J. Varjani, I. S. Thakur, Y. Wu, E. Gnansounou, M. Kumar, and S. Ravindran, "Sequestration and utilization of carbon dioxide by chemical and biological methods for biofuels and biomaterials by chemoautotrophs: Opportunities and challenges," *Bioresour. Technol.*, vol. 256, pp. 478–490, May 2018, doi: 10.1016/j.biortech.2018.02.039.

[8] S. V. Jørgensen, M. Z. Hauschild, and P. H. Nielsen, "The potential contribution to climate change mitigation from temporary carbon storage in biomaterials," *Int. J. Life Cycle Assess.*, vol. 20, no. 4, pp. 451–462, 2015, doi: 10.1007/s11367-015-0845-3.

[9] J. H. Arehart, J. Hart, F. Pomponi, and B. D'Amico, "Carbon sequestration and storage in the built environment," *Sustain. Prod. Consum.*, vol. 27, pp. 1047–1063, Jul. 2021, doi: 10.1016/J.SPC.2021.02.028.

[10] J. H. Williams *et al.*, "Pathways to Deep Decarbonization in the United States," 2015. Accessed: Nov. 22, 2019. [Online]. Available: http://usddpp.org/.

[11] M. Wei *et al.*, "Deep carbon reductions in California require electrification and integration across economic sectors," *Environ. Res. Lett*, vol. 8, pp. 14038–14048, Jan. 2013, doi: 10.1088/1748-9326/8/1/014038.

[12] M. Z. Jacobson and M. A. Delucchi, "Providing all global energy with wind, water, and solar power, Part I: Technologies, energy resources, quantities and areas of infrastructure, and materials," *Energy Policy*, vol. 39, no. 3, pp. 1154–1169, 2011, doi:

10.1016/j.enpol.2010.11.040.
[13] J. Rogelj *et al.*, “Energy system transformations for limiting end-of-century warming to below 1.5 °C,” *Nat. Clim. Chang.*, vol. 5, no. 6, pp. 519–527, Feb. 2015, doi: 10.1038/nclimate2572.
[14] A. Horvath, C. D. Scown, M. Taptich, and K. Piscopo, “The future of drop-in fuels,” Nov. 2016.
[15] C. D. Scown, M. Taptich, A. Horvath, T. E. McKone, and W. W. Nazaroff, “Achieving Deep Cuts in the Carbon Intensity of U.S. Automobile Transportation by 2050: Complementary Roles for Electricity and Biofuels,” *Environ. Sci. Technol.*, vol. 47, no. 16, pp. 9044–9052, Nov. 2013, doi: 10.1021/es4015635.
[16] D. L. Sanchez, J. H. Nelson, J. Johnston, A. Mileva, and D. M. Kammen, “Biomass enables the transition to a carbon-negative power system across western North America,” 2015, doi: 10.1038/NCLIMATE2488.
[17] J. Rogelj *et al.*, “Energy system transformations for limiting end-of-century warming to below 1.5 °C,” *Nat. Clim. Chang.*, vol. 5, no. 6, pp. 519–527, Jun. 2015, doi: 10.1038/nclimate2572.
[18] C. T. M. Clack *et al.*, “Evaluation of a proposal for reliable low-cost grid power with 100% wind, water, and solar,” vol. 114, no. 26, pp. 6722–6727, 2017, doi: 10.1073/pnas.1610381114.
[19] M. Z. Jacobson and M. A. Delucchi, “Providing all global energy with wind, water, and solar power, Part I: Technologies, energy resources, quantities and areas of infrastructure, and materials,” 2011, doi: 10.1016/j.enpol.2010.11.040.
[20] D. L. Sanchez and D. S. Callaway, “Optimal scale of carbon-negative energy facilities,” *Appl. Energy*, vol. 170, pp. 437–444, May 2016, doi: 10.1016/J.APENERGY.2016.02.134.
[21] J. F. D. Tapia *et al.*, “Design of biomass value chains that are synergistic with the food–energy–water nexus: Strategies and opportunities,” *Food Bioprod. Process.*, vol. 116, pp. 170–185, Jul. 2019, doi: 10.1016/J.FBP.2019.05.006.
[22] N. Shabani, S. Akhtari, and T. Sowlati, “Value chain optimization of forest biomass for bioenergy production: A review,” *Renew. Sustain. Energy Rev.*, vol. 23, pp. 299–311, Jul. 2013, doi: 10.1016/J.RSER.2013.03.005.
[23] B. Steubing, R. Zah, and C. Ludwig, “Heat, electricity, or transportation? the optimal use of residual and waste biomass in Europe from an environmental perspective,” *Environ. Sci. Technol.*, vol. 46, no. 1, pp. 164–171, Jan. 2012, doi: 10.1021/ES202154K/SUPPL_FILE/ES202154K_SI_001.PDF.
[24] V. Codina Gironès, S. Moret, E. Peduzzi, M. Nasato, and F. Maréchal, “Optimal use of biomass in large-scale energy systems: Insights for energy policy,” *Energy*, vol. 137, pp. 789–797, Oct. 2017, doi: 10.1016/J.ENERGY.2017.05.027.
[25] C. Vadenbo, D. Tonini, and T. F. Astrup, “Environmental Multiobjective Optimization of the Use of Biomass Resources for Energy,” *Environ. Sci. Technol.*, vol. 51, no. 6, pp. 3575–3583, Mar. 2017, doi: 10.1021/ACS.EST.6B06480/ASSET/IMAGES/LARGE/ES-2016-06480F_0004.JPEG.
[26] F. Schipfer, L. Kranzl, D. Leclère, L. Sylvain, N. Forsell, and H. Valin, “Advanced biomaterials scenarios for the EU28 up to 2050 and their respective biomass demand,” *Biomass and Bioenergy*, vol. 96, pp. 19–27, Jan. 2017, doi: 10.1016/J.BIOMBIOE.2016.11.002.

[27] P. Smith *et al.*, “Biophysical and economic limits to negative CO2 emissions,” *Nat. Clim. Chang.*, vol. 6, no. 1, pp. 42–50, 2016, doi: 10.1038/nclimate2870.
[28] L. J. Smith and M. S. Torn, “Ecological limits to terrestrial biological carbon dioxide removal,” *Clim. Change*, vol. 118, no. 1, pp. 89–103, May 2013, doi: 10.1007/s10584-012-0682-3.
[29] K. Riahi, R. Schaeffer, and J. Arango, “Mitigation Pathways Compatible with Long-Term Goals,” in *Climate Change 2021: The Physical Science Basis. Contribution of Working Group III to the Sixth Assessment Report of the Intergovernmental Panel on Climate Change*, P. R. Shukla, J. Skea, R. Slade, A. Al Khourdajie, R. van Diemen, D. McCollum, M. Pathak, S. Some, P. Vyas, R. Fradera, M. Belkacemi, A. Hasija, G. Lisboa, S. Luz, and J. Malley, Eds. Cambridge, United Kingdom and New York, NY, USA: Cambridge University Press, 2022.
[30] A. Babin, C. Vaneeckhaute, and M. C. Iliuta, “Potential and challenges of bioenergy with carbon capture and storage as a carbon-negative energy source: A review,” *Biomass and Bioenergy*, vol. 146, no. December 2020, 2021, doi: 10.1016/j.biombioe.2021.105968.
[31] A. Muscat, E. M. de Olde, I. J. M. de Boer, and R. Ripoll-Bosch, “The battle for biomass: A systematic review of food-feed-fuel competition,” *Glob. Food Sec.*, vol. 25, p. 100330, Jun. 2020, doi: 10.1016/J.GFS.2019.100330.
[32] L. J. Smith and M. S. Torn, “Ecological limits to terrestrial biological carbon dioxide removal,” *Clim. Change*, vol. 118, no. 1, pp. 89–103, Sep. 2013, doi: 10.1007/s10584-012-0682-3.
[33] R. Slade, A. Bauen, and R. Gross, “Global bioenergy resources,” *Nat. Clim. Chang.*, vol. 4, no. 2, pp. 99–105, 2014, doi: 10.1038/nclimate2097.
[34] U. S. D. of Energy, “2016 billion-ton report: Advancing domestic resources for a thriving bioeconomy, Volume 1: Economic Availability of Feedstocks,” 2016.
[35] IPCC, “Climate Change 2014 Mitigation of Climate Change - Working Group III Contribution to the Fifth Assessment of the Intergovernmental Panel on Climate Change,” *Cambridge Univ. Press*, p. 1454, 2014, [Online]. Available: https://www.ipcc.ch/site/assets/uploads/2018/05/uncertainty-guidance-note.pdf.%0Awww.cambridge.org.
[36] C. D. Scown, M. Taptich, A. Horvath, T. E. McKone, and W. W. Nazaroff, “Achieving Deep Cuts in the Carbon Intensity of U.S. Automobile Transportation by 2050: Complementary Roles for Electricity and Biofuels,” *Environ. Sci. Technol.*, vol. 47, no. 16, pp. 9044–9052, Aug. 2013, doi: 10.1021/es4015635.
[37] C. E. Lovelock and C. M. Duarte, “Dimensions of blue carbon and emerging perspectives,” *Biol. Lett.*, vol. 15, no. 3, pp. 1–5, 2019, doi: 10.1098/rsbl.2018.0781.
[38] P. I. Macreadie *et al.*, “The future of Blue Carbon science,” *Nat. Commun.*, vol. 10, no. 1, pp. 1–13, 2019, doi: 10.1038/s41467-019-11693-w.
[39] G. H. Rau, K. G. Knauss, W. H. Langer, and K. Caldeira, “Reducing energy-related CO2 emissions using accelerated weathering of limestone,” *Energy*, vol. 32, no. 8, pp. 1471–1477, 2007, doi: 10.1016/j.energy.2006.10.011.
[40] J. S. Kirchner, K. A. Lettmann, B. Schnetger, J. O. Wolff, and H. J. Brumsack, “Carbon capture via accelerated weathering of limestone: Modeling local impacts on the carbonate chemistry of the southern North Sea,” *Int. J. Greenh. Gas Control*, vol. 92, no. November 2019, p. 102855, 2020, doi: 10.1016/j.ijggc.2019.102855.
[41] M. Fasihi, O. Efimova, and C. Breyer, “Techno-economic assessment of CO 2 direct air

capture plants," *J. Clean. Prod.*, vol. 224, pp. 957–980, 2019, doi: 10.1016/j.jclepro.2019.03.086.
[42] National Academies of Science Engineering and Medicine, "Negative Emissions Technologies and Reliable Sequestration," Washington D.C., 2019. doi: 10.17226/25259.
[43] K. Anderson and G. Peters, "The trouble with negative emissions," *Science (80-. ).*, vol. 354, no. 6309, pp. 182–183, Oct. 2016, doi: 10.1126/SCIENCE.AAH4567/ASSET/99984170-6985-40D5-9667-5BC58A35A1EC/ASSETS/GRAPHIC/354_182_F1.JPEG.
[44] D. Sandalow, R. Aines, J. Friedmann, C. McCormick, and D. L. Sanchez, "Biomass Carbon Removal and Storage (BiRCS) Roadmap," Jan. 2021, doi: 10.2172/1763937.
[45] B. Mackey *et al.*, "Untangling the confusion around land carbon science and climate change mitigation policy," *Nature Climate Change*, vol. 3, no. 6. pp. 552–557, 2013, doi: 10.1038/nclimate1804.
[46] P. A. Arias *et al.*, "Technical Summary," in *Climate Change 2021: The Physical Science Basis. Contribution of Working Group I to the Sixth Assessment Report of the Intergovernmental Panel on Climate Change*, V. Masson-Delmotte, P. Zhai, A. Pirani, S. L. Connors, C. Péan, S. Berger, N. Caud, Y. Chen, L. Goldfarb, M. I. Gomis, M. Huang, K. Leitzell, E. Lonnoy, J. B. R. Matthews, T. K. Maycock, T. Waterfield, O. Yelekçi, R. Yu, and B. Zhou, Eds. Cambridge, United Kingdom and New York, NY, USA: Cambridge University Press, 2021, p. 33−144.
[47] J. G. Canadell *et al.*, "Global Carbon and other Biogeochemical Cycles and Feedbacks Supplementary Material," in *Climate Change 2021: The Physical Science Basis. Contribution of Working Group I to the Sixth Assessment Report of the Intergovernmental Panel on Climate Change*, V. Masson-Delmotte, P. Zhai, A. Pirani, S. L. Connors, C. Péan, S. Berger, N. Caud, Y. Chen, L. Goldfarb, M. I. Gomis, M. Huang, K. Leitzell, E. Lonnoy, J. B. R. Matthews, T. K. Maycock, T. Waterfield, O. Yelekçi, R. Yu, and B. Zhou, Eds. 2021.
[48] P. Friedlingstein *et al.*, "Global carbon budget 2019," *Earth Syst. Sci. Data*, vol. 11, no. 4, pp. 1783–1838, Dec. 2019, doi: 10.5194/ESSD-11-1783-2019.
[49] W. Carton, J. F. Lund, and K. Dooley, "Undoing Equivalence: Rethinking Carbon Accounting for Just Carbon Removal," *Front. Clim.*, vol. 3, no. April, pp. 1–7, 2021, doi: 10.3389/fclim.2021.664130.
[50] J. G. Canadell *et al.*, "Global Carbon and other Biogeochemical Cycles and Feedbacks," in *Climate Change 2021: The Physical Science Basis. Contribution of Working Group I to the Sixth Assessment Report of the Intergovernmental Panel on Climate Change*, V. Masson-Delmotte, P. Zhai, A. Pirani, S. L. Connors, C. Péan, S. Berger, N. Caud, Y. Chen, L. Goldfarb, M. I. Gomis, M. Huang, K. Leitzell, E. Lonnoy, J. B. R. Matthews, T. K. Maycock, T. Waterfield, O. Yelekçi, R. Yu, and B. Zhou, Eds. Cambridge, United Kingdom and New York, NY, USA: Cambridge University Press, 2021, pp. 673–816.
[51] H. D. Matthews and K. Caldeira, "Stabilizing climate requires near-zero emissions," *Geophys. Res. Lett.*, vol. 35, no. 4, p. 4705, Feb. 2008, doi: 10.1029/2007GL032388.
[52] K. B. Tokarska and K. Zickfeld, "The effectiveness of net negative carbon dioxide emissions in reversing anthropogenic climate change," *Environ. Res. Lett.*, vol. 10, no. 9, p. 094013, Sep. 2015, doi: 10.1088/1748-9326/10/9/094013.
[53] F. Saeed *et al.*, "How difficult is it to recover from dangerous levels of global warming? You may also like UK-Deformation Failure Mechanism and Motion Laws of Near-

horizontal Thick-layer with Thin-layer Columnar Dangerous Rock Mass in the Chishui Red Bed Area J Xie, G L Yang, Y G Qin et al.-From Paris to Makkah: heat stress risks for Muslim pilgrims at 1.5 ℃ and 2 ℃ How difficult is it to recover from dangerous levels of global warming?," vol. 4, p. 9, 2009, doi: 10.1088/1748-9326/4/1/014012.

[54] T. L. Frölicher and F. Joos, "Reversible and irreversible impacts of greenhouse gas emissions in multi-century projections with the NCAR global coupled carbon cycle-climate model," *Clim. Dyn.*, vol. 35, no. 7, pp. 1439–1459, Dec. 2010, doi: 10.1007/S00382-009-0727-0/FIGURES/13.

[55] M. Eby, K. Zickfeld, A. Montenegro, D. Archer, K. J. Meissner, and A. J. Weaver, "Lifetime of Anthropogenic Climate Change: Millennial Time Scales of Potential CO2 and Surface Temperature Perturbations," *J. Clim.*, vol. 22, no. 10, pp. 2501–2511, May 2009, doi: 10.1175/2008JCLI2554.1.

[56] S. Solomon, G. K. Plattner, R. Knutti, and P. Friedlingstein, "Irreversible climate change due to carbon dioxide emissions," *Proc. Natl. Acad. Sci. U. S. A.*, vol. 106, no. 6, pp. 1704–1709, Feb. 2009, doi: 10.1073/PNAS.0812721106.

[57] D. Archer, "Fate of fossil fuel CO2 in geologic time," *J. Geophys. Res. C Ocean.*, vol. 110, no. 9, pp. 1–6, 2005, doi: 10.1029/2004JC002625.

[58] J. C. Minx *et al.*, "Negative emissions—Part 1: Research landscape and synthesis," *Environ. Res. Lett.*, vol. 13, no. 6, p. 063001, Jun. 2018, doi: 10.1088/1748-9326/aabf9b.

[59] S. Fuss *et al.*, "Negative emissions—Part 2: Costs, potentials and side effects," *Environ. Res. Lett.*, vol. 13, no. 6, p. 63002, Sep. 2018, doi: 10.1088/1748-9326/aabf9f.

[60] O. Olsson *et al.*, "Deployment of BECCS / U value chains Technological pathways , policy options and business models," 2020. [Online]. Available: https://www.ieabioenergy.com/publications/new-publication-deployment-of-beccs-u-value-chains-technological-pathways-policy-options-and-business-models/.

[61] S. Fankhauser *et al.*, "The meaning of net zero and how to get it right," *Nature Climate Change*, vol. 12, no. 1. Nature Publishing Group, pp. 15–21, Dec. 20, 2022, doi: 10.1038/s41558-021-01245-w.

[62] IPCC, "IPCC Special Report: Global Warming of 1.5 ºC, Summary for Policymakers," 2018. Accessed: Dec. 06, 2021. [Online]. Available: https://www.ipcc.ch/sr15/chapter/spm/.

[63] F. Seymour, "Seeing the Forests as well as the (Trillion) Trees in Corporate Climate Strategies," *One Earth*, vol. 2, no. 5, pp. 390–393, May 2020, doi: 10.1016/J.ONEEAR.2020.05.006.

[64] California Air Resources Board, "California's Compliance Offset Program," 2021. https://ww2.arb.ca.gov/sites/default/files/2021-10/nc-forest_offset_faq_20211027.pdf (accessed Jul. 23, 2022).

[65] E. Mitchell-Larson and T. Bushman, "Carbon Direct Commentary: Release of the Voluntary Registry Offset Database," 2021. [Online]. Available: https://carbon-direct.com/wp-content/uploads/2021/04/CD-Commentary-on-Voluntary-Registry-Offsets-Database_April-2021.pdf.

[66] Berkeley Carbon Trading Project and Carbon Direct, "Voluntary Registry Offsets Database," 2021. https://gspp.berkeley.edu/faculty-and-impact/centers/cepp/projects/berkeley-carbon-trading-project/offsets-database (accessed Jul. 23, 2022).

[67] European Commission, "What is the Bioeconomy - Research - European Commission,"

2021. https://ec.europa.eu/research/bioeconomy/policy/bioeconomy_en.htm (accessed May 29, 2022).
[68] A. Aguilar, R. Wohlgemuth, and T. Twardowski, “Perspectives on bioeconomy,” *N. Biotechnol.*, vol. 40, no. Pt A, pp. 181–184, Jan. 2018, doi: 10.1016/J.NBT.2017.06.012.
[69] J. Jones, B. Verma, R. Mohtar, and M. Matlock, “Transforming food and agriculture to circular systems: a perspective for 2050,” *Resour. Mag.*, vol. 28, no. 2, 2021, Accessed: Apr. 17, 2022. [Online]. Available: www.asabe.org/advertise.
[70] P. Forster *et al.*, “The Earth’s Energy Budget, Climate Feedbacks, and Climate Sensitivity,” in *Climate Change 2021: The Physical Science Basis. Contribution of Working Group I to the Sixth Assessment Report of the Intergovernmental Panel on Climate Change*, V. Masson-Delmotte, P. Zhai, A. Pirani, S. L. Connors, C. Péan, S. Berger, N. Caud, Y. Chen, L. Goldfarb, M. I. Gomis, M. Huang, K. Leitzell, E. Lonnoy, J. B. R. Matthews, T. K. Maycock, T. Waterfield, O. Yelekçi, R. Yu, and B. Zhou, Eds. Cambridge, United Kingdom and New York, NY, USA: Cambridge University Press, 2021, pp. 923–1054.
[71] U.S. Department of Energy, “2016 billion-ton report: Advancing domestic resources for a thriving bioeconomy, Volume 1: Economic Availability of Feedstocks,” 2016. doi: 10.1089/ind.2016.29051.doe.
[72] J. Rogelj *et al.*, “Mitigation pathways compatible with 1.5 C in the context of sustainable development,” in *Global Warming of 1.5°C. An IPCC Special Report on the impacts of global warming of 1.5°C above pre-industrial levels and related global greenhouse gas emission pathways, in the context of strengthening the global response to the threat of climate change*, no. June 2018, V. Masson-Delmotte, P. Zhai, H.-O. Pörtner, D. Roberts, J. Skea, P. R. Shukla, A. Pirani, W. Moufouma-Okia, C. Péan, R. Pidcock, S. Connors, J. B. R. Matthews, Y. Chen, X. Zhou, M. I. Gomis, E. Lonnoy, T. Maycock, M. Tignor, and T. Waterfield, Eds. 2018, pp. 93–174.
[73] D. Y. C. Leung, G. Caramanna, and M. M. Maroto-Valer, “An overview of current status of carbon dioxide capture and storage technologies,” *Renew. Sustain. Energy Rev.*, vol. 39, pp. 426–443, Nov. 2014, doi: 10.1016/J.RSER.2014.07.093.
[74] W. J. Sagues and A. Woodley, “Building a Biotechnology Innovation Ecosystem to Mitigate Climate Change,” 2022. Accessed: Oct. 08, 2022. [Online]. Available: https://uidp.org/custom-type/innovation-in-the-bioeconomy-mitigating-climate-change/.
[75] M. He *et al.*, “Waste-derived biochar for water pollution control and sustainable development,” *Nat. Rev. Earth Environ. 2022 37*, vol. 3, no. 7, pp. 444–460, Jun. 2022, doi: 10.1038/s43017-022-00306-8.
[76] M. Honegger and D. Reiner, “The political economy of negative emissions technologies: consequences for international policy design,” *Clim. Policy*, vol. 18, no. 3, pp. 306–321, Mar. 2018, doi: 10.1080/14693062.2017.1413322.
[77] S. Fuss *et al.*, “Negative emissions—Part 2: Costs, potentials and side effects,” *Environ. Res. Lett.*, vol. 13, no. 6, p. 063002, Jun. 2018, doi: 10.1088/1748-9326/aabf9f.
[78] S. E. Tanzer and A. Ramírez, “When are negative emissions negative emissions?,” *Energy and Environmental Science*, vol. 12, no. 4. pp. 1210–1218, 2019, doi: 10.1039/c8ee03338b.
[79] A. Al-Mamoori, A. Krishnamurthy, A. A. Rownaghi, and F. Rezaei, “Carbon Capture and Utilization Update,” *Energy Technol.*, vol. 5, no. 6, pp. 834–849, Jun. 2017, doi: 10.1002/ENTE.201600747.

[80] R. M. Cuéllar-Franca and A. Azapagic, “Carbon capture, storage and utilisation technologies: A critical analysis and comparison of their life cycle environmental impacts,” *J. CO2 Util.*, vol. 9, pp. 82–102, Mar. 2015, doi: 10.1016/J.JCOU.2014.12.001.
[81] T. Terlouw, C. Bauer, L. Rosa, and M. Mazzotti, “Life cycle assessment of carbon dioxide removal technologies: a critical review,” *Energy Environ. Sci.*, vol. 14, no. 4, pp. 1701–1721, Apr. 2021, doi: 10.1039/D0EE03757E.
[82] F. Creutzig, C. Breyer, J. Hilaire, J. Minx, G. P. Peters, and R. Socolow, “The mutual dependence of negative emission technologies and energy systems,” *Energy Environ. Sci.*, vol. 12, no. 6, pp. 1805–1817, Jun. 2019, doi: 10.1039/C8EE03682A.
[83] Y. Cao, M. He, S. Dutta, G. Luo, S. Zhang, and D. C. W. Tsang, “Hydrothermal carbonization and liquefaction for sustainable production of hydrochar and aromatics,” *Renew. Sustain. Energy Rev.*, vol. 152, p. 111722, Dec. 2021, doi: 10.1016/J.RSER.2021.111722.
[84] L. J. Snowden-Swan *et al.*, “Wet Waste Hydrothermal Liquefaction and Biocrude Upgrading to Hydrocarbon Fuels: 2021 State of Technology,” doi: 10.2172/1863608.
[85] R. C. Brown, “The Role of Pyrolysis and Gasification in a Carbon Negative Economy,” *Process. 2021, Vol. 9, Page 882*, vol. 9, no. 5, p. 882, May 2021, doi: 10.3390/PR9050882.
[86] V. S. Sikarwar *et al.*, “An overview of advances in biomass gasification,” *Energy Environ. Sci.*, vol. 9, no. 10, pp. 2939–2977, Oct. 2016, doi: 10.1039/C6EE00935B.
[87] R. M. Swanson, J. A. Satrio, R. C. Brown, A. Platon, and D. D. Hsu, “Techno-Economic Analysis of Biofuels Production Based on Gasification,” 2010, Accessed: Sep. 27, 2022. [Online]. Available: http://www.osti.gov/bridge.
[88] A. Dutta *et al.*, “Ex Situ Catalytic Fast Pyrolysis of Lignocellulosic Biomass to Hydrocarbon Fuels: 2018 State of Technology and Future Research,” 2018, Accessed: Sep. 27, 2022. [Online]. Available: www.nrel.gov/publications.
[89] A. Bhave *et al.*, “Screening and techno-economic assessment of biomass-based power generation with CCS technologies to meet 2050 CO2 targets,” *Appl. Energy*, vol. 190, pp. 481–489, 2017, doi: 10.1016/j.apenergy.2016.12.120.
[90] H. P. Schmidt *et al.*, “Pyrogenic carbon capture and storage,” *GCB Bioenergy*, vol. 11, no. 4, pp. 573–591, Apr. 2019, doi: 10.1111/GCBB.12553.
[91] J. Hetland, P. Yowargana, S. Leduc, and F. Kraxner, “Carbon-negative emissions: Systemic impacts of biomass conversion. A case study on CO2 capture and storage options,” *Int. J. Greenh. Gas Control*, vol. 49, pp. 330–342, Jun. 2016, doi: 10.1016/J.IJGGC.2016.03.017.
[92] M. Langholtz *et al.*, “The Economic Accessibility of CO2 Sequestration through Bioenergy with Carbon Capture and Storage (BECCS) in the US,” *L. 2020, Vol. 9, Page 299*, vol. 9, no. 9, p. 299, Aug. 2020, doi: 10.3390/LAND9090299.
[93] D. L. Sanchez and D. M. Kammen, “A commercialization strategy for carbon-negative energy,” *Nat. Energy 2016 11*, vol. 1, no. 1, pp. 1–4, Jan. 2016, doi: 10.1038/NENERGY.2015.2.
[94] J. Full, S. Merseburg, R. Miehe, and A. Sauer, “A New Perspective for Climate Change Mitigation—Introducing Carbon-Negative Hydrogen Production from Biomass with Carbon Capture and Storage (HyBECCS),” *Sustain. 2021, Vol. 13, Page 4026*, vol. 13, no. 7, p. 4026, Apr. 2021, doi: 10.3390/SU13074026.
[95] S. E. Baker *et al.*, “Getting to Neutral: Options for Negative Carbon Emissions in

California," 2019, Accessed: Sep. 27, 2022. [Online]. Available: https://livermorelabfoundation.org/2019/12/19/getting-to-neutral/.
[96] Energy Transitions Commission, "Making the Hydrogen Economy Possible : accelerating clean hydrogen in an electrified economy," *Making Mission Possible Series*, 2021. https://www.energy-transitions.org/publications/making-clean-hydrogen-possible/ (accessed Sep. 27, 2022).
[97] C. Arnaiz del Pozo, S. Cloete, and Á. Jiménez Álvaro, "Carbon-negative hydrogen: Exploring the techno-economic potential of biomass co-gasification with CO2 capture," *Energy Convers. Manag.*, vol. 247, p. 114712, Nov. 2021, doi: 10.1016/J.ENCONMAN.2021.114712.
[98] M. Fajardy and N. Mac Dowell, "Can BECCS deliver sustainable and resource efficient negative emissions?," *Energy Environ. Sci.*, vol. 10, no. 6, pp. 1389–1426, 2017, doi: 10.1039/c7ee00465f.
[99] M. He, Z. Xu, Y. Sun, P. S. Chan, I. Lui, and D. C. W. Tsang, "Critical impacts of pyrolysis conditions and activation methods on application-oriented production of wood waste-derived biochar," *Bioresour. Technol.*, vol. 341, p. 125811, Dec. 2021, doi: 10.1016/J.BIORTECH.2021.125811.
[100] W. J. Sagues, S. Park, H. Jameel, and D. L. Sanchez, "Enhanced carbon dioxide removal from coupled direct air capture–bioenergy systems," *Sustain. Energy Fuels*, vol. 3, no. 11, pp. 3135–3146, Oct. 2019, doi: 10.1039/C9SE00384C.
[101] W. J. Sagues, H. Jameel, D. L. Sanchez, and S. Park, "Prospects for bioenergy with carbon capture & storage (BECCS) in the United States pulp and paper industry," *Energy Environ. Sci.*, vol. 13, no. 8, pp. 2243–2261, Aug. 2020, doi: 10.1039/D0EE01107J.
[102] Encyclopedia Britannica, "Arrhenius equation | Definition & Facts | Britannica," *Encyclopdedia Britannica*, 2022. https://www.britannica.com/science/Arrhenius-equation (accessed Sep. 29, 2022).
[103] D. Kardaś, P. Hercel, I. Wardach-Święcicka, and S. Polesek-Karczewska, "On the kinetic rate of biomass particle decomposition - Experimental and numerical analysis," *Energy*, vol. 219, p. 119575, Mar. 2021, doi: 10.1016/J.ENERGY.2020.119575.
[104] D. L. Sanchez, N. Johnson, S. T. McCoy, P. A. Turner, and K. J. Mach, "Near-term deployment of carbon capture and sequestration from biorefineries in the United States," *Proc. Natl. Acad. Sci. U. S. A.*, vol. 115, no. 19, pp. 4875–4880, 2018, doi: 10.1073/pnas.1719695115.
[105] U.S. EPA, "LMOP Landfill and Project Database | US EPA." https://www.epa.gov/lmop/lmop-landfill-and-project-database#access (accessed May 13, 2022).
[106] EPA, "Livestock Anaerobic Digester Database," *AgSTAR Livestock Anaerobic Digester Database*, 2016. https://www.epa.gov/agstar/livestock-anaerobic-digester-database (accessed May 13, 2022).
[107] JBEI, "BioSiting Tool: Select Map." https://biositing.jbei.org/ (accessed May 13, 2022).
[108] J. R. Moreira, V. Romeiro, S. Fuss, F. Kraxner, and S. A. Pacca, "BECCS potential in Brazil: Achieving negative emissions in ethanol and electricity production based on sugar cane bagasse and other residues," *Appl. Energy*, vol. 179, pp. 55–63, Oct. 2016, doi: 10.1016/J.APENERGY.2016.06.044.
[109] P. C. Psarras, S. Comello, P. Bains, P. Charoensawadpong, S. Reichelstein, and J. Wilcox, "Carbon Capture and Utilization in the Industrial Sector," *Environ. Sci. Technol.*, vol. 51,

no. 19, pp. 11440–11449, Oct. 2017, doi: 10.1021/ACS.EST.7B01723/SUPPL_FILE/ES7B01723_SI_006.XLSX.
[110] Y. Xu, L. Isom, and M. A. Hanna, "Adding value to carbon dioxide from ethanol fermentations," *Bioresour. Technol.*, vol. 101, no. 10, pp. 3311–3319, May 2010, doi: 10.1016/j.biortech.2010.01.006.
[111] P. M. Berger, L. Yoksoulian, J. T. Freiburg, S. K. Butler, and W. R. Roy, "Carbon sequestration at the Illinois Basin-Decatur Project: experimental results and geochemical simulations of storage," *Environ. Earth Sci. 2019 7822*, vol. 78, no. 22, pp. 1–10, Nov. 2019, doi: 10.1007/S12665-019-8659-4.
[112] J. N. Rosenberg, A. Mathias, K. Korth, M. J. Betenbaugh, and G. A. Oyler, "Microalgal biomass production and carbon dioxide sequestration from an integrated ethanol biorefinery in Iowa: A technical appraisal and economic feasibility evaluation," *Biomass and Bioenergy*, vol. 35, no. 9, pp. 3865–3876, Oct. 2011, doi: 10.1016/J.BIOMBIOE.2011.05.014.
[113] J. L. Field *et al.*, "Robust paths to net greenhouse gas mitigation and negative emissions via advanced biofuels," *Proc. Natl. Acad. Sci. U. S. A.*, vol. 117, no. 36, pp. 21968–21977, Sep. 2020, doi: 10.1073/PNAS.1920877117/SUPPL_FILE/PNAS.1920877117.SAPP.PDF.
[114] S. Kim *et al.*, "Carbon-Negative Biofuel Production," *Environ. Sci. Technol.*, vol. 54, no. 17, pp. 10797–10807, Sep. 2020, doi: 10.1021/ACS.EST.0C01097/ASSET/IMAGES/LARGE/ES0C01097_0003.JPEG.
[115] H. Li, Y. Tan, M. Ditaranto, J. Yan, and Z. Yu, "Capturing CO2 from Biogas Plants," *Energy Procedia*, vol. 114, pp. 6030–6035, Jul. 2017, doi: 10.1016/J.EGYPRO.2017.03.1738.
[116] K. Rajendran and G. S. Murthy, "Techno-economic and life cycle assessments of anaerobic digestion – A review," *Biocatal. Agric. Biotechnol.*, vol. 20, p. 101207, Jul. 2019, doi: 10.1016/J.BCAB.2019.101207.
[117] W. J. Nock, M. Walker, R. Kapoor, and S. Heaven, "Modeling the water scrubbing process and energy requirements for CO 2 capture to upgrade biogas to biomethane," *Ind. Eng. Chem. Res.*, vol. 53, no. 32, pp. 12783–12792, Aug. 2014, doi: 10.1021/IE501280P.
[118] G. Shah, E. Ahmad, K. K. Pant, and V. K. Vijay, "Comprehending the contemporary state of art in biogas enrichment and CO2 capture technologies via swing adsorption," *Int. J. Hydrogen Energy*, vol. 46, no. 9, pp. 6588–6612, Feb. 2021, doi: 10.1016/J.IJHYDENE.2020.11.116.
[119] M. S. Ivan, K. M. Vítězová, M. Struk, I. Kushkevych, and Á. M. Vítězová, "Biogas upgrading methods: recent advancements and emerging technologies Pressure swing adsorption PSB Purple sulphur bacteria VSA Vacuum swing adsorption," *Rev Env. Sci Biotechnol*, vol. 19, pp. 651–671, 2020, doi: 10.1007/s11157-020-09539-9.
[120] W. J. Sagues *et al.*, "Decarbonizing agriculture through the conversion of animal manure to dietary protein and ammonia fertilizer," *Bioresour. Technol.*, vol. 297, p. 122493, Feb. 2020, doi: 10.1016/J.BIORTECH.2019.122493.
[121] S. Wang, T. Zhang, M. Bao, H. Su, and P. Xu, "Microbial Production of Hydrogen by Mixed Culture Technologies: A Review," *www.biotechnology-journal.com*, 2019, doi: 10.1002/biot.201900297.
[122] P. A. Turner *et al.*, "The global overlap of bioenergy and carbon sequestration potential," *Clim. Change*, vol. 148, no. 1–2, pp. 1–10, May 2018, doi: 10.1007/S10584-018-2189-

Z/FIGURES/4.
[123] E. Baik, D. L. Sanchez, P. A. Turner, K. J. Mach, C. B. Field, and S. M. Benson, "Geospatial analysis of near-term potential for carbon-negative bioenergy in the United States," *Proc. Natl. Acad. Sci. U. S. A.*, vol. 115, no. 13, pp. 3290–3295, Mar. 2018, doi: 10.1073/PNAS.1720338115/ASSET/404C19EE-DBD9-4B1E-A8FD-DCE0181F773A/ASSETS/GRAPHIC/PNAS.1720338115FIG04.JPEG.
[124] R. Meys *et al.*, "Achieving net-zero greenhouse gas emission plastics by a circular carbon economy," *Science (80-. ).*, vol. 374, no. 6563, pp. 71–76, Oct. 2021, doi: 10.1126/SCIENCE.ABG9853/SUPPL_FILE/SCIENCE.ABG9853_SM.PDF.
[125] C. Smeaton, "Augmentation of global marine sedimentary carbon storage in the age of plastic," *Limnol. Oceanogr. Lett.*, vol. 6, no. 3, pp. 113–118, Jun. 2021, doi: 10.1002/LOL2.10187.
[126] United Nations Environment Programme, "Visual Feature | Beat Plastic Pollution," *UNEP*, 2022. https://www.unep.org/interactives/beat-plastic-pollution/ (accessed May 13, 2022).
[127] L. Parker, "A Whopping 91 Percent of Plastic Isn't Recycled | National Geographic Society," *National Geographic Societyo*, 2019. https://www.nationalgeographic.org/article/whopping-91-percent-plastic-isnt-recycled/ (accessed May 13, 2022).
[128] J. P. Dees, M. Ateia, and D. L. Sanchez, "Microplastics and Their Degradation Products in Surface Waters: A Missing Piece of the Global Carbon Cycle Puzzle," *ACS ES&T Water*, vol. 1, no. 2, pp. 214–216, 2021, doi: 10.1021/acsestwater.0c00205.
[129] Department of Ecology State of Washington, "Focus on Bioplastics: 'Biobased,' 'Biodegradable,' and 'Compostable,'" 2014. doi: 10.1520/D833-12.
[130] European Bioplastics, "Bioplastics market data," *european-bioplastics.org*, 2021. https://www.european-bioplastics.org/market/#iLightbox[gallery_image_1]/-1 (accessed May 13, 2022).
[131] R. Mülhaupt, "Green polymer chemistry and bio-based plastics: Dreams and reality," *Macromol. Chem. Phys.*, vol. 214, no. 2, pp. 159–174, 2013, doi: 10.1002/macp.201200439.
[132] T. A. Hottle, M. M. Bilec, and A. E. Landis, "Biopolymer production and end of life comparisons using life cycle assessment," *Resour. Conserv. Recycl.*, vol. 122, pp. 295–306, Jul. 2017, doi: 10.1016/J.RESCONREC.2017.03.002.
[133] F. Gironi and V. Piemonte, "Bioplastics Disposal: How To Manage It," *WIT Trans. Ecol. Environ.*, vol. 140, pp. 261–271, Jun. 2010, doi: 10.2495/WM100241.
[134] G. Vinci, R. Ruggieri, A. Billi, C. Pagnozzi, M. V. Di Loreto, and M. Ruggeri, "Sustainable management of organic waste and recycling for bioplastics: A lca approach for the italian case study," *Sustain.*, vol. 13, no. 11, 2021, doi: 10.3390/su13116385.
[135] E. T. H. Vink, K. R. Rábago, D. A. Glassner, and P. R. Gruber, "Applications of life cycle assessment to NatureWorks$^{TM}$ polylactide (PLA) production," *Polym. Degrad. Stab.*, vol. 80, no. 3, pp. 403–419, Jan. 2003, doi: 10.1016/S0141-3910(02)00372-5.
[136] R. Geyer, J. R. Jambeck, and K. L. Law, "Production, use, and fate of all plastics ever made," *Sci. Adv.*, vol. 3, no. 7, 2017, doi: 10.1126/sciadv.1700782.
[137] T. Leejarkpai, T. Mungcharoen, and U. Suwanmanee, "Comparative assessment of global warming impact and eco-efficiency of PS (polystyrene), PET (polyethylene terephthalate) and PLA (polylactic acid) boxes," *J. Clean. Prod.*, vol. 125, pp. 95–107, Jul. 2016, doi:

10.1016/J.JCLEPRO.2016.03.029.
[138] A. Morschbacker, “Bio-ethanol based ethylene,” *Polym. Rev.*, vol. 49, no. 2, pp. 79–84, Apr. 2009, doi: 10.1080/15583720902834791.
[139] N. Fackler *et al.*, “Stepping on the Gas to a Circular Economy: Accelerating Development of Carbon-Negative Chemical Production from Gas Fermentation,” *Annu. Rev. Chem. Biomol. Eng.*, vol. 12, pp. 439–470, 2021, doi: 10.1146/annurev-chembioeng-120120-021122.
[140] Y. Ni, G. M. Richter, O. N. Mwabonje, A. Qi, M. K. Patel, and J. Woods, “Novel integrated agricultural land management approach provides sustainable biomass feedstocks for bioplastics and supports the UK’s ‘net-zero’ target,” *Environ. Res. Lett.*, vol. 16, no. 1, p. 014023, Dec. 2020, doi: 10.1088/1748-9326/ABCF79.
[141] D. Tonini, D. Schrijvers, S. Nessi, P. Garcia-Gutierrez, and J. Giuntoli, “Carbon footprint of plastic from biomass and recycled feedstock: methodological insights,” *Int. J. Life Cycle Assess.*, vol. 26, no. 2, pp. 221–237, Feb. 2021, doi: 10.1007/S11367-020-01853-2/TABLES/3.
[142] Y. Zhu, C. Romain, and C. K. Williams, “Sustainable polymers from renewable resources,” *Nature*, vol. 540, no. 7633, pp. 354–362, Dec. 2016, doi: 10.1038/NATURE21001.
[143] D. Zhang, E. A. del Rio-Chanona, J. L. Wagner, and N. Shah, “Life cycle assessments of bio-based sustainable polylimonene carbonate production processes,” *Sustain. Prod. Consum.*, vol. 14, pp. 152–160, Apr. 2018, doi: 10.1016/J.SPC.2018.03.001.
[144] A. Rehman, F. Saleem, F. Javed, A. Ikhlaq, S. W. Ahmad, and A. Harvey, “Recent advances in the synthesis of cyclic carbonates via CO2 cycloaddition to epoxides,” *J. Environ. Chem. Eng.*, vol. 9, no. 2, p. 105113, Apr. 2021, doi: 10.1016/J.JECE.2021.105113.
[145] O. Hauenstein, M. Reiter, S. Agarwal, B. Rieger, and A. Greiner, “Bio-based polycarbonate from limonene oxide and CO2 with high molecular weight, excellent thermal resistance, hardness and transparency,” *Green Chem.*, vol. 18, no. 3, pp. 760–770, Feb. 2016, doi: 10.1039/C5GC01694K.
[146] O. Hauenstein, S. Agarwal, and A. Greiner, “Bio-based polycarbonate as synthetic toolbox,” *Nat. Commun. 2016 71*, vol. 7, no. 1, pp. 1–7, Jun. 2016, doi: 10.1038/NCOMMS11862.
[147] Z. Li, J. Yang, and X. J. Loh, “Polyhydroxyalkanoates: opening doors for a sustainable future,” *NPG Asia Mater. 2016 84*, vol. 8, no. 4, pp. e265–e265, Apr. 2016, doi: 10.1038/AM.2016.48.
[148] A. Z. Naser, I. Deiab, and B. M. Darras, “Poly(lactic acid) (PLA) and polyhydroxyalkanoates (PHAs), green alternatives to petroleum-based plastics: a review,” *RSC Adv.*, vol. 11, no. 28, pp. 17151–17196, May 2021, doi: 10.1039/D1RA02390J.
[149] J. Maroušek, M. Vochozka, J. Plachý, and J. Žák, “Glory and misery of biochar,” *Clean Technol. Environ. Policy 2016 192*, vol. 19, no. 2, pp. 311–317, Sep. 2016, doi: 10.1007/S10098-016-1284-Y.
[150] B. Wang, B. Gao, and J. Fang, “Recent advances in engineered biochar productions and applications,” *Crit. Rev. Environ. Sci. Technol.*, vol. 47, no. 22, pp. 2158–2207, Nov. 2017, doi: 10.1080/10643389.2017.1418580.
[151] X. Zhu *et al.*, “Machine learning exploration of the critical factors for CO2 adsorption capacity on porous carbon materials at different pressures,” *J. Clean. Prod.*, vol. 273, p.

122915, Nov. 2020, doi: 10.1016/J.JCLEPRO.2020.122915.
[152] A. A. Abd, M. R. Othman, and J. Kim, “A review on application of activated carbons for carbon dioxide capture: present performance, preparation, and surface modification for further improvement,” *Environ. Sci. Pollut. Res. 2021 2832*, vol. 28, no. 32, pp. 43329–43364, Jun. 2021, doi: 10.1007/S11356-021-15121-9.
[153] S. Jung, Y. K. Park, and E. E. Kwon, “Strategic use of biochar for CO2 capture and sequestration,” *J. CO2 Util.*, vol. 32, pp. 128–139, Jul. 2019, doi: 10.1016/J.JCOU.2019.04.012.
[154] Q. Yin, B. Zhang, R. Wang, and Z. Zhao, “Biochar as an adsorbent for inorganic nitrogen and phosphorus removal from water: a review,” *Environ. Sci. Pollut. Res. Int.*, vol. 24, no. 34, pp. 26297–26309, Dec. 2017, doi: 10.1007/S11356-017-0338-Y.
[155] W. Zhao, H. Yang, S. He, Q. Zhao, and L. Wei, “A review of biochar in anaerobic digestion to improve biogas production: Performances, mechanisms and economic assessments,” *Bioresour. Technol.*, vol. 341, p. 125797, Dec. 2021, doi: 10.1016/J.BIORTECH.2021.125797.
[156] M. Burton and E. Van Der Walt, “Electric-Car Revolution Shakes Up the Biggest Metals Markets,” *Bloomberg*, 2017. https://www.bloomberg.com/news/articles/2017-08-02/electric-car-revolution-is-shaking-up-the-biggest-metals-markets (accessed May 13, 2022).
[157] A. Mayyas, “Are there enough materials to cover li-ion batteries?,” *Joint Institute for Strategic Energy Analysis [NREL]*, 2018. https://www.jisea.org/20180815.html (accessed May 13, 2022).
[158] W. J. Sagues *et al.*, “A simple method for producing bio-based anode materials for lithium-ion batteries,” *Green Chem.*, vol. 22, no. 20, pp. 7093–7108, Oct. 2020, doi: 10.1039/D0GC02286A.
[159] L. Zhao, X. Zhao, L. T. Burke, J. C. Bennett, R. A. Dunlap, and M. N. Obrovac, “Voronoi-Tessellated Graphite Produced by Low-Temperature Catalytic Graphitization from Renewable Resources,” *ChemSusChem*, vol. 10, no. 17, pp. 3409–3418, Sep. 2017, doi: 10.1002/CSSC.201701211.
[160] J. Yang and S. Zuo, “Facile synthesis of graphitic mesoporous carbon materials from sucrose,” *Diam. Relat. Mater.*, vol. 95, pp. 1–4, May 2019, doi: 10.1016/J.DIAMOND.2019.03.018.
[161] M. N. Obrovac, X. Zhao, L. T. Burke, and R. A. Dunlap, “Reversible lithium insertion in catalytically graphitized sugar carbon,” *Electrochem. commun.*, vol. 60, pp. 221–224, Nov. 2015, doi: 10.1016/J.ELECOM.2015.09.015.
[162] S. Xia *et al.*, “Reaction kinetics, mechanism, and product analysis of the iron catalytic graphitization of cellulose,” *J. Clean. Prod.*, vol. 329, p. 129735, Dec. 2021, doi: 10.1016/J.JCLEPRO.2021.129735.
[163] E. Thompson, A. E. Danks, L. Bourgeois, and Z. Schnepp, “Iron-catalyzed graphitization of biomass,” *Green Chem.*, vol. 17, no. 1, pp. 551–556, Dec. 2014, doi: 10.1039/C4GC01673D.
[164] N. A. Banek, D. T. Abele, K. R. McKenzie, and M. J. Wagner, “Sustainable Conversion of Lignocellulose to High-Purity, Highly Crystalline Flake Potato Graphite,” *ACS Sustain. Chem. Eng.*, vol. 6, no. 10, pp. 13199–13207, Oct. 2018, doi: 10.1021/ACSSUSCHEMENG.8B02799/ASSET/IMAGES/LARGE/SC-2018-02799X_0009.JPEG.

[165] H. G. Chae *et al.*, "High strength and high modulus carbon fibers," *Carbon N. Y.*, vol. 93, pp. 81–87, Nov. 2015, doi: 10.1016/J.CARBON.2015.05.016.
[166] F. Souto, V. Calado, and N. Pereira, "Lignin-based carbon fiber: a current overview," *Mater. Res. Express*, vol. 5, no. 7, p. 072001, Jul. 2018, doi: 10.1088/2053-1591/AABA00.
[167] W. J. Sagues *et al.*, "Are lignin-derived carbon fibers graphitic enough?," *Green Chem.*, vol. 21, no. 16, pp. 4253–4265, Aug. 2019, doi: 10.1039/C9GC01806A.
[168] E. M. Karp *et al.*, "Renewable acrylonitrile production," *Science (80-. ).*, vol. 358, no. 6368, pp. 1307–1310, Dec. 2017, doi: 10.1126/SCIENCE.AAN1059/SUPPL_FILE/AAN1059_KARP_SM.PDF.
[169] M. Al Aiti, D. Jehnichen, D. Fischer, H. Brünig, and G. Heinrich, "On the morphology and structure formation of carbon fibers from polymer precursor systems," *Prog. Mater. Sci.*, vol. 98, pp. 477–551, Oct. 2018, doi: 10.1016/J.PMATSCI.2018.07.004.
[170] L. A. Biederman and W. Stanley Harpole, "Biochar and its effects on plant productivity and nutrient cycling: a meta-analysis," *GCB Bioenergy*, vol. 5, no. 2, pp. 202–214, Mar. 2013, doi: 10.1111/GCBB.12037.
[171] C. Zhang *et al.*, "Biochar for environmental management: Mitigating greenhouse gas emissions, contaminant treatment, and potential negative impacts," *Chem. Eng. J.*, vol. 373, pp. 902–922, Oct. 2019, doi: 10.1016/J.CEJ.2019.05.139.
[172] J. Wang, Z. Xiong, and Y. Kuzyakov, "Biochar stability in soil: meta-analysis of decomposition and priming effects," *GCB Bioenergy*, vol. 8, no. 3, pp. 512–523, May 2016, doi: 10.1111/gcbb.12266.
[173] P. Brassard, S. Godbout, and V. Raghavan, "Soil biochar amendment as a climate change mitigation tool: Key parameters and mechanisms involved," *J. Environ. Manage.*, vol. 181, pp. 484–497, Oct. 2016, doi: 10.1016/J.JENVMAN.2016.06.063.
[174] L. Leng and H. Huang, "An overview of the effect of pyrolysis process parameters on biochar stability," *Bioresour. Technol.*, vol. 270, pp. 627–642, Dec. 2018, doi: 10.1016/J.BIORTECH.2018.09.030.
[175] A. El-Naggar *et al.*, "Biochar composition-dependent impacts on soil nutrient release, carbon mineralization, and potential environmental risk: A review," *J. Environ. Manage.*, vol. 241, pp. 458–467, Jul. 2019, doi: 10.1016/J.JENVMAN.2019.02.044.
[176] R. R. Tan, "Data challenges in optimizing biochar-based carbon sequestration," *Renew. Sustain. Energy Rev.*, vol. 104, pp. 174–177, Apr. 2019, doi: 10.1016/J.RSER.2019.01.032.
[177] X. Zhu *et al.*, "Life-cycle assessment of pyrolysis processes for sustainable production of biochar from agro-residues," *Bioresour. Technol.*, vol. 360, p. 127601, Sep. 2022, doi: 10.1016/J.BIORTECH.2022.127601.
[178] J. Matuštík, T. Hnátková, and V. Kočí, "Life cycle assessment of biochar-to-soil systems: A review," *J. Clean. Prod.*, vol. 259, p. 120998, Jun. 2020, doi: 10.1016/J.JCLEPRO.2020.120998.
[179] K. E. Skog, "Sequestration of carbon in harvested wood products for the United States," *For. Prod. J.*, vol. 58, no. 6, pp. 56–72, 2008.
[180] R. Bergman, M. Puettmann, A. Taylor, and K. E. Skog, "The Carbon Impacts of Wood Products," *For. Prod. J.*, vol. 64, no. 7–8, pp. 220–231, Dec. 2014, doi: 10.13073/FPJ-D-14-00047.
[181] R. Sathre and J. O'Connor, "Meta-analysis of greenhouse gas displacement factors of

wood product substitution," *Environ. Sci. Policy*, vol. 13, no. 2, pp. 104–114, Apr. 2010, doi: 10.1016/j.envsci.2009.12.005.
[182] P. Brunet-Navarro, H. Jochheim, and B. Muys, "Modelling carbon stocks and fluxes in the wood product sector: a comparative review," *Glob. Chang. Biol.*, vol. 22, no. 7, pp. 2555–2569, Jul. 2016, doi: 10.1111/gcb.13235.
[183] X. Wang, J. M. Padgett, J. S. Powell, and M. A. Barlaz, "Decomposition of forest products buried in landfills," *Waste Manag.*, 2013, doi: 10.1016/j.wasman.2013.07.009.
[184] F. B. De la Cruz, J. P. Chanton, and M. A. Barlaz, "Measurement of carbon storage in landfills from the biogenic carbon content of excavated waste samples," *Waste Manag.*, vol. 33, no. 10, pp. 2001–2005, Oct. 2013, doi: 10.1016/J.WASMAN.2012.12.012.
[185] L. Arroja, A. C. Dias, and I. Capela, "The Role of Eucalyptus Globulus Forest and Products in Carbon Sequestration," *Clim. Chang. 2006 741*, vol. 74, no. 1, pp. 123–140, Feb. 2006, doi: 10.1007/S10584-006-3461-1.
[186] M. A. Carle, S. D'Amours, R. Azouzi, and M. Rönnqvist, "A Strategic Forest Management Model for Optimizing Timber Yield and Carbon Sequestration," *For. Sci.*, vol. 67, no. 2, pp. 205–218, Apr. 2021, doi: 10.1093/FORSCI/FXAA043.
[187] T. J. Fahey *et al.*, "Forest carbon storage: ecology, management, and policy," *Front. Ecol. Environ.*, vol. 8, no. 5, pp. 245–252, Jun. 2010, doi: 10.1890/080169.
[188] A. Favero, A. Daigneault, and B. Sohngen, "Forests: Carbon sequestration, biomass energy, or both?," *Sci. Adv.*, vol. 6, no. 13, 2020, doi: 10.1126/SCIADV.AAY6792/SUPPL_FILE/AAY6792_SM.PDF.
[189] E. L. Kalies and L. L. Yocom Kent, "Tamm Review: Are fuel treatments effective at achieving ecological and social objectives? A systematic review," *For. Ecol. Manage.*, vol. 375, pp. 84–95, 2016, doi: 10.1016/j.foreco.2016.05.021.
[190] S. L. Stephens, A. L. R. Westerling, M. D. Hurteau, M. Z. Peery, C. A. Schultz, and S. Thompson, "Fire and climate change: conserving seasonally dry forests is still possible," *Front. Ecol. Environ.*, vol. 18, no. 6, pp. 354–360, Aug. 2020, doi: 10.1002/FEE.2218.
[191] R. W. Malmsheimer *et al.*, "Managing forests because carbon matters: Integrating energy, products, and land management policy," *J. For.*, vol. 109, no. 7 SUPPL., 2011, [Online]. Available: https://academic.oup.com/jof/article/109/Suppl_1/S7/4598951.
[192] M. K. White, S. T. Gower, and D. E. Ahl, "Life cycle inventories of roundwood production in northern Wisconsin: Inputs into an industrial forest carbon budget," *For. Ecol. Manage.*, vol. 219, no. 1, pp. 13–28, Nov. 2005, doi: 10.1016/J.FORECO.2005.08.039.
[193] P. Saud, J. Wang, B. D. Sharma, and W. Liu, "Carbon impacts of hardwood lumber processing in the northeastern United States," *Can. J. For. Res.*, vol. 45, no. 12, pp. 1699–1710, Aug. 2015, doi: 10.1139/cjfr-2015-0082.
[194] W. E. Schlosser, J. H. Bassman, F. G. Wagner, and P. R. Wandschneider, "Increasing long-term storage of carbon sequestered in Russian softwood logs through enhanced lumber recovery," *For. Prod. J.*, vol. 52, no. 9, pp. 51–59, 2002.
[195] C. A. Bolin and S. Smith, "Life cycle assessment of ACQ-treated lumber with comparison to wood plastic composite decking," *J. Clean. Prod.*, vol. 19, no. 6–7, pp. 620–629, Apr. 2011, doi: 10.1016/J.JCLEPRO.2010.12.004.
[196] C. A. Bolin and S. T. Smith, "Life cycle assessment of borate-treated lumber with comparison to galvanized steel framing," *J. Clean. Prod.*, vol. 19, no. 6–7, pp. 630–639, Apr. 2011, doi: 10.1016/J.JCLEPRO.2010.12.005.

[197] D. . Sanchez, T. Zimring, C. Mater, and K. Harrell, “Literature Review and Evaluation of Research Gaps to Support Wood Products Innovatation,” 2020. Accessed: May 29, 2022. [Online]. Available: https://bof.fire.ca.gov/media/9688/full-12-a-jiwpi_formattedv12_3_05_2020.pdf.
[198] S. van Ewijk, J. A. Stegemann, and P. Ekins, “Limited climate benefits of global recycling of pulp and paper,” *Nat. Sustain.*, vol. 4, no. 2, pp. 180–187, 2021, doi: 10.1038/s41893-020-00624-z.
[199] S. van Ewijk, J. A. Stegemann, and P. Ekins, “Limited climate benefits of global recycling of pulp and paper,” *Nat. Sustain. 2020 42*, vol. 4, no. 2, pp. 180–187, Oct. 2020, doi: 10.1038/S41893-020-00624-Z.
[200] A. Haile *et al.*, “Pulp and paper mill wastes: utilizations and prospects for high value-added biomaterials,” *Bioresour. Bioprocess.*, vol. 8, no. 1, pp. 1–22, Dec. 2021, doi: 10.1186/S40643-021-00385-3/FIGURES/14.
[201] B. P. McGrail *et al.*, “Overcoming business model uncertainty in a carbon dioxide capture and sequestration project: Case study at the Boise White Paper Mill,” *Int. J. Greenh. Gas Control*, vol. 9, pp. 91–102, Jul. 2012, doi: 10.1016/J.IJGGC.2012.03.009.
[202] S. E. Tanzer, K. Blok, and A. Ramírez, “Can bioenergy with carbon capture and storage result in carbon negative steel?,” *Int. J. Greenh. Gas Control*, vol. 100, p. 103104, Sep. 2020, doi: 10.1016/J.IJGGC.2020.103104.
[203] A. T. Ubando, W. H. Chen, R. R. Tan, and S. R. Naqvi, “Optimal integration of a biomass-based polygeneration system in an iron production plant for negative carbon emissions,” *Int. J. Energy Res.*, vol. 44, no. 12, pp. 9350–9366, Oct. 2020, doi: 10.1002/ER.4902.
[204] S. Gupta, H. W. Kua, and S. D. Pang, “Biochar-mortar composite: Manufacturing, evaluation of physical properties and economic viability,” *Constr. Build. Mater.*, vol. 167, pp. 874–889, Apr. 2018, doi: 10.1016/J.CONBUILDMAT.2018.02.104.
[205] B. A. Akinyemi and A. Adesina, “Recent advancements in the use of biochar for cementitious applications: A review,” *J. Build. Eng.*, vol. 32, p. 101705, Nov. 2020, doi: 10.1016/J.JOBE.2020.101705.
[206] D. Cuthbertson, U. Berardi, C. Briens, and F. Berruti, “Biochar from residual biomass as a concrete filler for improved thermal and acoustic properties,” *Biomass and Bioenergy*, vol. 120, pp. 77–83, Jan. 2019, doi: 10.1016/J.BIOMBIOE.2018.11.007.
[207] S. Praneeth, R. Guo, T. Wang, B. K. Dubey, and A. K. Sarmah, “Accelerated carbonation of biochar reinforced cement-fly ash composites: Enhancing and sequestering CO2 in building materials,” *Constr. Build. Mater.*, vol. 244, p. 118363, May 2020, doi: 10.1016/J.CONBUILDMAT.2020.118363.
[208] L. Wang *et al.*, “Biochar as green additives in cement-based composites with carbon dioxide curing,” *J. Clean. Prod.*, vol. 258, p. 120678, Jun. 2020, doi: 10.1016/J.JCLEPRO.2020.120678.
[209] M. U. Hossain, L. Wang, I. K. M. Yu, D. C. W. Tsang, and C.-S. Poon, “Environmental and technical feasibility study of upcycling wood waste into cement-bonded particleboard,” *Constr. Build. Mater.*, vol. 173, pp. 474–480, Jun. 2018, doi: 10.1016/J.CONBUILDMAT.2018.04.066.
[210] J. Alcalde *et al.*, “Estimating geological CO2 storage security to deliver on climate mitigation,” *Nat. Commun.*, vol. 9, no. 1, Dec. 2018, doi: 10.1038/s41467-018-04423-1.
[211] U.S. Environmental Protection Agency, “Plastics: Material-Specific Data,” *Facts and*

*Figures about Materials, Waste and Recycling*, 2020. https://www.epa.gov/facts-and-figures-about-materials-waste-and-recycling/plastics-material-specific-data (accessed Jul. 10, 2020).
[212] C. P. Ward and C. M. Reddy, "We need better data about the environmental persistence of plastic goods," *Proc. Natl. Acad. Sci. U. S. A.*, vol. 117, no. 26, pp. 14618–14621, 2020, doi: 10.1073/pnas.2008009117.
[213] S. Ghatge, Y. Yang, J.-H. Ahn, and H.-G. Hur, "Biodegradation of polyethylene: a brief review," *Appl Biol Chem*, vol. 63, p. 27, 2020, doi: 10.1186/s13765-020-00511-3.
[214] A. A. Shah, F. Hasan, A. Hameed, and S. Ahmed, "Biological degradation of plastics: A comprehensive review," *Biotechnol. Adv.*, vol. 26, no. 3, pp. 246–265, 2008, doi: 10.1016/j.biotechadv.2007.12.005.
[215] A. Chamas *et al.*, "Degradation Rates of Plastics in the Environment," *ACS Sustain. Chem. Eng.*, vol. 8, no. 9, pp. 3494–3511, 2020, doi: 10.1021/acssuschemeng.9b06635.
[216] W. C. Stewart and G. M. Nakamura, "Documenting the full climate benefits of harvested wood products in northern california: Linking harvests to the us greenhouse gas inventory," *For. Prod. J.*, vol. 62, no. 5, pp. 340–353, 2012, doi: 10.13073/0015-7473-62.5.340.
[217] F. Santos, M. S. Torn, and J. A. Bird, "Biological degradation of pyrogenic organic matter in temperate forest soils," *Soil Biol. Biochem.*, vol. 51, pp. 115–124, 2012, doi: 10.1016/j.soilbio.2012.04.005.
[218] N. P. Gurwick, L. A. Moore, C. Kelly, and P. Elias, "A Systematic Review of Biochar Research, with a Focus on Its Stability in situ and Its Promise as a Climate Mitigation Strategy," *PLoS One*, vol. 8, no. 9, p. e75932, Sep. 2013, doi: 10.1371/journal.pone.0075932.
[219] B. P. Singh, A. L. Cowie, and R. J. Smernik, "Biochar carbon stability in a clayey soil as a function of feedstock and pyrolysis temperature," *Environ. Sci. Technol.*, vol. 46, no. 21, pp. 11770–11778, 2012, doi: 10.1021/es302545b.
[220] A. Enders, K. Hanley, T. Whitman, S. Joseph, and J. Lehmann, "Characterization of biochars to evaluate recalcitrance and agronomic performance," *Bioresour. Technol.*, vol. 114, pp. 644–653, 2012, doi: 10.1016/j.biortech.2012.03.022.
[221] J. Huang, B. Mendoza, J. S. Daniel, C. J. Nielsen, L. Rotstayn, and O. Wild, "Anthropogenic and natural radiative forcing," *Clim. Chang. 2013 Phys. Sci. Basis Work. Gr. I Contrib. to Fifth Assess. Rep. Intergov. Panel Clim. Chang.*, vol. 9781107057, pp. 659–740, 2013, doi: 10.1017/CBO9781107415324.018.
[222] A. Levasseur, P. Lesage, M. Margni, L. Deschênes, and R. Samson, "Considering time in LCA: Dynamic LCA and its application to global warming impact assessments," *Environ. Sci. Technol.*, vol. 44, no. 8, pp. 3169–3174, 2010, doi: 10.1021/es9030003.
[223] M. A. Sanderson, P. R. Adler, A. A. Boateng, M. D. Casler, and G. Sarath, "Switchgrass as a biofuels feedstock in the USA," *Can. J. Plant Sci.*, vol. 86, no. 5, pp. 1315–1325, 2006, doi: 10.4141/p06-136.
[224] T. D. Montgomery, H. S. Han, and A. R. Kizha, "Modeling work plan logistics for centralized biomass recovery operations in mountainous terrain," *Biomass and Bioenergy*, vol. 85, pp. 262–270, 2016, doi: 10.1016/j.biombioe.2015.11.023.
[225] G. M. Pedroso *et al.*, "Switchgrass is a promising, high-yielding crop for California biofuel," *Calif. Agric.*, vol. 65, no. 3, pp. 168–173, 2011, doi: 10.3733/ca.E.v065n03p168.
[226] D. S. Newsome, "The Water-Gas Shift Reaction," *Catal. Rev.*, vol. 21, no. 2, pp. 275–318,

1980, doi: 10.1080/03602458008067535.
[227] M. Kanniche, R. Gros-Bonnivard, P. Jaud, J. Valle-Marcos, J. M. Amann, and C. Bouallou, “Pre-combustion, post-combustion and oxy-combustion in thermal power plant for CO2 capture,” *Appl. Therm. Eng.*, vol. 30, no. 1, pp. 53–62, 2010, doi: 10.1016/j.applthermaleng.2009.05.005.
[228] C. Kunze and H. Spliethoff, “Assessment of oxy-fuel, pre- and post-combustion-based carbon capture for future IGCC plants,” *Appl. Energy*, vol. 94, pp. 109–116, 2012, doi: 10.1016/j.apenergy.2012.01.013.
[229] M. Wang *et al.*, “Greenhouse gases, Regulated Emissions, and Energy use in Transportation Model ® (2018 .Net).” Oct. 2018, doi: 10.11578/GREET-Net-2018/dc.20200803.8.
[230] S. K. Thengane, K. Kung, R. York, S. Sokhansanj, C. J. Lim, and D. L. Sanchez, “Technoeconomic and emissions evaluation of mobile in-woods biochar production,” *Energy Convers. Manag.*, vol. 223, p. 113305, Nov. 2020, doi: 10.1016/j.enconman.2020.113305.
[231] J. Jin, S. Chen, and R. Wellwood, “Oriented Strand Board: Opportunities and Potential Products in China,” *Bioresources*, vol. 11, no. 4, pp. 10585–10603, 2016, doi: 10.15376/biores.11.4.
[232] M. Puettmann, E. Oniel, E. Kline, and L. Johnson, “Cradle to Gate Life Cycle Assessment of Oriented Strandboard Production from the Southeast,” 2012.
[233] D. E. Kline, “Gate-to-gate life-cycle inventory of oriented strandboard production,” *Wood Fiber Sci.*, vol. 37, pp. 74–84, 2005.
[234] T. D. Searchinger *et al.*, “Fixing a critical climate accounting error,” *Science (80-. ).*, vol. 326, no. 5952, 2009.
[235] J. Goodwin, M. Gillenwater, D. Romano, and K. Radunsky, “Chapter 1 Introduction To National Ghg Inventories,” *Refinement to 2006 IPCC Guidel. Natl. Greenh. Gas Invent.*, vol. 1, pp. 1–22, 2019.
[236] A. Levasseur, P. Lesage, M. Margni, and R. Samson, “Biogenic Carbon and Temporary Storage Addressed with Dynamic Life Cycle Assessment,” *J. Ind. Ecol.*, vol. 17, no. 1, pp. 117–128, 2013, doi: 10.1111/j.1530-9290.2012.00503.x.
[237] A. Abel De Souza Machado, W. Kloas, C. Zarfl, S. Hempel, and M. C. Rillig, “Microplastics as an emerging threat to terrestrial ecosystems,” doi: 10.1111/gcb.14020.
[238] IEA, “Emissions – Global Energy & CO2 Status Report 2019 – Analysis - IEA,” *IEA*, 2019. https://www.iea.org/reports/global-energy-co2-status-report-2019 (accessed Jun. 27, 2020).
[239] “The global bio-based polymer market in 2019,” *Bioplastics Magazine*, 2020. https://www.bioplasticsmagazine.com/en/news/meldungen/20200127-The-global-bio-based-polymer-market-in-2019-A-revised-view.php (accessed Jul. 05, 2020).
[240] J. Brahney, M. Hallerud, E. Heim, M. Hahnenberger, and S. Sukumaran, “Plastic rain in protected areas of the United States,” *Science (80-. ).*, vol. 368, no. 6496, pp. 1257–1260, Jun. 2020, doi: 10.1126/science.aaz5819.
[241] S. C. Bolyard, A. M. Motlagh, D. Lozinski, and D. R. Reinhart, “Impact of organic matter from leachate discharged to wastewater treatment plants on effluent quality and UV disinfection,” *Waste Manag.*, vol. 88, pp. 257–267, Apr. 2019, doi: 10.1016/j.wasman.2019.03.036.
[242] F. Zhu, C. Zhu, C. Wang, and C. Gu, “Occurrence and Ecological Impacts of

Microplastics in Soil Systems: A Review," *Bull. Environ. Contam. Toxicol.*, vol. 102, no. 6, pp. 741–749, 2019, doi: 10.1007/s00128-019-02623-z.
[243] C. P. Ward and C. M. Reddy, "Opinion: We need better data about the environmental persistence of plastic goods," *Proc. Natl. Acad. Sci.*, p. 202008009, 2020, doi: 10.1073/pnas.2008009117.
[244] C. P. Ward, C. J. Armstrong, A. N. Walsh, J. H. Jackson, and C. M. Reddy, "Sunlight Converts Polystyrene to Carbon Dioxide and Dissolved Organic Carbon," *Environ. Sci. Technol. Lett.*, vol. 6, no. 11, pp. 669–674, 2019, doi: 10.1021/acs.estlett.9b00532.
[245] L. Zhu, S. Zhao, T. B. Bittar, A. Stubbins, and D. Li, "Photochemical dissolution of buoyant microplastics to dissolved organic carbon: Rates and microbial impacts," *J. Hazard. Mater.*, vol. 383, no. July 2019, p. 121065, 2020, doi: 10.1016/j.jhazmat.2019.121065.
[246] B. Gewert, M. Plassmann, O. Sandblom, and M. Macleod, "Identification of Chain Scission Products Released to Water by Plastic Exposed to Ultraviolet Light," *Environ. Sci. Technol. Lett.*, vol. 5, no. 5, pp. 272–276, 2018, doi: 10.1021/acs.estlett.8b00119.
[247] M. Ateia, A. Kanan, and T. Karanfil, "Microplastics release precursors of chlorinated and brominated disinfection byproducts in water," *Chemosphere*, vol. 251, p. 126452, Jul. 2020, doi: 10.1016/j.chemosphere.2020.126452.
[248] D. Hu, M. Shen, Y. Zhang, and G. Zeng, "Micro(nano)plastics: An un-ignorable carbon source?," *Sci. Total Environ.*, vol. 657, pp. 108–110, 2019, doi: 10.1016/j.scitotenv.2018.12.046.
[249] M. U. F. Kirschbaum, G. Zeng, F. Ximenes, D. L. Giltrap, and J. R. Zeldis, "Towards a more complete quantification of the global carbon cycle," *Biogeosciences*, vol. 16, no. 3, pp. 831–846, 2019, doi: 10.5194/bg-16-831-2019.
[250] C. M. Rochman and T. Hoellein, "The global odyssey of plastic pollution," *Science*, vol. 368, no. 6496, pp. 1184–1185, 2020, doi: 10.1126/science.abc4428.
[251] Intergovernmental Panel on Climate Change, *Climate Change 2014: Synthesis Report. Contribution of Working Groups I, II and III to the Fifth Assessment Report of the Intergovernmental Panel on Climate Change*. 2014.
[252] J. H. Williams *et al.*, "The Technology Path to Deep Greenhouse Gas Emissions Cuts by 2050: The Pivotal Role of Electricity Downloaded from," 2012. Accessed: Jan. 24, 2019. [Online]. Available: www.sciencemag.orgsciencevolhttp://science.sciencemag.org/.
[253] M. Wei *et al.*, "Deep carbon reductions in California require electrification and integration across economic sectors," *Environ. Res. Lett*, vol. 8, pp. 14038–14048, 2013, doi: 10.1088/1748-9326/8/1/014038.
[254] L. M. Fulton, L. R. Lynd, A. Körner, N. Greene, and L. R. Tonachel, "The need for biofuels as part of a low carbon energy future," *Biofuels, Bioprod. Biorefining*, vol. 9, no. 5, pp. 476–483, Apr. 2015, doi: 10.1002/bbb.1559.
[255] M. Yang, N. R. Baral, A. Anastasopoulou, H. M. Breunig, and C. D. Scown, "Cost and Life-Cycle Greenhouse Gas Implications of Integrating Biogas Upgrading and Carbon Capture Technologies in Cellulosic Biorefineries," *Environ. Sci. Technol.*, p. acs.est.0c02816, 2020, doi: 10.1021/acs.est.0c02816.
[256] "Use of energy for transportation - U.S. Energy Information Administration (EIA)." Apr. 12, 2022, [Online]. Available: https://www.eia.gov/energyexplained/use-of-energy/transportation.php.
[257] I. E. A. Bioenergy, "Implementation of bioenergy in Brazil - 2021 update," IEA

Bioenergy, 2021. [Online]. Available: https://www.ieabioenergy.com/wp-content/uploads/2021/11/CountryReport2021_Brazil_final.pdf.
[258] C. M. Quintella *et al.*, "Brazilian potential for CCS for negative balance emission of CO2 from biomass energy," *10th Int. Conf. Greenh. Gas Control Technol.*, vol. 4, pp. 2926–2932, 2011, doi: 10.1016/j.egypro.2011.02.200.
[259] US Energy Information Adminstration (EIA), "U.S. Fuel Ethanol Production Capacity Increased by 3% in 2019," *Today in Energy*, 2020. https://www.eia.gov/todayinenergy/detail.php?id=45316 (accessed Jul. 08, 2022).
[260] S. Barros, "Biofuels Annual - Brazil 2021," United States Department of Agriculture, 2021. [Online]. Available: https://apps.fas.usda.gov/newgainapi/api/Report/DownloadReportByFileName?fileName=Biofuels Annual_Sao Paulo ATO_Brazil_08-02-2021.pdf.
[261] S. Barros, "USDA GAIN Report: Brazil Biofuels Annual 2021," United States Department of Agriculture, Apr. 2021. [Online]. Available: https://apps.fas.usda.gov/newgainapi/api/Report/DownloadReportByFileName?fileName=Biofuels Annual_Sao Paulo ATO_Brazil_08-02-2021.pdf.
[262] L. Tao, J. N. Markham, Z. Haq, and M. J. Biddy, "Techno-economic analysis for upgrading the biomass-derived ethanol-to-jet blendstocks," *Green Chem.*, vol. 19, no. 4, pp. 1082–1101, 2017, doi: 10.1039/c6gc02800d.
[263] H. S. Kheshgi and R. C. Prince, "Sequestration of fermentation CO2from ethanol production," *Energy*, vol. 30, no. 10, pp. 1865–1871, Jul. 2005, doi: 10.1016/j.energy.2004.11.004.
[264] Y. Xu, L. Isom, and M. A. Hanna, "Adding value to carbon dioxide from ethanol fermentations," *Bioresour. Technol.*, vol. 101, no. 10, pp. 3311–3319, May 2010, doi: 10.1016/J.BIORTECH.2010.01.006.
[265] National Energy Technology Laboratory, "Cost of Capturing CO2 from Industrial Sources," 2014. Accessed: Sep. 11, 2019. [Online]. Available: https://sequestration.mit.edu/pdf/2013_Summers_Capture_Costs_Industrial_Sources.pdf.
[266] S. Gollakota and S. McDonald, "CO $_2$ capture from ethanol production and storage into the Mt Simon Sandstone," *Greenh. Gases Sci. Technol.*, vol. 2, no. 5, pp. 346–351, Oct. 2012, doi: 10.1002/ghg.1305.
[267] "Aemetis cuts carbon score of Keyes ethanol plant | EthanolProducer.com." May 12, 2022, [Online]. Available: http://ethanolproducer.com/articles/16435/aemetis-cuts-carbon-score-of-keyes-ethanol-plant.
[268] L. Douglas and L. Douglas, "Summit says carbon pipeline project has secured 20% of Iowa route," *Reuters*, May 12, 2022.
[269] "How a Houston oil giant is pushing the needle on commercial-scale direct air capture," *Houston Inno*. May 12, 2022, [Online]. Available: https://www.bizjournals.com/houston/inno/stories/inno-insights/2021/04/15/1pointfive-oxy-low-carbon-ventures.html.
[270] "Navigator CO2, Big River announce CCUS agreement | EthanolProducer.com." May 12, 2022, [Online]. Available: http://www.ethanolproducer.com/articles/19249/navigator-co2-big-river-announce-ccus-agreement.
[271] "NDIC approves Class VI well for Red Trail Energy's CCS project | EthanolProducer.com." May 12, 2022, [Online]. Available: http://www.ethanolproducer.com/articles/18669/ndic-approves-class-vi-well-for-red-trail-

energyundefineds-ccs-project.
[272] K. Bracmort, “The Renewable Fuel Standard (RFS): An Overview,” Congressional Research Service, Oct. 2020. [Online]. Available: http://www.crs.gov.
[273] *California Low Carbon Fuel Standard*, vol. Title 17,. 2009.
[274] U.S., *Credit for carbon oxide sequestration*, vol. Title 26 S. .
[275] C. E. F. Vian, L. Rodrigues, and H. J. T. da Silva, “Evolution in Public Policies Designed to Develop the Sugar–Energy Industry in Brazil,” in *Advances in Sugarcane Biorefinery*, Elsevier, 2018, pp. 279–306.
[276] S. Barros, “USDA GAIN Report: Brazil Biofuels Annual 2019,” 2019.
[277] C. Grangeia, L. Santos, and L. L. B. Lazaro, “The Brazilian biofuel policy (RenovaBio) and its uncertainties: An assessment of technical, socioeconomic and institutional aspects,” *Energy Convers. Manag. X*, vol. 13, p. 100156, Jan. 2022, doi: 10.1016/J.ECMX.2021.100156.
[278] “Global Sustainable Aviation Fuel Market (2021 to 2030) -.” Apr. 12, 2022, [Online]. Available: https://www.globenewswire.com/news-release/2022/02/21/2388550/28124/en/Global-Sustainable-Aviation-Fuel-Market-2021-to-2030-Rising-Demand-for-SAF-by-Airlines-Across-the-Globe-Presents-Opportunities.html.
[279] E. G. Lindfeldt and M. O. Westermark, “Biofuel production with CCS as a strategy for creating a CO2 -neutral road transport sector,” *Greenh. Gas Control Technol. 9*, vol. 1, no. 1, pp. 4111–4118, 2009, doi: 10.1016/j.egypro.2009.02.219.
[280] J. Lask *et al.*, “Lignocellulosic ethanol production combined with CCS—A study of GHG reductions and potential environmental trade-offs,” *GCB Bioenergy*, vol. 13, no. 2, pp. 336–347, Nov. 2021, doi: 10.1111/gcbb.12781.
[281] A. Carroll and C. Somerville, “Cellulosic Biofuels,” 2009, doi: 10.1146/annurev.arplant.043008.092125.
[282] D. Humbird *et al.*, “Process Design and Economics for Biochemical Conversion of Lignocellulosic Biomass to Ethanol,” 2002, Accessed: Feb. 05, 2019. [Online]. Available: http://www.osti.gov/bridge.
[283] J. Baeyens, Q. Kang, L. Appels, R. Dewil, Y. Lv, and T. Tan, “Challenges and opportunities in improving the production of bio-ethanol,” *Prog. Energy Combust. Sci.*, vol. 47, pp. 60–88, 2015, doi: 10.1016/j.pecs.2014.10.003.
[284] M. A. Collura and W. L. Luyben, “Energy-saving distillation designs in ethanol production,” *ACS Publications*. Apr. 12, 2002, [Online]. Available: https://pubs.acs.org/doi/pdf/10.1021/ie00081a021.
[285] R. Karuppiah, A. Peschel, I. E. Grossmann, M. Martín, W. Martinson, and L. Zullo, “Energy optimization for the design of corn-based ethanol plants,” *AIChE J.*, vol. 54, no. 6, pp. 1499–1525, Jun. 2008, doi: 10.1002/aic.11480.
[286] B. S. Moraes, M. Zaiat, and A. Bonomi, “Anaerobic digestion of vinasse from sugarcane ethanol production in Brazil: Challenges and perspectives,” *Renew. Sustain. Energy Rev.*, vol. 44, pp. 888–903, 2015, doi: 10.1016/j.rser.2015.01.023.
[287] M. J. De Kam, R. V Morey, and D. G. Tiffany, “INTEGRATING BIOMASS TO PRODUCE HEAT AND POWER AT ETHANOL PLANTS,” *Appl. Eng. Agric.*, vol. 25, p. 18, [Online]. Available: https://elibrary-asabe-org.libproxy.berkeley.edu/pdfviewer.asp?param1=s:/8y9u8/q8qu/tq9q/5tv/J/quqzIGGP/IL/I/VfUNMJP.5tv&param2=M/HG/IGII&param3=HIO.JI.HG.IJG&param4=26320.

[288] A. Laude, O. Ricci, G. Bureau, J. Royer-Adnot, and A. Fabbri, “CO2 capture and storage from a bioethanol plant: Carbon and energy footprint and economic assessment,” *Int. J. Greenh. Gas Control*, vol. 5, no. 5, pp. 1220–1231, Sep. 2011, doi: 10.1016/J.IJGGC.2011.06.004.
[289] A. Bhave *et al.*, “Screening and techno-economic assessment of biomass-based power generation with CCS technologies to meet 2050 CO2 targets,” *Appl. Energy*, vol. 190, pp. 481–489, Mar. 2017, doi: 10.1016/j.apenergy.2016.12.120.
[290] C. Kunze and H. Spliethoff, “Assessment of oxy-fuel, pre- and post-combustion-based carbon capture for future IGCC plants,” *Appl. Energy*, vol. 94, pp. 109–116, 2012, doi: 10.1016/j.apenergy.2012.01.013.
[291] A. Komaki, T. Gotou, T. Uchida, T. Yamada, T. Kiga, and C. Spero, “Operation Experiences of Oxyfuel Power Plant in Callide Oxyfuel Project,” 2014, vol. 63, pp. 490–496, doi: 10.1016/j.egypro.2014.11.053.
[292] R. Stanger *et al.*, “Oxyfuel combustion for CO2 capture in power plants,” *Int. J. Greenh. Gas Control*, vol. 40, pp. 55–125, 2015, doi: https://doi.org/10.1016/j.ijggc.2015.06.010.
[293] T. Fujimori and T. Yamada, “Realization of oxyfuel combustion for near zero emission power generation,” *Proc. Combust. Inst.*, vol. 34, no. 2, pp. 2111–2130, 2013, doi: https://doi.org/10.1016/j.proci.2012.10.004.
[294] D. Leeson, N. Mac Dowell, N. Shah, C. Petit, and P. S. Fennell, “A Techno-economic analysis and systematic review of carbon capture and storage (CCS) applied to the iron and steel, cement, oil refining and pulp and paper industries, as well as other high purity sources,” *Int. J. Greenh. Gas Control*, vol. 61, pp. 71–84, Jun. 2017, doi: 10.1016/j.ijggc.2017.03.020.
[295] L. F. de Mello *et al.*, “A technical and economical evaluation of CO2 capture from FCC units,” *Energy Procedia*, vol. 1, no. 1, pp. 117–124, Apr. 2009, doi: 10.1016/j.egypro.2009.01.018.
[296] M. Ditaranto and J. Bakken, “Study of a full scale oxy-fuel cement rotary kiln,” *Int. J. Greenh. Gas Control*, vol. 83, pp. 166–175, Apr. 2019, doi: 10.1016/j.ijggc.2019.02.008.
[297] D. Gielen, “CO2 removal in the iron and steel industry,” *Energy Convers. Manag.*, vol. 44, no. 7, pp. 1027–1037, Apr. 2003, doi: 10.1016/S0196-8904(02)00111-5.
[298] M. Bui *et al.*, “Carbon capture and storage (CCS): the way forward,” *Energy Environ. Sci.*, vol. 11, no. 5, pp. 1062–1176, Jun. 2018, doi: 10.1039/C7EE02342A.
[299] C. L. Senior, W. Morris, and T. A. Lewandowski, “Emissions and risks associated with oxyfuel combustion: State of the science and critical data gaps,” *J. Air Waste Manag. Assoc.*, vol. 63, no. 7, pp. 832–843, 2013, doi: 10.1080/10962247.2013.791892.
[300] J. Ahn and H.-J. Kim, “Combustion Characteristics of 0.5 MW Class Oxy-Fuel FGR (Flue Gas Recirculation) Boiler for CO2 Capture,” *Energies*, vol. 14, no. 14, p. 4333, Aug. 2021, doi: 10.3390/en14144333.
[301] C. R. Burrows and M. S. Appold, “Hydrology of the Forest City basin, Mid-Continent, USA: implications for CO2 sequestration in the St. Peter Sandstone,” *Environ. Earth Sci.*, vol. 73, no. 4, pp. 1409–1425, Jun. 2015, doi: 10.1007/s12665-014-3494-0.
[302] M. Wang *et al.*, “Greenhouse gases, Regulated Emissions, and Energy use in Transportation Model ® (2019 .Net).” Oct. 2019, doi: 10.11578/GREET-Net-2019/dc.20200706.2.
[303] S. Mueller, “2008 National dry mill corn ethanol survey,” *Biotechnol. Lett.*, vol. 32, no. 9, pp. 1261–1264, May 2010, doi: 10.1007/s10529-010-0296-7.

[304] J. R. Kwiatkowski, A. J. McAloon, F. Taylor, and D. B. Johnston, “Modeling the process and costs of fuel ethanol production by the corn dry-grind process,” *Ind. Crops Prod.*, vol. 23, no. 3, pp. 288–296, 2006, doi: 10.1016/j.indcrop.2005.08.004.
[305] BBI International Project Development Division, “Corn Ethanol Industry Process Data Corn Ethanol Industry Process Data,” no. February, 2009, Accessed: Jul. 10, 2022. [Online]. Available: http://www.osti.gov/bridge.
[306] G. H.E., N. T.B., and C. J.C., “Projected process economics for ethanol production from corn.” 1992.
[307] A. McAloon, F. Taylor, and W. Yee, “Determining the Cost of Producing Ethanol from Corn Starch and Lignocellulosic Feedstocks,” p. 44, 2000, [Online]. Available: https://www.nrel.gov/docs/fy01osti/28893.pdf.
[308] S. D. Phillips, J. K. Tarud, M. J. Biddy, and A. Dutta, “Gasoline from Woody Biomass via Thermochemical Gasification, Methanol Synthesis, and Methanol-to-Gasoline Technologies: A Technoeconomic Analysis,” *Ind. Eng. Chem. Res.*, vol. 50, no. 20, pp. 11734–11745, 2011, doi: 10.1021/ie2010675.
[309] S. Jones *et al.*, “Process Design and Economics for the Conversion of Algal Biomass to Hydrocarbons: Whole Algae Hydrothermal Liquefaction and Upgrading,” Pacific Northwest National Laboratory, 2014.
[310] R. Davis, J. Markham, C. Kinchin, N. Grundl, E. Tan, and D. Humbird, “Process Design and Economics for the Production of Algal Biomass: Algal Biomass Production in Open Pond Systems and Processing Through Dewatering for Downstream Conversion,” National Renewable Energy Laboratory (NREL), 2016. [Online]. Available: https://www.nrel.gov/docs/fy16osti/64772.pdf.
[311] U. S. B. of L. Statistics, “Average hourly earnings of production and nonsupervisory employees, chemicals, not seasonally adjusted,” U.S. Bureau of Labor Statistics, 2022. [Online]. Available: https://beta.bls.gov/dataViewer/view/timeseries/CEU3232500008.
[312] U. S. B. of L. Statistics, “Producer Price Index by Commodity: Chemicals and Allied Products: Basic Inorganic Chemicals,” U.S. Bureau of Labor Statistics, 2022. [Online]. Available: https://fred.stlouisfed.org/series/WPU0613#0.
[313] C. E. Magazine, “Chemical Engineering Plant Cost Index,” 2021.
[314] “A Detailed Approach for Cost Analysis for Early CCS Projects: A Case Study from the Illinois Basin - Decatur Project by Sallie Greenberg, Keri Canaday, Austyn Vance, Ray McKaskle, John Koenig :: SSRN.” Apr. 25, 2022, [Online]. Available: https://papers.ssrn.com/sol3/papers.cfm?abstract_id=3365964.
[315] “Technology Handbook,” *Air Liquide*. Apr. 25, 2021, [Online]. Available: https://www.engineering-airliquide.com/technology-handbook.
[316] C. A. R. B. (CARB), “Current Fuel Pathways [Spreadsheet].” CARB LCFS Program, May 01, 2022.
[317] D. Hofstrand, “Ag Decision Maker D1-10: Ethanol Profitability.” Iowa State University Extension and Outreach, Feb. 15, 2022, [Online]. Available: https://www.extension.iastate.edu/agdm/energy/html/d1-10.html.
[318] A. Baylin-Stern and N. Berghout, “Is carbon capture too expensive,” International Energy Agency (IEA), 2021. [Online]. Available: https://www.iea.org/commentaries/is-carbon-capture-too-expensive.
[319] D. Kearns, H. Liu, and C. Consoli, “Technology readiness and costs of CCS,” 2021. Accessed: Aug. 12, 2022. [Online]. Available:

https://scienceforsustainability.org/w/images/b/bc/Technology-Readiness-and-Costs-for-CCS-2021-1.pdf.
[320] U. Lee, H. Kwon, M. Wu, and M. Wang, “Retrospective analysis of the U.S. corn ethanol industry for 2005–2019: implications for greenhouse gas emission reductions,” *Biofuels, Bioprod. Biorefining*, vol. 15, no. 5, pp. 1318–1331, May 2021, doi: 10.1002/bbb.2225.
[321] Y. Chen *et al.*, “Quantifying Regional Methane Emissions in the New Mexico Permian Basin with a Comprehensive Aerial Survey,” *Environ. Sci. Technol.*, vol. 56, no. 7, pp. 4317–4323, Apr. 2022, doi: 10.1021/acs.est.1c06458.
[322] D. Mazzone, J. Witcover, and C. Murphy, “Multijurisdictional Status Review of Low Carbon Fuel Standards, 2010–2020 Q2: California, Oregon, and British Columbia,” Jun. 2021, doi: 10.7922/G2SN0771.
[323] I. Daniel Posen, W. Michael Griffin, H. Scott Matthews, and L. Azevedo, “Changing the Renewable Fuel Standard to a Renewable Material Standard: Bioethylene Case Study,” 2014, doi: 10.1021/es503521r.
[324] S. Gota, C. Huizenga, K. Peet, N. Medimorec, and S. Bakker, “Decarbonising transport to achieve Paris Agreement targets,” *Energy Effic.*, vol. 12, no. 2, pp. 363–386, 2019, doi: 10.1007/s12053-018-9671-3.
[325] W. F. Lamb *et al.*, “A review of trends and drivers of greenhouse gas emissions by sector from 1990 to 2018,” *Environ. Res. Lett.*, vol. 16, no. 7, p. 073005, Jun. 2021, doi: 10.1088/1748-9326/ABEE4E.
[326] J. C. Minx *et al.*, “A comprehensive and synthetic dataset for global, regional, and national greenhouse gas emissions by sector 1970-2018 with an extension to 2019,” *Earth Syst. Sci. Data*, vol. 13, no. 11, pp. 5213–5252, Nov. 2021, doi: 10.5194/ESSD-13-5213-2021.
[327] K. Haustein *et al.*, “A real-time Global Warming Index,” *Sci. Reports 2017 71*, vol. 7, no. 1, pp. 1–6, Nov. 2017, doi: 10.1038/s41598-017-14828-5.
[328] C. P. Morice *et al.*, “An Updated Assessment of Near-Surface Temperature Change From 1850: The HadCRUT5 Data Set,” *J. Geophys. Res. Atmos.*, vol. 126, no. 3, p. e2019JD032361, Feb. 2021, doi: 10.1029/2019JD032361.
[329] M. Klöwer, M. R. Allen, D. S. Lee, S. R. Proud, L. Gallagher, and A. Skowron, “Quantifying aviation’s contribution to global warming,” *Environ. Res. Lett.*, vol. 16, no. 10, p. 104027, Nov. 2021, doi: 10.1088/1748-9326/AC286E.
[330] D. F. Finger, C. Braun, and C. Bil, “Impact of Battery Performance on the Initial Sizing of Hybrid-Electric General Aviation Aircraft,” *J. Aerosp. Eng.*, vol. 33, no. 3, p. 04020007, Feb. 2020, doi: 10.1061/(ASCE)AS.1943-5525.0001113.
[331] J. Larsson, A. Elofsson, T. Sterner, and J. Åkerman, “International and national climate policies for aviation: a review,” *https://doi-org.libproxy.berkeley.edu/10.1080/14693062.2018.1562871*, vol. 19, no. 6, pp. 787–799, Jul. 2019, doi: 10.1080/14693062.2018.1562871.
[332] I. Dincer and C. Acar, “A review on potential use of hydrogen in aviation applications,” *Int. J. Sustain. Aviat.*, vol. 2, no. 1, p. 74, 2016, doi: 10.1504/IJSA.2016.076077.
[333] IATA Economics, “Economic Performance of the Airline Industry Key Points,” 2020. Accessed: May 20, 2022. [Online]. Available: www.iata.org/economics.
[334] R. Mawhood, E. Gazis, S. de Jong, R. Hoefnagels, and R. Slade, “Production pathways for renewable jet fuel: a review of commercialization status and future prospects,” *Biofuels, Bioproducts and Biorefining*, vol. 10, no. 4. John Wiley & Sons, Ltd, pp. 462–484, Jul. 01,

2016, doi: 10.1002/bbb.1644.
[335] M. Prussi, A. O'Connell, and L. Lonza, "Analysis of current aviation biofuel technical production potential in EU28," *Biomass and Bioenergy*, vol. 130, p. 105371, Nov. 2019, doi: 10.1016/j.biombioe.2019.105371.
[336] IATA, "Fact Sheet 2: Sustainable Aviation Fuel: Technical Certification," 2020.
[337] C. Gutiérrez-Antonio, F. I. Gómez-Castro, J. A. de Lira-Flores, and S. Hernández, "A review on the production processes of renewable jet fuel," *Renewable and Sustainable Energy Reviews*, vol. 79. Pergamon, pp. 709–729, Nov. 01, 2017, doi: 10.1016/j.rser.2017.05.108.
[338] T. G. Kreutz, E. D. Larson, C. Elsido, E. Martelli, C. Greig, and R. H. Williams, "Techno-economic prospects for producing Fischer-Tropsch jet fuel and electricity from lignite and woody biomass with CO2 capture for EOR," *Appl. Energy*, vol. 279, no. August, p. 115841, 2020, doi: 10.1016/j.apenergy.2020.115841.
[339] S. Gollakota and S. McDonald, "Commercial-scale CCS Project in Decatur, Illinois – Construction Status and Operational Plans for Demonstration," *Energy Procedia*, vol. 63, pp. 5986–5993, Jun. 2014, doi: 10.1016/j.egypro.2014.11.633.
[340] ICAO, "Collaborative Aviation Climate Action Takes Flight," *ICAO*. 2014, Accessed: Jul. 04, 2022. [Online]. Available: https://www.icao.int/newsroom/pages/collaborative-aviation-climate-action-takes-flight.aspx.
[341] International Civil Aviation Organization and Air Transport Action Group, "TRANSPORT-AVIATON Action Statement," 2014.
[342] S. S. Doliente, A. Narayan, J. F. D. Tapia, N. J. Samsatli, Y. Zhao, and S. Samsatli, "Bio-aviation Fuel: A Comprehensive Review and Analysis of the Supply Chain Components," *Front. Energy Res.*, vol. 8, no. July, pp. 1–38, 2020, doi: 10.3389/fenrg.2020.00110.
[343] C. Gutiérrez-Antonio, F. Israel Gómez-Castro, J. G. Segovia-Hernández, and A. Briones-Ramírez, "Simulation and optimization of a biojet fuel production process," in *Computer Aided Chemical Engineering*, vol. 32, 2013, pp. 13–18.
[344] D. S. Lee *et al.*, "The contribution of global aviation to anthropogenic climate forcing for 2000 to 2018," *Atmos. Environ.*, vol. 244, p. 117834, Jan. 2021, doi: 10.1016/J.ATMOSENV.2020.117834.
[345] Bronwen Thornton and Maruxa Cardama, "SLOCAT Transport and Climate Change Global Status Report - 2nd edition," p. 365, 2021, Accessed: Jul. 01, 2022. [Online]. Available: https://tcc-gsr.com/.
[346] P. D. S. Lee, L. L. Lim, and B. Owen, "Bridging the aviation CO2 emissions gap: why emissions trading is needed," *Dalt. Res. Inst.*, p. 29, 2013.
[347] M. Prussi *et al.*, "CORSIA: The first internationally adopted approach to calculate life-cycle GHG emissions for aviation fuels," *Renewable and Sustainable Energy Reviews*, vol. 150. 2021, doi: 10.1016/j.rser.2021.111398.
[348] ICAO, "ICAO document INTERNATIONAL CIVIL AVIATION ORGANIZATION CORSIA Sustainability Criteria for CORSIA Eligible Fuels C RSIA Carbon Offsetting and Reduction Scheme for International Aviation," 2021.
[349] E. Korkut and L. B. Fowler, "Regulatory and Policy Analysis of Production, Development and Use of Sustainable Aviation Fuels in the United States," *Front. Energy Res.*, vol. 9, no. November, pp. 1–18, 2021, doi: 10.3389/fenrg.2021.750514.
[350] M. D. Staples, R. Malina, P. Suresh, J. I. Hileman, and S. R. H. Barrett, "Aviation CO2 emissions reductions from the use of alternative jet fuels," *Energy Policy*, vol. 114, pp.

342–354, 2018, doi: 10.1016/j.enpol.2017.12.007.
[351] M. Prussi *et al.*, “CORSIA: The first internationally adopted approach to calculate life-cycle GHG emissions for aviation fuels,” 2021, doi: 10.1016/j.rser.2021.111398.
[352] T. Searchinger *et al.*, “Use of U.S. croplands for biofuels increases greenhouse gases through emissions from land-use change,” *Science (80-. ).*, vol. 319, no. 5867, pp. 1238–1240, 2008, doi: 10.1126/science.1151861.
[353] S. C. de Vries, G. W. J. van de Ven, M. K. van Ittersum, and K. E. Giller, “Resource use efficiency and environmental performance of nine major biofuel crops, processed by first-generation conversion techniques,” *Biomass and Bioenergy*, vol. 34, no. 5, pp. 588–601, May 2010, doi: 10.1016/J.BIOMBIOE.2010.01.001.
[354] E. M. Aro, “From first generation biofuels to advanced solar biofuels,” *Ambio*, vol. 45, no. 1, pp. 24–31, Jan. 2016, doi: 10.1007/S13280-015-0730-0/FIGURES/1.
[355] K. G. Cassman and A. J. Liska, “Food and fuel for all: realistic or foolish?,” *Biofuels, Bioprod. Biorefining*, vol. 1, no. 1, pp. 18–23, Sep. 2007, doi: 10.1002/BBB.3.
[356] Z. Zhang, L. Lohr, C. Escalante, and M. Wetzstein, “Food versus fuel: What do prices tell us?,” *Energy Policy*, vol. 38, no. 1, pp. 445–451, Jan. 2010, doi: 10.1016/J.ENPOL.2009.09.034.
[357] U.S. Energy Information Association, “U.S. fuel ethanol production capacity increased by 3% in 2019,” *Today in Energy*, 2020. https://www.eia.gov/todayinenergy/detail.php?id=45316 (accessed Oct. 18, 2020).
[358] USDA Foreign Agricultural Service, “Ethanol 2019 Export Highlights,” *USDA Foreign Agricultural Service*, 2019. https://www.fas.usda.gov/ethanol-2019-export-highlights (accessed Jul. 08, 2022).
[359] Minnesota Biofuels Association, “The ‘Blend Wall,’” 2020. https://www.mnbiofuels.org/resources/facts-about-ethanol/the-blend-wall (accessed Jul. 08, 2022).
[360] Alternative Fuels Data Center, “Maps and Data - Global Ethanol Production,” *Alternative Fuels Data Center*, 2021. https://afdc.energy.gov/data/10331 (accessed Apr. 16, 2021).
[361] USDA Foreign Agricultural Service, “Brazil: Sugar Semi-Annual,” *USDA Foreign Agricultural Service*, 2020. https://www.fas.usda.gov/data/brazil-sugar-semi-annual-6.
[362] Transport Policy, “Brazil: Fuels: Biofuels,” *TransportPolicy.net*, 2021. https://www.transportpolicy.net/standard/brazil-fuels-biofuels/ (accessed Jul. 08, 2022).
[363] USDA Foreign Agricultural Service, “Oilseed: World Markets and Trade (April 2021),” 2021.
[364] USDA Foreign Agricultural Service, “Oilseet: World Markets and Trade April 2021,” *USDA Foreign Agricultural Service*, 2021. https://downloads.usda.library.cornell.edu/usda-esmis/files/tx31qh68h/0c484n813/6d5712933/oilseeds.pdf.
[365] T. Radich, “The Flight Paths for Biojet Fuel,” 2015. Accessed: Apr. 17, 2021. [Online]. Available: www.eia.gov.
[366] H. A. Alalwan, A. H. Alminshid, and H. A. S. Aljaafari, “Promising evolution of biofuel generations. Subject review,” *Renew. Energy Focus*, vol. 28, pp. 127–139, Mar. 2019, doi: 10.1016/J.REF.2018.12.006.
[367] U.S. Department of Energy, “Executive Summary/Overview -Stepwise Supply Curves,” *Bioenergy KDF*, 2021. https://bioenergykdf.net/executive-summaryoverview?chapterNumber=1&tabNumber=1 (accessed Apr. 17, 2021).

[368] K. L. Kadam and J. D. McMillan, “Availability of corn stover as a sustainable feedstock for bioethanol production,” *Bioresour. Technol.*, vol. 88, no. 1, pp. 17–25, May 2003, doi: 10.1016/S0960-8524(02)00269-9.
[369] G. D. P. S. Augustus, M. Jayabalan, and G. J. Seiler, “Evaluation and bioinduction of energy components of Jatropha curcas,” *Biomass and Bioenergy*, vol. 23, no. 3, pp. 161–164, Sep. 2002, doi: 10.1016/S0961-9534(02)00044-2.
[370] K. Openshaw, “A review of Jatropha curcas: an oil plant of unfulfilled promise,” *Biomass and Bioenergy*, vol. 19, no. 1, pp. 1–15, Jul. 2000, doi: 10.1016/S0961-9534(00)00019-2.
[371] L. Tao, A. Milbrandt, Y. Zhang, and W. C. Wang, “Techno-economic and resource analysis of hydroprocessed renewable jet fuel,” *Biotechnol. Biofuels*, vol. 10, no. 1, pp. 1–16, Nov. 2017, doi: 10.1186/S13068-017-0945-3/FIGURES/7.
[372] G. Heinrich, “Jatropha curcas L. -An alternative oil crop,” *Biokerosene Status Prospect.*, pp. 237–257, Aug. 2017, doi: 10.1007/978-3-662-53065-8_11/COVER/.
[373] S. S. Doliente, A. Narayan, J. F. D. Tapia, N. J. Samsatli, Y. Zhao, and S. Samsatli, “Bio-aviation Fuel: A Comprehensive Review and Analysis of the Supply Chain Components,” *Front. Energy Res.*, vol. 8, no. July, pp. 1–38, 2020, doi: 10.3389/fenrg.2020.00110.
[374] B. Sims, “Neste Oil expands input stream to include jatropha, camelina,” *BiodieselMagazine.com*, 2011. https://biodieselmagazine.com/articles/7931/neste-oil-expands-input-stream-to-include-jatropha-camelina (accessed Jul. 15, 2022).
[375] E. Voegele, “Jatenergy sells jatropha oil to Lufthansa,” *BiodieselMagazine.com*, 2011. https://biodieselmagazine.com/articles/8061/jatenergy-sells-jatropha-oil-to-lufthansa (accessed Jul. 15, 2022).
[376] M. Molefe, D. Nkazi, and H. E. Mukaya, “Method Selection for Biojet and Biogasoline Fuel Production from Castor Oil: A Review,” *Energy & Fuels*, vol. 33, no. 7, pp. 5918–5932, Jul. 2019, doi: 10.1021/ACS.ENERGYFUELS.9B00384.
[377] United Nations, “Castor oil seed,” *UN Data*, 2022. http://data.un.org/Data.aspx?d=FAO&f=itemCode%3A265 (accessed Jul. 15, 2022).
[378] T. H. Tsui and J. W. C. Wong, “A critical review: emerging bioeconomy and waste-to-energy technologies for sustainable municipal solid waste management,” *Waste Disposal and Sustainable Energy*, vol. 1, no. 3. Springer, pp. 151–167, Aug. 07, 2019, doi: 10.1007/s42768-019-00013-z.
[379] A. E. Ladd, “Opposition to Solid Waste Incineration: Pre- Implementation Anxieties Surrounding a New Environmental Controversy*,” *Sociol. Inq.*, vol. 61, no. 3, pp. 299–313, Jul. 1991, doi: 10.1111/J.1475-682X.1991.TB00163.X.
[380] M. Wang, Z. Wang, X. Gong, and Z. Guo, “The intensification technologies to water electrolysis for hydrogen production – A review,” *Renew. Sustain. Energy Rev.*, vol. 29, pp. 573–588, Jan. 2014, doi: 10.1016/J.RSER.2013.08.090.
[381] J. Wilcox, P. C. Psarras, and S. Liguori, “Assessment of reasonable opportunities for direct air capture,” *Environ. Res. Lett.*, vol. 12, no. 6, p. 065001, May 2017, doi: 10.1088/1748-9326/AA6DE5.
[382] X. Su, X. Yang, B. Zhao, and Y. Huang, “Designing of highly selective and high-temperature endurable RWGS heterogeneous catalysts: recent advances and the future directions,” *J. Energy Chem.*, vol. 26, no. 5, pp. 854–867, Sep. 2017, doi: 10.1016/J.JECHEM.2017.07.006.
[383] O. Schmidt, A. Gambhir, I. Staffell, A. Hawkes, J. Nelson, and S. Few, “Future cost and performance of water electrolysis: An expert elicitation study,” *Int. J. Hydrogen Energy*,

vol. 42, no. 52, pp. 30470–30492, Dec. 2017, doi: 10.1016/J.IJHYDENE.2017.10.045.
[384] M. Wang, "California GREET 3.0." Argonne National Laboratory, 2016, [Online]. Available: https://www.arb.ca.gov/fuels/lcfs/ca-greet/ca-greet30-corrected.xlsm?_ga=2.184007590.1258986997.1657325441-361084880.1654188250.
[385] O. Edenhofer, *Climate Change 2014: Mitigation of Climate Change. Contribution of Working Group III to the Fifth Assessment Report of the Intergovernmental Panel on Climate Change [Edenhofer, O., R. Pichs-Madruga, Y. Sokona, E. Farahani, S. Kadner, K. Seyboth, A. Adler,*. Cambridge, United Kingdom and New York, NY, USA: Cambridge University Press, 2014.
[386] E. D. Larson, G. Fiorese, G. Liu, R. H. Williams, T. G. Kreutz, and S. Consonni, "Co-production of decarbonized synfuels and electricity from coal + biomass with CO2 capture and storage: An Illinois case study," *Energy Environ. Sci.*, vol. 3, no. 1, pp. 28–42, 2010, doi: 10.1039/b911529c.
[387] N. McQueen, M. J. Desmond, R. H. Socolow, P. Psarras, and J. Wilcox, "Natural Gas vs. Electricity for Solvent-Based Direct Air Capture," *Front. Clim.*, vol. 2, p. 618644, Jan. 2021, doi: 10.3389/fclim.2020.618644.
[388] M. A. Pellow, C. J. M. Emmott, C. J. Barnhart, and S. M. Benson, "Hydrogen or batteries for grid storage? A net energy analysis," *Energy Environ. Sci.*, vol. 8, no. 7, 2015, doi: 10.1039/C4EE04041D.
[389] NREL, "Renewable Electricity Futures Study: Exploration of High-Penetration Renewable Electricity Futures, Volume 1," *Natl. Renew. Energy Lab.*, vol. 1, p. 280, 2012, doi: NREL/TP-6A20-52409-1.
[390] E. Rezaei and S. Dzuryk, "Techno-economic comparison of reverse water gas shift reaction to steam and dry methane reforming reactions for syngas production," *Chem. Eng. Res. Des.*, vol. 144, pp. 354–369, Apr. 2019, doi: 10.1016/j.cherd.2019.02.005.
[391] J. Han, L. Tao, and M. Wang, "Well-to-wake analysis of ethanol-to-jet and sugar-to-jet pathways," *Biotechnol. Biofuels*, vol. 10, no. 1, pp. 1–15, 2017, doi: 10.1186/s13068-017-0698-z.
[392] M. N. Pearlson, "A Techno-economic and Environmental Assessment of Hydroprocessed Renewable Distillate Fuels," *Dep. Aeronaut. Astronaut.*, p. 106, 2011, [Online]. Available: http://dspace.mit.edu/bitstream/handle/1721.1/65508/746766700.pdf?sequence=1.
[393] R. W. Stratton, H. M. Wong, and J. I. Hileman, "Quantifying variability in life cycle greenhouse gas inventories of alternative middle distillate transportation fuels," *Environ. Sci. Technol.*, vol. 45, no. 10, pp. 4637–4644, 2011, doi: 10.1021/es102597f.
[394] M. M. Wright, D. E. Daugaard, J. A. Satrio, and R. C. Brown, "Techno-economic analysis of biomass fast pyrolysis to transportation fuels," *Fuel*, vol. 89, no. SUPPL. 1, pp. S2–S10, 2010, doi: 10.1016/j.fuel.2010.07.029.
[395] S. B. Jones, J. E. Holladay, C. Valkenburg, D. J. Stevens, C. W. Walton, and C. Kinchin, "Production of Gasoline and Diesel from Biomass via Fast Pyrolysis, Hydrotreating and Hydrocracking: A Design Case," 2009.
[396] E. D. Larson, G. Fiorese, G. Liu, R. H. Williams, T. G. Kreutz, and S. Consonni, "Co-production of decarbonized synfuels and electricity from coal + biomass with $CO_2$ capture and storage: an Illinois case study," *Energy Environ. Sci.*, vol. 3, no. 1, pp. 28–42, Jan. 2010, doi: 10.1039/B911529C.
[397] O. Schmidt, A. Gambhir, I. Staffell, A. Hawkes, J. Nelson, and S. Few, "Future cost and

performance of water electrolysis: An expert elicitation study," *Int. J. Hydrogen Energy*, vol. 42, no. 52, pp. 30470–30492, Dec. 2017, doi: 10.1016/j.ijhydene.2017.10.045.
[398] N. McQueen, K. V. Gomes, C. McCormick, K. Blumanthal, M. Pisciotta, and J. Wilcox, "A review of direct air capture (DAC): scaling up commercial technologies and innovating for the future," *Prog. Energy*, vol. 3, no. 3, p. 032001, Jul. 2021, doi: 10.1088/2516-1083/abf1ce.
[399] M. Wang *et al.*, "Greenhouse gases, Regulated Emissions, and Energy use in Technologies Model ® (2020 .Net)." Oct. 2020, doi: 10.11578/GREET-Net-2020/dc.20200913.1.
[400] S. Restrepo-Valencia and A. Walter, "Techno-economic assessment of bio-energy with carbon capture and storage systems in a typical sugarcane mill in Brazil," *Energies*, vol. 12, no. 6, p. 1129, Mar. 2019, doi: 10.3390/en12061129.
[401] S. Liguori, K. Kian, N. Buggy, B. H. Anzelmo, and J. Wilcox, "Opportunities and challenges of low-carbon hydrogen via metallic membranes," *Prog. Energy Combust. Sci.*, vol. 80, p. 100851, Sep. 2020, doi: 10.1016/J.PECS.2020.100851.
[402] M. Stahmer, "Polyethylene - the optimum gas pipe material? [technical memo]," vol. 4130, pp. 1–2, 2008.
[403] J. Colt, W. Driscoll, and R. Freed, "Work Assignment 239, Task 2: Carbon Sequestration in Landfills [Memorandum]." United State Environmental Protection Agency, 1995, Accessed: Jul. 10, 2020. [Online]. Available: https://19january2017snapshot.epa.gov/www3/epawaste/conserve/tools/warm/pdfs/ICF_Memo_Carbon_Sequestration_in_Landfills.pdf.
[404] U.S. Environmental Protection Agency, "Advancing Sustainable Materials Management: 2014 Fact Sheet Assessing Trends in Material Generation, Recycling, Composting, Combustion with Energy Recovery and Landfilling in the United States," 2014.
[405] U.S. Environmental Protection Agency Office of Resource Conservation, "Documentation for Greenhouse Gas Emission and Energy Factors Used in the Waste Reduction Model (WARM) - Containers, Packaging, and Non-Durable Goods Materials Chapters," 2016.
[406] A. C. Albertsson, "The shape of the biodegradation curve for low and high density polyethenes in prolonged series of experiments," *Eur. Polym. J.*, vol. 16, no. 7, pp. 623–630, 1980, doi: 10.1016/0014-3057(80)90100-7.
[407] A. A. Shah, F. Hasan, A. Hameed, and S. Ahmed, "Biological degradation of plastics: A comprehensive review," *Biotechnology Advances*, vol. 26, no. 3. pp. 246–265, May 2008, doi: 10.1016/j.biotechadv.2007.12.005.
[408] U. Lee, J. Han, and M. Wang, "Evaluation of landfill gas emissions from municipal solid waste landfills for the life-cycle analysis of waste-to-energy pathways," *J. Clean. Prod.*, vol. 166, pp. 335–342, 2017, doi: 10.1016/j.jclepro.2017.08.016.
[409] Intergovernmental Panel on Climate Change (IPCC), "2006 IPCC Guidelines for National Greenhouse Gas Inventories: Vol 5 Chapter 3 Solid Waste Disposal," *2006 IPCC Guidel. Natl. Greenh. Gas Invent.*, vol. 5, pp. 6.1-6.49, 2006, doi: 10.1111/j.1749-6632.2009.05320.x.
[410] J. S. Rhodes and D. W. Keith, "Biomass Energy with Geological Sequestration of CO2: Two for the Price of One?," *Greenh. Gas Control Technol. - 6th Int. Conf.*, vol. II, no. i, pp. 1371–1376, 2003, doi: http://dx.doi.org/10.1016/B978-008044276-1/50217-8.
[411] S. T. McCoy and E. S. Rubin, "An engineering-economic model of pipeline transport of CO2 with application to carbon capture and storage," *Int. J. Greenh. Gas Control*, vol. 2,

no. 2, pp. 219–229, 2008, doi: 10.1016/S1750-5836(07)00119-3.
[412] L. S. Heath, R. A. Birdsey, C. Row, and A. J. Plantinga, “Carbon pools and fluxes in U.S. forest products,” in *Forest Ecosystems, Forest Management and the Global Carbon Cycle*, Berlin, Heidelberg: Springer Berlin Heidelberg, 1996, pp. 271–278.
[413] Z. Qin, J. B. Dunn, H. Kwon, S. Mueller, and M. M. Wander, “Influence of spatially dependent, modeled soil carbon emission factors on life-cycle greenhouse gas emissions of corn and cellulosic ethanol,” *GCB Bioenergy*, vol. 8, no. 6, pp. 1136–1149, Nov. 2016, doi: 10.1111/gcbb.12333.
[414] M. Mermertaş and F. Germirli Babuna, “Life Cycle Environmental Impact Analysis of HDPE Packaging Materials for Different Disposal Options,” Springer, Cham, 2019, pp. 55–61.
[415] M. Puettmann, K. Wilson, and E. Oneil, “Life cycle assessment of biochar from post-harvest forest residues (Draft Report),” 2017.
[416] J. B. Wilson, “Life-cycle inventory of formaldehyde-based resins used in wood composites in terms of resources, emissions, energy and carbon,” *Wood Fiber Sci.*, vol. 42, no. SUPPL. 1, pp. 125–143, 2010, Accessed: Dec. 31, 2019. [Online]. Available: www.corrim.
[417] Franklin Associates, “Cradle-To-Gate Life Cycle Inventory of Nine Plastic Resins,” *Am. Chem. Counc.*, pp. 1–198, 2011, [Online]. Available: https://plastics.americanchemistry.com/LifeCycle-Inventory-of-9-Plastics-Resins-and-4-Polyurethane-Precursors-Rpt-Only/.
[418] “National_Renewable_Energy_Laboratory/USLCI | LCA Collaboration Server.” https://www.lcacommons.gov/lca-collaboration/National_Renewable_Energy_Laboratory/USLCI/dataset/PROCESS/2c79b9d3-e5f9-34a8-990e-b7d6f9e4dd08 (accessed Jul. 20, 2020).
[419] Beck Group, “California Assessment of Wood Business Innovation Opportunities and Markets ( CAWBIOM ),” 2015.
[420] “18R-97: Cost Estimate Classification System – As Applied in Engineering, Procurement, and Construction for the Process Industries,” p. 7, 2020.
[421] G. P. Towler and R. K. Sinnot, *Chemical engineering design: principles, practice, and economics of plant and process design*, 2nd ed. Boston, MA: Butterworth-Heinemann, 2013.
[422] I. R. E. James, D. Keairns, M. Turner, M. Woods, N. Kuehn, and A. Zoelle, “Cost and Performance Baseline for Fossil Energy Plants Volume 1: Bituminous Coal and Natural Gas to Electricity,” Sep. 2019, doi: 10.2172/1569246.
[423] M. Woods, M. Matuszewski, and R. Brasington, “Advancing Oxycombustion Technology for Bituminous Coal Power Plants: An R&D Guide,” Apr. 2012, doi: 10.2172/1489759.
[424] M. J. Turner and L. L. Pinkerton, “Quality Guidelines for Energy System Studies: Capital Cost Scaling Methodology,” Jan. 2013, doi: 10.2172/1513277.
[425] C. N. Hamelinck, A. P. C. Faaij, H. den Uil, and H. Boerrigter, “Production of FT transportation fuels from biomass; technical options, process analysis and optimisation, and development potential,” *Energy*, vol. 29, no. 11, pp. 1743–1771, Sep. 2004, doi: 10.1016/J.ENERGY.2004.01.002.
[426] Air Liquide Engineering and Construction, “Technology Handbook,” 2021. https://www.engineering-airliquide.com/technology-handbook (accessed Oct. 21, 2021).
[427] T. Uchida, T. Goto, T. Yamada, T. Kiga, and C. Spero, “Oxyfuel Combustion as CO2

Capture Technology Advancing for Practical use - callide Oxyfuel Project -," *Energy Procedia*, vol. 37, pp. 1471–1479, Jan. 2013, doi: 10.1016/J.EGYPRO.2013.06.022.

## APPENDIX A. Supplementary information for Leveraging the bioeconomy for carbon drawdown

The supplementary information in subsequent sections provides a detailed explanation of the methods used to derive 10,000-year estimates of carbon sequestration (A1) and the life cycle GHG emissions of the four biomass conversion pathways analyzed (A2.3 - A2.6). A more complete exposition of analysis results, combining the cradle-to-gate analyses in (A2) with the long-term sequestration estimates in (A1) is presented for switchgrass IGCC with CCS (A2.3.2), corn stover polyethylene with CCS (A2.4.2), biochar from forest residues (A2.5.2), and oriented strand board from forest residues (A2.6.2).

## A1 Sequestration technologies

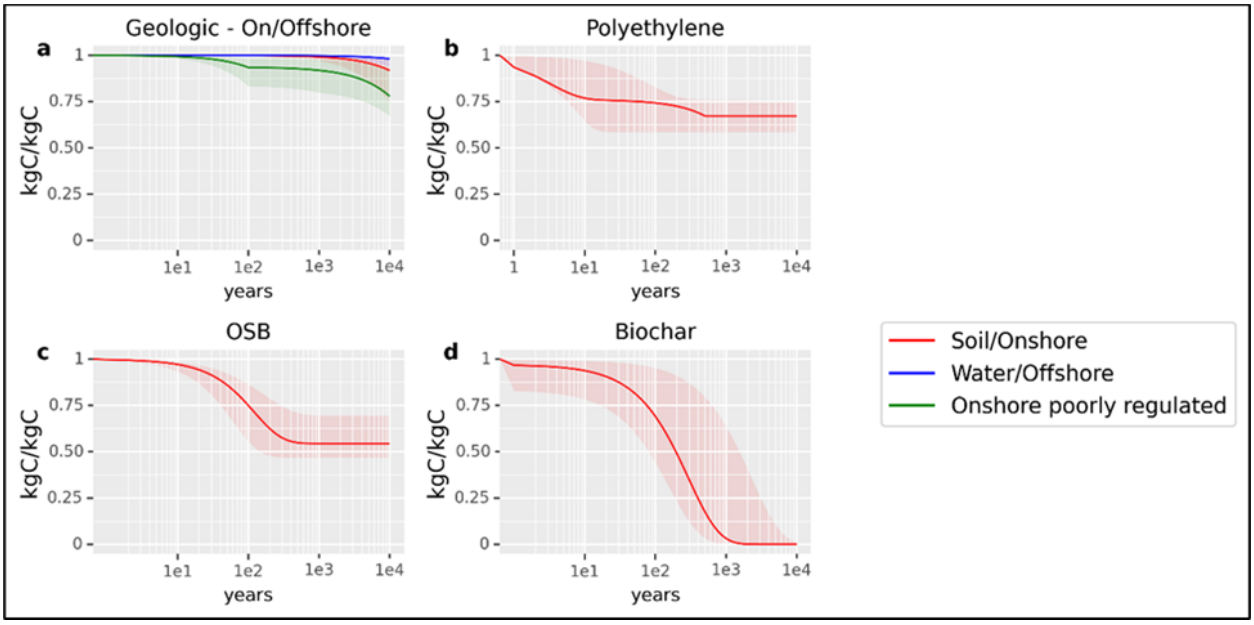


**Figure A1** – Estimated carbon sequestration over time. This figure illustrates a range of optimistic, pessimistic, and moderate cases for carbon sequestration over time. The dark red line in each panel is the moderate estimate for each analyzed scenario. The dark blue and dark green lines in panel (a) represent the P50 estimate (see A1.1) for offshore and onshore poorly-regulated geologic sequestration. The dark red line in panel (a) is the P50 scenario for onshore, well-regulated wells. This is the baseline case for geological sequestration in this analysis. The functional form in each case considers a pulse of carbon entering the carbon cycle in the form of a product or sequestration co-product. From the production gate, the function may consider (where appropriate) operational use-life, recycling, secondary use, and sequestration of carbon in the product or biosphere. Panels: **a.** Geologic sequestration of industrially captured $CO_2$ in either onshore well-regulated or poorly-regulated or offshore well-regulated reservoirs **b.** carbon sequestered in a polyethylene product. Note that the discontinuity and shape of the function results from the interaction of both linear (landfill decay) and exponential (use-life decay) components in the function. **c.** carbon sequestered in oriented strand board (OSB) construction material **d.** carbon sequestered in biochar soil ammendment applied to agricultural soil.

### A1.1 Geological Storage

Our estimates are adapted from Alcalde et al. (2018)[210], who used a Monte Carlo modeling approach to estimate $CO_2$ leakage from geologic reservoirs over 10,000 years. The analysis considers well-regulated onshore and offshore wells and poorly regulated wells (onshore only). **Table A1** shows the $5^{th}$, $50^{th}$, and $95^{th}$ percentile thresholds for the % of $CO_2$ leaked at the time in years. P95 indicates that 95% of the values in model runs were greater than that value. P5 indicates that 5% of the model runs returned values greater than the indicated value.

**Table A1** Percentage of geologically sequestered carbon leakage over time (adapted from Alcalde et al. (2018)

| **Time since sequestration (years)** | **Onshore Geological (Well-regulated) – CO2 leaked (%)** | | | **Offshore Geological (Well-regulated) - – CO2 leaked (%)** | | | **Onshore Geological (Poorly-regulated) - – CO2 leaked (%)** | | |
|---|---|---|---|---|---|---|---|---|---|
| | P95 | P50 | P5 | P95 | P50 | P5 | P95 | P50 | P5 |
| 1 | 0.0013 | 0.0022 | 0.0045 | 0.0005 | 0.0008 | 0.0014 | 0.0517 | 0.202 | 0.521 |
| 100 | 0.0737 | 0.156 | 0.358 | 0.0249 | 0.0447 | 0.0888 | 1.70 | 6.41 | 16.5 |
| 1000 | 0.246 | 0.888 | 2.96 | 0.0709 | 0.213 | 0.646 | 2.39 | 8.05 | 20.0 |
| 10000 | 1.81 | 8.18 | 25.71 | 0.483 | 1.89 | 6.29 | 6.91 | 22.0 | 32.6 |

We convert the leakage values in **Table A1** to % $CO_2$ (or % carbon) remaining sequestered by subtracting each cell from 100 (**Table A2**). P95 now indicates that 95% of values are less than the indicated value while P5 indicates that 5% of modeled values are less than the indicated value.

**Table A2** Percentage of carbon remaining geologically sequestered over time.

| **Time since sequestration (years)** | **Onshore Geological (Well-regulated) – $CO_2$ remaining in storage (%)** | | | **Offshore Geological (Well-regulated) – $CO_2$ remaining in storage (%)** | | | **Offshore Geological (Poorly-regulated) – $CO_2$ remaining in storage (%)** | | |
|---|---|---|---|---|---|---|---|---|---|
| | P95 | **P50** | P5 | P95 | P50 | P5 | P95 | P50 | P5 |
| 1 | 99.9987 | **99.9978** | 99.9955 | 99.9995 | 99.9992 | 99.9986 | 99.9483 | 99.798 | 99.479 |
| 100 | 99.9263 | **99.844** | 99.642 | 99.9751 | 99.9553 | 99.9112 | 98.3 | 93.59 | 83.5 |
| 1000 | 99.754 | **99.112** | 97.04 | 99.9291 | 99.787 | 99.354 | 97.61 | 91.95 | 80 |
| 10000 | 98.19 | **91.82** | 74.29 | 99.517 | 98.11 | 93.71 | 93.09 | 78 | 67.4 |

We fit a first-order decay function to the P95, P50, and P5 values to calculate % $CO_2$ remaining sequestered at any time (t) where *r* is the decay rate. The onshore and offshore well-regulated cases are modeled with single decay function and rate. The onshore poorly regulated case is modeled with three different decay rates for 0-100; 101-1,000; and 1001-10,000 years in each of the probability divisions.

Eq. 1

$$C_{geo}(t) = C_0 e^{-rt}$$

The decay function matches the Monte Carlo results within < 1% in each referenced period. This is the function reported in **Figure A1a**, with P95, P50, and P5 for both onshore and offshore representing optimistic, midrange, and pessimistic bounds, respectively.

In the life cycle analyses in Part II of our paper, we estimate the emissions from geological sequestration in the IGCC and polyethylene pathways from the onshore, well-regulated scenario only.

### A1.2 Carbon sequestered in polyethylene and landfills

We model the sequestration of carbon in plastic goods as a multi-stage process, including a use phase, a recycling or up-cycling phase, and eventual end-of-life (EOL) as waste in a managed or unmanaged environment or as a feedstock for energy production. We consider only the most common EOL pathways in the U.S. Using 2017 estimates from the EPA[211], we assume that 8% of polyethylene is recycled, 16% is combusted, and 76% enters landfills. To represent optimistic, moderate, and pessimistic cases for polyethylene (PE) carbon in landfills (**Figure A1b**), we consider low-density polyethylene (LDPE) grocery bags, high-density polyethylene (HDPE) bottles, and HDPE water pipe, respectively. We conservatively assume a 2-year half-life in use for a given stock of LDPE bags or HDPE bottles. Industry literature reports that HDPE pipe can last as long as 100 years.[402] We assume a 50-year half-life to represent the use phase for a given stock of HDPE pipe. The use phase stock ($PE_{UL}$) of carbon remaining in polyethylene from a production pulse of PE ($PE_0$) is estimated by a first-order decay function of the form:

Eq. 2

$$PE_{UL}(t) = PE_0 e^{-rt}$$

Where *r* is the decay rate determined by the half-life and *t* is time.

As a pulse of PE exits its use-life, it may be recycled, combusted for energy, or it enters a managed landfill (we only consider "best management practices"). Recycled plastics are typically processed into a lower grade product than the original product. However, for simplicity, we track the carbon sequestered in recycled plastics by adding the carbon back to the stock at each time *t*. Combusted PE is assumed to release all carbon as $CO_2$.

Determining the degradation rate of carbon stored in PE once it reaches landfill is challenging due to a wide variety of environmental conditions and the timescales required to observe degradation in field settings. However, indirect methods (e.g. accelerated degradation) as well as extrapolations from short-duration experiments do offer some insight.

Conventional greenhouse gas accounting of municipal solid waste as adopted by the U.S. EPA assumes that the carbon in plastics in landfills is permanently sequestered.[403]–[405] However, studies have indicated the potential for plastics such as PE to break down into mineralized carbon under the conditions found in a landfill environment.[213], [406] In order to be released as landfill gasses via biodegradation, highly stable PE would first need to undergo chemical decomposition via physical processes (photodegradation from UV light, thermo-oxidation, and hydrolysis).[407] Degradation rates are subject to a number of environmental factors (temperature, humidity, pH, presence of oxygen).

In our analysis, we do not attempt to model biodegradation and instead adopt a physical decay model as a proxy. We implement a zeroth-order linear decay model based on physical processes as adapted from Chamas et al. (2020).[215] Physical degradation is a function of surface area and material density.[215] We assume that between 1% and 23% of the carbon in landfilled PE is subject to decay. The upper bound of 23% is a somewhat arbitrary and conservative limit

based on the labile fraction assumption for harvest wood products[179] while the lower bound of 1% approximates the EPA assumption. We selected a simple midpoint of 11.5% for the moderate case. Chamas et al. (2020) reports a range of degradation half-lives from the literature for LDPE bags, HDPE bottles, and HDPE pipe degrading in soil: 4.6 years, 230-280 (250) years, and 4,600-5,500 (5,000) years, respectively. The half-lives in parenthesis (and the 4.6 years for LDPE bags) are the estimates modeled by Chamas et al. (2020). We calculate decay rates from these half-lives.

We then calculate the quantity of carbon remaining sequestered in PE in use or in landfills at any time $t$ = 1 to 10,000 years (**Figure A1b**), where:

The proportion of PE carbon in use-life at any time *t*:

If $PE_{UL}(0) = 1$ then $PE_{UL}(t)$ can be sequentially calculated to account for recycling:

Eq. 3

$$PE_{UL}(t) = PE_{UL}(t-1)e^{u} + [0.08(PE_{UL}(t-1) - PE_{UL}(t-1)e^{u})]$$

Where *u* is the use-life decay rate and the portion of the function in the brackets is equal to the recycled fraction (8%) of PE leaving use-life at any time *t.*
Or:

Eq. 4

$$PE_{UL}(t) = PE_{UL}(t-1)[e^{u} + 0.08[1 - e^{u}]]$$

The pulse of PE carbon exiting use-life at any time *t*:

Eq. 5

$$PE_{W}(t) = PE_{UL}(t-1) - PE_{UL}(t)$$

And entering landfills:

Eq. 6

$$PE_{New}(t) = 0.76PE_{W}(t)$$

The carbon remaining sequestered in the landfills at any time *t:*

Eq. 7

$$PE_{LF}(t) = \sum_{i=1}^{t} f_{labile}PE_{New}(i)\,(1 - r(t-i)) + f_{recalc}PE_{New}(i)$$

where *r* is the linear decay rate of the PE in landfills, and $f_{labile}$ and $f_{recalc}$ represent the labile and recalcitrant fractions of carbon, respectively.

Total carbon remaining sequestered at any time *t:*
Carbon sequestered at time *t* is the sum of the fraction of carbon remaining in its useful life and the fraction remaining sequestered in the landfill.

Eq. 8

$$PE_{seq}(t) = PE_{UL}(t) + PE_{LF}(t)$$

The fraction of carbon remaining in PE and landfills at time t is shown in **Figure A1b**. The estimated carbon loss to the atmosphere in each case is shown in **Table A3**.

**Table A3** Percentage of polyethylene and landfill carbon loss to atmosphere over time. Values in bold-face reflect moderate case assumptions used in the main text.

| Time since sequestration (years) | Carbon loss from polyethylene and landfills (%) - Optimistic | Carbon loss from polyethylene and landfills (%) - Moderate | Carbon loss from polyethylene and landfills (%) - Pessimistic |
|---|---|---|---|
| 100 | 0.172 | **0.257** | 0.415 |
| 1,000 | 0.241 | **0.327** | 0.415 |
| 10,000 | 0.248 | **0.327** | 0.415 |

### A1.2.1 Landfill emissions

We assume that carbon escapes from landfills as either $CO_2$ or $CH_4$. Given the paucity of data on PE degradation in landfills, we are unable to establish the ratio of carbon degradation products specific to PE. Thus, we assume emissions profiles consistent with landfill gas more generally. In the absence of methane management infrastructure such as methane flaring or energy production from landfill gas (LFG), we assume that 50% of carbon is released as $CO_2$ while 50% is released as $CH_4$.[408] This is a simplifying assumption because a fraction (up to 10%) of $CH_4$ will oxidize into $CO_2$ upon exiting the landfill. We do not account for that fraction. In the case of flaring or energy production from LFG, we assume that 75% of methane is oxidized via combustion.[408] The resulting fraction of carbon emissions in this case is 87.5% $CO_2$ compared to 12.5% emitted as $CH_4$. $CH_4$ emission are multiplied by their 100-year global warming potential (GWP) of 28, irrespective of when the emissions occur.[229] This amplifies the impact of $CH_4$ emissions when considering only a 100-year timeframe.[222] In the main body of our analysis, we report only the landfill case with flaring.
The fraction of total polyethylene carbon released as $CO_2$ emissions from polyethylene and landfills at any time *t*:

Fraction of polyethylene carbon released from energy combustion at time *t:*

Eq. 9

$$C_{energy}(t) = \sum_{i=1}^{t} 0.16 PE_W(i)$$

Fraction of polyethylene carbon released from landfill at time *t:*

Eq. 10

$$C_{LF}(t) = (1 - PE_{seq}) - C_{energy}(t)$$

At a landfill that flares 75% of methane into $CO_2$ the fraction of total C emissions that become $CO_2$ at time *t*:

Eq. 11

$$C_{CO2,flare}(t) = C_{energy}(t) + 0.875C_{LF}(t)$$

At a landfill that does not flare methane into $CO_2$ the fraction of total C emissions that become $CO_2$ at time *t*:

Eq. 12

$$C_{CO2,no-flare}(t) = C_{energy}(t) + 0.50C_{LF}(t)$$

The fraction of total polyethylene carbon released as $CH_4$ emissions from landfills at any time *t*: At a landfill that flares 75% of methane into $CO_2$ the fraction of total C emissions that become $CH_4$ at time *t*:

Eq. 13

$$C_{CH4,flare}(t) = 0.125C_{LF}(t)$$

At a landfill that does not flare methane into $CO_2$ the fraction of total C emissions that become $CO_2$ at time *t*:

Eq. 14

$$C_{CH4,no-flare}(t) = 0.50C_{LF}(t)$$

### A1.3 Oriented strand board

We model the sequestration of carbon in oriented strand board (OSB) as a multi-phase process, with a use phase and then an end-of-life phase that may involve recycling, secondary use, and a significant portion managed in landfills or open dumps. The optimistic, moderate, and pessimistic cases for sequestration of carbon in OSB are derived from Skog (2008) and Stewart and Nakamura (2012), combining half-life estimates for the useful life of wood construction materials in single, multi-family, and residential upkeep scenarios with half-life estimates for wood construction materials decaying landfills.[179], [216] The optimistic case assumes a useful half-life of 115 years based on OSB utilization in single family home construction. The pessimistic case assumes a useful half-life of 30 years based on OSB utilization in residential upkeep. The moderate case assumes a useful half-life of 72 years based on an end-use weighted average of half-lives for single family, multi-family, and residential upkeep construction. The

stock of carbon remaining in OSB in use ($OSB_{UL}$) from a production pulse of OSB ($OSB_0$) is estimated by a first-order decay model of the form:

Eq. 15

$$OSB_{UL}(t) = OSB_0 e^{-rt}$$

Where *r* is the decay rate determined by the half-life and *t* is time.

As a pulse of OSB exits its use-life, our analysis assumes the two most common end-of-life scenarios in the U.S.—landfill and energy production. We assume 70% of OSB waste is landfilled and 30% combusted for energy, which is consistent with estimates for California[216] and similar to national estimates in the literature [179]. Combusted OSB is assumed to release all of its carbon as $CO_2$.

In our analysis, we use a first-order exponential decay model with a decay rate based on landfill half-lives of 35, 29, and 20 years, for the optimistic, moderate, and pessimistic cases [179], [409]. We assume that in the moderate case no more than 23% of the carbon in OSB in landfills is subject to decay, with lower and upper bounds at 1.3% and 34.6%.[179] The large recalcitrant fraction of OSB carbon is due in part to the recalcitrance of the lignin in wood products. Moreover, biological degradation rates are impacted by changes in chemical and environmental conditions (moisture, pH, oxygen) in landfill soils over time. For a more complete treatment of these topics, see Skog (2008) [179].

We then calculate the quantity of carbon remaining sequestered in OSB in-use or in landfills at any time *t* = 1 to 10,000 years (shown in **Figure A1c**) where:

<u>The proportion of OSB carbon in use-life at any time *t*:</u>

If $OSB_{UL}(0) = 1$ then $OSB_{UL}(t)$ is calculated as:

Eq. 16

$$OSB_{UL}(t) = OSB_{UL}(0) e^{ut}$$

Where *u* is the use-life decay and *t* is time.

<u>The pulse of OSB carbon exiting use-life at any time *t*:</u>

Eq. 17

$$OSB_W(t) = OSB_{UL}(t-1) - OSB_{UL}(t)$$

<u>And entering landfills:</u>

Eq. 18

$$OSB_{New}(t) = 0.70 OSB_{W}(t)$$

The carbon remaining sequestered in the landfills at any time *t:*

Eq. 19

$$OSB_{LF}(t) = \sum_{i=1}^{t} f_{labile} OSB_{New}(i)\, e^{r(t-i)} + f_{recalc} OSB_{New}(i)$$

where *r* is the exponential decay rate of the OSB in landfills, and $f_{labile}$ and $f_{recalc}$ represent the labile and recalcitrant fractions of carbon, respectively.

Total carbon remaining sequestered at any time *t:*

Total carbon remaining sequestered is the sum of the fraction of carbon remaining in its useful life and the fraction remaining sequestered in the landfill.

Eq. 20

$$OSB_{seq}(t) = OSB_{UL}(t) + OSB_{LF}(t)$$

The fraction of carbon remaining in polyethylene and landfills at time t is shown in **Figure A1c**. The estimated carbon loss to the atmosphere in each case is shown in **Table A4**.

**Table A4** Percentage of OSB and landfill carbon loss to atmosphere over time. Values in bold-face reflect moderate assumptions used in the main text.

| Time since sequestration (years) | Carbon loss from OSB and landfills (%) - Optimistic | Carbon loss from OSB and landfills (%) - Moderate | Carbon loss from OSB and landfills (%) - Pessimistic |
|---|---|---|---|
| 100 | 0.135 | **0.249** | 0.441 |
| 1,000 | 0.304 | **0.456** | 0.532 |
| 10,000 | 0.305 | **0.456** | 0.532 |

### A1.3.1 Landfills

The assumptions for the fate of carbon in landfills are same as in the PE case. See **Appendix A1.2.1** for more details.

The fraction of total OSB carbon released as $CO_2$ emissions from OSB and landfills at any time *t*:

Fraction of OSB carbon released from energy combustion at time *t:*

Eq. 21

$$C_{energy}(t) = \sum_{i=1}^{t} 0.30 OSB_W(i)$$

Fraction of OSB carbon released from landfill at time *t:*

Eq. 22

$$C_{LF}(t) = (1 - OSB_{seq}) - C_{energy}(t)$$

At a landfill that flares 75% of methane into $CO_2$ the fraction of total C emissions that become $CO_2$ at time *t*:

Eq. 23

$$C_{CO2,flare}(t) = C_{energy}(t) + 0.875 C_{LF}(t)$$

At a landfill that does not flare methane into $CO_2$ the fraction of total C emissions that become $CO_2$ at time *t*:

Eq. 24

$$C_{CO2,no-flare}(t) = C_{energy}(t) + 0.50 C_{LF}(t)$$

The fraction of total OSB carbon released as $CH_4$ emissions from landfills at any time *t*:

At a landfill that flares 75% of methane into $CO_2$ the fraction of total C emissions that become $CH_4$ at time *t*:

Eq. 25

$$C_{CH4,flare}(t) = 0.125 C_{LF}(t)$$

At a landfill that does not flare methane into $CO_2$ the fraction of total C emissions that become $CO_2$ at time *t*:

Eq. 26

$$C_{CH4,no-flare}(t) = 0.50 C_{LF}(t)$$

**A1.4 Biochar**

Our analysis assumes that biochar is produced as an agricultural soil amendment. Physical characteristics of the biochar (e.g. the O:C and H:C ratios) as well as environmental factors such as precipitation and soil conditions influence biochar stability; as such, there is a large degree of uncertainty in the durability of sequestration [218]–[220]. However, we have constrained our analysis to biochar manufactured for carbon storage purposes, and thus we set bounds on the

quality of the biochar and the application conditions. These imposed constraints limit the fraction of labile carbon in the biochar. We calculate carbon sequestered in biochar in soils over 10,000 years using a two-pool model, representing the differing degradation rates of the labile and recalcitrant carbon fractions in the biochar. The carbon remaining in soils over time *t* is calculated with a double first-order exponential decay function of the form:

Eq. 27

$$C_{soil}(t) = C_{labile}e^{-r_{labile}t} + C_{recalc}e^{-r_{recalc}t}$$

Where $C_{soil}$ is the fraction of the original carbon pulse sequestered in biochar in soils, $C_{labile}$ is the labile fraction, $C_{recalc}$ is the recalcitrant fraction and $r_{labile}$ and $r_{recalc}$ are the decay constants of the fast and slow decaying biochar pools. The moderate case labile and recalcitrant fractions are assumed to be 3% and 97%, respectively, as treated in Wang, Xiong, and Kuzyiakov (2016) [172]. For the optimistic case, we place a lower limit of 0.5% on the labile fraction. For the pessimistic case, the labile fraction is two standard deviations larger than the moderate case (~12%) based on the standard error reported in the source publication. The values for $r_{labile}$ and $r_{recalc}$ are taken from Santos, Torn, and Bird (2012), with the optimistic case estimates derived from andesite soils (table 3 in the referenced publication) minus two standard deviations [217]. The pessimistic case values are derived from the granite soil estimates plus two standard deviations. Decay rates for the fast (labile) and slow pools for each scenario are shown in **Table A5**. The moderate case values are the average of the unadjusted andesite and granite soil values. The estimated carbon remaining sequestered in biochar over 10,000 years is shown in **Figure A1d**. The estimated cumulative fraction of biochar carbon returning to the atmosphere is shown in **Table A6**.

**Table A5** Labile and recalcitrant pool decay rates for three scenarios

| | **Optimistic** | **Moderate** | **Pessimistic** |
|---|---|---|---|
| $\mathbf{r_{labile}}$ | 1.97 | 18.51 | 35.04 |
| $\mathbf{r_{recalc}}$ | 4.45e-4 | 3.40e-3 | 6.35e-3 |

**Table A6** Percentage of biochar soil carbon leakage over time. Values in bold-face reflect moderate case assumptions used in the main text.

| **Time since sequestration (years)** | **Optimistic** | **Moderate** | **Pessimistic** |
|---|---|---|---|
| 100 | 0.048 | **0.31** | 0.56 |
| 1,000 | 0.36 | **0.97** | ~1.0 |
| 10,000 | 0.99 | **~1.0** | 1.0 |

## A2. Four biomass conversion pathways and life cycle emissions

This analysis is intended to highlight opportunities for carbon drawdown within a broad bioeconomy. The four selected pathways are not exhaustive, nor should the analysis be interpreted as prescriptive. There are numerous economic, social, and ecological considerations that are not captured in a calculation of life cycle greenhouse gas emissions. We selected four pathways to represent a variety of conversion technologies and potential feedstocks. The selected pathways were deemed technically viable in the near-term, meaning that literature review and the authors' judgement selected for pathways that are presently commercial, in the demonstration phase, or have a combination of process components that have demonstrated technical viability.

Some components of the life cycle analysis (e.g. electric grid emissions) are regionally specific to California. This is due in part to existing policy support, commitment to decarbonization, and the state's willingness to be a test bed for innovative climate policy, such as the low-carbon fuel standard (LCFS). California also boasts significant biomass resources from its forestry, agricultural, and waste management sectors. Where possible, we rely on life cycle emissions estimates from Argonne National Laboratory's Greenhouse Gases, Regulated Emissions, and Energy Use in Transportation (GREET) model.[229] A variant of this model is used by participants in California's LCFS program to assess the carbon intensity of fuel pathways.

### A2.1 Notes on methodology

#### A2.1.1 Carbon accounting

GREET takes a net-zero approach to biogenic carbon, i.e. when $CO_2$ is emitted from a biogenic source in a combustion process GREET accounts an equal offsetting biogenic credit. This is commensurate with the IPCC GHG national accounting methodology which takes a stock-change approach whereby emissions from biomass are assumed to occur at the point of harvest.[235] Hence, biogenic emissions from combustion or decay in later stages in the life cycle are assumed to be zero. This avoids double-counting in some policy contexts. However, this method ignores the climate impacts of biogenic carbon emissions from feedstocks with long regrowth cycles ("carbon debt"[352]), and it offers no way to credit the stocks of sequestered carbon in durable goods, landfills, and soil amendments.[236] Thus, we present results in two different ways. Our tabular results are presented the way GREET calculates emissions while our figures take a "flow-based" approach whereby carbon uptake is tracked from photosynthesis to final emission or storage. We maintain the tabular data consistent with GREET's methodology for cross-comparability.

For simplicity, we apply 100-year global warming potentials (GWP) to all GHG emissions, regardless of when they occur in time. This decision amplifies the relative climate impact of emissions that occur late in a project's lifetime (e.g. landfill emissions) when considering the 100-year time horizon, causing the estimates of net carbon removal presented here to be conservative within the GWP framework.[222] Dynamic life cycle assessment methods[222], [236] can be used to account for these temporal discrepancies, but for the illustrative purposes here, we focus on the physical carbon drawdown rather than assessing the benefits of delayed impacts over a fixed time horizon. The temporal impact considerations are out-of-scope and

would only serve to enhance the apparent climate benefits of pathways that delay release of stored carbon ($CO_2$ emissions occurring near year 100 would approach zero impact). This is a distraction from the nominal carbon removal estimate we are after.

### A2.2 Feedstock selection

#### A2.2.1 Switchgrass

Switchgrass is a fast-growing perennial crop that can generate high yields in diverse environments, including marginal lands unsuitable for conventional agriculture.[223] This is especially beneficial since limited land resources and competition for food production are key challenges for scaling up biomass production for carbon drawdown.

#### A2.2.2 Corn stover

Corn stover is a waste agricultural feedstock. Agricultural wastes have the advantage of not requiring additional land for cultivation. Most of the resources have already been expended to produce the primary agricultural good. The wastes would otherwise degrade in situ, releasing a significant portion of their carbon back into the atmosphere.

#### A2.2.3 Forest residues

Residues consist of the unmerchantable wood left over from logging activities in managed forests. Transport of residues presents logistical challenges.[224] When it is not cost-effective to transport or utilize residues, they may be burned onsite or left to decompose.

### A2.3 Switchgrass to electricity with CCS

We analyze the “cradle-to-grave” life cycle of an integrated gasification combined cycle (IGCC) power plant using the energy crop switchgrass as fuel. Carbon capture is accomplished with pre-combustion (solvent) removal of $CO_2$ from the shifted syngas.

**Table A7** IGCC data sources

| **Process** | **LCI Source** |
|---|---|
| IGCC process emissions | GREET.net 2018[229] |
| Feedstock supply and transport | GREET.net 2018 |
| Captured $CO_2$ emissions | (Calculated) Excel model based on GREET carbon balance |
| CCS technical requirements | Kanniche et al. (2010)[227] |
| CCS energy emissions | Reduction in plant efficiency. No additional. |

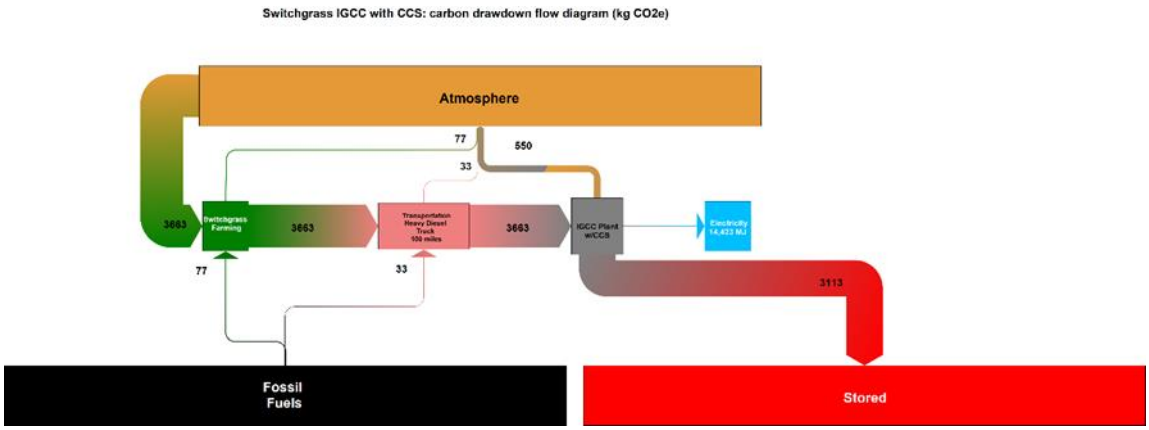


**Figure A2** Carbon flow through switchgrass IGCC system as $CO_2e$ per tonne of feedstock

*Switchgrass Farming* – We assume switchgrass production takes place in California. There are suitable conditions for growing switchgrass throughout the state.[225] Electricity emissions are modeled using GREET's California distributed mix. Switchgrass travels 100 km by heavy diesel truck to the IGCC plant, under the assumption that the feedstock, IGCC power plant, and geological sequestration sites for $CO_2$ can be located proximately in California. We assume switchgrass feedstock is 46.6% elemental carbon by mass. This is equivalent to approximately 1,707 kg of potential atmospheric $CO_2$ per tonne of feedstock. Approximately 2.15 tonnes of feedstock are equivalent to the functional unit of 1 tonne C.

*IGCC Plant and Electricity Generation* – We assume the IGCC electric plant is also located in California, proximate (within 140 km) to depleted oil and gas reservoirs dispersed across the state where captured $CO_2$ might be sequestered. The feedstock functional unit of 1 tonne C (2.15 tonnes switchgrass) will yield 14,423 MJ of electricity under an assumption of 40% conversion efficiency, as modeled in GREET without carbon capture. Since this is the primary and only product from this process, we do not apply credits for displacement of grid electricity.

*Pre-combustion Carbon Capture and Compression* – We model pre-combustion capture of $CO_2$ after physical scrubbing with a methanol-based system as described in an analysis of a coal slurry IGCC system.[227] CSS system operation causes a 22% relative drop in plant efficiency in order to achieve an 85% capture rate. Earlier analyses of suboptimal bio-based IGCC reported capture efficiencies of around 50% at plant thermal efficiencies as low as 28%. [410] However, we assume the coal case to be closer to approximating what is possible in a modern optimized biomass IGCC facility with greater heat integration. The relative drop in plant efficiency reduces the overall thermal conversion efficiency of the plant from 40% to 31.2%. As a result, after scrubbing, capturing, and compressing process emissions, the output of the plant is reduced from 14,423MJ/tC to 11,250 MJ/tC in switchgrass.

*Land-use change* – GREET does not explicitly model land use change impacts for switchgrass or other dedicated energy crops used for electricity production. No credit or penalty is assigned in our analysis for this pathway.

### A2.3.1 Switchgrass to electricity results

**Table A8** shows the cradle-to-grave life cycle $CO_2$ emissions for switchgrass-IGCC without the benefit of CCS. The raw process emissions from electricity production are 3,772 kg $CO_2$/tC. However, 3,664 kg of that total are biogenic in nature and do not represent a positive emission to the atmosphere. Prior to CCS, the process yields net positive emission of 108 kg $CO_2$/tC, primarily resulting from feedstock production and transportation.

**Table A8** Life cycle CO2 emissions for switchgrass to electricity (kg/tC)

| **Life cycle emissions per 1 tonne C in feedstock** | | |
|---|---|---|
| **Products** | | |
| Electricity to grid (w/o CCS) | 14422.96 | MJ |
| **CO2 Emissions** | | |
| Process Emissions (Switchgrass Farming) | 24.96 | kg |
| Process Emissions (IGCC) | 3661.87 | kg |
| Upstream Emissions (Switchgrass Farming) | 51.78 | kg |
| Transport Emissions (Farm to Plant) | 33.38 | kg |
| **Total Emissions** | **3771.99** | **kg** |
| Biogenic Credit (IGCC) | -3663.51 | kg |
| Biogenic Credit (Switchgrass Farming) | -0.05 | kg |
| **Lifecycle CO2 (w/o CCS)** | **108.43** | **kg** |

We estimate 3,112 kg$CO_2$/tC (see **Table A9**) is captured from syngas clean-up by the CCS system. Electricity required to compress and pump the captured $CO_2$ to nearby geological sequestration sites is generated on-site. These emissions are already accounted for in the production process. As mentioned previously, the parasitic load for CCS results in a 3,173 MJ reduction in electricity generation. The final life cycle $CO_2$ emissions total -3,004 kg $CO_2$/tC once adjustments are made to reflect the CCS credit.

**Table A9** Life cycle $CO_2$ adjustment for switchgrass IGCC pre-combustion CCS (per t C)

| **Life cycle emissions per 1 tonne C in feedstock** | | |
|---|---|---|
| | | |
| Captured CO2 Credit | -3112.59 | kg |
| **Power Plant Efficiency Losses** | | |
| Carbon Capture Process Energy | 3173.05 | MJ |
| **Final Electricity to Grid** | **11249.91** | MJ |
| **Life Cycle CO2 (w/ capture)** | **-3004.17** | **kg** |

The final greenhouse gas potential is reflected in **Table A10**. Methane and nitrous oxide emissions are multiplied by their 100-year emissions factor to calculate the carbon dioxide equivalent ($CO_2$e) impact on climate. Nitrous oxide makes up the largest portion of this non-$CO_2$

impact, somewhat evenly distributed between the switchgrass cultivation process and the combustion at the IGCC plant. The additional 193 kg$CO_2$e/tC from these emissions bring the total GHG impact of the bioelectricity process to -2,811 kg$CO_2$e/tC.

3,124 kWh (11,249 MJ)

**Table A10** Non-GHG Emissions for Electricity Production from Switchgrass (kg/tC)

| Non-CO2 GHG Emissions (GHG 100 CO2e) | | |
|---|---|---|
| | | |
| CH4 (Process) x 28 CO2e | 10.10 | kg |
| N20 (Process) x 265 CO2e | 182.96 | kg |
| Total Non GHG CO2e | **193.06** | **kg** |
| **Life Cycle CO2e (w/ capture)** | **-2811.10** | **kg** |

### A2.3.2 IGCC drawdown over 100; 1,000; and 10,000 years

Here we combine cradle-to-gate emissions for IGCC electricity production with the sequestration models described in A1.1 to estimate the long-term sequestration benefit of the conversion pathway. At $t = 0$, 849 kgC (3,113 kg$CO_2$e) is sequestered in geological storage. Per the decay function described in Eq. 1 and the durability percentages described in **Table A2**, the cumulative $CO_2$e leaked at each time $t$ is shown in **Table A11**.

**Table A11** IGCC $CO_2$ leaked from geological sequestration over time (representative case in bold)

| **Case** | **100 years (kg $CO_2$e/t)** | **1,000 years (kg $CO_2$e/t)** | **10,000 years (kg $CO_2$e/t)** |
|---|---|---|---|
| Onshore - optimistic | 0.56 | 5.67 | 56.33 |
| **Onshore - moderate** | **2.63** | **26.42** | **254.56** |
| Onshore - pessimistic | 9.14 | 91.05 | 800.10 |
| Offshore - optimistic | 0.15 | 1.51 | 15.03 |
| Offshore - moderate | 0.59 | 5.93 | 58.82 |
| Offshore - pessimistic | 2.00 | 20.13 | 195.74 |

The moderate onshore case is selected as the representative case in our analysis. The 10,000-year drawdown profile of the pathway is shown in **Figure A3**. At 100; 1,000; and 10,000 years, 99.9%, 99% and 91% of the original drawdown benefit remain, respectively.

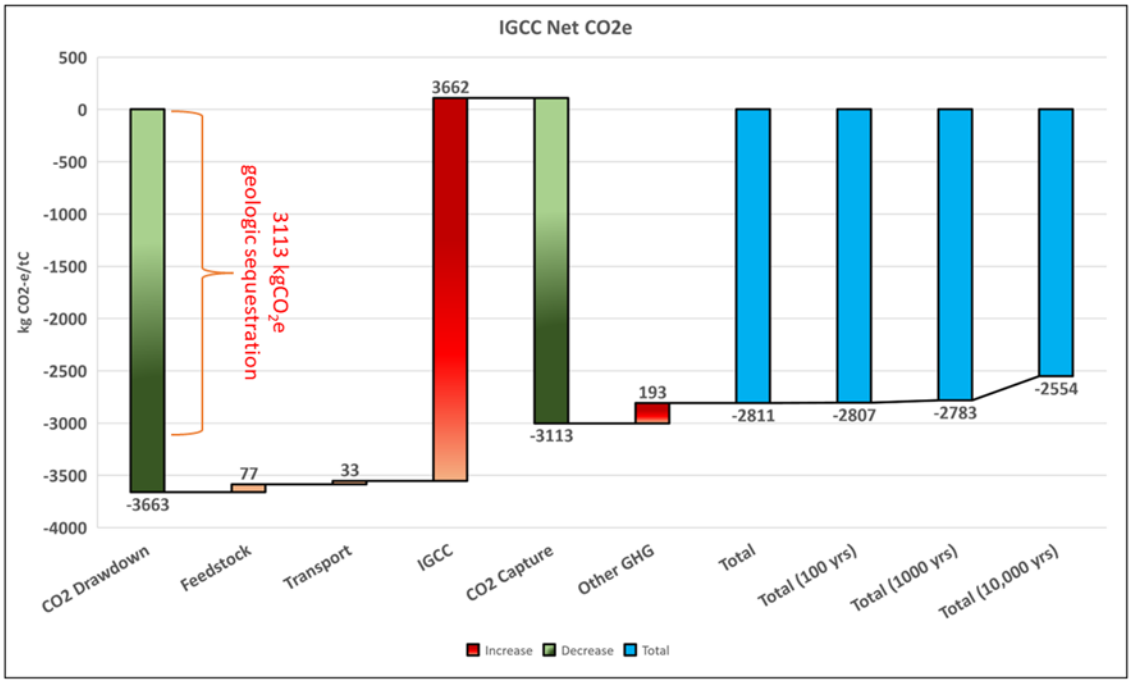


**Figure A3** IGCC-CCS electricity production from switchgrass - drawdown over 10,000 years (moderate case). Note that in the waterfall diagrams, green and red bars represent magnitudes of drawdown and emissions subsequent to the initial drawdown in biomass. The blue bars represent totals. The sum of all red and green bars is equal to the first blue bar.

### A2.4 Corn stover to polyethylene with CCS

We analyze the "cradle-to-grave" life cycle of a bio-polyethylene (PE) production supply chain based on lignocellulosic ethanol production from corn stover. Conversion of ethanol ($C_2H_5OH$) to bioethylene ($C_2H_4$) to polyethylene $(C_2H_4)_n$ is assumed to take place in the same refinery. The modeled facility integrates CCS to capture fermentation stage $CO_2$ during ethanol production.

**Table A12** Polyethylene data sources

| **Process** | **LCI Source** |
|---|---|
| Feedstock handling and transport | GREET.net 2018[229] |
| Ethanol, bioethylene, and polyethylene process emissions | GREET.net 2018 |
| Captured $CO_2$ emissions | (Calculated) Excel model based on GREET carbon balance |
| CCS technical requirements | NETL[265] |
| CCS energy emissions | GREET – California distributed grid mix |

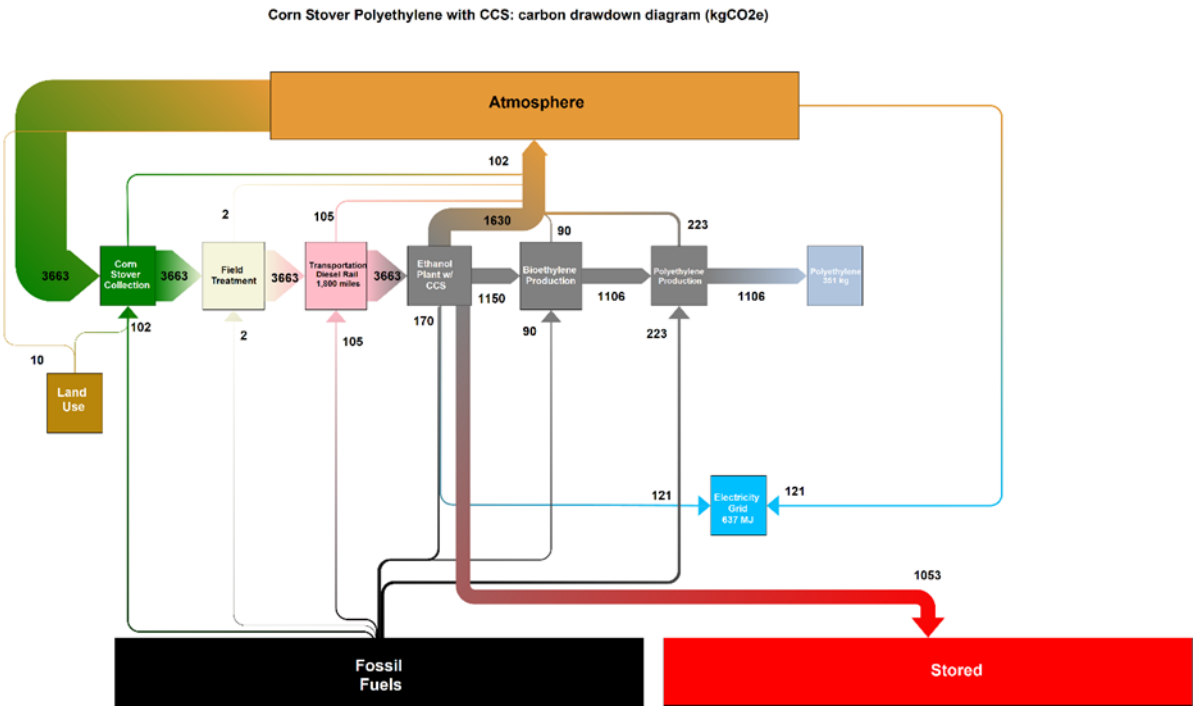


**Figure A4** Carbon flow through corn stover to polyethylene system with CCS as $CO_2e$ per tonne of feedstock. Embodied fossil emissions as well as upstream fossil emissions associated with production inputs are included in the flow diagram at the point where those inputs enter the production process. Thus, fossil emissions exiting a box in the diagram include both onsite emissions and emissions associated with upstream production of inputs. This diagram only shows the life cycle up to the point of resin production. Fabrication into finished products and the impact on the overall carbon intenisty of the process are discussed and calculated below.

*Corn stover collection and field treatment* – Collection and treatment of corn stover is assumed to take place in Iowa, utilizing the GREET average U.S. Central and Southern Plains electric grid mix and associated transmission and distribution losses. Stover feedstock is assumed to travel 1,800 miles by diesel rail from farm to the refinery in California. Corn stover is assumed to be 46.6% elemental carbon by mass. This is equivalent to approximately 3,663 kg of potential atmospheric $CO_2$ per tonne C in feedstock. Approximately 2.15 tonnes of feedstock are equivalent to the functional unit of 1 tonne C.

*Ethanol production from corn stover* – The modeled refinery is assumed to be co-located with bioethylene and PE upgrading facilities. We assume the facility is located near Fresno County, which is the approximate location of existing ethanol refineries. This location is also proximate to nearby oil and gas fields, which we are assuming would be amenable to geological sequestration. We are unaware of existing refineries in this region that convert lignocellulosic biomass to polyethylene, but this seems a suitable a location was such a facility to exist. Using GREET model yields, 1 ton of stover feedstock is equivalent to 280 kg (93 gal) of ethanol (EtOH) intermediate.

*Co-production of process and grid electricity from biomass* – Other than a small amount of energy from diesel—about 180 btu/gal EtOH—all process energy for the conversion of stover to ethanol is assumed to come from combustion of a fraction of the stover feedstock to supply boiler heat and power generation. Approximately 400 kg/t of stover (858 kg/tC) is combusted on-site to deliver process heat and to generate power. The ethanol refinery is assumed to generate 814 MJ (1,746 MJ/tC) of electricity in excess of facility requirements. However, the excess is reduced to 637 MJ (1,366 MJ/tC) to account for the demands of capture and compression of $CO_2$, discussed in the subsequent sections. This remaining excess generation is exported to the grid and credits the life cycle carbon intensity of the plant by displacing an equivalent amount electricity from the average California grid.

*Carbon dioxide emissions from fermentation* - Carbon dioxide emissions are assumed to be internally consistent with the carbon content assumptions of resources and products employed by the GREET model. We assume that 46.6% of the mass of corn stover feedstock is carbon and 52.2% of the mass of the ethanol product is carbon. Approximately 40% of the stover is combusted for energy onsite. By mass-balance in Eq. 28, we obtain a fermentation emissions rate of 491 $kgCO_2e$/t of stover (or 1,053 $kgCO_2e$/tC).

Eq. 28

$$(\mathbf{0.466 \times 1000}\boldsymbol{kg\ Stover}) - (\mathbf{0.522} \times \mathbf{280}\boldsymbol{kg\ EtOH}) - (\mathbf{0.466} \times \mathbf{400}\boldsymbol{kg\ Stover}) \approx \mathbf{134}\boldsymbol{kg\ Carbon}$$

$$\mathbf{134}\boldsymbol{kg\ C} \times \frac{\mathbf{44}\boldsymbol{kgCO_2}}{\mathbf{12}\boldsymbol{kgC}} \approx \mathbf{491}\boldsymbol{kgCO_2}$$

*Capture and compression of fermentation carbon dioxide* - We employ a simple model of fermentation $CO_2$ capture. Fermentation $CO_2$ streams are relatively pure, and we assume a 90% concentration coming from the fermentation vent.[265] Clean-up and capture of the $CO_2$ requires only dehydration and compression to a supercritical pipeline pressure. We assume a 100% capture rate and calculate the energy demand and associated emissions of a five stage $CO_2$ compressor with a suction pressure of 17.4 psia at 81° F. [265] Assuming a pressure drop of 35 kPa/km (5.07 psia/km) and a minimum outlet pressure of 10.3 MPa (1494 psia) [411] and excluding elevation, this pressure is sufficient to pump compressed $CO_2$ roughly 140 km**.** The energetic cost of this process is estimated to be 100.09 kWh/t $CO_2$ captured.[265] Electricity for capture and compression is modeled as a reduction in excess co-product electricity. The energy requirement to capture fermentation $CO_2$ is approximately 49 kWh/t of stover processed as shown in Eq. 29.

Eq. 29

$$(\mathbf{0.10009}\boldsymbol{kWh})/\boldsymbol{kgCO_2} \times \mathbf{490}\boldsymbol{kgCO_2/t\ Stover} \approx \mathbf{49.1}\ \boldsymbol{kWh/t\ stover}$$

*Land use change*— GREET's assumptions for land use change (LUC) account for both direct (domestic) and indirect (international) land use change using the CCLUB model. Land use change scenarios from biofuels production are modeled using Purdue University's Global Trade Analysis Project (GTAP) model, which is a computable general equilibrium model. GTAP determines potential land use changes domestically and internationally contingent on a set of biomass-to-ethanol production scenarios. This analysis utilizes the Stover Ethanol scenario and associated LUC elasticities. This scenario assumes a growth in corn ethanol production from

3.41 billion gallons (BG) to 15 BG and an additional 9 BG of ethanol from stover between 2004 and 2034, which is the end of the recommended 30-year production horizon in the CCLUB model. This expansion of ethanol is also consistent with U.S. Department of Energy [71] Billion-Ton Report assumptions. Domestic emissions are modeled using the CENTURY model while international emissions are modeled using the Winrock model. The LUC emissions amortization period is set equivalent with the production period at 30 years. The model considers 100 cm soil depth for soil organic carbon (SOC) calculations, and it is assumed that, internationally, biomass is burned to clear land. Within the CENTURY model, tilling practices are set as the U.S. average, and the yield scenario assumes a 1% increasing annual yield. Where the model predicts forest conversion to cropland, the model settings adopt a Harvested Wood Products (HWP) assumption from Heath *et al.* [412]. This setting assumes that 60% of converted forest live and dead wood will be harvested. 21% of the harvested portion will end up in durable wood products. 21% will be burned for energy. 18% will be released as $CO_2$ to the atmosphere. The remaining 40% of waste wood will also be released to the atmosphere. Notably, the stover scenario results in net carbon sequestration even though there is equivalent corn ethanol production as in the corn ethanol scenario. This is because the "GTAP [model] predicts a small amount of gains in forest lands that result in carbon sequestration, offsetting carbon emissions from limited conversion of cropland pasture to corn agriculture." [413]

*Ethanol conversion to bioethylene and polyethylene*— Bioethylene and polyethylene production are assumed to be co-located with the ethanol refinery. However, natural gas and power are provided by conventional utilities rather than direct integration with the ethanol facility. The ethylene process consumes natural gas at a rate of 2,457 btu/kg of bioethylene. Electricity consumption is 1,189 btu/kg of bioethylene. Electricity use is modeled as distributed from the average California grid mix. Similarly, bioethylene conversion to polyethylene requires natural gas, electricity, residual oil, and liquified petroleum gas combustion onsite. The energy consumption rates are 7.230 btu/kg, 2,005 btu/kg, 55.11 btu/kg, and 0.90 btu/kg of polyethylene produced, respectively. The yield ratios from ethanol to ethylene to PE are approximately 1.71 **:** 1.01 **:** 1 on a mass basis. There is unreacted and recycled material in the ethanol to bioethylene conversion process. This results in roughly 9.3 kg of carbon (34 kg$CO_2$e) exiting the mass balance of the process. Some of this material would be recycled, but for simplicity, we chose to track this material but not update the feedstock requirements.

*Upgrading polyethylene to products*

This cradle-to-gate assessment is intended to represent a general polyethylene resin production process. There are many varieties and end-uses of polyethylene (e.g. LDPE, HDPE, LLDPE). After production of the PE resin, further life cycle steps will be undertaken to transform PE resin to end-products. Potential processes include the production of films, injection molding, compression molding, and extrusion. All these processes will incur additional process emissions. In the tabular data below, we exclude the final product phase. But for the representative case, we include additional emissions from injection molding. HDPE bottles we selected as the representative case for PE. Bottles are produced by blow molding, which is a form of injection molding whereby PE is heated and injected into a mold and then compressed air expansion is used to form a hollow receptacle. Emissions factors from GREET for compressions molding,

injection molding, and extrusion are shown in **Table A13**. We note that GREET's emissions estimates for injection molding are lower than other published LCAs.[414]

**Table A13** Conversion of polyethylene resin to products process emissions

| | **Compression Mold (kg $CO_2$e/t feed)** | | | **Extrusion (kg $CO_2$e/t feed)** | | | **Injection Mold (kg $CO_2$e/t feed)** | | |
|---|---|---|---|---|---|---|---|---|---|
| | **$CO_2$** | **$CH_4$** | **$N_2O$** | **$CO_2$** | **$CH_4$** | **$N_2O$** | **$CO_2$** | **$CH_4$** | **$N_2O$** |
| **LDPE** | 158 | 7.56 | 0.64 | 29 | 2.26 | 0.17 | 150 | 8.2 | 0.6 |
| **HDPE** | 99 | 7.56 | 0.64 | 29 | 2.26 | 0.17 | 150 | 8.2 | 0.6 |

### A2.4.1 Corn Stover to Polyethylene Results

The stover to PE process with CCS yields a net drawdown of -1,595 kg $CO_2$e/tC. As illustrated in **Figure A4**, photosynthetic drawdown for the feedstock stage is around 3,663 kg$CO_2$/tC. The polyethylene product stores 1,106 kg $CO_2$e of the biogenic carbon. Excess process electricity is provided to the grid, displacing alternative electricity generation. Capture of fermentation $CO_2$ further improves the performance of this process, bringing it well into the net negative emissions (drawdown) range.

Cradle-to-gate life cycle $CO_2$ emissions for stover polyethylene resin without the benefit of CCS are shown in **Table A14**. The product yield for polyethylene is 351 kg/tC. The process generates an excess 1,747 MJ/tC of electricity, but the parasitic load of the CCS system reduces excess generation to 1,367 MJ/tC. The process emissions from ethanol production are significant but since they originate from stover combustion, they do not contribute significantly to the carbon intensity of the process. The process is credited -121 kg$CO_2$e/tC for displacement of grid electricity, and land use further credits the process -10 kg$CO_2$e/tC, implying an increase in terrestrial carbon stocks (see Land Use section above for full explanation). Before accounting CCS removals, the process stands at a net negative emission of approximately -542 kg$CO_2$e/tC.

**Table A14** Life cycle $CO_2$ emissions for 1 ton of corn stover converted to polyethylene

| **Life cycle emissions per 1 tonne C in feedstock** | | |
|---|---|---|
| **Products** | | |
| Polyethylene | 350.80 | kg |
| Electricity to grid (Ethanol Stage) | 1366.95 | MJ |
| **CO2 Emissions** | | |
| Process Emissions (Stover Collection at Farm) | 47.87 | kg |
| Upstream Emissions (Stover Collection at Farm) | 53.88 | kg |
| Process Emissions (TDCHS) | 0.00 | kg |
| Upstream Emissions (TDCHS) | 1.66 | kg |
| Transport (stover) | 105.15 | kg |
| Process Emissions (Ethanol) | 1472.64 | kg |
| Upstream Emissions (Ethanol) | 169.60 | kg |
| Process Emissions (Bioethylene) | 51.60 | kg |

| | | |
|---|---|---|
| Upstream Emissions (Bioethylene) | 38.39 | kg |
| Process Emissions (Polyethylene) | 153.17 | kg |
| Upstream Emissions (Polyethylene) | 69.62 | kg |
| Total Emissions | **2163.58** | **kg** |
| Displaced Electricity credit | -120.71 | kg |
| Total w/ Co-product credits | **2042.87** | kg |
| Biogenic Credit (Stover Collection) | -0.07 | kg |
| Biogenic Credit (Ethanol) | -1468.61 | kg |
| LUC | -10.10 | kg |
| (Direct) | -2.83 | kg |
| (Indirect) | -7.26 | kg |
| CO2 Stored in Polyethylene Credit | -1106.16 | kg |
| "Cradle to Gate" CO2 | **-542.07** | **kg** |

Carbon captured from the fermentation stage of ethanol production is estimated to be 1,053 $kgCO_2/tC$, as shown in **Table A15**. Electricity required to compress and pump the captured $CO_2$ to nearby geological sequestration sites is generated on-site. These emissions are already accounted for in the production process emissions. The impact of the CCS system is a reduction of excess electricity provided to the grid. The parasitic load for CCS results in a 380 MJ reduction in electricity export. The final life cycle $CO_2$ emissions totals -1,595 $kgCO_2/tC$ .

**Table A15** Life cycle CO2 adjustment for stover to polyethylene fermentation CCS

| **Life cycle emissions per 1 tonne C in feedstock** | | |
|---|---|---|
| | | |
| Captured CO2 Credit | **-1053.34** | kg |
| Life Cycle CO2 (w/ capture) | **-1595.41** | **kg** |

The final $CO_2e$ intensity is reflected in **Table A16**. Methane and nitrous oxide emissions are multiplied by their 100-year emissions factor to calculate the carbon dioxide equivalent (CO2e) impact on climate. Methane makes up the largest portion of this non-$CO_2$ impact, and those emissions primarily originate upstream from the stover collection process in the production of nitrogen fertilizer. The additional 58 $kgCO_2e/tC$ from these emissions bring the total cradle-to-gate emissions to -1,538 $kgCO_2e/tC$ before upgrading of PE to final product. Note, these are the cumulative emissions for the PE resin only. We incorporate extrusion molding in the next section.

**Table A16** Non-GHG Emissions for polyethylene production from corn stover

| **Non-CO2 GHG Emissions and Total Life-cycle CO2e** |
|---|
| |

| | | |
|---|---|---|
| CH4 (Process) x 28 CO2e | 41.47 | kg |
| N20 (Process) x 265 CO2e | 16.40 | kg |
| **Total Non GHG CO2e** | **57.86** | **kg** |
| **Life Cycle CO2e (w/ capture)** | **-1537.55** | **kg** |

### A2.4.2 Polyethylene drawdown over 100; 1,000; and 10,000 years

Here we combine cradle-to-gate emissions for polyethylene production with the sequestration models described in Appendix A1.2 to estimate the long-term sequestration benefit of the conversion pathway. At $t = 0$, 302 kgC (1,106 kg $CO_2e$) is sequestered in the polyethylene product and 287 kgC (1,053 kg$CO_2e$) is sequestered in geological storage.

Per the decay function described in Eq. 1 and the sequestration percentages described in **Table A2**, the cumulative $CO_2e$ emitted at each time $t$ from geological sequestration is shown in **Table A16**.

**Table A17** Polyethylene $CO_2$ emitted from geological sequestration over time (representative case in bold)

| **Case** | **100 years (kg $CO_2e$/t)** | **1,000 years (kg $CO_2e$/t)** | **10,000 years (kg $CO_2e$/t)** |
|---|---|---|---|
| Poly. (geologic onshore) optimistic | 0.19 | 1.94 | 19.26 |
| **Poly. (geologic onshore) moderate** | **0.90** | **9.03** | **87.04** |
| Poly. (geologic onshore) pessimistic | 3.13 | 31.13 | 273.55 |

The carbon remaining in the polyethylene at 100; 1,000; and 10,000 years is estimated according to the functions described by Eq. 3 through Eq. 8, The quantity of polyethylene carbon emitted at $t$ is calculated by Eq. 9 and Eq. 10. The quantity of $CO_2$ and $CH_4$ emissions from energy production and landfill emissions at each time $t$ is calculated by Eq. 11 and Eq. 13 in the case of a landfill that flares fugitive methane emissions.

**Table A18** Flaring case landfill emissions (representative case in bold)

| **Case** | **Emission** | **100 years (kg $CO_2e$/tC)** | **1,000 years (kg $CO_2e$/tC)** | **10,000 years (kg $CO_2e$/tC)** |
|---|---|---|---|---|
| Poly (product C) optimistic | $CO_2$ (energy) | 138.58 | 192.35 | 192.35 |
| | $CO_2$ (landfill) | 45.28 | 64.63 | 71.25 |
| | $CH_4$ (landfill) | 65.86 | 94.01 | 103.64 |
| **Poly (product C) moderate** | **$CO_2$ (energy)** | **192.35** | **192.35** | **192.35** |
| | **$CO_2$ (landfill)** | **80.07** | **148.54** | **148.54** |
| | **$CH_4$ (landfill)** | **116.47** | **216.05** | **216.05** |
| Poly (product C) | $CO_2$ (energy) | 192.35 | 192.35 | 192.35 |

| | | | | |
|---|---|---|---|---|
| pessimistic | $CO_2$ (landfill) | 233.12 | 233.12 | 233.12 |
| | $CH_4$ (landfill) | 339.08 | 339.08 | 339.08 |

In the case of a landfill that does not flare fugitive landfill emissions, $CO_2$ and $CH_4$ are calculated by Eq. 12 and Eq. 14. In this case, $CH_4$ emissions are much greater.

**Table A19** Non-flaring case landfill emissions (representative case in bold)

| **Case** | **Emission** | **100 years (kg $CO_2$e/tC)** | **1,000 years (kg $CO_2$e/tC)** | **10,000 years (kg $CO_2$e/tC)** |
|---|---|---|---|---|
| Poly (product C) optimistic | $CO_2$ (energy) | 138.58 | 192.35 | 192.35 |
| | $CO_2$ (landfill) | 25.87 | 36.93 | 40.72 |
| | $CH_4$ (landfill) | 263.43 | 376.04 | 414.56 |
| **Poly (product C) moderate** | **$CO_2$ (energy)** | **192.35** | **192.35** | **192.35** |
| | **$CO_2$ (landfill)** | **45.76** | **84.88** | **84.88** |
| | **$CH_4$ (landfill)** | **465.89** | **864.22** | **864.22** |
| Poly (product C) pessimistic | $CO_2$ (energy) | 192.35 | 192.35 | 192.35 |
| | $CO_2$ (landfill) | 133.21 | 133.21 | 133.21 |
| | $CH_4$ (landfill) | 1356.32 | 1356.32 | 1356.32 |

The full emissions profile of corn stover to polyethylene bottles (moderate case), assuming that landfills combust or flare methane emissions, is shown in **Figure A5**. This calculation also includes the additional fabrication emissions (341 kg $CO_2$e/tC) for injection molding shown in **Table A13**, bringing the cradle-to-gate emissions to -1,197 kg$CO_2$e/tC. At 100; 1,000; and 10,000 years, 67%, 53% and 46% of the original drawdown benefit remain, respectively.

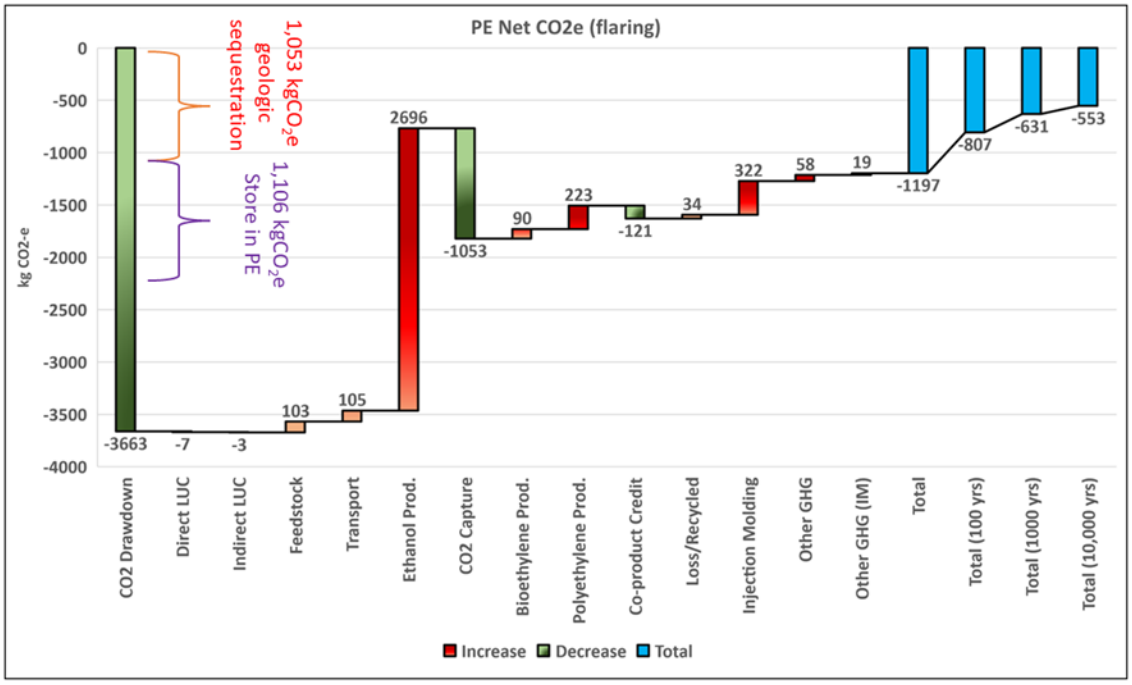


**Figure A5** Polyethylene with CCS drawdown over 10,000 years (moderate case/flared landfills). Note that in the waterfall diagrams, green and red bars represent magnitudes of drawdown and emissions subsequent to the initial drawdown in biomass. The blue bars represent totals. The sum of all red and green bars is equal to the first blue bar.

The full emissions profile of corn stover to polyethylene bottles (moderate case) assuming that landfills do not control methane emissions by flaring is shown in **Figure A6**. This calculation also includes the additional fabrication emissions (341 kg $CO_2$e/tC) for injection molding shown in **Table A13**, bringing the cradle-to-gate emissions to -1,197 kg$CO_2$e/tC. At 100; 1,000; and 10,000 years, 41%, 4% and 0% of the original drawdown benefit remain, respectively. At the 10,000 years, the conversion process yields net emissions.

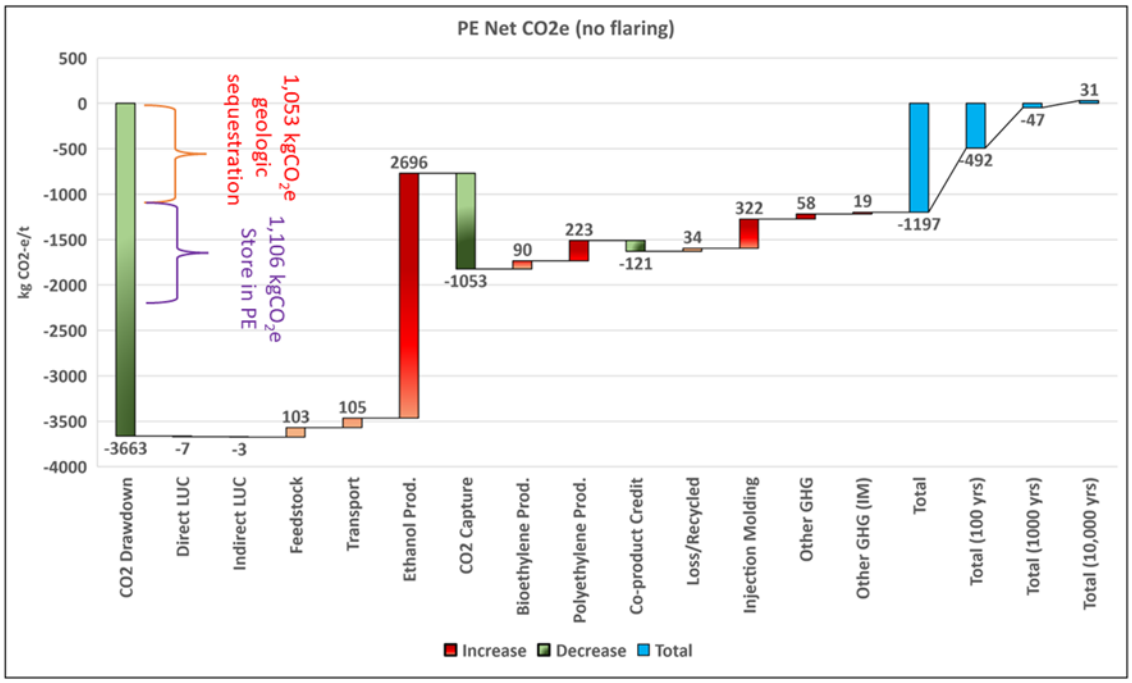


**Figure A6** Polyethylene with CCS drawdown over 10,000 years (moderate case/unflared landfills). Note that in the waterfall diagrams, green and red bars represent magnitudes of drawdown and emissions subsequent to the initial drawdown in biomass. The blue bars represent totals. The sum of all red and green bars is equal to the first blue bar.

### A2.5 Forest residues to biochar

We model the "cradle-to-grave" life cycle emissions of a commercial forest residue to biochar system incorporating an air curtain burner. Carbon sequestration is achieved through physical storage in the biochar product and subsequent agricultural soil amendment. We analyze a simple biochar process using an air curtain burner (ACB). An ACB is typically used for the complete combustion of biomass. However, operations can be modified to achieve "flame cap" pyrolysis, with slow pyrolysis taking place in the base of the firebox alongside complete combustion in the upper layer. The ACB can be set up at remote locations for the management of forest residues.

**Table A20** Biochar data sources

| **Process** | **LCI Source** |
|---|---|
| Feedstock handling and transport | GREET.net 2018[229] |
| Gate-to-gate airburner yields and emissions | Puettmann (2017)[415] |
| Upstream energy and fuels | GREET.net 2018 |

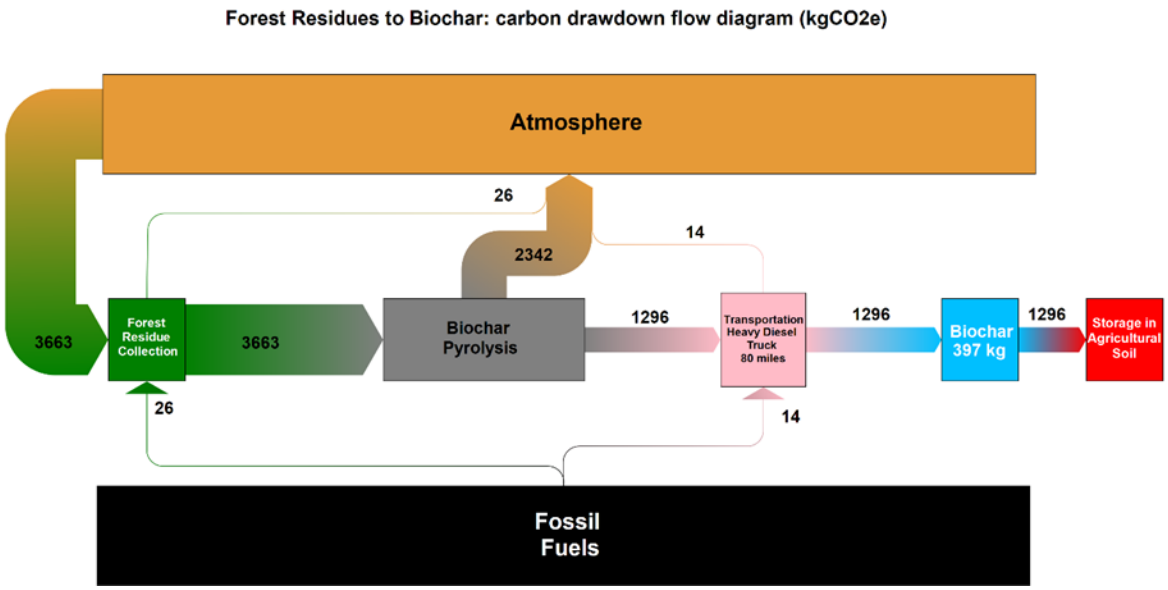


**Figure A7** Carbon flow through forest residues to biochar system as $CO_2e$ per tonne of feedstock. Note that carbon in methane and carbon monoxide emissions are not shown in this figure. These emissions account for the balance of carbon in the feedstock. Embodied fossil emissions as well as upstream fossil emissions associated with production inputs are included in the flow diagram at the point where those inputs enter the production process. Thus, fossil emissions exiting a box in the diagram include both onsite emissions and emissions associated with upstream production of inputs.

*Forest Residue Collection* – forest residue collection is assumed to take place in Northern California. The feedstock is co-located with the biochar process, as the ACB is designed to be mobile. The forest residue is assumed to be 50.3% carbon by mass which is equivalent to 1,844 kg of atmospheric $CO_2$/t of feedstock. Feedstock handling energy and emissions are taken from GREET. We note that the energy requirement assumptions for feedstock handling in GREET are substantially smaller than those reported in Puettmann (2017).[415] GREET assumes about 139 MJ (131,750 Btu) or approximately 4 L of diesel per ton of feedstock handled. While Puettmann assumes 2,300 MJ (2.18 MMBtu) or roughly 88 L of propane/LPG per ton of feedstock. We rely on the GREET estimate for consistency with our other pathways.

*Biochar Production via Pyrolysis* – The ACB is a relatively simple technology comprised of a refractory-lined box with a high-powered blower. The modeled process draws upon conversion efficiencies and GHG emission factors from Puettmann (2017).[415] The modeled process converts 5,000 kg (bone dry basis) of forest residue to 1,000 kg of biochar with carbon content of 89%. We modified the carbon mass-balance for consistency with GREET. The carbon balance in the source literature implies a forest residue carbon content of 39% or an unreported bio-oil or liquid VOC fraction. Assuming that in the latter case, bio-oil would be combusted in an air burner batch process, we adjust biochar conversion $CO_2$ emissions up from 0.78 kg/kg of forest residues to 1.18 kg/kg. This is consistent with a forest residue carbon content of 50.3% as in GREET and the OSB pathway we analyzed. For simplicity, non-$CO_2$ carbon emissions in the carbon balance ($CH_4$ & CO) as adapted from the reference literature are held constant.

*Biochar End-of-Life* – Produced biochar is assumed to be transported roughly 80 miles by truck from forest site to agricultural soils in the California Central Valley region.

### A2.5.1 Forest Residue to Biochar Results

The biochar technology in this analysis has potential as a negative emissions pathway at -963kg $CO_2$e/tC. Cradle-to-gate life cycle $CO_2$ emissions for forest residue to biochar are shown in **Table A21.** The biochar production yield is 397 kg/tC. Photosynthetic drawdown in the feedstock is 3,663 kg$CO_2$/tC of forest residue (see **Figure A7**). The onsite and upstream process $CO_2$ emissions for biochar production total 2,343 kg $CO_2$/tC, all of which are biogenic. Carbon is physically stored (-1,296 kg$CO_2$e/tC) in agricultural soils. When considering only $CO_2$ emissions, the cradle-to-gate emissions are roughly -1,281 kg$CO_2$/tC.

**Table A21** Life cycle $CO_2$ emissions for biochar production

| **Life cycle emissions per 1 tonne C in feedstock** | | |
|---|---|---|
| **Products** | | |
| Biochar | 397 | kg |
| **CO2 Emissions** | | |
| Process Emissions (Forest Residue Collection) | 22.43 | kg |
| Upstream Emissions (Forest Residue Collection) | 4.09 | kg |
| Process Emissions (Biochar Production) | **2342.41** | kg |
| Upstream Emissions (Biochar Production) | 0.00 | kg |
| Transport Biochar to Farm | 14.44 | kg |
| Total Emissions | **2383.37** | **kg** |
| Biogenic Credit (Biochar Production) | -2342.41 | kg |
| Biogenic Credit (To balance non-CO2 emissions) | -25.81 | kg |
| CO2 Stored in Biochar Credit | -1295.73 | kg |
| "Cradle to Gate" CO2 | -**1280.58** | **kg** |

However, the non-$CO_2$ GHG emissions have a significant impact on the final emissions intensity. The combined effect of methane (~145 kg$CO_2$e/tC) and $N_2O$ (~173 kg$CO_2$e/tC) bring the cradle-to-gate emissions to -963 kg$CO_2$e/tC, as shown in **Table A22**.

**Table A22** Non-GHG emissions for biochar production

| **Non-CO2 GHG emissions (GHG 100 CO2e) and total life cycle CO2e** | | |
|---|---|---|
| | | |
| CH4 (Process) x 28 CO2e | 145.42 | kg |
| N20 (Process) x 265 CO2e | 172.56 | kg |
| **Total Non GHG CO2e** | **317.98** | **kg** |

| Life cycle CO2e | -962.59 | kg |
|---|---|---|

**Figure A8**Error! Reference source not found. shows sources and sinks of emissions in the biochar process. Emissions contributions are largely biogenic from the pyrolysis process. About 35% of available biogenic carbon is stored in the biochar. Non-$CO_2$ GHG emissions represent 12% of total emissions when biogenic $CO_2$ is included. Non-$CO_2$ GHG's are almost eight times greater than fossil $CO_2$ emissions.

### A2.5.2 Biochar drawdown over 100; 1,000; and 10,000 years

Here we combine cradle-to-gate emissions for forest residues converted to a biochar soil amendment with the sequestration models described in Appendix A1.4 to estimate the long-term sequestration benefit of the conversion pathway. At $t = 0$, 353 kgC (1,296 kg$CO_2$e/tC) is sequestered in the biochar in soils. Per the decay function described in Eq. 27 and the sequestration losses described in **Table A6**, the cumulative $CO_2$e emitted at each time $t$ is shown in **Table A23**.

**Table A23** Biochar $CO_2$ emitted from soil sequestration over time (representative case in bold)

| **Case** | **100 years (kg $CO_2$e/tC)** | **1,000 years (kg $CO_2$e/tC)** | **10,000 years (kg $CO_2$e/tC)** |
|---|---|---|---|
| Biochar - optimistic | 62.09 | 469.46 | 1280.72 |
| **Biochar - moderate** | **397.95** | **1253.58** | **1295.73** |
| Biochar - pessimistic | 719.34 | 1293.83 | 1295.73 |

The moderate case is selected as the representative case. The 10,000-year drawdown profile of the pathway is shown in **Figure A8**. At 100 years, 59% of the original drawdown benefit remains. At 1,000 and 10,000 years, the process yields net positive emissions.

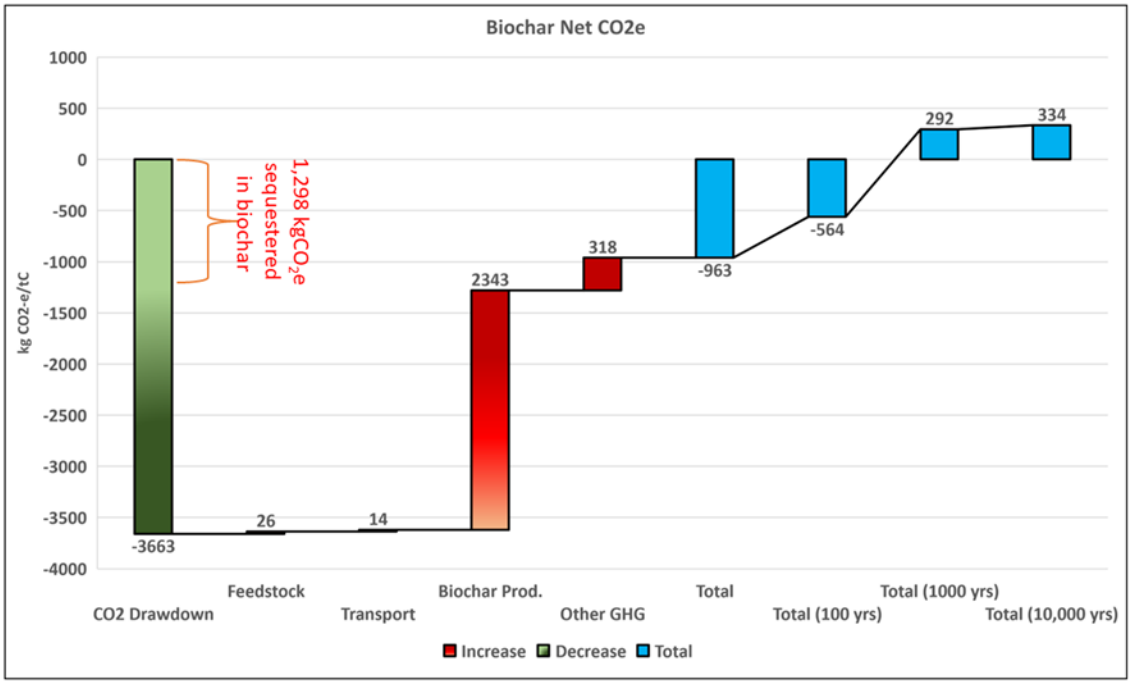


**Figure A8** Biochar soil amendment drawdown over 100 years (moderate case). Note that in the waterfall diagrams, green and red bars represent magnitudes of drawdown and emissions subsequent to the initial drawdown in biomass. The blue bars represent totals. The sum of all red and green bars is equal to the first blue bar.

### A2.6 Forest Residues to OSB

We analyze the "cradle-to-grave" life cycle of oriented strand board (OSB) construction material from forest residues. A standard production unit of OSB is measured at 1,000 $ft^2$ at 3/8" thickness. A tonne of forest residue feedstock will produce roughly 1.3 units with an estimated mass of 769 kg. To produced OSB, wood strands approximately 2.5 cm x 15 cm are layered at opposing angles and compressed under high temperatures with resin and wax (about 5% by mass)[232] to produce a strong construction material.

We rely on gate-to-gate life cycle data from Kline (2005), which relies on survey data from operations in the Southeastern U.S.[233] To remain consistent with other pathways in this analysis, we rely on GREET data for forest residue handling and transportation emissions. We compared results with published cradle-to-gate LCA results for conventional OSB production (from harvested wood feedstock, rather than residues).[232] Despite differences in upstream processes and our exclusion of packaging and handling after production, we find similar results. Kline (2005) assumes a feedstock carbon content of 51.3%. We recalculate the carbon mass-balance to be consistent with a carbon content of 50.3%, as in GREET and our other forest residue pathway. Finally, there are roughly 16 kg of wood feedstock reported as unaccounted in Kline (2005). This unaccounted portion is a function of the mass balance assumptions made in the source literature and is highly sensitive to those assumptions. We add this material to the

final mass of the OSB product. This adjustment is for internal consistency in carbon accounting and the mass difference is within the variance of OSB product mass.

**Table A24** OSB data sources

| **Process** | **LCI Source** |
|---|---|
| Feedstock characteristics, collection, and transport | GREET.net 2018[229] |
| Gate to Gate OSB process emissions | Kline (2005)[233] |
| Fossil fuel inputs (upstream) and supply chain transportation emissions | GREET.net 2018 |
| PF Resin | Wilson (2010)[416] |
| MDI Resin | Franklin Associates (2011)[417] |
| Slack Wax, at plant, US SE | NREL / USLCI – Federal LCA Commons[418] |
| Co-product EOL | Offsite combustion for energy assumed / No displacement credits |

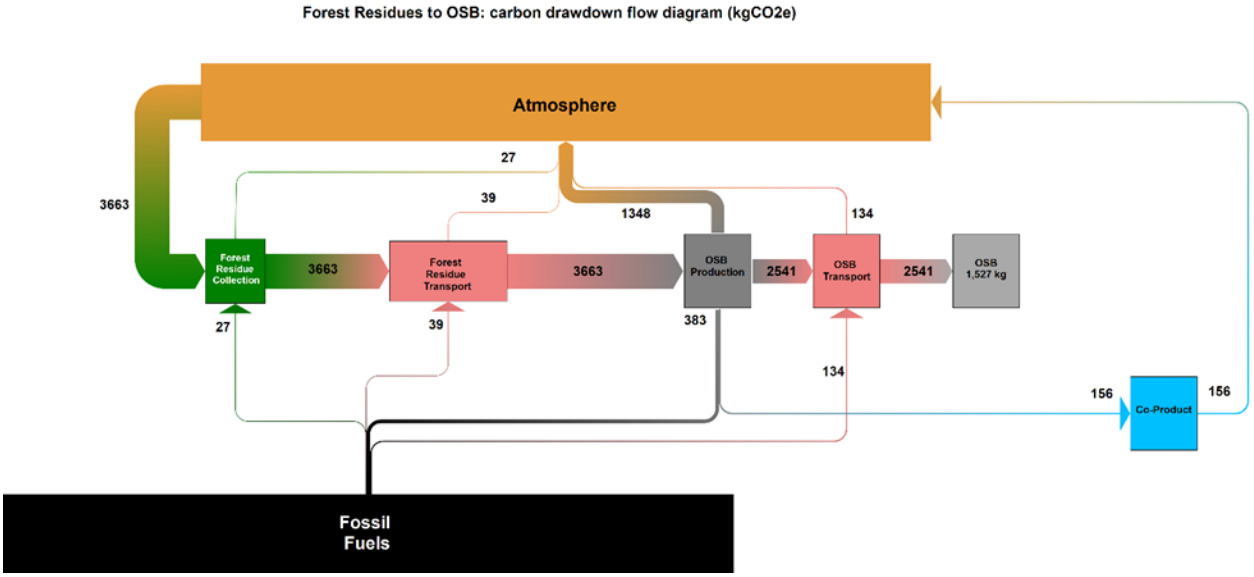


**Figure A9** Carbon flow through forest residues to OSB system as CO2e per tonne of feedstock. Embodied fossil emissions as well as upstream fossil emissions associated with production inputs are included in the flow diagram at the point where those inputs enter the production process. Thus, fossil emissions exiting a box in the diagram include both onsite emissions and emissions associated with upstream production of inputs. Note that carbon in methane and carbon monoxide emissions are not shown in this figure. These emissions account for the balance of carbon in the feedstock.

*Forest Residue Collection* - Forest residue collection is assumed to take place in Northern California. The residue travels 90 miles by heavy duty truck to the OSB mill. The forest residue is assumed to be 50.3% carbon by mass which is equivalent to roughly 1,844 kg of atmospheric

$CO_2$/t of feedstock. Approximately 1.99 tonnes of forest residue are equivalent to the functional unit.

*OSB production from forest residues* -- We assume a hypothetical OSB production facility located in Northern California.[419] Since OSB is highly standardized product due to building codes and regulations, we assume that the on relevant differences between OSB production in California as opposed to the Southeastern U.S. will be the emissions intensity of energy sources and the end-of-life disposition of waste co-products. The OSB production process involves feedstock handling, flaking of logs, drying and screening, blending, mat formation and pressing, and finishing. In addition, heat is required for emissions control (combustion of VOCs). The process requires about 235 kW of electricity to process 1 tonne of forest residues. Electricity is assumed to have the emissions intensity of the average California distributed grid mix. Onsite wood fuel provides 89.6% (or 4,764 MJ per ton of residues) of the onsite heat energy requirement. The remainder of heat energy comes from natural gas, LPG, and fuel oil. About 80% of the heat energy requirement is used in the drying phase. Other heat requirements include pressing and emissions control. Onsite emissions for fossil fuels are taken from Kline (2005). Upstream emissions for fossil fuel production use North American values from the GREET model. Fossil fuels are also required for onsite material handling equipment. See Kline (2005) for additional details. In addition to wood feedstock, 25 kg of PF resin, 5 kg of MDI resin, and 11 kg of slack wax per ton of forest residue processed. The data sources for upstream emissions from these inputs are listed in **Table A24**.

*OSB Co-products*—The OSB process creates 26 kg of bark mulch, 11 kg of fines, and 6 kg of dust and scrap per ton of feedstock processed. For simplicity, this small amount of co-product is assumed to be combusted offsite. The emissions are biogenic, ultimately yielding no contribution the overall emissions intensity. We do not assign emissions credits for displacement of energy products.

*OSB End-of-life*—We do not attempt to calculate emissions from transportation of OSB to point-of-sale or point-of-use. Additional end-of-life assumptions for OSB are detailed in S.I 1.3 and 2.4.2.

### A2.6.1 Forest residue to OSB results

Life cycle OSB greenhouse gas emissions at the facility gate are -1,806 $kgCO_2e$/tC. Photosynthetic drawdown in the feedstock is 3,663 $kgCO_2$/tC of forest residue (see **Figure A9),** In **Table A25**, process and transportation $CO_2$ emissions total 1548 $kgCO_2$/tC. Of those emissions, 964 $kgCO_2$/tC is biogenic, mostly from combustion of wood for heat energy, with a smaller portion arising from the combustion of VOCs as a result of abatement measures. 2,541 $kgCO_2$/tC is sequestered in the final OSB product. An additional 156 $kgCO_2e$/tC is sequestered in the wood co-products (bark, fines, waste), but it is ultimately assumed to be released via combustion offsite. The net $CO_2$ balance before consideration of non-$CO_2$ GHGs is -1,958 $kgCO_2$/tC.

**Table A25** Life cycle $CO_2$ of forest residue converted to OSB

| Life cycle emissions per 1 tonne C in feedstock |
|---|

| | | |
|---|---|---|
| **Products** | | |
| Oriented Strand Board (Mass basis) | 1526.88 | kg |
| Oriented Strand Board (Functional Unit Basis) | 2.57 | units |
| **CO2 Emissions** | | |
| Process Emissions (Forest Residue Collection) | 22.43 | kg |
| Upstream Emissions (Forest Residue Collection) | 4.09 | kg |
| Forest Residue Transport | 38.95 | kg |
| Process Emissions (OSB Production) | 1078.22 | kg |
| Upstream Emissions (OSB Production) | 269.52 | kg |
| OSB Transport | 134.41 | kg |
| Total Emissions | **1547.61** | **kg** |
| Biogenic Credit (OSB Production) | -964.70 | kg |
| CO2 in Co-Products | -156.14 | kg |
| CO2 Sequestered in OSB Wood | -2541.20 | kg |
| Total w/ Biogenic Credit and Product Sequestration | **-2114.43** | **kg** |
| End-of-Life (Co-product combustion) | 156.14 | kg |
| Total Cradle to Grave Emissions | **-1958.29** | **kg** |

When the added impact of non-$CO_2$ GHG emissions is considered, as shown in **Table A26**, the final cradle-to-gate emissions total -1,806 kg$CO_2$e/tC.

**Table A26** Non-CO2 GHG emissions for OSB production

| Non-CO2 GHG Emissions and Total Life-cycle CO2e | | |
|---|---|---|
| | | |
| CH4 (Process) x 28 CO2e | 100.82 | kg |
| N20 (Process) x 265 CO2e | 51.60 | kg |
| **Total Non GHG CO2e** | **152.41** | **kg** |
| **Life Cycle CO2e (w/ capture)** | **-1805.87** | **kg** |

### A2.6.2 OSB drawdown over 100; 1,000; and 10,000 years

Here we combine cradle-to-gate emissions for OSB production with the sequestration models described in Appendix A1.3 to estimate the long-term sequestration benefit of the conversion pathway. At $t = 0$, 693 kgC (2.541 kg$CO_2$/tC) is sequestered in the OSB product.

Per the sequestration functions described by Eq. 16 through Eq. 20, the carbon remaining in OSB at 100; 1,000; and 10,000 years is estimated. The quantity of OSB carbon emitted at $t$ is calculated by Eq. 21 and Eq. 22. The quantity of $CO_2$ and $CH_4$ emissions from energy production and landfill emissions at each time $t$ is calculated by Eq. 23 and Eq. 25 in the case of a landfill

that flares fugitive methane emissions. The emissions over time for the flaring case are shown in **Table A27**.

**Table A27** OSB Flaring case emissions (representative case in bold)

| Case | Emission | 100 years (kg $CO_2e$/t) | 1,000 years (kg $CO_2e$/t) | 10,000 years (kg $CO_2e$/t) |
|---|---|---|---|---|
| OSB (product C) optimistic | $CO_2$ (energy) | 342.37 | 760.50 | 762.36 |
| | $CO_2$ (landfill) | 1.40 | 11.06 | 11.11 |
| | $CH_4$ (landfill) | 2.03 | 16.09 | 16.15 |
| **OSB (product C) moderate** | **$CO_2$ (energy)** | **468.79** | **762.31** | **762.36** |
| | **$CO_2$ (landfill)** | **142.80** | **346.46** | **346.50** |
| | **$CH_4$ (landfill)** | **207.71** | **503.95** | **504.00** |
| OSB (product C) pessimistic | $CO_2$ (energy) | 682.14 | 762.36 | 762.36 |
| | $CO_2$ (landfill) | 385.7 | 515.23 | 515.23 |
| | $CH_4$ (landfill) | 561.02 | 749.43 | 749.43 |

The full emissions profile for OSB production (moderate case) assuming that landfills flare methane emissions is shown in **Figure A10**. Cradle-to-gate emissions are -1806 kg$CO_2$e/tC. At 100 years, 55% of the original drawdown remains. This falls to 11% at 1,000 and 10,000 years.

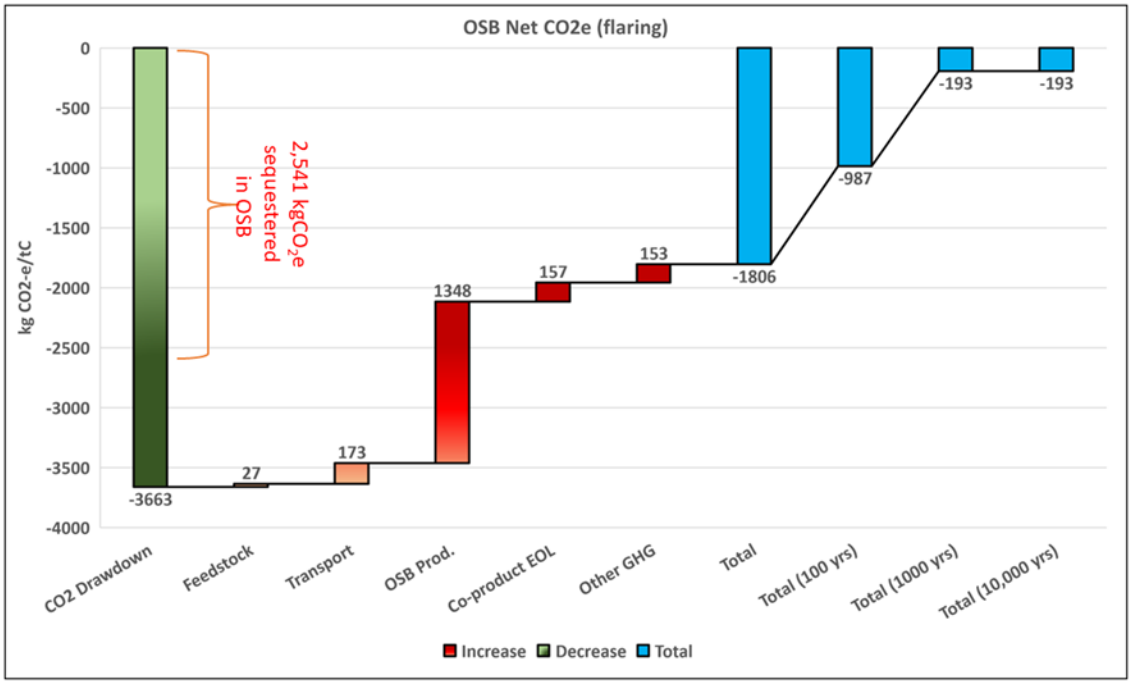


**Figure A10** OSB drawdown over 10,000 years (moderate case/flared landfills). Note that in the waterfall diagrams, green and red bars represent magnitudes of drawdown and emissions subsequent to the initial drawdown in biomass. The blue bars represent totals. The sum of all red and green bars is equal to the first blue bar.

For the scenario where landfills do not flare methane emissions, the quantity of $CO_2$ and $CH_4$ emissions from energy production and landfill emissions at each time *t* is calculated by Eq. 24 and Eq. 26. The emissions over time for the no-flaring case are shown in **Table A28**.

**Table A28** OSB non-flaring case emissions (representative case in bold)

| **Case** | **Emission** | **100 years (kg $CO_2$e/t)** | **1,000 years (kg $CO_2$e/t)** | **10,000 years (kg $CO_2$e/t)** |
|---|---|---|---|---|
| OSB (product C) optimistic | $CO_2$ (energy) | 342.37 | 760.50 | 762.36 |
| | $CO_2$ (landfill) | 0.80 | 6.32 | 6.35 |
| | $CH_4$ (landfill) | 8.13 | 64.36 | 64.63 |
| **OSB (product C) moderate** | **$CO_2$ (energy)** | **468.79** | **762.31** | **762.36** |
| | **$CO_2$ (landfill)** | **81.60** | **197.98** | **198.00** |
| | **$CH_4$ (landfill)** | **830.82** | **2015.79** | **2016.02** |
| OSB (product C) pessimistic | $CO_2$ (energy) | 682.14 | 762.36 | 762.36 |
| | $CO_2$ (landfill) | 220.40 | 294.42 | 294.42 |
| | $CH_4$ (landfill) | 2244.09 | 2997.70 | 2997.70 |

The full 10,000-year (moderate case) emissions profile of the OSB pathway assuming that landfills do not manage methane emissions is shown in **Figure A11**. Cradle-to-gate emissions are -1,806 kgCO2e/tC. At 100 years 24% of the original drawdown benefit remains. At 1,000 and 10,000 years, the pathway yields significant net emissions. This is primarily due to high GWP of methane emissions in the landfill.

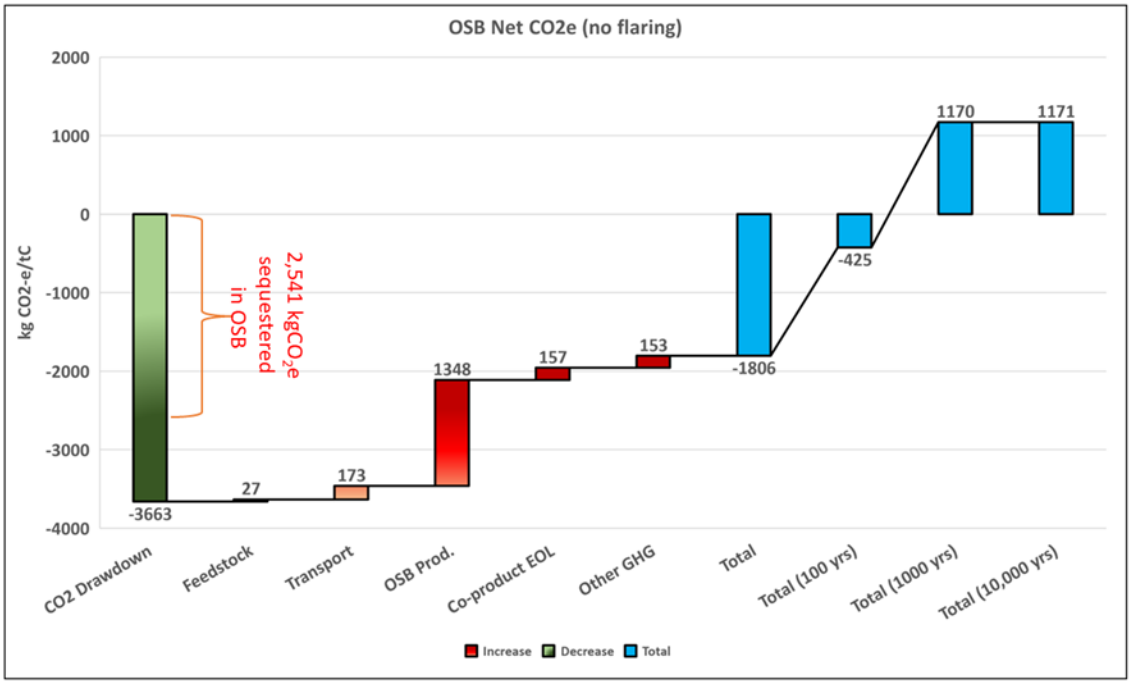


**Figure A11** OSB drawdown over 10,000 years (moderate case/unflared landfills). Note that in the waterfall diagrams, green and red bars represent magnitudes of drawdown and emissions subsequent to the initial drawdown in biomass. The blue bars represent totals. The sum of all red and green bars is equal to the first blue bar.

### A2.6.3 OSB counterfactual selection

From the meta-analysis by Sathre and O'Connor, we draw our range of displacement factors from Table 2: Low, middle, and high estimates of displacement factors of wood product substitution (tC emission reduction per tC of additional wood products used) based on data from 21 studies. We select only consider the subset of estimates from the literature that explicitly involve "building" construction, i.e. scenarios where OSB is a plausible wood substitute. We selected the lowest and highest displacement factors from the middle range column of estimates to arrive at 0.4 to 6.0 tC displaced per tonne of wood C utilized. In our manuscript, we report these values to $tCO_2$/t wood C (1.5 – 22.0 $tCO_2$/C).

# APPENDIX B. Supplementary Information: Oxyfuel combustion with carbon capture and sequestration to produce low-carbon ethanol

## B1. Mass and Energy Balance

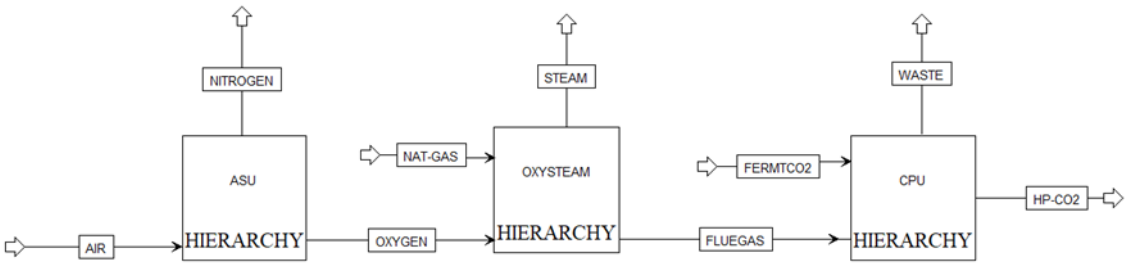


**Figure B1** Block flow representation/ Scope of ASPEN Model

### B1.1 Material balance

The material balance of the quantity of CO2 capturable from a 40 million gallon per year denatured (2.5 vol%) ethanol plant, running 358 days/annum is stated below. The composition of corn used is reviewed from literature sources [285], [304], [305], [307] and given in **Table B1**. Fermentation is assumed to have 93.2% conversion efficiency, while liquefaction and saccharification conversion efficiency and ethanol recovery is 99%. Corn is assumed to compose of 40.52% carbon. Density of ethanol is 0.79 kg/L. The reaction equations are stated below.

Liquefaction of starch to maltose

$$2(C_6H_{10}O_5)_n + nH_2O \xrightarrow{\alpha-amylase} nC_{12}H_{22}O_{11}$$

Saccharification of maltose to glucose

$$C_{12}H_{22}O_{11} + H_2O \xrightarrow{glucoamylase} 2C_6H_{12}O_6$$

Fermentation of glucose to ethanol

$$C_6H_{12}O_6 \xrightarrow{yeast} 2C_2H_6O + 2CO_2$$

From the above equations, 1kg of starch produces 1.06 kg of maltose and 1kg of maltose produce 1.05 kg of glucose. 1kg of glucose produces 0.51 kg of ethanol and 0.49 kg of $CO_2$.

### B1.2 Energy balance

Mueller (2008) reported the thermal energy requirements of a dry grind ethanol mill in US as 8.08 MJ/L[303]. In this work, we have modelled the steam requirement of a 40 million gallon per year (189 million litre per year) ethanol plant supplied by oxyfuel combustion of natural gas, capturing the $CO_2$ produced during the combustion and fermentation step using ASPEN plus V11. Peng-Robinson (PENG-ROB) equations of state is the property methods selected.

**Table B1** Corn composition

| **Component** | **%wt basis** |
|---|---|
| Starch | 62.9 |
| Glucose | 1.70 |
| Cellulose/Hemicellulose | 7.2 |
| Protein | 8.1 |
| Oil | 3.8 |
| Ash | 1.3 |
| Water | 15.0 |
| **Total** | **100.0** |
| Shelled corn (lb/bu) | 56 |

**Table B2** ASU modelling parameters

| | **Scenario 1 – Direct Dry** | **Scenario 2 – Steam Dry** | |
|---|---|---|---|
| **Parameter** | **Value** | **Value** | **Unit** |
| Flowrate | 25100 | 40635 | $Nm^3/hr$ |
| Pressure | 1 | 1 | bar |
| Temperature | 15 | 15 | $^oC$ |
| $N_2$ | 78.1 | 78.1 | % |
| $O_2$ | 21 | 21 | % |
| Ar | 0.9 | 0.9 | % |
| Compressor efficiency | 85 | 85 | % |
| $O_2$ purity | 95 | 95 | % |
| $O_2$ pressure | 1.2 | 1.2 | bar |

**Table B3** Carbon balance for both cases

| **Scenario 1 – Direct Dry** | **Carbon in** | **Carbon out** |
|---|---|---|

| Source | | Flowrate | %C | C in kg/hr | | Flowrate | %C | C in kg/hr |
|---|---|---|---|---|---|---|---|---|
| Fermentation | Corn | 40951 | 40.52% | 16595 | EtOH | 13701 | 52% | 7143 |
| | | | | | DDGS | 11514 | 49% | 5642 |
| | | | | | Corn oil | 313 | 76% | 238 |
| Oxyfuel | Natural gas | | | 1383 | Oxy vents | 5.5 | 27% | 1.5 |
| | | | | | Ferment vents | 6.5 | 27% | 1.8 |
| | | | | | $CO_2$ product | 18145 | 27% | 4952 |
| **Total** | | | | **17978** | | | | **17978** |
| **Scenario 2 – Steam Dry** | **Carbon in** | | | | **Carbon out** | | | |
| Source | | Flowrate | %C | C in kg/hr | | Flowrate | %C | C in kg/hr |
| Fermentation | Corn | 40951 | 40.52% | 16595 | EtOH | 13701 | 52% | 7143 |
| | | | | | DDGS | 11514 | 49% | 5642 |
| | | | | | Corn oil | 313 | 76% | 238 |
| Oxyfuel | Natural gas | | | 2239 | Oxy vents | 9.2 | 27% | 2.52 |
| | | | | | Ferment vents | 6.5 | 27% | 1.78 |
| | | | | | $CO_2$ product | 21278 | 27% | 5807 |
| **Total** | | | | **18834** | | | | **18834** |

**Table B4** Results summary

| **Parameter** | **Scenario 1 – Direct Dry** | **Scenario 2 – Steam Dry** |
|---|---|---|
| Air flow rate (t/d) | 776 | 1256 |
| $O_2$ flow rate (t/d) | 189 | 306 |
| $N_2$ flow rate (t/d) | 873 | 950 |
| Natural gas flow rate (t/d) | 46 | 74 |
| Steam flow rate (t/d) | 779 | 1265 |
| $CO_2$ product flow rate (t/d) | 435 | 511 |
| ASU SER (kWh/t $O_2$) | 196 | 196 |
| CPU SER (kWh/t $CO_2$) | 115 | 117 |
| Combustion temperature ($^oC$) | 1053 | 1053 |

## B2. LCA Assumptions and Extended Analysis

### B2.1 Life Cycle Inventory

**Table B5** LCA Inventory. Aggregate emissions factors will differ somewhat from GREET.net assumptions. Raw data was extracted and tabulated independently in an Excel model. We use AR5 GWP factors for $CH_4$ and $N_2O$ whereas GREET uses AR4 factors.

| Input | Qty | $gCO_2e$ | Source |
|---|---|---|---|
| Corn (g) | 1.12E2 | 3.70E1 | GREET.net 2019 |
| Alpha amylase (g) | 3.17E-2 | 3.84E-2 | GREET.net 2019 |
| Gluco amylase (g) | 6.82E-2 | 3.77E-1 | GREET.net 2019 |
| Yeast (g) | 3.46E-2 | 8.69E-2 | GREET.net 2019 |
| Process water (gal) | 3.42E-2 | 0.00 | GREET.net 2019 |
| Sulfuric acid (g) | 5.86E-2 | 2.59E-3 | GREET.net 2019 |
| Ammonia (g) | 2.25E-1 | 5.62E-1 | GREET.net 2019 |
| Sodium Hydroxide (g) | 2.82E-1 | 5.65E-1 | GREET.net 2019 |
| Calcium Oxide (g) | 1.34E-1 | 1.72E-1 | GREET.net 2019 |
| Natural gas (boiler) – Direct dry (Btu) | 2.22E2 | 1.48E1 | GREET.net 2019 NA Shale/Conventional + Utility boiler |
| Natural gas (dryer) – Direct dry (Btu) | 1.38E2 | 9.10E0 | GREET.net 2019 Shale/Conventional + Dryer |
| Natural gas (boiler) – Steam dry (Btu) | 3.60E2 | 2.41E1 | GREET.net 2019 Shale/Conventional + Utility boiler |
| Natural gas (oxyfuel boiler) – Direct dry (Btu) | 2.22E2 | 1.48E1 | GREET.net 2019 + Aspen |
| Natural gas (oxyfuel boiler) – Steam dry (Btu) | 3.60E2 | 2.41E1 | GREET.net 2019 + Aspen |
| Electricity – BASE (Btu) | 3.08E1 | 6.02E0 | GREET.net 2019 MROW Distributed |
| Additional Electricity FERMCCS (Btu) | 1.41E1 | 2.76E0 | GREET.net 2019 MROW Distributed |
| Additional Electricity FERMOXYCCS (Btu) | 3.39E1 | 6.63E0 | GREET.net 2019 MROW Distributed |
| Additional Electricity SD-FERMOXYCCS (Btu) | 4.66E1 | 9.11E0 | GREET.net 2019 MROW Distributed |
| **Output** | | | |
| Ethanol (MJ) | 1.00 | | Aspen Yield |
| DDGS (g) | 3.15E1 | -1.16E1 | Aspen Yield + GREET Displacement EF |
| Corn oil (g) | 8.57E1 | -2.10E-1 | Aspen Yield + GREET Displacement EF |

### B2.2 Extended LCA Results

We chose to focus our analysis on a conservative subset of cases wherein a direct drying system is used to dry the DDGS co-product. In the direct dry configuration, only 62% of the natural gas

is combusted in the boiler, thus only the $CO_2$ emissions from the boiler fraction of fuel combustion is available to the capture system. However, we model an alternative scenario where all natural gas is combusted in the boiler and DDGS is dried indirectly via the steam dry configuration. In **Figure B2,** the direct dry cases BASE, FERMCCS, and FERMOXYCSS reported in the manuscript are on the far left. BASE-RNG, FERMCCS-RNG, and FERMOXYCCS-RNG model the same direct dry cases but substitute renewable natural gas (RNG) from upgraded landfill gas (described in manuscript sensitivity analysis) for conventional natural gas. The six cases on the right-hand side of the figure with the SD- designation represent the life cycle GHG intensity of the "steam dryer" configuration of each of the direct dry scenarios. The net CI reduction between FERMOXYCCS and SD-FERMOXYCCS is -6 $gCO_2e/MJ$. The steam dry configuration enables an additional 8 $gCO_2e/MJ$ of avoided emissions relative to the direct dry case. However, the process also generates a little over 2 $gCO_2e/MJ$ more emissions from the electric grid, as additional power is required to support the ASU and CPU due to more fuel in oxyfuel boiler.

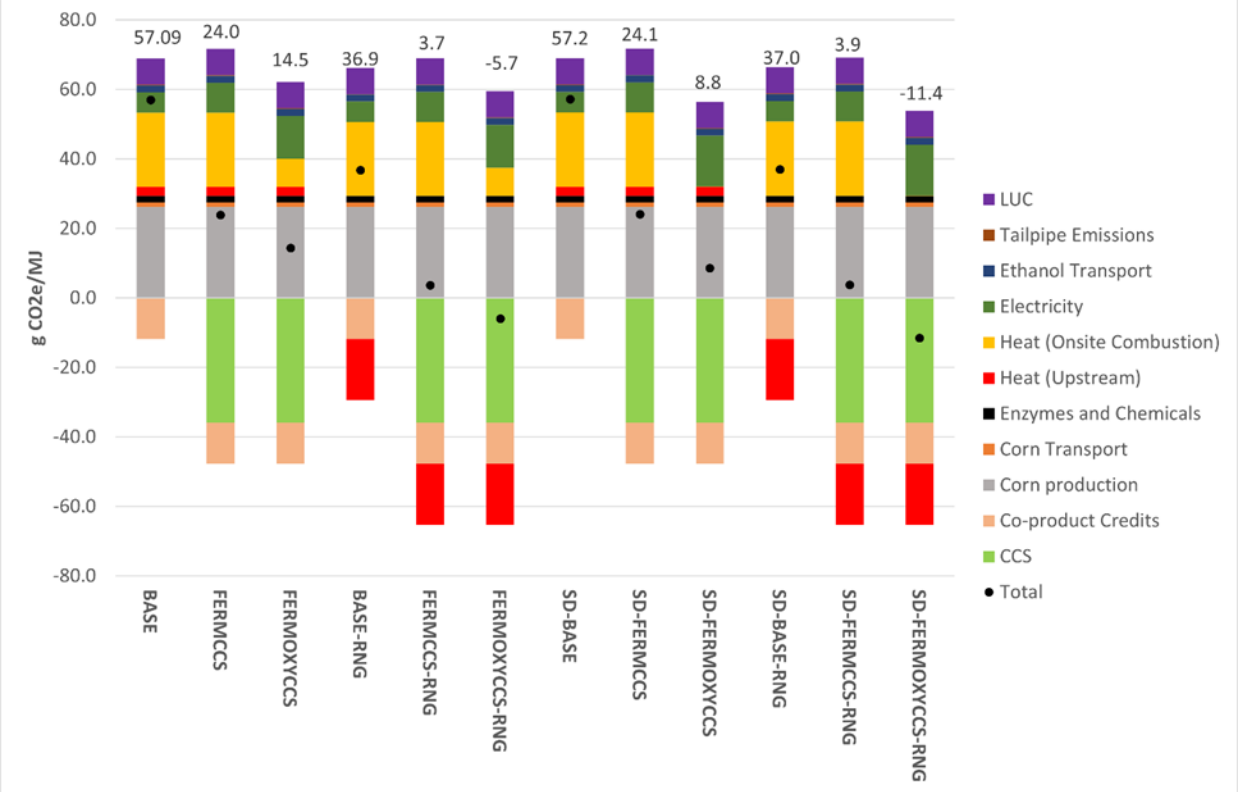


**Figure B2** Life cycle carbon intensity (CI) of twelve ethanol process configurations BASE = Baseline facility with direct drying of DDGS, FERMCCS = CCS on fermentation gas only, FERMOXYCCS = Oxyfuel boiler added with CCS on both fermentation and boiler flue gas streams, CCS = Carbon Capture and Sequestration, RNG= Renewable natural gas substituted for conventional NG, SD – Steam Dry configuration, i.e., all natural gas fuel is combusted in boiler, LUC = Land Use Change.

## B3. $CO_2$ Capture Cost Model

### B3.1 Air separation unit (ASU)

The cost-to-capacity method for computing order-of-magnitude cost estimates meaning using known cost and capacity of an existing plant or equipment to calculate cost of a new plant or equipment. The calculated cost from this method gives a Class 4 or 5 estimate as specified by Association for the Advancement of Cost Engineering (AACE) International[420].
The cost to capacity's concept is that cost of different sizes of equipment or facilities using similar technology vary nonlinearly which is associated with economies of scale. That is, it tends to cost less to build larger plants per unit capacity. The governing equation is given below.

$$C_2 = C_1 \left[\frac{S_2}{S_1}\right]^n \quad \ldots 1$$

Where, $C_1$ = known capital cost of the plant 1
$C_2$ = Required capital cost of the plant 2
$S_1$ = Capacity of the plant 1
$S_2$ = Capacity of the plant 2
$n$ = Scaling exponent

The technology for oxygen separation from air is the cryogenic distillation. The equipment cost is the direct cost of the process equipment excluding labour, material, installation, direct, and indirect costs. Two sources in literature with corresponding base year are listed in **Table B6**. The reference cost has been updated to 2020 dollars using the Chemical Engineering Plant Cost Index (CEPCI).

The relationship is given as[421]:

$$C_2 = C_1 \left[\frac{Cost\ Index\ in\ year\ 2}{Cost\ Index\ in\ year\ 1}\right] \quad \ldots 2$$

**Table B6** Reviewed ASU equipment cost (2020) and capacities

| Label | Source | Cost year | Capacity (tonnes$O_2$/day) | Updated Equipment Cost (M$2020) |
|---|---|---|---|---|
| A | NETL-2019[422] | 2018 | 3665 | $52.68 |
| B | NETL-2019 [422] | 2018 | 3687 | $52.90 |
| C | NETL-2019 [421] | 2018 | 3954 | $55.54 |
| D | NETL-2019 [422] | 2018 | 4186 | $57.81 |

| | | | | |
|---|---|---|---|---|
| E | NETL-2019 [422] | 2018 | 4288 | $58.80 |
| F | NETL-2012 [423] | 2007 | 11681 | $126.35 |
| G | NETL-2012 [423] | 2007 | 12798 | $133.46 |
| H | NETL-2012 [423] | 2007 | 12955 | $134.45 |

To determine the scaling exponent of the ASU, a power law scaling curve of cost vs capacity is plotted. **Figure B3** shows the cost versus capacity power regression analysis. The exponent is calculated as 0.75. The suggested scaling exponent for ASUs given by "Quality Guideline for Energy System Studies – Capital Cost Scaling Methodology" QGESS[424] and Hamelinck *et al.* [425] are 0.70 and 0.75 respectively.

Therefore, the governing scaling equation for calculating the cost of cryogenic ASU using the capacity of oxygen produced as scaling parameter is:

$$ASU\ Equipment\ Cost\ (M_{2020}\ USD) = 0.1126\left[Capacity\left(\frac{tonne\ O_2}{day}\right)\right]^{0.75} \quad ...3$$

Therefore, for a cryogenic ASU capacity of 377 tpd $O_2$, the equipment cost is calculated as $9.63M. According to Air Liquide Engineering and Construction technology 2021 handbook [426], the cost of a Sigma – Standard Air Separation Unit, which produces 110 to 380 tpd O2 up to 99.8% purity is between 5.37 – 9.67M$2020. Based on this validation, ASU is scaled from Air Liquide cost with a scaling exponent of 0.75.

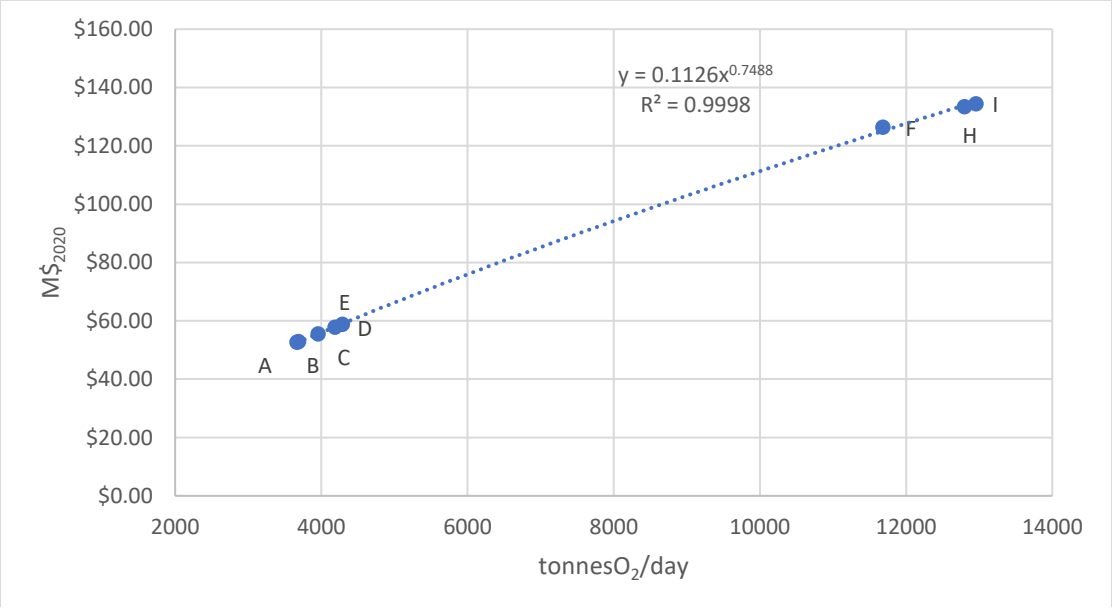


**Figure B3** Cost versus capacity power regression analysis

### B3.2 $CO_2$ purification unit (CPU)

The CPU was scaled directly from the Illinois Basin Decatur Project (IBDP) [426] with a scaling exponent of 0.8 for compression and dehydration equipment, and 0.6 for electrical transmission line, instrumentation, and controls.

### B3.3 Oxyfuel boiler

There is very limited literature cost of oxyfuel utility boilers. For this analysis, the cost of oxyfuel boiler is based off the air combustion utility boiler. An installation factor of 4 is suggested for the additional modification. Such modifications include[427]:

- Oxyburners as opposed to normal burners
- Flue gas recycling ducts and fans
- Air preheater replaced by economizer
- Superheater and attemperators

**B4. California Low-Carbon Fuel Standard (LCFS) Credit Calculations**

The following formula is used to calculate credits and deficits generated under California's LCFS program. Deficit generators (sellers of fossil fuels whose fuels do not meet the CI standard) must purchase credits from credit generators (alternative fuel producers whose fuel has a CI lower than the CI standard) such that all deficits are cancelled by credits and the average CI of fuel sold in California meets the CI criteria for the current year. The formula below is adapted from **Title 17, California Code of Regulations (CCR), section §95486.1. "Generating and Calculating Credits and Deficits Using Fuel Pathways."**

$$\boldsymbol{Credits_i^{XD}\ or\ Deficits_i^{XD}(MT) = \left(CI_{standard}^{XD} - CI_{reported}^{XD}\right) \times E_{displaced}^{XD} \times C}$$

**Where:**

$\boldsymbol{Credits_i^{XD}\ or\ Deficits_i^{XD}(MT)}$ is either the number of LCFS credits generated (a zero or positive value), or deficits incurred (a negative value), in metric tons, by a fuel or blendstock under the average carbon intensity requirement for gasoline (XD = "Gasoline"), diesel (XD = "Diesel"), or jet fuel (XD = "jet fuel).

$\boldsymbol{CI_{standard}^{XD}}$ is the average carbon intensity requirement of the either gasoline, diesel, or jet fuel for a given year.
$\boldsymbol{CI_{reported}^{XD}}$ is the adjusted carbon intensity value of a fuel or blendstock in gCO2e/MJ
$\boldsymbol{E_{displaced}^{XD}}$ is the total quantity of gasoline, diesel, or jet fuel displaced in MJ
**C** is a factor used to convert credits to units of metric tons from gCO2e and has the value of:
$C = 1.0 \times 10^{-6} \frac{(MT)}{(gCO2e)}$

## APPENDIX C. Supplementary Information for A comparison of sustainable aviation fuel pathways across emissions, cost, and feedstock sustainability criteria

### C1. Technology Readiness Level

**Table C1** BECCS Technology Readiness Levels as defined by the DOE. Adapted from NASEM 2019 [42]

| | TRL | DOE Definition | BECCS Description |
|---|---|---|---|
| Applied Research | 1 | Basic principles observed and reported | Lowest level of technology readiness. Scientific research begins to be translated into applied R&D. Examples include paper studies of a technology's basic properties. |
| | 2 | Technology concept and/or application formulated | Invention begins. Once basic principles are observed, practical applications can be invented. Applications are speculative and there may be no proof or detailed analysis to support the assumptions. Examples are still limited to analytic studies. |
| | 3 | Analytical and experimental critical function and/or characteristic proof of concept | Active R&D is initiated. This includes analytical and laboratory-scale studies to physically validate the analytical predictions of separate elements of the technology (e.g., individual technology components have undergone laboratory-scale testing). |
| Development | 4 | Component and/or system validation in a laboratory environment | Bench-scale components and/or system has been developed and validated in the laboratory environment. Bench-scale prototype is defined as <1% of final scale (e.g.; technology has undergone bench-scale testing w/ biomass feed stock/simulated feedstock of 0.1-1 t/d) |
| | 5 | Laboratory-scale similar- system validation in a relevant environment | The basic technological components are integrated so that the bench-scale system configuration is similar to the final application in almost all respects. Bench-scale prototype is defined as less than 1% of final scale (e.g.; complete technology has undergone bench-scale testing using actual dry biomass feedstock of 0.01-1 t/d). |
| | 6 | Engineering/pilot-scale prototypical system demonstrated in a relevant environment | Engineering-scale models or prototypes are tested in a relevant environment. Pilot-scale prototype is defined as being 1-5% percent final scale (e.g., complete technology has undergone small pilot-scale testing using actual dry biomass at a scale of ~ 10-50 t/d). |
| Demonst | 7 | System prototype demonstrated in a plant environment | This represents a major step up from TRL 6, requiring demonstration of an actual system prototype in a relevant environment. Final design is virtually complete. Demonstration-scale prototype is defined as 5–25% of final scale or design and development of a 50-250 t/d dry biomass plant (e.g., complete technology has undergone large pilot-scale testing using dry biomass feedstock at a scale equivalent to approximately 50-250 t/d). |

| | | | |
|---|---|---|---|
| **r a t i o n** | **8** | Actual system completed and qualified through test and demonstration in a plant environment | The technology has been proven to work in its final form and under expected conditions. In almost all cases, this TRL represents the end of true system development. Examples include startup, testing, and evaluation of the system within a 50-250 t/d dry biomass capacity plant (e.g., complete and fully integrated technology has been initiated at full-scale demonstration including startup, testing, and evaluation of using dry biomass |
| | **9** | Actual system operated over the full range of expected conditions | The technology is in its final form and operated under the full range of operating conditions. The scale of this technology is expected to be 50-250 t/d dry biomass capacity plant (e.g., complete and fully integrated technology has undergone full-scale demonstration testing using dry biomass feedstock at a scale equivalent to approximately 50 t/d dry or greater) |

**Table C2** Assessment of SAF pathway Technology Readiness Levels

| Technology | Assigned TRL | Justification |
|---|---|---|
| Corn ATJ | 8 | Commercial except ethanol-to-jet conversion (demonstrated but not yet commercial) |
| Corn ATJ CCS | 7 | CCS demonstrated on corn ethanol but not yet practiced at scale |
| Cellulosic ATJ | 8 | Commercial except ethanol-to-jet conversion |
| Cellulosic ATJ CCS | 7 | CCS demonstrated on cellulosic ethanol but not yet practiced at scale |
| Sugar ATJ | 8 | Commercial except ethanol-to-jet conversion |
| Sugar ATJ CCS | 7 | CCS demonstrated on sugar ethanol but not yet practiced at scale |
| Palm HEFA | 9 | Commercial |
| Soy HEFA | 9 | Commercial |
| Jatropha HEFA | 7 | HEFA is commercial; jatropha not yet commercialized within modern agriculture systems |
| UCO HEFA | 8 | Practiced at commercial scale, but supply chains for UCO are immature |
| Cellulosic HDCJ | 6 | Only deployed at pilot scale |
| MSW HDCJ | 5 | Not yet deployed at pilot scale |
| Cellulosic FT | 7 | Red Rock Biofuels currently building full-scale facility |
| Cellulosic FT CCS | 6 | CCS demonstrated on FT but not practiced |

| | | |
|---|---|---|
| MSW FT | 7 | Fulcrum Bioenergy currently building full-scale facility |
| MSW FT CCS | 6 | CCS demonstrated on FT but not practiced |
| ATF_electro (green) | 7 | Norsk e-fuel facility planned for 2023, 10 million liters/yr |
| ATF_co_electro (blue) | 5-6 | SOEC installs in Europe at the scale of ~150 kW |
| ATF_rwgs (orange) | 6 | Deployed at pilot scale by Carbon Engineering |

## C2. Selected Life Cycle Assessment Results

NOTE ON WATERFALL DIAGRAMS – Waterfall diagrams do not account for co-product credits nor do they account for allocation of emissions burdens among various co-products. Their purpose here is to track the "actual" emissions balance of the life cycle, thus waterfall totals will not match life cycle calculations. Waterfalls show totals both with and without CCS where appropriate. CCS total includes LUC emissions.

NOTE ON SYSTEM FLOW DIAGRAMS (SANKEYS) – The system flow diagrams track only carbon moving through the system, whether of biogenic or fossil origin. Non-CO2 GHGs and LUC are not tracked on these figures.

NOTE ON TABULAR DATA – The tabular data contains the LCA calculations including all credits, penalties, and allocations assessed. Grey cells at each stage tabulate total emissions from previous stages allocated to final SAF.

## C2.1 Alcohol to Jet

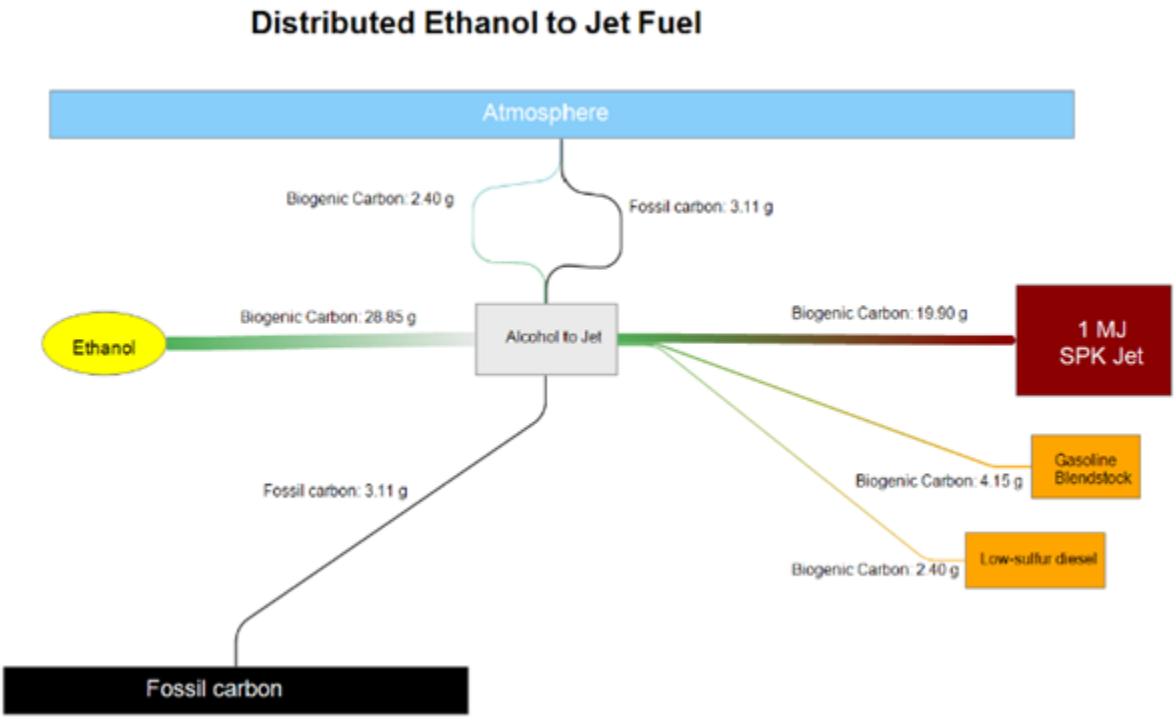


**Figure C1** Ethanol to Jet carbon flow diagram - 1.49 MJ of ethanol input to produce 1 MJ of SPK Jet

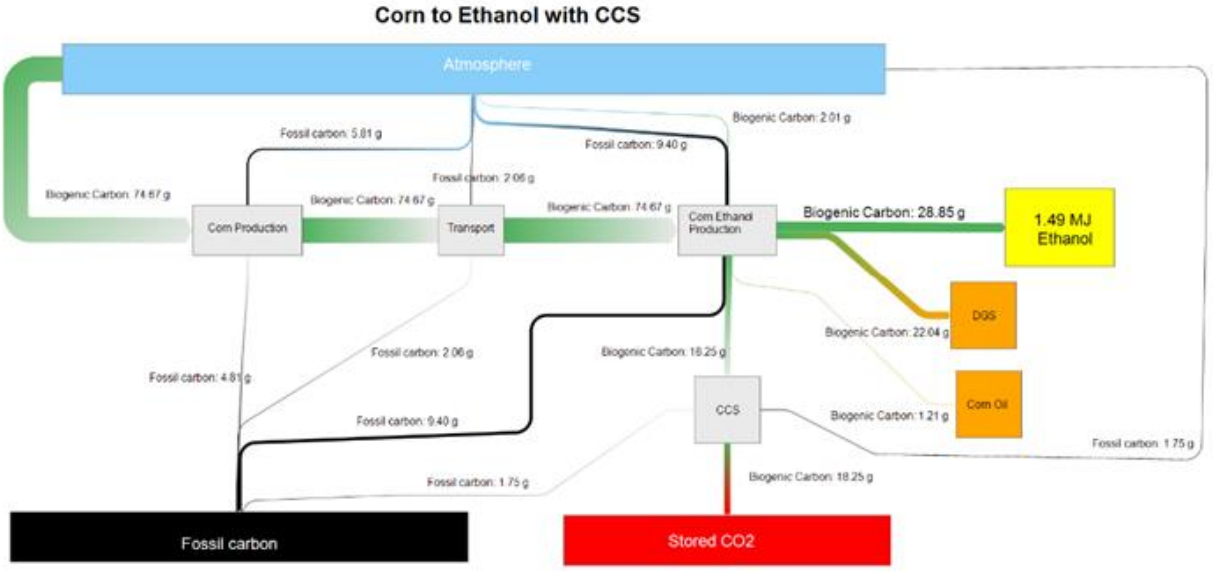


**Figure C2** Corn starch ethanol with CCS carbon flow diagram

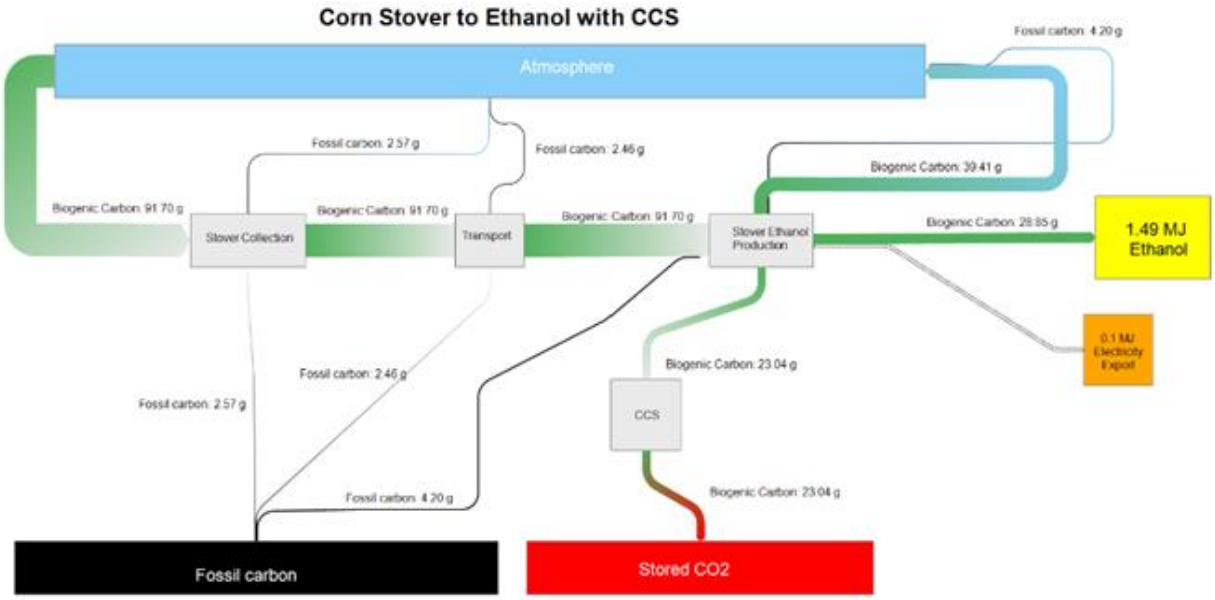


**Figure C3** Corn stover ethanol with CCS carbon flow diagram

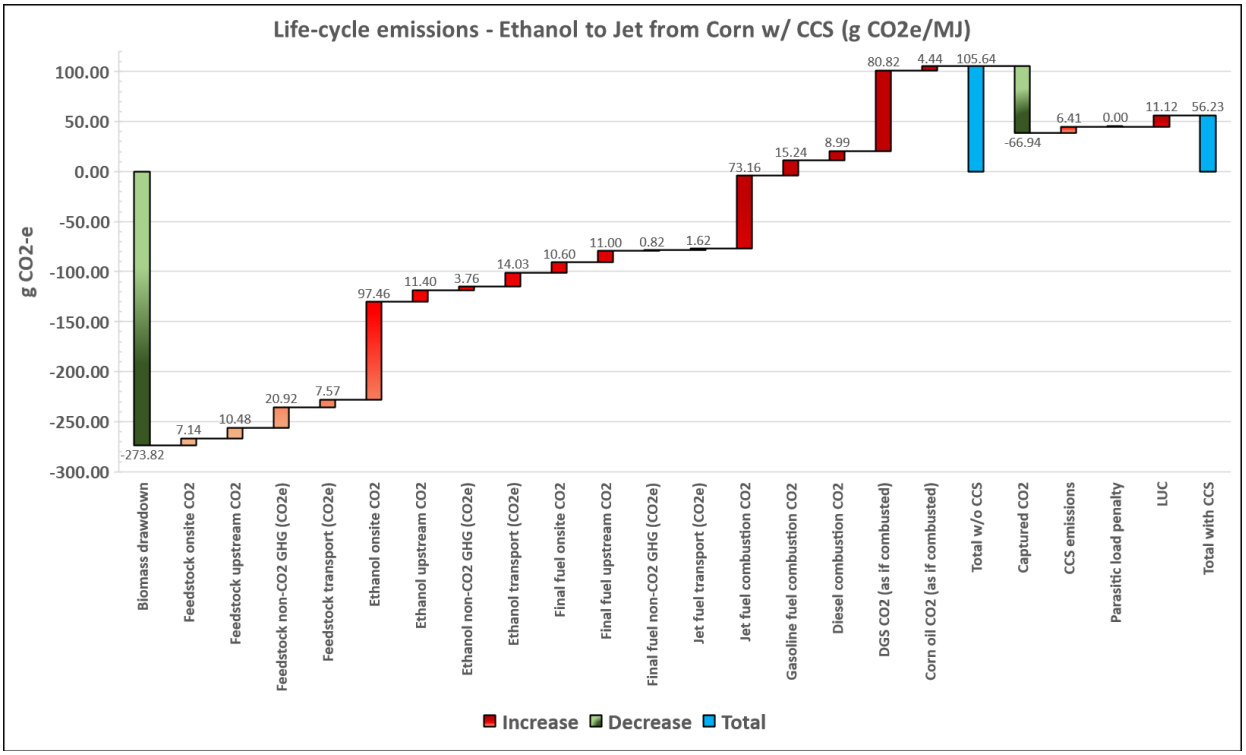


**Figure C4** Waterfall diagram for Corn starch ethanol to SAF with CCS emissions - illustrates carbon uptake in biomass (initial green bar) and sources of emissions and removals along product supply chain. First total (blue) represents net emissions, not including co-product credits or allocation, without CCS. To the right of the first total, CCS capture, and LUC impacts are added in. Without credits and co-product allocation, these totals will not match LCA total. Figure represents physical processes only. Degradable or combustible products and co-products are assumed to return to the atmosphere as $CO_2$.

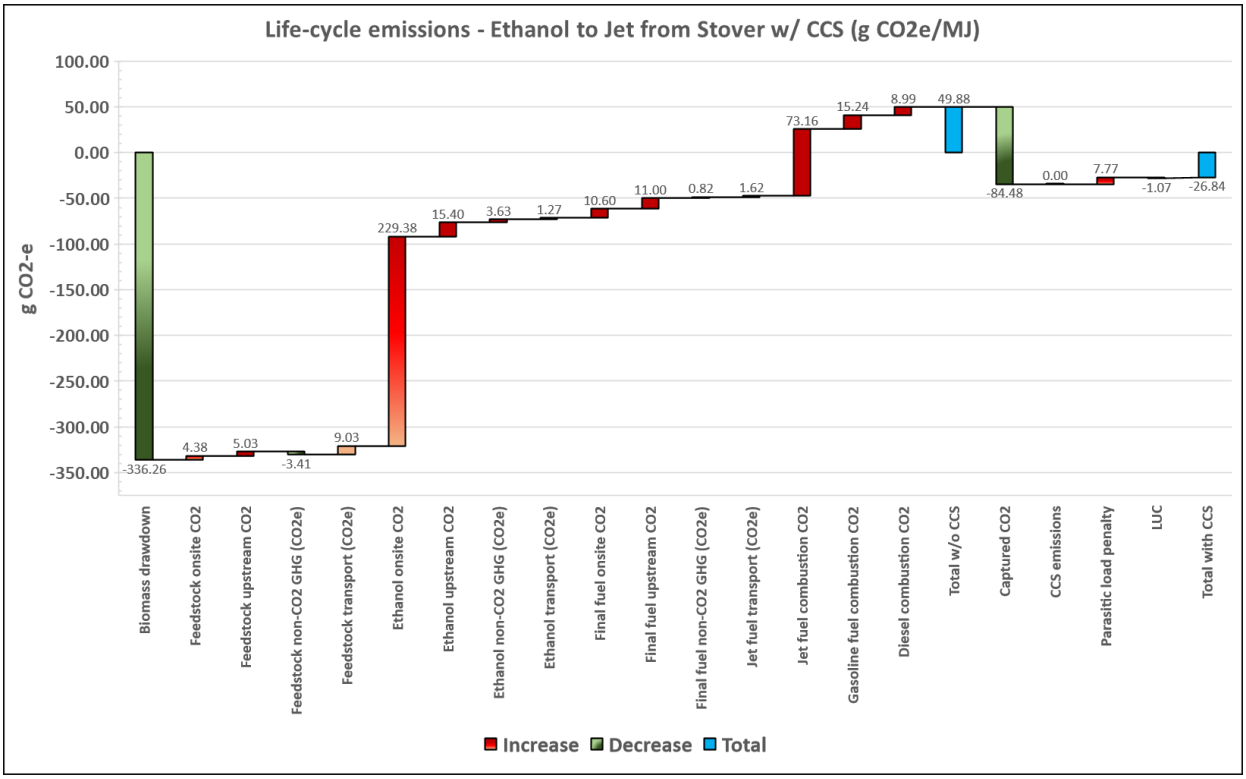


**Figure C5** Waterfall diagram for Corn stover ethanol to SAF with CCS emissions - illustrates carbon uptake in biomass (initial green bar) and sources of emissions and removals along product supply chain. First total (blue) represents net emissions, not including co-product credits or allocation, without CCS. To the right of the first total, CCS capture, and LUC impacts are added in. Without credits and co-product allocation, these totals will not match LCA total. Figure represents physical processes only. Degradable or combustible products and co-products are assumed to return to the atmosphere as $CO_2$.

| Corn Ethanol to Jet Fuel | | |
|---|---|---|
| **Final Fuel Products** | | |
| SPK Jet Fuel | 1 | MJ |
| Gasoline | 0.21 | MJ |
| Low Sulfur Diesel | 0.12 | MJ |
| **Upstream Co-products** | | |
| Distillers Grains | 0.099 | lbs |
| Corn Oil | 0.004 | lbs |

| Feedstock Emissions | | |
|---|---|---|
| Feedstock onsite CO2 | 7.14 | g |
| Feedstock upstream CO2 | 10.48 | g |
| Feedstock biogenic CO2 credit | -0.01 | g |
| Feedstock non-CO2 GHG (CO2e) | 20.92 | g |
| Feedstock total CO2e | 38.52 | g |
| **Feedstock Transport** | | |
| Feedstock transport (CO2e) | 7.57 | g |

| Ethanol Emissions | | |
|---|---|---|
| **Feedstock emissions allocated** | **46.09** | **g** |
| Ethanol onsite CO2 | 97.46 | g |
| Ethanol upstream CO2 | 11.40 | g |
| Ethanol biogenic CO2 credit | -74.39 | g |
| Ethanol non-CO2 GHG (CO2e) | 3.76 | g |
| DGS displacement credit | -16.56 | g |
| Corn oil displacement credit | 0.00 | g |
| Ethanol total CO2e | 67.76 | g |
| **Ethanol Transport** | | |
| Ethanol transport (CO2e) | 1.27 | g |

| Jet Fuel Emissions | | |
|---|---|---|
| **Ethanol emissions allocated** | **51.91** | **g** |
| Final fuel onsite CO2 | 7.97 | g |
| Final fuel upstream CO2 | 8.27 | g |
| Final fuel biogenic CO2 credit | -8.01 | g |
| Final fuel non-CO2 GHG (CO2e) | 0.62 | g |
| Gasoline credit | 0.00 | g |
| LS Diesel credit | 8.84 | g |
| Final fuel total CO2e | 51.91 | g |
| **Jet Fuel Transport** | | |
| Jet fuel transport (CO2e) | 0.69 | g |
| **End-of-life** | | |
| Jet fuel combustion CO2 | 73.16358 | g |
| Biogenic credit | -73.1636 | g |
| **No CCS - Total** | | |
| **No CCS - Total** | **52.60** | **g** |

| CCS - Total | | |
|---|---|---|
| Captured CO2 | -50.3329 | g |
| CCS emissions | 4.82075 | g |
| **CCS Total** | **7.09** | **g** |

| Include LUC - Total | | |
|---|---|---|
| LUC | 15.39 | g |
| **Total without CCS** | **67.99** | **g** |
| **Total with CCS** | **22.48** | **g** |

| Stover Ethanol to Jet Fuel | | |
|---|---|---|
| **Final Fuel Products** | | |
| SPK Jet Fuel | 1 | MJ |
| Gasoline | 0.21 | MJ |
| Low Sulfur Diesel | 0.12 | MJ |
| **Upstream Co-products** | | |
| Electricity | 0.161 | MJ |
| Electricity with CCS | 0.115 | MJ |

| Feedstock Emissions | | |
|---|---|---|
| Feedstock onsite CO2 | 4.38 | g |
| Feedstock upstream CO2 | 5.03 | g |
| Feedstock biogenic CO2 credit | -0.02 | g |
| Feedstock non-CO2 GHG (CO2e) | -3.41 | g |
| Feedstock total CO2e | 5.98 | g |
| **Feedstock Transport** | | |
| Feedstock transport (CO2e) | 9.03 | g |

| Ethanol Emissions | | |
|---|---|---|
| **Feedstock emissions allocated** | **15.02** | **g** |
| Ethanol onsite CO2 | 229.38 | g |
| Ethanol upstream CO2 | 15.40 | g |
| Ethanol biogenic CO2 credit | -229.14 | g |
| Ethanol non-CO2 GHG (CO2e) | 3.63 | g |
| Electricity credit | -20.51 | g |
| | | |
| Ethanol total CO2e | -1.25 | g |
| **Ethanol Transport** | | |
| Ethanol transport (CO2e) | 1.27 | g |

| Jet Fuel Emissions | | |
|---|---|---|
| **Ethanol emissions allocated** | **0.02** | **g** |
| Final fuel onsite CO2 | 7.97 | g |
| Final fuel upstream CO2 | 8.27 | g |
| Final fuel biogenic CO2 credit | -8.01 | g |
| Final fuel non-CO2 GHG (CO2e) | 0.62 | g |
| Gasoline credit | 0.00 | g |
| LS Diesel credit | 8.84 | g |
| Final fuel total CO2e | 0.02 | g |
| **Jet Fuel Transport** | | |
| Jet fuel transport (CO2e) | 0.69 | g |
| **End-of-life** | | |
| Jet fuel combustion CO2 | 73.16358 | g |
| Biogenic credit | -73.1636 | g |
| **No CCS - Total** | | |
| **No CCS - Total** | **0.71** | **g** |

| CCS - Total | | |
|---|---|---|
| Captured CO2 | -63.5211 | g |
| Parasitic load penalty | 5.838663 | g |
| **CCS Total** | **-56.97** | **g** |

| Include LUC - Total | | |
|---|---|---|
| LUC | -1.0668 | g |
| **Total without CCS** | **-0.36** | **g** |
| **Total with CCS** | **-58.04** | **g** |

| Sugarcane Ethanol to Jet Fuel | | |
|---|---|---|
| **Final Fuel Products** | | |
| SPK Jet Fuel | 1 | MJ |
| Gasoline | 0.21 | MJ |
| Low Sulfur Diesel | 0.12 | MJ |
| **Upstream Co-products** | | |
| Electricity | 0.493 | MJ |
| Electricity with CCS | 0.442 | MJ |

| Feedstock Emissions | | |
|---|---|---|
| Feedstock onsite CO2 | 33.99 | 0 |
| Feedstock upstream CO2 | 5.11 | 0 |
| Feedstock biogenic CO2 credit | -30.39 | 0 |
| Feedstock non-CO2 GHG (CO2e) | 11.59 | 0 |
| Feedstock total CO2e | 20.31 | 0 |
| **Feedstock Transport** | | |
| Feedstock transport (CO2e) | 39.79 | g |

| Ethanol Emissions | | |
|---|---|---|
| **Feedstock emissions allocated** | **60.09** | **g** |
| Ethanol onsite CO2 | 376.72 | g |
| Ethanol upstream CO2 | 11.81 | g |
| Ethanol biogenic CO2 credit | -377.05 | g |
| Ethanol non-CO2 GHG (CO2e) | 4.51 | g |
| Electricity credit | -29.70 | g |
| | | |
| Ethanol total CO2e | 46.39 | g |
| **Ethanol Transport** | | |
| Ethanol transport (CO2e) | 1.27 | g |

| Jet Fuel Emissions | | |
|---|---|---|
| **Ethanol emissions allocated** | **35.84** | **g** |
| Final fuel onsite CO2 | 7.97 | g |
| Final fuel upstream CO2 | 8.27 | g |
| Final fuel biogenic CO2 credit | -8.01 | g |
| Final fuel non-CO2 GHG (CO2e) | 0.62 | g |
| Gasoline credit | 0.00 | g |
| LS Diesel credit | 8.84 | g |
| Final fuel total CO2e | 35.84 | g |
| **Jet Fuel Transport** | | |
| Jet fuel transport (CO2e) | 1.62 | g |
| **End-of-life** | | |
| Jet fuel combustion CO2 | 73.16358 | g |
| Biogenic credit | -73.1636 | g |
| **No CCS - Total** | | |
| **No CCS - Total** | **37.46** | **g** |

| CCS - Total | | |
|---|---|---|
| Captured CO2 | -70.0981 | g |
| Parasitic load penalty | 3.042959 | g |
| **CCS Total** | **-29.60** | **g** |

| Include LUC - Total | | |
|---|---|---|
| LUC | 17.582 | g |
| **Total without CCS** | **55.04** | **g** |
| **Total with CCS** | **-12.02** | **g** |

**Figure C6** Screenshot of ATJ tabular data taken from Excel model.

## C2.2 HEFA

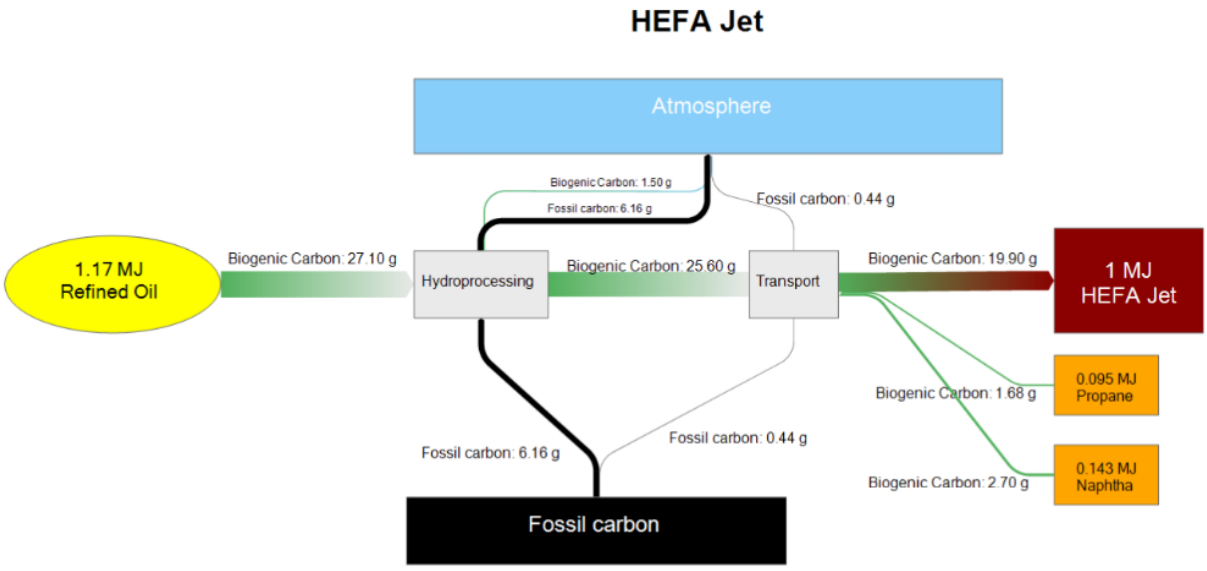


**Figure C7** HEFA Jet fuel from refined fats and oils carbon flow diagram

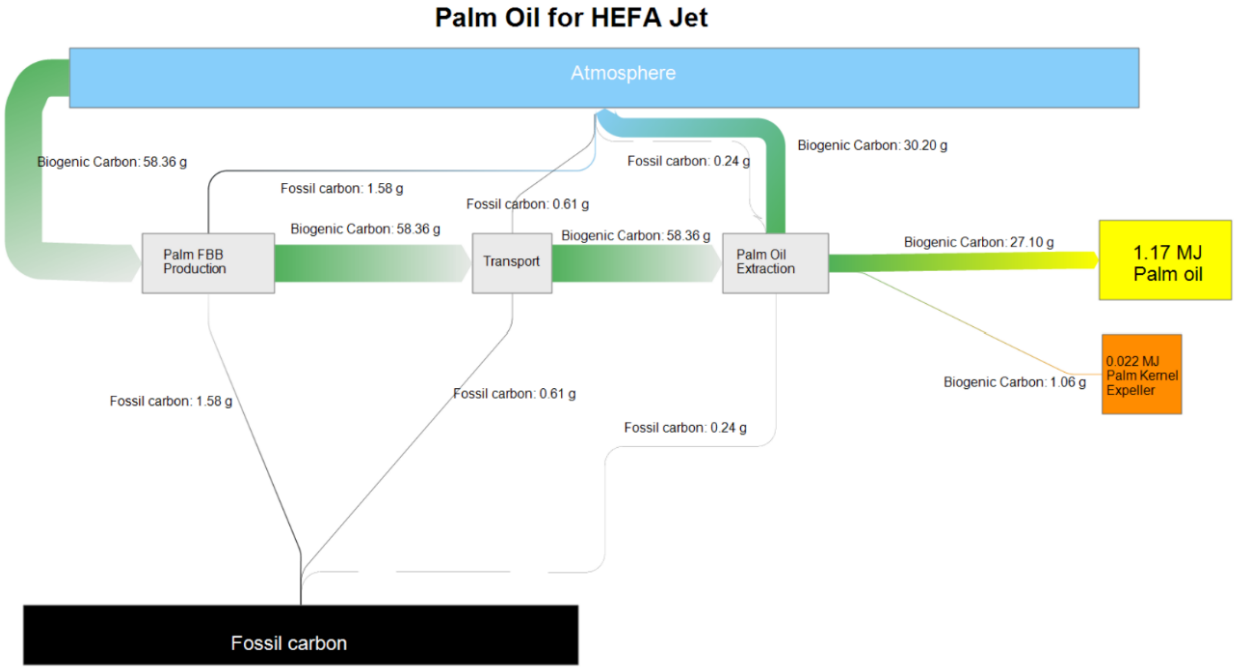


**Figure C8** Palm Oil carbon flow diagram

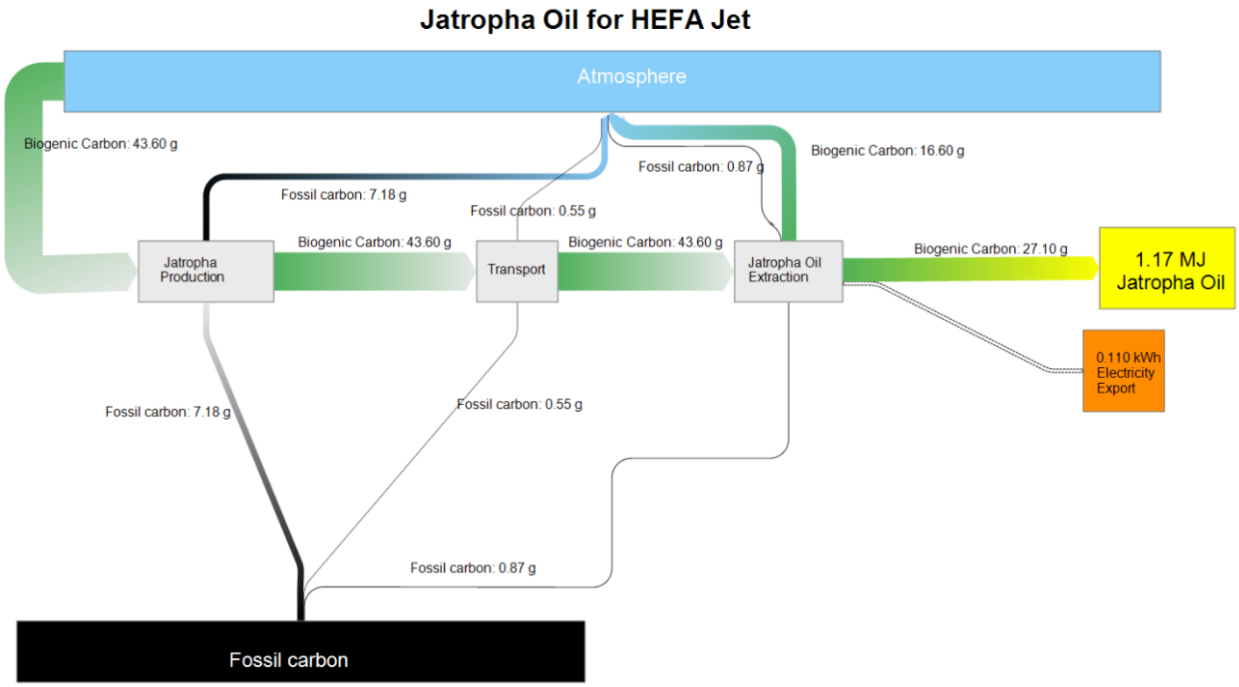


**Figure C9** Jatropha Oil carbon flow diagram

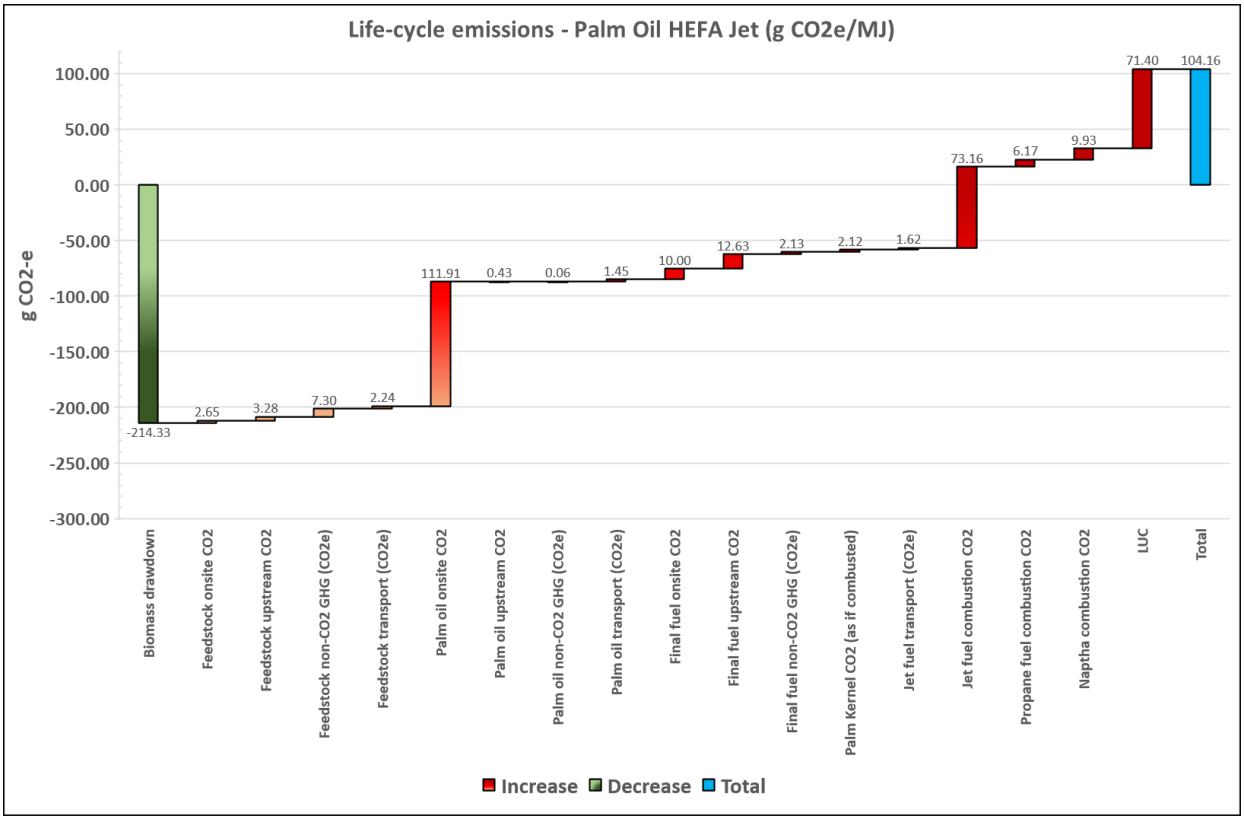


**Figure C10** Waterfall diagram for Palm Oil HEFA SAF emissions - illustrates carbon uptake in biomass (initial green bar) and sources of emissions and removals along product supply chain. First total (blue) represents net emissions, not including co-product credits or allocation. Without credits and co-product allocation, these totals will not match LCA total. Figure represents physical processes only. Degradable or combustible products and co-products are assumed to return to the atmosphere as $CO_2$.

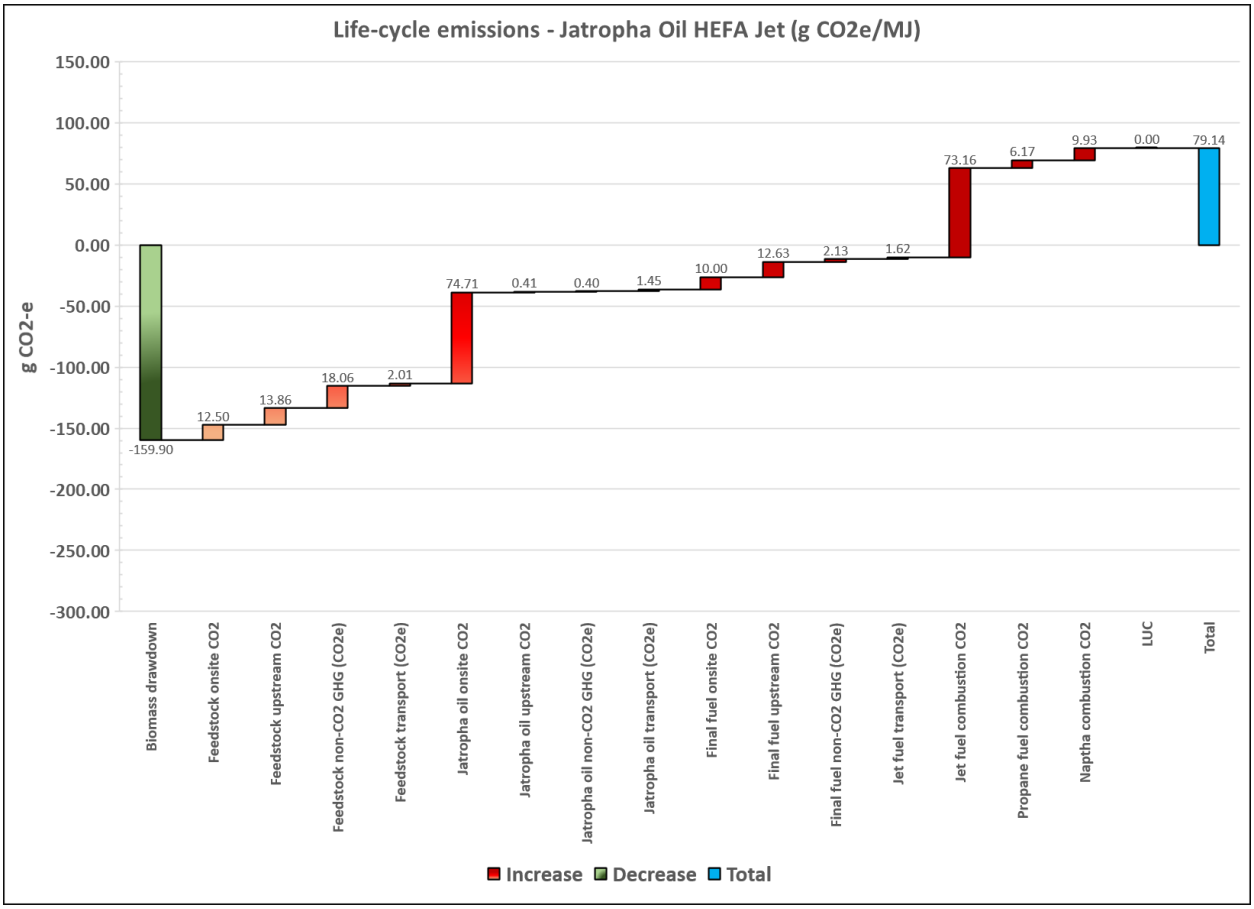


**Figure C11** Waterfall diagram for Jatropha Oil HEFA SAF emissions - illustrates carbon uptake in biomass (initial green bar) and sources of emissions and removals along product supply chain. First total (blue) represents net emissions, not including co-product credits or allocation. Without credits and co-product allocation, these totals will not match LCA total. Figure represents physical processes only. Degradable or combustible products and co-products are assumed to return to the atmosphere as $CO_2$.

| HEFA Jet from Palm FBB | | |
|---|---|---|
| **Final Fuel Products** | | |
| SPK Jet Fuel | 1 | MJ |
| Propane | 0.10 | MJ |
| Naptha | 0.14 | MJ |
| **Upstream Co-products** | | |
| Palm Kernel | 3.613 | g |
| **Feedstock Emissions** | | |
| Feedstock onsite CO2 | 2.65 | g |
| Feedstock upstream CO2 | 3.28 | g |
| Feedstock biogenic CO2 credit | 0.00 | g |
| Feedstock non-CO2 GHG (CO2e) | 7.30 | g |
| Feedstock total CO2e | 13.23 | g |
| **Feedstock Transport** | | |
| Feedstock transport (CO2e) | 2.24 | g |
| **Palm Oil Emissions** | | |
| **Feedstock emissions allocated** | **15.16** | **g** |
| Palm oil onsite CO2 | 111.91 | g |
| Palm oil upstream CO2 | 0.43 | g |
| Palm oil biogenic CO2 credit | -111.01 | g |
| Palm oil non-CO2 GHG (CO2e) | 0.06 | g |
| | | |
| Palm oil total CO2e | 16.55 | g |
| **Ethanol Transport** | | |
| Palm oil transport (CO2e) | 1.45 | g |
| **Jet Fuel Emissions** | | |
| **Palm oil emissions allocated** | **14.54** | **g** |
| Final fuel onsite CO2 | 8.07 | g |
| Final fuel upstream CO2 | 10.20 | g |
| Final fuel biogenic CO2 credit | -0.01 | g |
| Final fuel non-CO2 GHG (CO2e) | 1.72 | g |
| Propane displacement credit | 0.00 | g |
| Naptha displacement credit | 0.00 | g |
| Final fuel total CO2e | 34.53 | g |
| **Jet Fuel Transport** | | |
| Jet fuel transport (CO2e) | 1.62 | g |
| **End-of-life** | | |
| Jet fuel combustion CO2 | 73.16358 | g |
| Biogenic credit | -73.1636 | g |
| **No CCS - Total** | | |
| **No CCS - Total** | **36.15** | **g** |
| **Include LUC - Total** | | |
| LUC | 71.4 | g |
| **Total without CCS** | **107.55** | **g** |

| HEFA Jet from Jatropha | | |
|---|---|---|
| **Final Fuel Products** | | |
| SPK Jet Fuel | 1.00 | MJ |
| Propane | 0.10 | MJ |
| Naptha | 0.14 | MJ |
| **Upstream Co-products** | | |
| Electricity | 0.397 | MJ |
| **Feedstock Emissions** | | |
| Feedstock onsite CO2 | 12.50 | g |
| Feedstock upstream CO2 | 13.86 | g |
| Feedstock biogenic CO2 credit | -0.03 | g |
| Feedstock non-CO2 GHG (CO2e) | 18.06 | g |
| Feedstock total CO2e | 44.39 | g |
| **Feedstock Transport** | | |
| Feedstock transport (CO2e) | 2.01 | g |
| **Jatropha Oil Emissions** | | |
| **Feedstock emissions allocated** | **46.40** | **g** |
| Jatropha oil onsite CO2 | 74.71 | g |
| Jatropha oil upstream CO2 | 0.41 | g |
| Jatropha oil biogenic CO2 credit | -71.50 | g |
| Jatropha oil non-CO2 GHG (CO2e) | 0.40 | g |
| Electricity credit | -51.29 | g |
| Jatropha oil total CO2e | -0.87 | g |
| **Ethanol Transport** | | |
| Jatropha oil transport (CO2e) | 1.45 | g |
| **Jet Fuel Emissions** | | |
| **Jatropha oil emissions allocated** | **0.47** | **g** |
| Final fuel onsite CO2 | 8.07 | g |
| Final fuel upstream CO2 | 10.20 | g |
| Final fuel biogenic CO2 credit | -0.01 | g |
| Final fuel non-CO2 GHG (CO2e) | 1.72 | g |
| Propane displacement credit | 0.00 | g |
| Naptha displacement credit | 0.00 | g |
| Final fuel total CO2e | 20.46 | g |
| **Jet Fuel Transport** | | |
| Jet fuel transport (CO2e) | 1.62 | g |
| **End-of-life** | | |
| Jet fuel combustion CO2 | 73.16358 | g |
| Biogenic credit | -73.1636 | g |
| **No CCS - Total** | | |
| **No CCS - Total** | **22.08** | **g** |
| **Include LUC - Total** | | |
| LUC | 0 | g |
| **Total without CCS** | **22.08** | **g** |

**Figure C12** Snapshot of Palm Oil HEFA and Jatropha HEFA tabular data

| HEFA Jet from Waste Oil | | |
|---|---|---|
| **Final Fuel Products** | | |
| SPK Jet Fuel | 1.00 | MJ |
| Propane | 0.14 | MJ |
| Naptha | 0.11 | MJ |
| **Upstream Co-products** | | |
| Electricity | 0.000 | MJ |

| **Feedstock Emissions** | | |
|---|---|---|
| Waste oil collection | 10.37 | g |
| | 0.00 | g |
| | 0.00 | g |
| | 1.15 | g |
| Feedstock total CO2e | 11.52 | g |
| **Feedstock Transport** | | |
| Feedstock transport (CO2e) | 0.00 | g |

| **Waste Oil Purification Emissions** | | |
|---|---|---|
| **Feedstock emissions allocated** | **11.52** | **g** |
| Purification onsite CO2 | 0.00 | g |
| | 0.00 | g |
| | 0.00 | g |
| | 0.00 | g |
| | 0.00 | g |
| Waste oil total CO2e | 11.52 | g |
| **Ethanol Transport** | | |
| Waste oil transport (CO2e) | 1.45 | g |

| **Jet Fuel Emissions** | | |
|---|---|---|
| **Waste oil emissions allocated** | **10.48** | **g** |
| Final fuel onsite CO2 | 8.07 | g |
| Final fuel upstream CO2 | 10.20 | g |
| Final fuel biogenic CO2 credit | -0.01 | g |
| Final fuel non-CO2 GHG (CO2e) | 1.72 | g |
| Propane displacement credit | 0.00 | g |
| Naptha displacement credit | 0.00 | g |
| Final fuel total CO2e | 30.47 | g |
| **Jet Fuel Transport** | | |
| Jet fuel transport (CO2e) | 0.69 | g |
| **End-of-life** | | |
| Jet fuel combustion CO2 | 73.16358 | g |
| Biogenic credit | -73.1636 | g |
| **No CCS - Total** | | |
| **No CCS - Total** | **31.16** | **g** |

| **Include LUC - Total** | | |
|---|---|---|
| LUC | 0 | g |
| **Total without CCS** | **31.16** | **g** |

| HEFA Jet from Soybean | | |
|---|---|---|
| **Final Fuel Products** | | |
| SPK Jet Fuel | 1.00 | MJ |
| Propane | 0.14 | MJ |
| Naptha | 0.11 | MJ |
| **Upstream Co-products** | | |
| Soybean Meal | 1.529 | MJ |

| **Feedstock Emissions** | | |
|---|---|---|
| Feedstock onsite CO2 | 8.42 | g |
| Feedstock upstream CO2 | 7.63 | g |
| Feedstock biogenic CO2 credit | -0.01 | g |
| Feedstock non-CO2 GHG (CO2e) | 32.20 | g |
| Feedstock total CO2e | 48.24 | g |
| **Feedstock Transport** | | |
| Feedstock transport (CO2e) | 3.36 | g |

| **Soy Oil Emissions** | | |
|---|---|---|
| **Feedstock emissions allocated** | **22.18** | **g** |
| Soy oil onsite CO2 | 9.99 | g |
| Soy oil upstream CO2 | 3.27 | g |
| Soy oil biogenic CO2 credit | -0.03 | g |
| Soy oil non-CO2 GHG (CO2e) | 1.04 | g |
| Soy meal credit | 0.00 | g |
| Soy oil total CO2e | 36.45 | g |
| **Ethanol Transport** | | |
| Ethanol transport (CO2e) | 1.45 | g |

| **Jet Fuel Emissions** | | |
|---|---|---|
| **Soy oil emissions allocated** | **30.61** | **g** |
| Final fuel onsite CO2 | 8.07 | g |
| Final fuel upstream CO2 | 10.20 | g |
| Final fuel biogenic CO2 credit | -0.01 | g |
| Final fuel non-CO2 GHG (CO2e) | 1.72 | g |
| Propane displacement credit | 0.00 | g |
| Naptha displacement credit | 0.00 | g |
| Final fuel total CO2e | 50.60 | g |
| **Jet Fuel Transport** | | |
| Jet fuel transport (CO2e) | 0.69 | g |
| **End-of-life** | | |
| Jet fuel combustion CO2 | 73.16358 | g |
| Biogenic credit | -73.1636 | g |
| **No CCS - Total** | | |
| **No CCS - Total** | **51.30** | **g** |

| **Include LUC - Total** | | |
|---|---|---|
| LUC | 29.77 | g |
| **Total without CCS** | **81.07** | **g** |

**Figure C13** Snapshot of UCO HEFA and Soy Oil HEFA tabular data

## C2.3 HDCJ

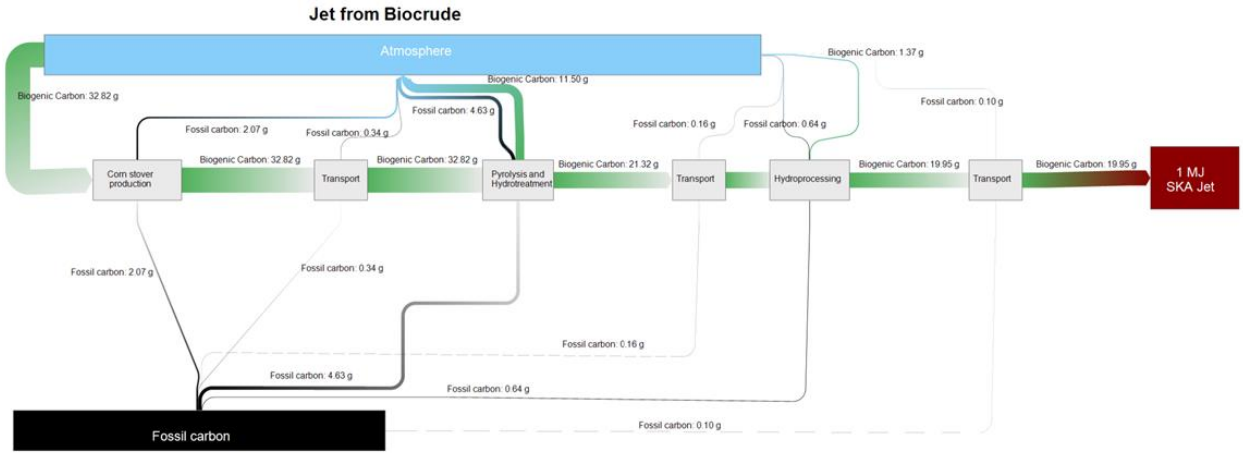


**Figure C14** Integrated Corn Stover to Pyrolysis Oil to SAF carbon flow diagram

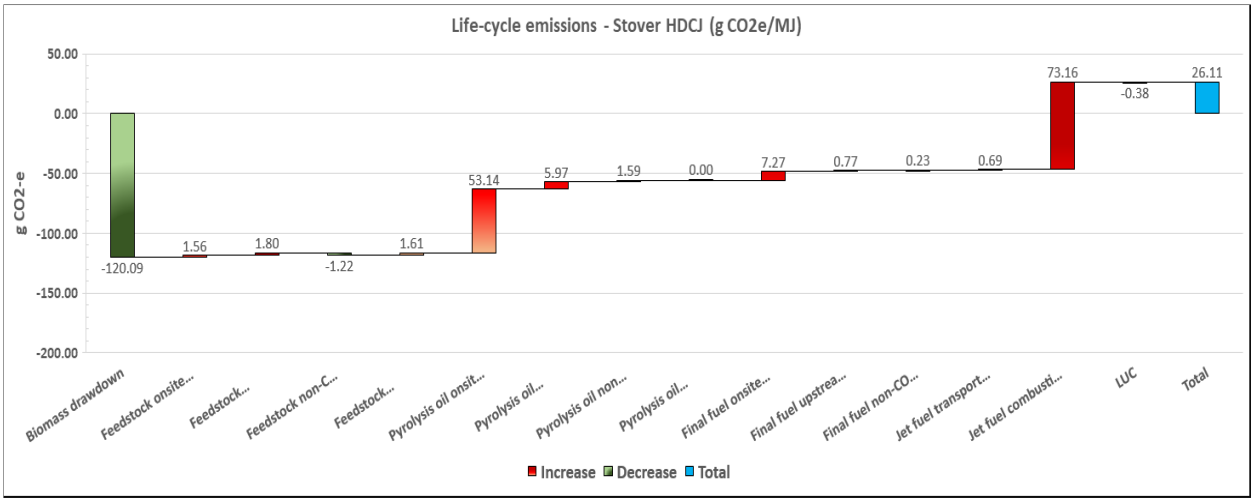


**Figure C15** Waterfall diagram for Stover HDCJ SAF emissions - illustrates carbon uptake in biomass (initial green bar) and sources of emissions and removals along product supply chain. First total (blue) represents net emissions, not including co-product credits or allocation. There are no credits or co-product allocations, thus this set of waterfalls closely resembles final LCA calculations. Degradable or combustible products and co-products are assumed to return to the atmosphere as $CO_2$.

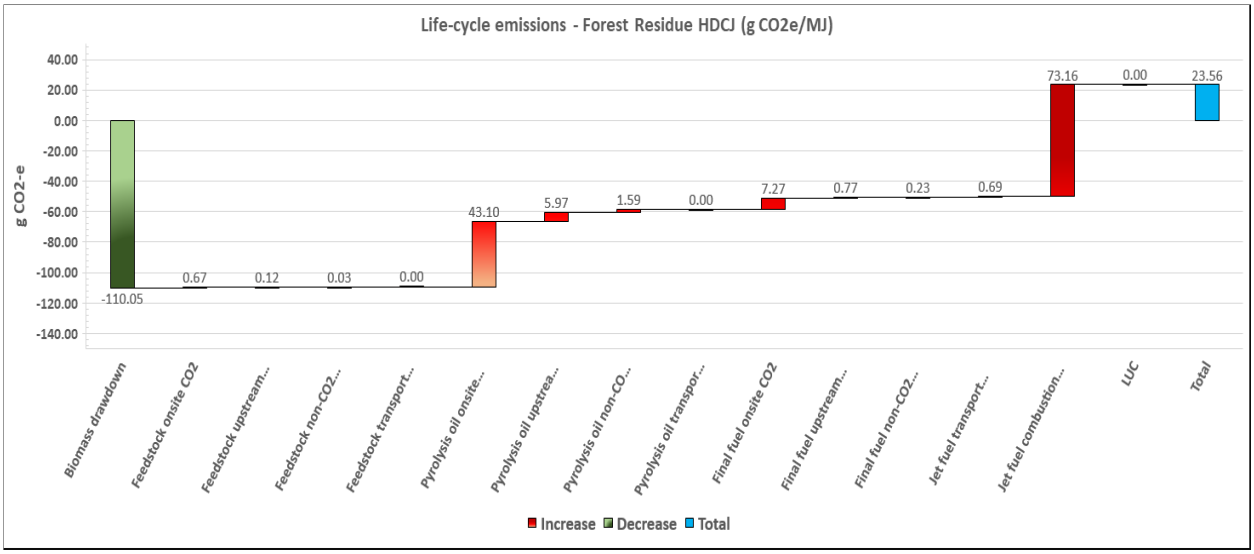


**Figure C16** Waterfall diagram for Forest Residue HDCJ SAF emissions - illustrates carbon uptake in biomass (initial green bar) and sources of emissions and removals along product supply chain. First total (blue) represents net emissions, not including co-product credits or allocation. There are no credits or co-product allocations, thus this set of waterfalls closely resembles final LCA calculations. Degradable or combustible products and co-products are assumed to return to the atmosphere as $CO_2$.

| Stover Biocrude to Jet Fuel | | |
|---|---|---|
| **Final Fuel Products** | | |
| SKA Jet Fuel | 1 | MJ |
| **Feedstock Emissions** | | |
| Feedstock onsite CO2 | 1.56 | g |
| Feedstock upstream CO2 | 1.80 | g |
| Feedstock biogenic CO2 credit | -0.01 | g |
| Feedstock non-CO2 GHG (CO2e) | -1.22 | g |
| Feedstock total CO2e | 2.14 | g |
| **Feedstock Transport** | | |
| Feedstock transport (CO2e) | 1.61 | g |
| **Hydrotreated Pyrolysis Oil Emissions** | | |
| **Feedstock emissions allocated** | **3.75** | **g** |
| Pyrolysis oil onsite CO2 | 53.14 | g |
| Pyrolysis oil upstream CO2 | 5.97 | g |
| Pyrolysis oil biogenic CO2 credit | -42.10 | g |
| Pyrolysis oil non-CO2 GHG (CO2e) | 1.59 | g |
| Pyrolysis oil total CO2e | 22.35 | g |
| **Ethanol Transport** | | |
| Pyrolysis oil transport (CO2e) | 0.00 | g |
| **Jet Fuel Emissions** | | |
| **Py-oil emissions allocated** | **22.35** | **g** |
| Final fuel onsite CO2 | 7.27 | g |
| Final fuel upstream CO2 | 0.77 | g |
| Final fuel biogenic CO2 credit | -4.92 | g |
| Final fuel non-CO2 GHG (CO2e) | 0.23 | g |
| Final fuel total CO2e | 25.71 | g |
| **Jet Fuel Transport** | | |
| Jet fuel transport (CO2e) | 0.69 | g |
| **End-of-life** | | |
| Jet fuel combustion CO2 | 73.16358 | g |
| Biogenic credit | -73.1636 | g |
| **No CCS - Total** | | |
| **No CCS - Total** | **26.40** | **g** |
| **Include LUC - Total** | | |
| LUC | -0.381 | g |
| **Total without CCS** | **26.02** | **g** |

| Forest Residue Biocrude to Jet Fuel | | |
|---|---|---|
| **Final Fuel Products** | | |
| SKA Jet Fuel | 1 | MJ |
| **Feedstock Emissions** | | |
| Feedstock onsite CO2 | 0.67 | g |
| Feedstock upstream CO2 | 0.12 | g |
| Feedstock biogenic CO2 credit | 0.00 | g |
| Feedstock non-CO2 GHG (CO2e) | 0.03 | g |
| Feedstock total CO2e | 0.83 | g |
| **Feedstock Transport** | | |
| Feedstock transport (CO2e) | 1.37 | g |
| **Hydrotreated Pyrolysis Oil Emissions** | | |
| **Feedstock emissions allocated** | **2.20** | **g** |
| Pyrolysis oil onsite CO2 | 43.10 | g |
| Pyrolysis oil upstream CO2 | 5.97 | g |
| Pyrolysis oil biogenic CO2 credit | -32.05 | g |
| Pyrolysis oil non-CO2 GHG (CO2e) | 1.59 | g |
| Pyrolysis oil total CO2e | 20.80 | g |
| **Ethanol Transport** | | |
| Pyrolysis oil transport (CO2e) | 0.00 | g |
| **Jet Fuel Emissions** | | |
| **Py-oil emissions allocated** | **20.80** | **g** |
| Final fuel onsite CO2 | 7.27 | g |
| Final fuel upstream CO2 | 0.77 | g |
| Final fuel biogenic CO2 credit | -4.92 | g |
| Final fuel non-CO2 GHG (CO2e) | 0.23 | g |
| Final fuel total CO2e | 24.15 | g |
| **Jet Fuel Transport** | | |
| Jet fuel transport (CO2e) | 0.69 | g |
| **End-of-life** | | |
| Jet fuel combustion CO2 | 73.16358 | g |
| Biogenic credit | -73.1636 | g |
| **No CCS - Total** | | |
| **No CCS - Total** | **24.85** | **g** |
| **Include LUC - Total** | | |
| LUC | 0 | g |
| **Total without CCS** | **24.85** | **g** |

| RDF Biocrude to Jet Fuel | | |
|---|---|---|
| **Final Fuel Products** | | |
| SKA Jet Fuel | 1 | MJ |
| **Feedstock Emissions** | | |
| Feedstock onsite CO2 | 1.24 | 0 |
| Feedstock upstream CO2 | 0.00 | 0 |
| Feedstock biogenic CO2 credit | 0.00 | 0 |
| Feedstock non-CO2 GHG (CO2e) | -55.87 | 0 |
| Feedstock total CO2e | -54.63 | 0 |
| **Feedstock Transport** | | |
| Feedstock transport (CO2e) | 1.84 | g |
| **Hydrotreated Pyrolysis Oil Emissions** | | |
| **Feedstock emissions allocated** | **-52.79** | **g** |
| Pyrolysis oil onsite CO2 | 43.10 | g |
| Pyrolysis oil upstream CO2 | 5.97 | g |
| Pyrolysis oil biogenic CO2 credit | -32.05 | g |
| Pyrolysis oil non-CO2 GHG (CO2e) | 1.59 | g |
| Pyrolysis oil total CO2e | -34.19 | g |
| **Ethanol Transport** | | |
| Pyrolysis oil transport (CO2e) | 0.00 | g |
| **Jet Fuel Emissions** | | |
| **Py-oil emissions allocated** | **-34.19** | **g** |
| Final fuel onsite CO2 | 7.27 | g |
| Final fuel upstream CO2 | 0.77 | g |
| Final fuel biogenic CO2 credit | -4.92 | g |
| Final fuel non-CO2 GHG (CO2e) | 0.23 | g |
| Final fuel total CO2e | -30.83 | g |
| **Jet Fuel Transport** | | |
| Jet fuel transport (CO2e) | 0.69 | g |
| **End-of-life** | | |
| Jet fuel combustion CO2 | 73.16358 | g |
| Biogenic credit | -73.1636 | g |
| **No CCS - Total** | | |
| **No CCS - Total** | **-30.14** | **g** |
| **Include LUC - Total** | | |
| LUC | 0 | g |
| **Total without CCS** | **-30.14** | **g** |

**Figure C17** Snapshot of HDCJ SAF tabular data

## C2.4 FT Jet

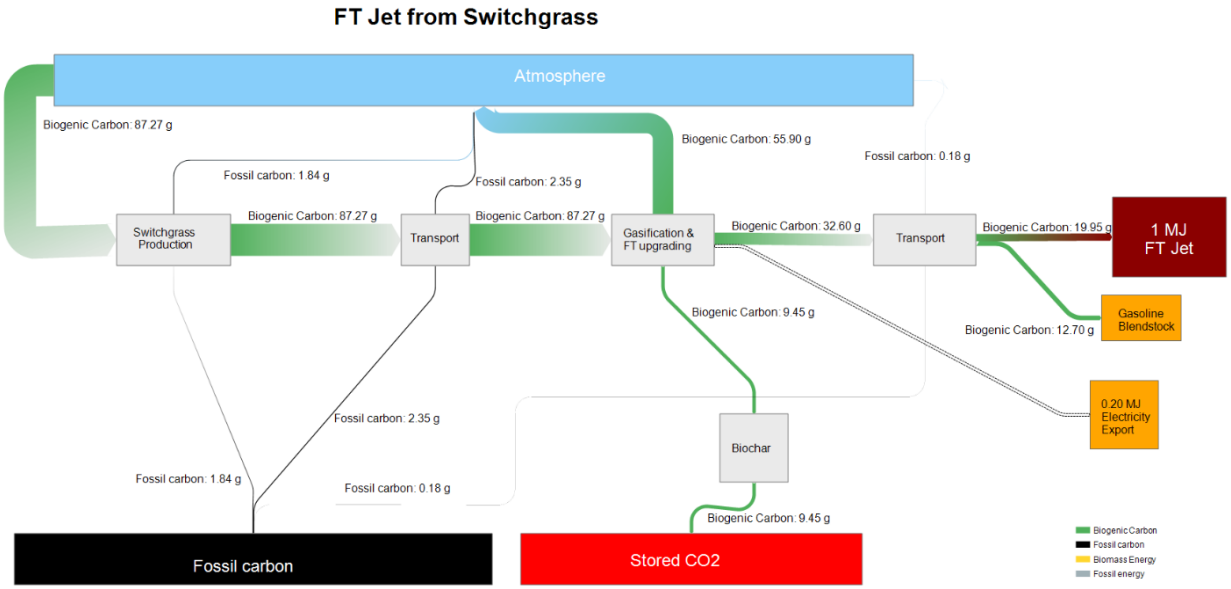


**Figure C18** Switchgrass Fischer-Tropsch to SAF carbon flow diagram

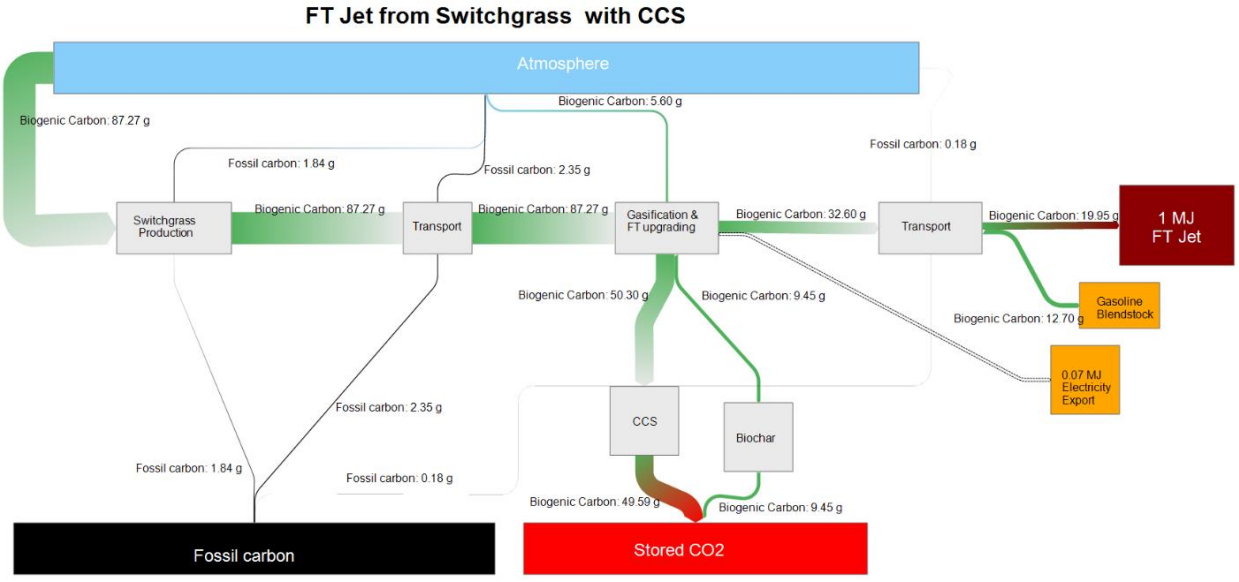


**Figure C19** Switchgrass Fischer-Tropsch to SAF with CCS carbon flow diagram

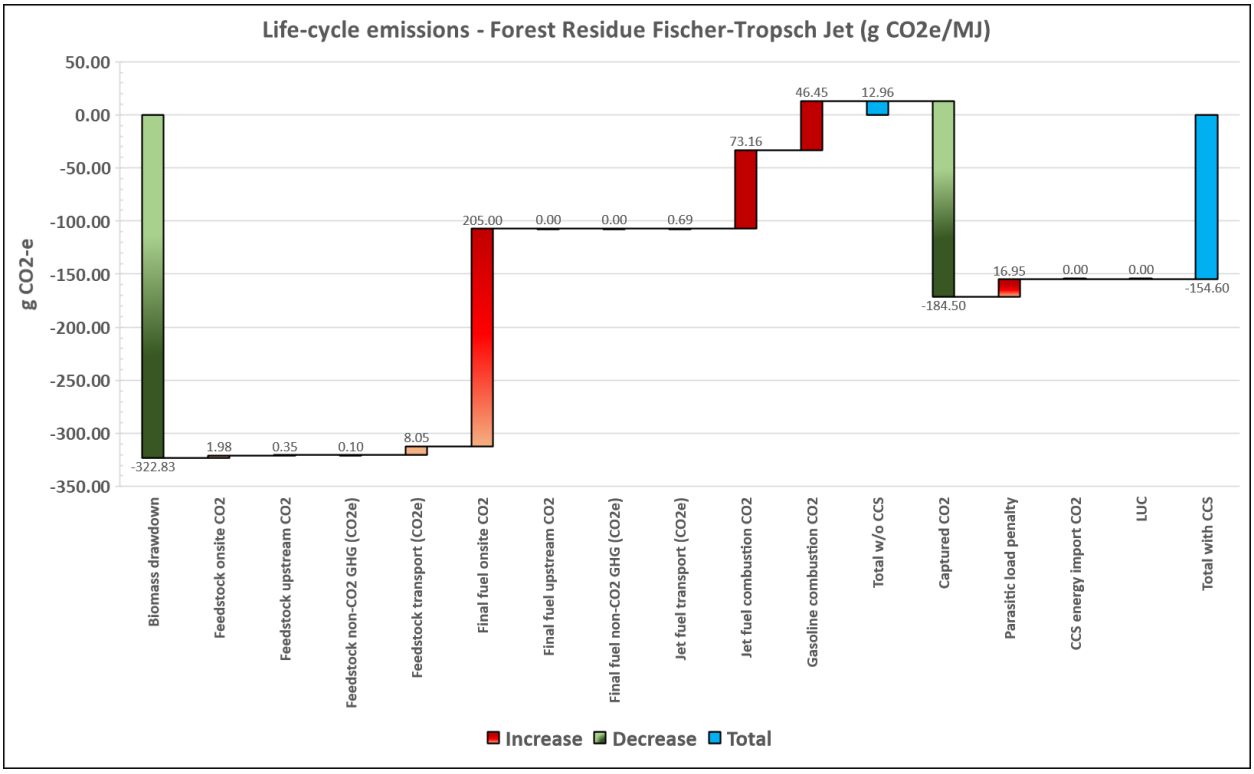


**Figure C20** Waterfall diagram for Forest Residue FT SAF emissions - illustrates carbon uptake in biomass (initial green bar) and sources of emissions and removals along product supply chain. First total (blue) represents net emissions, not including co-product credits or allocation, without CCS. To the right of the first total, CCS capture and LUC impacts are added in. Without credits and co-product allocation, these totals will not match LCA total. Figure represents physical processes only. Degradable or combustible products and co-products are assumed to return to the atmosphere as $CO_2$

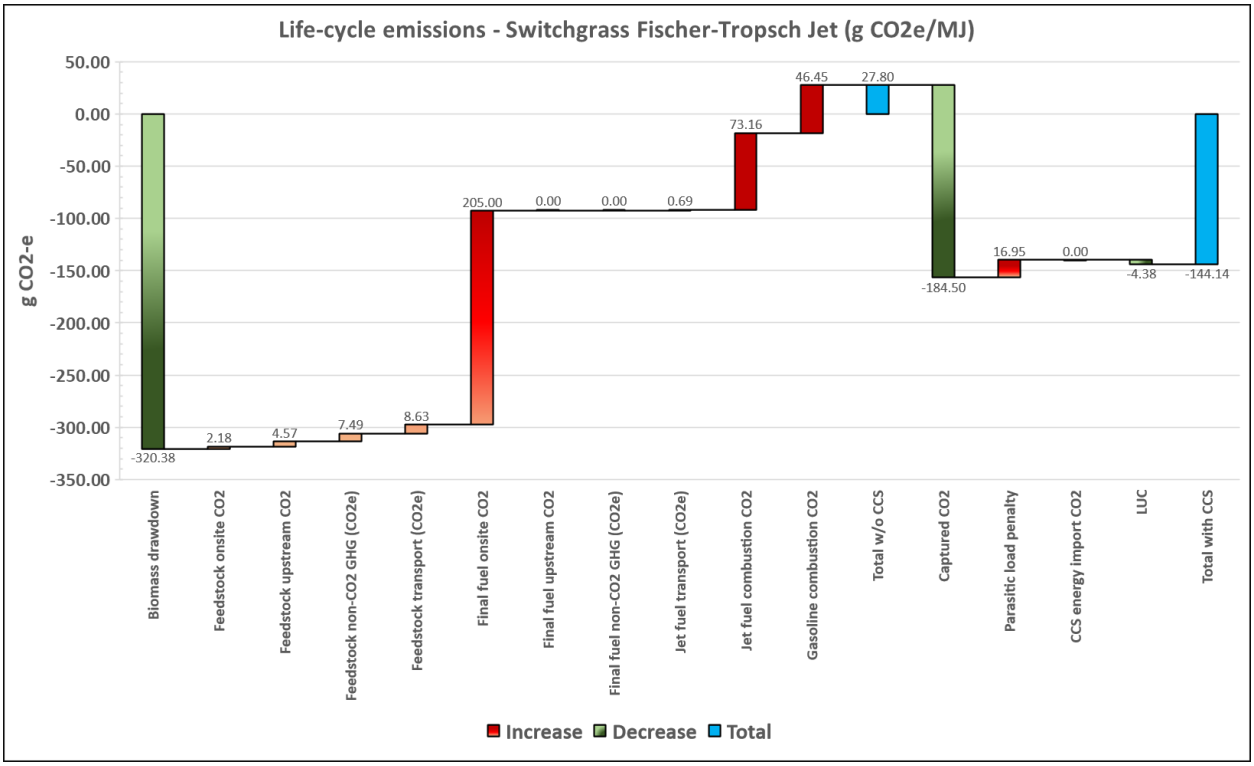


**Figure C21** Waterfall diagram for Switchgrass FT SAF emissions - illustrates carbon uptake in biomass (initial green bar) and sources of emissions and removals along product supply chain. First total (blue) represents net emissions, not including co-product credits or allocation, without CCS. To the right of the first total, CCS capture, and LUC impacts are added in. Without credits and co-product allocation, these totals will not match LCA total. Figure represents physical processes only. Degradable or combustible products and co-products are assumed to return to the atmosphere as $CO_2$

| Forest Residue to FT Jet Fuel | | |
|---|---|---|
| **Final Fuel Products** | | |
| FT Jet | 1.00 | MJ |
| Gasoline | 0.64 | MJ |
| Electricity | 0.20 | MJ |
| Electricity with CCS | 0.13 | MJ |
| Biochar | 0.21 | MJ |
| **Feedstock Emissions** | | |
| Feedstock onsite CO2 | 1.98 | g |
| Feedstock upstream CO2 | 0.35 | g |
| Feedstock biogenic CO2 credit | 0.00 | g |
| Feedstock non-CO2 GHG (CO2e) | 0.10 | g |
| Feedstock total CO2e | 2.43 | g |
| **Feedstock Transport** | | |
| Feedstock transport (CO2e) | 8.05 | g |
| **Jet Fuel Emissions** | | |
| **Feedstock emissions allocated** | **5.70** | **g** |
| Final fuel onsite CO2 | 111.47 | g |
| Final fuel upstream CO2 | 0.00 | g |
| Final fuel biogenic CO2 credit | -111.47 | g |
| Final fuel non-CO2 GHG (CO2e) | 0.00 | g |
| Electricity displacement credit | 0.00 | g |
| Gasoline displacement credit | 0.00 | g |
| Final fuel total CO2e | 5.70 | g |
| **Jet Fuel Transport** | | |
| Jet fuel transport (CO2e) | 0.69 | g |
| **End-of-life** | | |
| Jet fuel combustion CO2 | 73.16358 | g |
| Biogenic credit | -73.1636 | g |
| **No CCS - Total** | | |
| **No CCS - Total** | **6.39** | **g** |
| **CCS - Total** | | |
| Captured CO2 | -100.326 | g |
| Parasitic load penalty | -6.07 | g |
| CCS energy import CO2 | 0.00 | g |
| **CCS Total** | **-100.01** | **g** |
| **Include LUC - Total** | | |
| LUC | 0 | g |
| **Total without CCS** | **6.39** | **g** |
| **Total with CCS** | **-100.01** | **g** |

| Switchgrass to FT Jet Fuel | | |
|---|---|---|
| **Final Fuel Products** | | |
| FT Jet | 1.00 | MJ |
| Gasoline | 0.64 | MJ |
| Electricity | 0.20 | MJ |
| Electricity with CCS | 0.13 | MJ |
| Biochar | 0.21 | MJ |
| **Feedstock Emissions** | | |
| Feedstock onsite CO2 | 2.18 | g |
| Feedstock upstream CO2 | 4.57 | g |
| Feedstock biogenic CO2 credit | -0.01 | g |
| Feedstock non-CO2 GHG (CO2e) | 7.49 | g |
| Feedstock total CO2e | 14.23 | g |
| **Feedstock Transport** | | |
| Feedstock transport (CO2e) | 8.63 | g |
| **Jet Fuel Emissions** | | |
| **Feedstock emissions allocated** | **12.43** | **g** |
| Final fuel onsite CO2 | 111.47 | g |
| Final fuel upstream CO2 | 0.00 | g |
| Final fuel biogenic CO2 credit | -111.47 | g |
| Final fuel non-CO2 GHG (CO2e) | 0.00 | g |
| Electricity displacement credit | 0.00 | g |
| Gasoline displacement credit | 0.00 | g |
| Final fuel total CO2e | 12.43 | g |
| **Jet Fuel Transport** | | |
| Jet fuel transport (CO2e) | 0.69 | g |
| **End-of-life** | | |
| Jet fuel combustion CO2 | 73.16358 | g |
| Biogenic credit | -73.1636 | g |
| **No CCS - Total** | | |
| **No CCS - Total** | **13.12** | **g** |
| **CCS - Total** | | |
| Captured CO2 | -100.326 | g |
| Parasitic load penalty | -6.07 | g |
| CCS energy import CO2 | 0.00 | g |
| **CCS Total** | **-93.28** | **g** |
| **Include LUC - Total** | | |
| LUC | -4.38285 | g |
| **Total without CCS** | **8.74** | **g** |
| **Total with CCS** | **-97.66** | **g** |

| RDF to FT Jet Fuel | | |
|---|---|---|
| **Final Fuel Products** | | |
| FT Jet | 1.00 | MJ |
| Gasoline | 0.64 | MJ |
| Electricity | 0.20 | MJ |
| Electricity with CCS | 0.13 | MJ |
| Biochar | 0.21 | MJ |
| **Feedstock Emissions** | | |
| Feedstock onsite CO2 | 3.65 | g |
| Feedstock upstream CO2 | 0.00 | g |
| Feedstock biogenic CO2 credit | 0.00 | g |
| Feedstock non-CO2 GHG (CO2e) | -163.90 | g |
| Feedstock total CO2e | -160.25 | g |
| **Feedstock Transport** | | |
| Feedstock transport (CO2e) | 10.79 | g |
| **Jet Fuel Emissions** | | |
| **Feedstock emissions allocated** | **-81.27** | **g** |
| Final fuel onsite CO2 | 111.47 | g |
| Final fuel upstream CO2 | 0.00 | g |
| Final fuel biogenic CO2 credit | -111.47 | g |
| Final fuel non-CO2 GHG (CO2e) | 0.00 | g |
| Electricity displacement credit | 0.00 | g |
| Gasoline displacement credit | 0.00 | g |
| Final fuel total CO2e | -81.27 | g |
| **Jet Fuel Transport** | | |
| Jet fuel transport (CO2e) | 0.69 | g |
| **End-of-life** | | |
| Jet fuel combustion CO2 | 73.16358 | g |
| Biogenic credit | -73.1636 | g |
| **No CCS - Total** | | |
| **No CCS - Total** | **-80.57** | **g** |
| **CCS - Total** | | |
| Captured CO2 | -100.326 | g |
| Parasitic load penalty | -6.07 | g |
| CCS energy import CO2 | 0.00 | g |
| **CCS Total** | **-186.97** | **g** |
| **Include LUC - Total** | | |
| LUC | 0 | g |
| **Total without CCS** | **-80.57** | **g** |
| **Total with CCS** | **-186.97** | **g** |

**Figure C22** Snapshot of FT SAF tabular data

## C2.5 Air to Fuels

| ATF - H2 / CO2 Separate Electrolysis / FT | | |
|---|---|---|
| **Final Fuel Products** | | |
| FT Jet | 1.00 | MJ |
| Gasoline | 0.64 | MJ |
| Electricity | 0.20 | MJ |
| Electricity with CCS | 0.13 | MJ |

| Direct Air Capture Block | | |
|---|---|---|
| Direct Emissions | 0.01 | kgCO2e/kgCO2 captured |
| Embodied Em. DAC | 0.00 | kgCO2e/kgCO2 captured |
| Embodied Em. Energy | 0.00 | kgCO2e/kgCO2 captured |
| Nat. Gas Supply Chain CO2 | 0.05 | kgCO2e/kgCO2 captured |
| Methane Leakage | 0.12 | kgCO2e/kgCO2 captured |
| CO2 requirement | 0.07 | kgCO2 captured/MJ fuel |
| **Total** | **12.86** | **gCO2e/MJ fuel** |

| Hydrogen Electrolysis Block | | |
|---|---|---|
| One time upstream | 75.87 | kgCO2e/kW |
| Ongoing | 16.73 | kgCO2e/kW |
| Lifetime | 20 | years |
| Electrolyzer Efficiency | 52.28 | kWh/kg H2 |
| Electrolyzer Operating | 8585 | hrs/yr |
| H2 Requirement | 0.00667 | kg H2/ MJ fuel |
| Solar and Li-Ion CI | 25 | gCO2e/kWh |
| Embodied Emissions - Electrolysis | 0.19 | gCO2e/MJ fuel |
| Embodied Emissions - Solar | 8.71 | gCO2e/MJ fuel |
| **Total** | **8.90** | **gCO2e/MJ fuel** |

| CO Electrolysis Block | | |
|---|---|---|
| One time upstream | 75.87 | kgCO2e/kW |
| Ongoing | 16.73 | kgCO2e/kW |
| Lifetime | 20 | years |
| Electrolyzer Efficiency | 6 | kWh/Nm3 CO |
| Electrolyzer Operating | 8585 | hrs/yr |
| CO Requirement | 0.034573 | Nm3/MJ Fuel |
| Solar and Li-Ion CI | 25 | gCO2e/kWh |
| Embodied Emissions - Electrolysis | 0.11 | gCO2e/MJ fuel |
| Embodied Emissions - Solar | 5.19 | gCO2e/MJ fuel |
| **Total** | **5.30** | **gCO2e/MJ fuel** |

| Fischer-Tropsch Block | | |
|---|---|---|
| Vented CO2 | 444 | kg CO2e / bbl FT liq product |
| Combustion of Flue Gas CO2 | 48 | kg CO2e / bbl FT liq product |
| Incineration of Flue Gas CO2 | 18 | kg CO2e / bbl FT liq product |
| Vented credit (ambient) CO2 | -444 | kg CO2e / bbl FT liq product |
| Ancillary Sources CO2 | 20 | kg CO2e / bbl FT liq product |
| Combustion of Flue Gas CH4 | 0.015 | kg CO2e / bbl FT liq product |
| Fugitive and Flaring CH4 | 0.15 | kg CO2e / bbl FT liq product |
| Ancillary Sources CH4 | 1 | kg CO2e / bbl FT liq product |
| Combustion of Flue Gas N2O | 0.3 | kg CO2e / bbl FT liq product |
| Ancillary Sources N2O | 0.3 | kg CO2e / bbl FT liq product |
| Fugitive CO2 | 0.88 | kg CO2e / bbl FT liq product |
| **Total** | **15.25** | **gCO2e/MJ fuel** |

| Electricity Credit | | |
|---|---|---|
| Electricity Production | 0.11 | MJ / MJ fuel |
| Average Grid CI | 470 | gCO2e/kWh |
| **Total** | **-14.36** | **gCO2e/MJ fuel** |

| ATF - H2 / CO2 Separate Electrolysis / FT | | |
|---|---|---|
| **Total** | **27.95** | **gCO2e/MJ fuel** |

| ATF - H2 / CO2 Co-Electrolysis / FT | | |
|---|---|---|
| **Final Fuel Products** | | |
| FT Jet | 1.00 | MJ |
| Gasoline | 0.64 | MJ |
| Electricity | 0.20 | MJ |
| Electricity with CCS | 0.13 | MJ |

| Direct Air Capture Block | | |
|---|---|---|
| Direct Emissions | 0.01 | kgCO2e/kgCO2 captured |
| Embodied Em. DAC | 0.00 | kgCO2e/kgCO2 captured |
| Embodied Em. Energy | 0.00 | kgCO2e/kgCO2 captured |
| Nat. Gas Supply Chain CO2 | 0.05 | kgCO2e/kgCO2 captured |
| Methane Leakage | 0.12 | kgCO2e/kgCO2 captured |
| CO2 requirement | 0.09 | kgCO2 captured/MJ fuel |
| **Total** | **17.15** | **gCO2e/MJ fuel** |

| Syngas Block (2:1) | | |
|---|---|---|
| One time upstream | 75.87 | kgCO2e/kW |
| Ongoing | 16.73 | kgCO2e/kW |
| Lifetime | 20 | years |
| Electrolyzer Efficiency | 3.85 | kWh/Nm3 syngas |
| Electrolyzer Operating | 8585 | hrs/yr |
| Syngas req | 0.09179 | Nm3/MJ fuel |
| Solar and Li-Ion CI | 25 | gCO2e/kWh |
| Embodied Emissions - Electrolysis | 0.19 | gCO2e/MJ fuel |
| Embodied Emissions - Solar | 8.84 | gCO2e/MJ fuel |
| **Total** | **9.03** | **gCO2e/MJ fuel** |

| Fischer-Tropsch Block | | |
|---|---|---|
| Vented CO2 | 444 | kg CO2e / bbl FT liq product |
| Combustion of Flue Gas CO2 | 48 | kg CO2e / bbl FT liq product |
| Incineration of Flue Gas CO2 | 18 | kg CO2e / bbl FT liq product |
| Vented credit (ambient) CO2 | -444 | kg CO2e / bbl FT liq product |
| Ancillary Sources CO2 | 20 | kg CO2e / bbl FT liq product |
| Combustion of Flue Gas CH4 | 0.015 | kg CO2e / bbl FT liq product |
| Fugitive and Flaring CH4 | 0.15 | kg CO2e / bbl FT liq product |
| Ancillary Sources CH4 | 1 | kg CO2e / bbl FT liq product |
| Combustion of Flue Gas N2O | 0.3 | kg CO2e / bbl FT liq product |
| Ancillary Sources N2O | 0.3 | kg CO2e / bbl FT liq product |
| Fugitive CO2 | 0.88 | kg CO2e / bbl FT liq product |
| **Total** | **15.25** | **gCO2e/MJ fuel** |

| Electricity Credit | | |
|---|---|---|
| Electricity Production | 0.11 | MJ / MJ fuel |
| Average Grid CI | 470 | gCO2e/kWh |
| **Total** | **-14.36** | **gCO2e/MJ fuel** |

| ATF - H2 / CO2 Co-Electrolysis / FT | | |
|---|---|---|
| **Total** | **27.07** | **gCO2e/MJ fuel** |

| ATF - RWGS/FT | | |
|---|---|---|
| **Final Fuel Products** | | |
| FT Jet | 1.00 | MJ |
| Gasoline | 0.64 | MJ |
| Electricity | 0.20 | MJ |
| Electricity with CCS | 0.13 | MJ |

| Direct Air Capture Block | | |
|---|---|---|
| Direct Emissions | 0.01 | kgCO2e/kgCO2 captured |
| Embodied Em. DAC | 0.00 | kgCO2e/kgCO2 captured |
| Embodied Em. Energy | 0.00 | kgCO2e/kgCO2 captured |
| Nat. Gas Supply Chain CO2 | 0.05 | kgCO2e/kgCO2 captured |
| Methane Leakage | 0.12 | kgCO2e/kgCO2 captured |
| CO2 requirement | 0.06 | kgCO2 captured/MJ fuel |
| **Total** | **11.81** | **gCO2e/MJ fuel** |

| Hydrogen Electrolysis Block | | |
|---|---|---|
| One time upstream | 75.87 | kgCO2e/kW |
| Ongoing | 16.73 | kgCO2e/kW |
| Lifetime | 20 | years |
| Electrolyzer Efficiency | 52.28 | kWh/kg H2 |
| Electrolyzer Operating | 8585 | hrs/yr |
| H2 Requirement | 0.00802 | kg H2/ MJ fuel |
| Solar and Li-Ion CI | 25 | gCO2e/kWh |
| Embodied Emissions - Electrolysis | 0.23 | gCO2e/MJ fuel |
| Embodied Emissions - Solar | 10.48 | gCO2e/MJ fuel |
| **Total** | **10.71** | **gCO2e/MJ fuel** |

| RWGS Block | | |
|---|---|---|
| Natural Gas Demand | 7.33E-02 | MJ/ MJ fuel |
| Electricity Demand | 1.90E-02 | kWh/ MJ fuel |
| Lifetime | 20 | years |
| Heat for HPS | 0.0009 | MJ/ MJ fuel |
| Heat for LPS | 0.2232 | MJ/ MJ fuel |
| Natural Gas Emissions | 227.0 | gCO2e/kWh |
| Solar and Li-Ion CI | 25 | gCO2e/kWh |
| Electricity Emissions | 0.48 | gCO2e/MJ fuel |
| Natural Gas Emissions | 18.75 | gCO2e/MJ fuel |
| **Total** | **19.23** | **gCO2e/MJ fuel** |

| Fischer-Tropsch Block | | |
|---|---|---|
| Vented CO2 | 444 | kg CO2e / bbl FT liq product |
| Combustion of Flue Gas CO2 | 48 | kg CO2e / bbl FT liq product |
| Incineration of Flue Gas CO2 | 18 | kg CO2e / bbl FT liq product |
| Vented credit (ambient) CO2 | -444 | kg CO2e / bbl FT liq product |
| Ancillary Sources CO2 | 20 | kg CO2e / bbl FT liq product |
| Combustion of Flue Gas CH4 | 0.015 | kg CO2e / bbl FT liq product |
| Fugitive and Flaring CH4 | 0.15 | kg CO2e / bbl FT liq product |
| Ancillary Sources CH4 | 1 | kg CO2e / bbl FT liq product |
| Combustion of Flue Gas N2O | 0.3 | kg CO2e / bbl FT liq product |
| Ancillary Sources N2O | 0.3 | kg CO2e / bbl FT liq product |
| Fugitive CO2 | 0.88 | kg CO2e / bbl FT liq product |
| **Total** | **15.25** | **gCO2e/MJ fuel** |

| Electricity Credit | | |
|---|---|---|
| Electricity Production | 0.11 | MJ / MJ fuel |
| Average Grid CI | 470 | gCO2e/kWh |
| **Total** | **-14.36** | **gCO2e/MJ fuel** |

| ATF - RWGS/FT | | |
|---|---|---|
| **Total** | **42.64** | **gCO2e/MJ fuel** |

**Figure C23** Snapshot of Air to Fuels tabular data

## C3. Snapshot of Discounted Cash Flow Model used in TEA

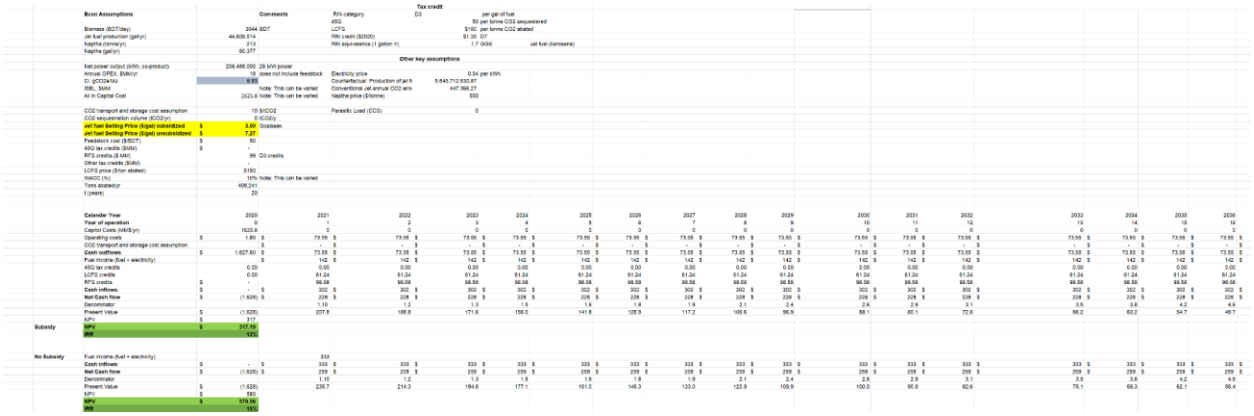

**Figure C24** Snapshot of discounted cash flow model for FT SAF without CCS